October 2014

Adaptive relay techniques for OFDM-based cooperative communication systems

Xin Gao
The University of Western Ontario

Supervisor
Xianbin, Wang
The University of Western Ontario

ADAPTIVE RELAY TECHNIQUES FOR OFDM-BASED COOPERATIVE
COMMUNICATION SYSTEMS
(Thesis format: Monograph)

by

Xin <u>Gao</u>

Graduate Program in Electrical and Computer Engineering

A thesis submitted in partial fulfillment
of the requirements for the degree of
Doctor of Philosophy

The School of Graduate and Postdoctoral Studies
The University of Western Ontario
London, Ontario, Canada

© Xin Gao 2014

Abstract

Cooperative communication has recently been considered as a key technology for modern wireless standards and next generation wireless networks to improve the quality-of-service (QoS) and extend transmission coverage in a cost-effective manner. In this thesis, we aim to address the challenges of wireless cooperative communications, and design the efficient OFDM-based relay systems.

Starting with the channel accumulation problem in the amplify-and-forward (AF) relay system, we proposed two adaptive guard interval (GI) schemes for single/multiple-relay networks respectively to cover the accumulated delay spread and enhance the transmission efficiency. Distinct from the traditional adaptive GI, the dynamical GI length can be detected by the destination individually. Numerical results show that the proposed scheme can further save the control signaling overhead without any symbol error rate (SER) performance loss. For multiple-relay systems, a novel relay selection criterion is proposed to achieve the trade-off between the transmission reliability and overhead by considering both the channel gain and the accumulated delay spread. From computer simulations, the proposed relay selection scheme significantly improves the efficient throughput over the multipath channel with variable channel length.

Moreover, cooperative systems require an accuracy resource allocation to achieve the high capacity in the two-way decode-and-forward (DF) relay system with time-varying channels and the bidirectional asymmetric traffic. We propose two allocation algorithms, where the total capacity is maximized under a capacity ratio constraint which depends on the traffic-load difference between the uplink and downlink. The balanced capacity performance shows that the proposed schemes can assure the fairs data rate of the two terminals and improve the overall QoS of the relay network. A low-complexity suboptimal allocation algorithm is proposed for the frequency-division model which separates subcarrier and time/power allocation. Verifying by simulations, the suboptimal scheme can achieve the similar performance with the optimal one with reduced complexity.

In order to further enhance the transmission reliability and maintain low processing delay, we propose a novel equalize-and-forward (EF) relay scheme, which can equalizes the channel between source and relay and eliminate the channel accumulation effect. The relay processing time is reduced by performing the channel estimation and equalization in parallel. In the EF relay, free-delay equalization is realized by presetting the equalizer with the current channel response that is predicted in parallel. Numerical results show that the EF relay can achieve comparable SER performance as the DF relay with much less latency and exhibit low outage probability at the same data rate as compared to traditional AF and DF schemes.

Keywords: wireless networks, cooperative communications, relay techniques, orthogonal frequency division multiplexing (OFDM), multipath channel.

Dedication

To my parents and my husband.

Acknowledgements

I am grateful to my supervisor Dr. Xianbin Wang. I have benefited tremendously from countless interactions and discussions with him. His emphasis on the fundamental nature of techniques and problems has not only inspired many aspects of this dissertation, but also instilled me with a better understanding of research. His precise and thorough approach to research has set up an example that I wish to follow in my future career. He also deserves many, many thanks for carefully reading my manuscripts and patiently improving my English writing.

I would like to extend my gratitude to Professors Jagath Samarabandu, Raveendra Rao and Jiandong Ren from Western University, and Professor Xiaodong Lin from the University of Ontario Institute of Technology for serving as my thesis examiners and a critical reading of the dissertation. Their insightful advice and comments improves the quality of this dissertation.

Thanks go to all present and former members of our group for the time that we spent both at work and after work. Especially I want to thank Dr. Aydin Behnad for intensive technical discussions on various parts of the dissertation. Thanks also go to all my friends both at UWO and elsewhere who made the last four years full of fun. I wish to thank my husband, Xiaoxu Ji, and my parents for their patience and constant support. My husband's understanding and encouragement has meant more than what I can express in a few words here. I am forever indebted to my parent for their support throughout these many years. I hope to have something better than this dissertation to dedicate to them in the future.

Contents

List of Figures

List of Tables

List of Abbreviations

3GPP	Third Generation partnership project
4G	Fourth Generation
5G	Fifth Generation
ADSL	Asymmetric digital subscriber line
AF	Amplify-and-forward
AWGN	Additive white Gaussian noise
BDFE	Block decision feedback equalizer
BER	Bit error rate
BF	Beamforming
BPSK	Binary phase shift keying
CDF	Cumulative distribution function
CP	Cyclic prefix
CSI	Channel state information
D/A	Digital-to-analog
DF	Decode-and-forward
DFT	Discrete Fourier transform
DSTC	Distributed space-time coding
EF	Equalize-and-forward
FD	Frequency division
FIR	Finite impulse response
FFT	Fast Fourier transform
GI	Guard interval
IFFT	Inverse fast Fourier transform

iid	Independent identically distributed
IIR	Infinite impulse response
ISI	Intersymbol interference
LTE	Long-term evolution
MCM	Multicarrier communications
MGF	Moment generating function
MIMO	Multiple-input and multiple-output
MRC	Maximum ratio combing
M-QAM	Multi-level quadrature amplitude modulation
NMSE	Normalized mean square error
OFDM	Orthogonal frequency division multiplexing
OFDMA	Orthogonal frequency division Multiple Access
PDF	Probability density function
PSK	Phase shift keying
P/S	Parallel-to-serial
QoS	Quality of service
QPSK	Quadrature phase shift keying
RF	Radio frequency
RS	Relay selection
SDF	Soft-decide-and-forward
SER	Symbol error rate
SNR	Signal-to-noise ratio
TD	Time division
UMB	Ultra mobile broadband
WiMAX	Worldwide interpretability for microwave access
WLAN	Wireless local area networks
WSSUS	Wide-sense stationary uncorrelated scattering

Chapter 1

INTRODUCTION

1.1 Research Motivations

1.1.1 Challenges in the explosive growth of wireless communications

Over the last decades, wireless communication has experienced a significantly fast development and has become indispensable to modern society, for instance, the latest generations of cellular systems, data networks and wireless local area networks (WLAN) for wireless computers, home and personal networking, etc. Between 2009 and 2014, global mobile traffic increased 66 times with an annual growth rate of 131 percent [1]. Today, mobile telephone services surpassed fixed line telephone services in terms of both availability and number of subscribers, and turned into an important tool in social and business communications. Mobile ad hoc networks are implemented in homes, campuses, hotels and airports, and provide a freedom for users to access Internet from anywhere at anytime. The next generation wireless communications systems are expected to offer high speed Internet access, wireless multimedia services and mobile computing with higher Quality of Service (QoS) requirements. The explosive growth of wireless communications is creating the demand for high-speed, reliable, and spectrally efficient communication over the wireless medium.

Obviously, there is a huge gap between the growth of wireless data traffic demand and the capacity growth rates of new wireless access technologies. There are several challenges in attempts to provide high-quality service in the dynamic wireless environment. This has

increased the effort in the investigation and implementation of wireless communication systems to accommodate communication reliability, coverage, and high data rate services for various applications.

A fundamental challenge of the wireless communication is the low reliability of the wireless channels. These pertain to the channel impairment due to multipath, fading, and shadowing, which is caused by receiving different versions of the source signal from different paths. The propagate paths result from scattering, reflection and diffraction of the transmitted signals by objects in the environment [2], such as buildings, trees, etc. Therefore, the capacity of a wireless channel has very high variability.

In addition to the unreliable channel, the spectrum resource over wireless channel is limited. Meanwhile, the required spectrum is increased as a consequence of high demand of high data rate services. Therefore, in order to reuse the frequency resource and satisfy the QoS requirements, the cellular coverage is restricted. Moreover, the increasing demand of high data rate transmission and the migration to high carrier frequency regions greatly limits the coverage of the wireless network. With the potential use of millimeter wave band in next generation wireless systems [3, 4], the cell size is reduced because by the Friis free-space equation, a millimeter wave signal experiences tens of dB more attenuation than a microwave signal. On other hand, to improve the transmission bit rate, more spectrum is required, and it also leads to coverage reduction. For instance, the coverage area has to reduce by 13 times, if the corresponding transmission bit rate rises by 100 times [5]. The natural method to address the coverage issue is to increase the number of the base stations in a region. However, it significantly raises the infrastructure cost.

Furthermore, energy consumption and environmental issue are caused by the fast growing data traffic volume and remarkable expansion of network infrastructures. From [6], approximately 18% of the Operation Expenditure results from the energy bill in the mature European market and at least 32% in India. Meanwhile, the enormous escalation of energy consumption due to the explosive development of wireless communications will directly result in the increase of greenhouse gas emission and becomes one of the major challenges in meeting the cost reduction and green environment targets [7].

Many techniques of wireless communications are emerging that suggest different architec-

tures for the described problems above. Cooperative communications as an attractive alternative is suggested by the standard task group in IEEE 802.16j Mobile Multihop Relay to extend the coverage of a base station by deploying several relay stations around the base station [8].

1.1.2   Advantages of cooperative communications

It is well known that signal fading arising from multipath propagation can be mitigated through the use of diversity. Diversity is to provide the destination node with several copies of the transmitted signal, so if one copy undergoes deep fading, the destination still can detect the received signal successfully using the other received copies. Diversity in wireless system can be achieved through time diversity, frequency diversity, and spatial diversity. A popular technique to achieve spatial diversity is the multiple-input and multiple-output (MIMO). This technique is attractive for its significant improvement to information rate and transmission reliability [9] [10]. However, high cost and complicate implementation issues bring challenges to MIMO systems.

Cooperative communications, shown in Fig. 1.1, have recently become a key technology for the modern wireless networks as an effective means of saving power, attaining broader coverage range, and mitigating channel impairments resulting from fading. It has been incorporated into many wireless standards, such as 3GPP long-term evolution (LTE) [11–13], IEEE 802.11s (mesh networking) [14], IEEE 802.16j (wireless multihop relay) [8], IEEE 802.16m (WiMAX2) [15, 16] and Femtocell [17].

Relay communication, which is a specific kind of wireless cooperative communication, has been demonstrated to be an effective way to combat wireless fading by providing spatial diversity without the need of multi-antenna configurations [18]. The fundamental idea of relay communication is that several relay terminals participate in communications by retransmitting
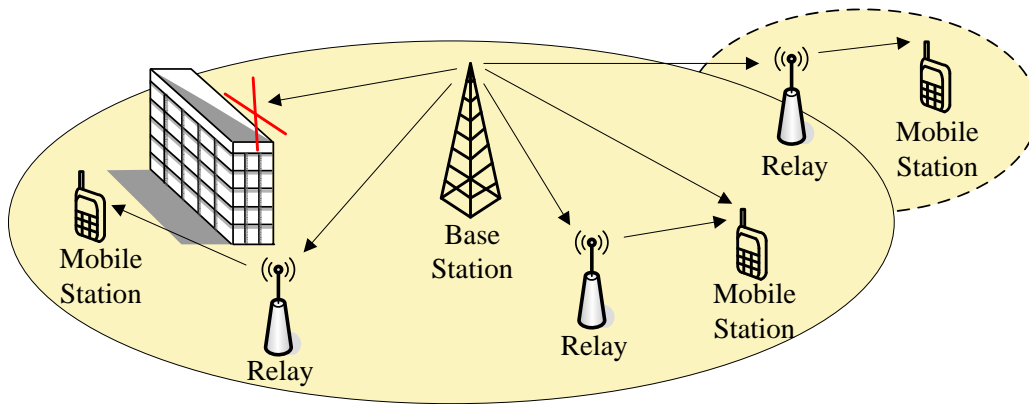
Figure 1.1: Cooperative communications in a wireless network.

a signal from a source to a destination by forming a distributed multi-antenna system [19, 20]. Relaying mimics MIMO communications by establishing interactions among the distributed nodes that serve as virtual multiple antennas both at the transmitter and receiver sides. The final destination receives multiple versions of the transmitted signals through the cooperative relay nodes and combines them forming the final received signal. In relay systems, the received and retransmitted signals at any relay node is typically orthogonalized to avoid the interference. It means the transmissions of source-relay and relay-destination are performed in different time slots or frequency bandwidths.

The application of relays in cellular systems can permit economical design for the case that there is few or infrequent user at the edge of cellular. Since the relay does not need a wired connection to the backhaul, it can eliminate the costs of the backplane that serves as the interface between the BS and the wired backhaul network. Besides, relay communications will reduce the required transmit power compared to those for a base station (BS) due to the smaller coverage. Moreover, if the density of relays in a cell is moderately high, the propagation loss from the relay to a terminal is much lower than from a BS to the terminal. Thereby higher data rates can be achieved in larger cells [21].

Furthermore, multi-hop relay cooperation scheme is a attractive approach to solve the area-coverage problem with a reasonable infrastructure cost. In a cellular, all idle users can act as relays to participate in the communication by establishing independent paths between the source and the destination. Hence, there is a potentially large number of relays which are able to help the base station to forward the signals. When the target mobile station is out of the service coverage of the base station, one or more relay node can retransmit the signals from the base station towards the destination. As a result, the coverage is substantially extended with the assist of relay nodes.

All the aforementioned benefits of the cooperative communication motivate us to investigate it as a promising techniques which can be used to combat the challenges of wireless networks.

1.2   Technical Challenges in Relay Communications

Although the relay technology is promising in improving communication quality, the involvement of multiple relay nodes and multi-hop transmissions also poses many challenges to the reliability and efficiency of the systems.

In relay communications, the diversity is achieved by exploiting the relay node to retransmit the source signal. Based on the signal processing methods employed by the relay node, cooperative schemes can be divided into two main protocols: amplify-and-forward (AF) and decode-and-forward (DF). In AF, the relay simply captures the waveform received from the source, amplifies it, then re-transmits a noisy version of source transmission. In DF, the relay implements a full physical layer transceiver. It decodes a transmission by the source, re-encodes the entire received signal, then retransmits.

One of the major challenges of cooperative communications is the low transmission reliability due to channel characteristic of the transmission links (i.e., the source-relay link, and the relay-destination link). In the broadband wireless systems, the channels take place over multipath propagation which leads to frequency selective fading and delay spread. In non-coherent cooperative relay systems, the channel condition will become rougher because of the accumulation of multipath fading in the multiple hops if there is no channel compensation techniques at relay nodes. The overall channel impulse response from the source via the relay to the destination is the convolution of the impulse responses of the multiple frequency-selective channels. As a result, the delay spread in the different links add together to form the overall delay spread of the concatenated channel, and the delay spread of the relaying link increases proportionally to the number of relays [22]. Meanwhile, in frequency domain, the frequency selectivity of overall channel response is also grown, which is the product of the frequency selectivity of each hop. Compared to the DF scheme, it is obvious that the AF scheme has simpler operation. However, without channel compensation techniques at AF relay nodes, the severe channel response will increase the noise level in the system, and cause the reduction the transmission reliability of the relay link [18].

Meanwhile, in the cooperative network with multiple available relay nodes, the trade-off of system reliability and efficiency becomes complicated to achieve. The cooperative multiple-

relay system, enabling the architecture called virtual MIMO, has become promising in various networks as it is able to enhance the overall system performance by achieving full cooperative diversity. Although the diversity order is high compared to a single-relay cooperative system, the operation becomes very complicated and the system suffers the additional resource consumption. The repetition-based cooperation schemes are bandwidth inefficient, since the larger number of relay nodes used for cooperative transmission reduces the spectral efficiency and increase the power consumption due to the transmission over orthogonal channels. The required resources in multiple-relay system increase by the number of available relay nodes. In order to benefit from the multiple-relay systems, relay selection (RS) is an alternative efficient transmission scheme which provides all the advantages of the cooperative diversity while minimizing the overhead without the need of synchronization across relays. Relay selection chooses a single best relay according to some criterion to participate in the transmission between relay and destination. However, in the specified situation with accumulated multipath fading channels, the relay selection schemes only based on the channel gain or signal-to-noise ratio (SNR) cannot achieve high transmission efficiency without considering the effect of the accumulated channel delay spread and relaying delay.

Besides, the multi-hop transmission involved in cooperative systems requires an accuracy resource allocation to achieve the high capacity. Especially, in the scenario with time-varying channels and the bidirectional asymmetric traffic, the traditional allocation which only depends on the channel condition causes the fairness issue and degradation of the overall QoS of the relay network. Practical relay systems typically avoid the interference between the received and retransmitted signals at any relay node by orthogonalizing these signals. Two common methods for orthogonal relay transmission are frequency division (FD) and time division (TD) where the available bandwidth or time frame, respectively, are shared. Due to the path loss and fading effects, the channel condition and capacity of these orthogonal channels are considerably different. Also, taking the mobility of the relay and terminal nodes into account, the channels fadings are time-variant. Therefore, allocating transmission resources to the hops equally and statically will lead to the overall system capacity reduction. It is important to make a wireless relay system which adaptively allocates the transmission resource, such as time slot, bandwidth and power. Meanwhile, in two-way relay systems, the traffic loads of down-link and up-link are

asymmetric in most practical cases [23–25]. Hence, the resource allocation algorithm without considering the asymmetric traffic loads leads to the fairness issue. Simply maximizing the total end-to-end capacity will result in the lopsided allocation of the resource, i.e., light traffic flows would obtain relatively excessive resource. On the other hand, forcing the two terminals with different traffic loads achieve the same capacity only according to the channel condition causes a problem such that the heavy traffic flows is deprived of resources and suffers low data rate. Moreover, the allocation scheme to achieve the equal capacity of two terminals does not take into account the notion that the two terminals might have different data rate requirements, eg., in the systems with service level differentiation or flexible billing mechanisms for different classes of users. Therefore, ignoring the asymmetric traffic in resource allocation lowers the overall quality of service of the relay network. For the bidirectional asymmetric traffic scenario, the traffic-load ratio between the two terminals should also be one of the factor to determine the resource allocation algorithm.

Furthermore, the channel compensation techniques applied at relay nodes, which have high complexity and long processing delay, results in additional delay overhead and reduce the end-to-end transmission time utilization rate particularly in packet and interactive communications. In order to improve the quality of retransmission, some relay schemes apply error correction techniques at relay nodes, such as DF relay. However, this high-complexity techniques result in another challenge of relay system, i.e., the reduction of transmission efficiency. In relay systems, the additive processing delay at relay nodes will increase the transmission overhead. Specifically, in the DF relay which completes the entire receiving and regenerating operations, the FFT/IFFT will take over $10\mu s$ delay [26], and de/interleaving and de/encoding need even much more processing time. Furthermore, in some decoding schemes, to achieve high throughput, the relay has to collect all coded packets in a block before being able to decode. It indicates that the long processing time at the relay is not negligible at all. This overhead reduces the transmission efficiency especially in the packet and interactive communications. Besides, for the delay sensitive and realtime application which requires imminently feedback information, the stringent latency requirement cannot tolerate high-complexity operations and long processing time of relay nodes.

1.3 Main Contributions of This Thesis

The above mentioned issues and factors encourage us to investigate the relay communication systems and propose several solutions. Specifically, motivated by the benefits of orthogonal frequency division multiplexing (OFDM) in terms of supporting the high bit rate transmission and combating the multipath channels, we use OFDM as the underlying modulation technique for our physical layer design.

The major contributions of this thesis is summarized as follows:

- Beginning with the transmission reliability and efficiency problem in AF relay systems, we proposed an adaptive GI scheme which can eliminate the overall transmission overhead by dynamically choosing the suitable GI length. The destination can detect the GI length individually. Hence, the proposed adaptive GI scheme can be implemented without any extra control signal transmitted by the source to notify the destination about the GI used. Numerical results show that the proposed scheme (without additional control signal) can achieve the same symbol error rate (SER) performance as the conventional adaptive GI approaches (with control signal), and further save the control signaling overhead without any SER performance loss.

  Next, we extend this work to multiple-relay systems. Based on the adaptive GI scheme for AF relay network, we propose a novel RS scheme to minimize the overhead as well as enhance the overall transmission reliability. In the proposed strategy, an effective throughput is defined as the selection criterion which depends on both the end-to-end channel gain and the accumulated delay spread. Both the theoretical analysis and simulation results show that when the channel delay spread varies, the proposed scheme can dramatically improve the effective data transmission throughput.

- We then consider resource allocation problem in the two-way DF relay system with asymmetric traffic loads. Two resource allocation algorithms are investigated to optimize the end-to-end capacity of the two-way system under the constraints which includes the total transmission time/power and the capacity ratio between the bidirectional transmissions.

In the first scheme where the two-way communication is executed by time-division, the total end-to-end capacity is maximized by optimizing the transmission time and power allocations under the capacity ratio and total transmission time/power constraints. The performance of this scheme is compared with different allocation schemes through simulations. The results show that the proposed optimal allocation can significantly improve the balanced capacity compared to the random and equal allocation schemes.

By exploiting the orthogonality of the subchannels in OFDM systems, the two-way communication in the second allocation scheme is performed by frequency-division model. In this scenario, subcarriers, subcarrier power and time slot are optimized to achieve the maximum balanced capacity. Since the optimal solution is extremely computationally complex to obtain, we propose a low-complexity suboptimal allocation algorithm which separates subcarrier allocation and time/power allocation. Simulation results verify that the suboptimal algorithm can provide the similar performance with the optimal one.

- To further improve the transmission reliability under multiple multipath channels, we present a novel equalize-and-forward (EF) relay scheme. To eliminate the accumulation of both delay spread and frequency selectivity, the relay node estimates and equalizes the channel between source and relay. To shorten the processing time, estimation and equalization are performed in two parallel parts. In main path, delay-free equalization is realized by passing data symbols through an equalizer preset with the up-to-date channel response from parallel path. In parallel path, the current channel condition are estimated and predicted from multiple past channel responses. Compared to AF and DF relay schemes, the proposed EF relay scheme has an efficient structure to eliminate the multipath channel effect as well as the relay overhead.

1.4   Thesis Structure

The remainder of this dissertation is organized as follows.

The background subjects is briefly introduced in Chapter 2, including the motivation for using the frequency agile multicarrier modulation technique in frequency-selective fading chan-

nels, the basic principles of OFDM-based communication systems, the benefits of cooperative communications and the classification of cooperative schemes. The chapter also provides a literature survey of cooperative communication systems related to our research.

Beginning with the channel accumulation problem in AF relay systems, two adaptive relay schemes against the accumulation of delay spread are proposed in Chapter 3. For the signel-relay networks, we introduced an adaptive GI scheme which can eliminate the overall transmission overhead by dynamically choosing the suitable GI length. Extending the adaptive GI scheme to multiple-relay systems, a novel relay selection (RS) scheme is proposed to minimize the overhead as well as enhance the overall transmission reliability. In the proposed strategy, an effective throughput is defined as the selection criterion which depends on both the end-to-end channel gain and the accumulated delay spread to maximize the transmission efficiency. The performance of the proposed scheme are evaluated through numerical simulations.

In Chapter 4, we present the adaptive resource allocation schemes for the two-way DF relay systems. Considering the different capacity requirements due to the asymmetric traffic loads of two-way communications, the transmission resources, including transmission time and power, are dynamically allocated to each hop. For the time-division systems, the end-to-end channel capacity is maximized under the constraints. Moreover, exploiting the orthogonal subchannels of OFDM systems, the two-way relay communications are performed simultaneously on different subchannels, i.e., frequency-division systems. Based on this scenario, a low-complexity subcarrier allocation algorithm is also introduced. Finally, numerical examples of the proposed schemes are presented.

To further improve the transmission reliability under multiple multipath channels, a novel equalize-and-forward (EF) relay scheme is presented in Chapter 5. First, we investigate the performance impact of the multihop transmission in relay systems. We then provide the EF relay design, which adopted an efficient parallel structure to shorten the processing time and to achieve both transmission reliability and low processing delay. Finally, the performances of EF relay scheme is compared to AF and DF relay schemes through computer simulations.

The conclusions of the thesis are summarized in Chapter 6. In addition, the future research directions relevant to the work in this thesis are discussed.

Chapter 2

Background and Literature Review

This chapter briefly introduce the background subjects related to our research. It includes the multicarrier modulation technique for frequency-selective fading channels, the basic principles of OFDM-based communication systems, the benefits of cooperative communications and the classification of cooperative schemes. We then review the development and important results in the major issues associated with cooperative communication from a broad array of related references. Specifically, we discusses considerations involved in the study of this dissertation, i.e., OFDM-based cooperative communications, relay techniques for multipath channels, relay selection and resource allocation in relay systems, and transmission efficiency improvement of relay communications. The motivation of this chapter is to familiarize the readers with the field of study and lay the foundation for the rest of the dissertation.

2.1 Principles of Multicarrier Communication

2.1.1 Multi-Carrier Modulation

In recent years, wireless applications are widely used and becoming more and more sophisticated, meanwhile the demand for high data-rate communications has increased substantially. Therefore, a communication system should be able to achieve high data-rates for transmission with the limited spectrum resource. The multicarrier communications (MCM) approach can supporting huge data-rates by dividing the transmitted bit stream into several parallel bit

Multi-carrier

Channel
fading

B

Single-carrier

Channel
fading

B
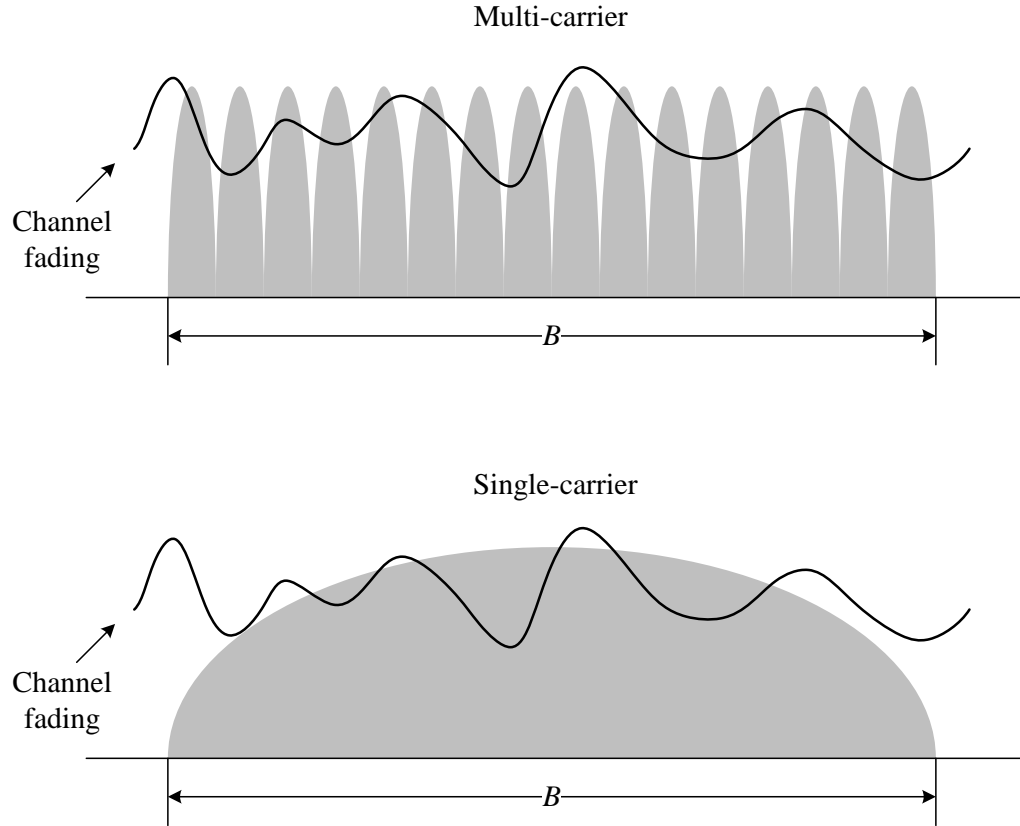
Figure 2.1: Comparison of the effect of frequency-selective fading channel on the signle-carrierr vs. the multi-carrier communications

streams and modulating these sub-streams with different narrowband subcarriers [27]. The number of the subcarriers is chosen to ensure that each subchannel experiences flat fading, where the intersymbol interference (ISI) on each subchannel is negligible. As a result, M-CM is robust to frequency selective fading, hence MCM becomes a prime candidate for high data-rate transmissions.

The coherence bandwidth for a channel is defined as B_c, over which the signal propagation characteristics are correlated. The coherence bandwidth can be approximately estimated by the inverse of the maximum path delay spread, τ_{max}. Consider a linearly modulated system with data rate R and bandwidth B. The channel is frequency selective if the signal bandwidth is larger than the coherence bandwidth, i.e., $B_c > B$. And the signal experiences frequency-selective fading. On the other hand, if B is smaller than B_c, the channel can be approximately considered flat. The comparison of the MCM and single carrier communications is shown in Fig. 2.1. Compared to single carrier systems, the fading of each subchannel in MCM communications

can be considered relatively flat since the subcarrier bandwidth is small compared to the coher-
ence bandwidth of the channel. Moreover, in a MCM system, a single fade or interferer only
affects a small percentage of the subcarriers. However, in a single carrier system, it can cause
the entire link to fail.

Due to different delays on different propagation paths, ISI is caused by the delay spread
when adjacent symbols overlap and interfere with each other. The symbol duration of the
signal, T_s, is defined as the inverse of the signal bandwidth, B. In a single-carrier modulated
system, the number of interfering symbols is given by

$$N_{\text{ISI}} = \left\lceil \frac{B}{B_c} \right\rceil = \left\lceil \frac{\tau_{\max}}{T_s} \right\rceil, \tag{2.1}$$

where $\lceil \cdot \rceil$ is ceiling operation. When the data rate is high, the symbol duration of the single-
carrier-modulated system will be very short, consequently, the bandwidth B becomes large, i.e.
$B > B_c$, then the effect of ISI will significantly increase.

On the other hand, if the signal bandwidth is much smaller than the coherence bandwidth,
$B \ll B_c$, the amount of ISI will become negligible. This effect is exploited in the multicarrier
systems. The basic premise of multicarrier modulations is to break this wideband system into
N linearly modulated sub-systems in parallel, each with subchannel bandwidth $B_N = B/N$ and
data rate $R_N \approx R/N$. In this case, the number of interfering symbols in multi-carrier modulated
systems becomes

$$N_{\text{ISI}} = \left\lceil \frac{B}{NB_c} \right\rceil = \left\lceil \frac{\tau_{\max}}{NT_s} \right\rceil. \tag{2.2}$$

For sufficiently large N, the subchannel bandwidth $B_N \ll B_c$, which ensures relatively flat
fading on each subchannel. In the time domain, the symbol time T_N of the modulated signals
in each subchannel is approximate to $N \times T_s$. So $B_N \ll B_c$ implies that $T_N \gg \tau_{\max}$. Thus, the
ISI degradation in MCM systems is much lower than that in single-carrier systems.

Moreover, there are some other advantages of the MCM systems. The multi-carrier system-
s are less susceptible to impulse noise, since the energy of the impulse noise only distributes
over several subchannels at the multi-carrier receiver, thereby its effect reduces. Besides, multi-
carrier systems can perform adaptive power and bit loading, which can enhance performance
with respect to maximizing throughput or minimizing power consumption. Multicarrier com-

munications require separated modulators and demodulators on each subchannel, which was too complex to implement in the early years. However, the development of simple and cheap implementations of the discrete Fourier transform (DFT) and its inverse reduces the computational complexity of MCM systems and ignited MCM's widespread use. Furthermore, low complexity equalizers can be adopted for satisfactory equalization in multi-carrier implementation, while more complex equalizers are required in a single carrier system.

2.1.2 Orthogonal frequency division multiplexing (OFDM)

(a) Transmitter

(b) Receiver
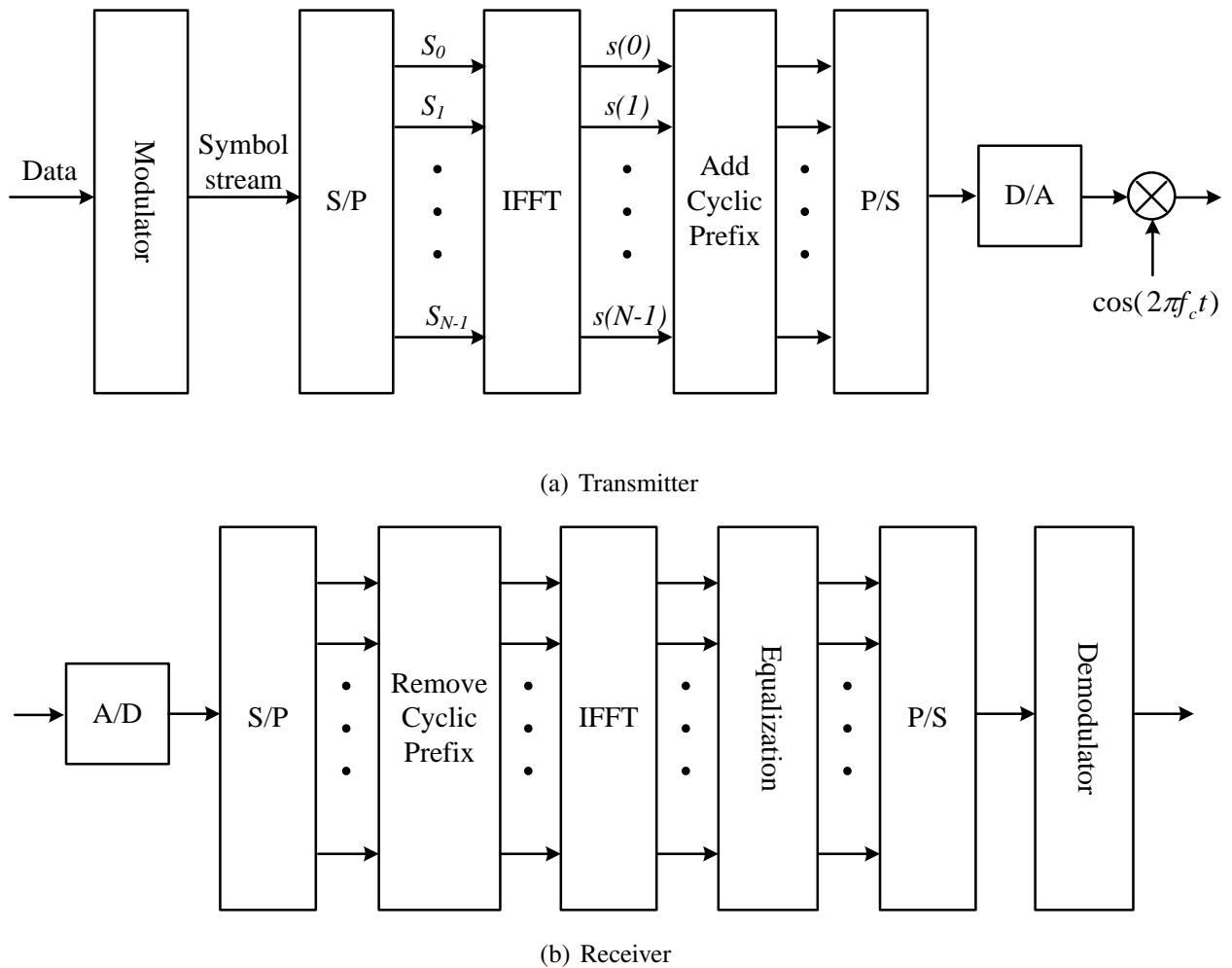
Figure 2.2: Block diagram of an OFDM system

In this thesis, we mainly focus on OFDM-based relay systems, which is a multi-carrier

transmission technique, and fundamentals of OFDM is described in this section.

OFDM is a popular scheme for many existing and future wideband digital communication systems, whether wireless or over wirelines, such as asymmetric digital subscriber line (ADSL) broadband internet access systems [28], digital video and audio broadcasting systems [29], IEEE 802.11a [30], IEEE 802.11g [31] and IEEE 802.11n [32] Wi-Fi systems, IEEE 802.16 WiMAX systems [33], and 4G mobile cellular communication systems, such as LTE and UMB.

The basic principle of OFDM is to divide the available spectrum into N subcarriers, with each subcarrier containing a low rate data stream. The subcarriers have appropriate spacing and passband filter shape to satisfy orthogonality. The block diagram of an OFDM system is shown in Figure 2.2. First, the high data rate stream of symbols is passed through serial to parallel converter resulting in a block of N low rate parallel data streams. This serial to parallel conversion increases the symbol duration by a factor of N. Then these streams are modulated individually by exploiting M-ary quadrature amplitude modulation (QAM) or M-ary phase shift keying (PSK). The low rate streams are loaded onto N orthogonal subcarrier and summed up to yield an OFDM symbol. The baseband transmitted signal for a single OFDM block corresponds to

$$s(t) = \frac{1}{N} \sum_{k=0}^{N-1} S_k e^{j2\pi k \Delta f t}, \tag{2.3}$$

where S_k, $k = 0, 1, \ldots, N-1$, represents the complex symbols of the k-th subcarrier, and Δf is the frequency spacing between adjacent subcarriers [2]. The baseband OFDM signal given in (2.3) is equivalent to the implemented by IFFT of N M-ary PSK (or M-ary QAM) input symbols. Therefore, the IDFT and DFT are used to modulating and demodulating the data constellations on the orthogonal subcarriers. The discrete sample of the OFDM symbol is written as

$$s(n) = \frac{1}{N} \sum_{k=0}^{N-1} S_k e^{\frac{j2\pi kn}{N}}, \quad n = 0, 1, \ldots, N-1. \tag{2.4}$$

As compared to the traditional parallel systems, frequency division multiplexing (FDM), OFDM can achieve a higher spectrally efficient. In FDM systems shown in Fig. 2.3, when adjacent subcarriers are located without sufficient guard spacing, spectral bleeding into adjacent subcarriers results in the distortion of the signal. Therefore, a guard band is necessary between subcarriers, which leads to an inefficient usage of spectrum. However, OFDM systems resolve

FDM multi-carrier modulation

frequency

OFDM multi-carrier modulation

←————Bandwidth saving————→
frequency
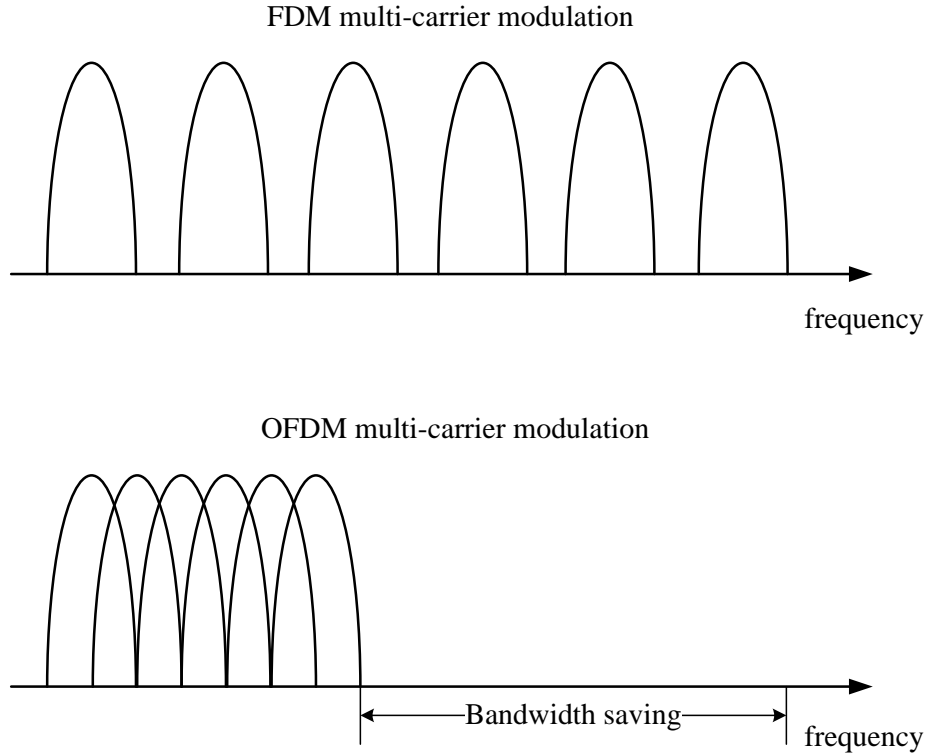
Figure 2.3: Comparison of the bandwidth utilization between the FDM and the OFDM systems

this issue by insuring that any two subcarriers are mutually orthogonal. Then, OFDM can uses overlapping spectrum of orthogonal subcarriers, which leads to effective usage of spectrum, as shown in Fig. 2.3 [34].

Before the samples in (2.4) are sent to the digital to analogue converter (D/A), the guard interval (GI) or cyclic prefix (CP) is appended to the OFDM symbols. CP was an important contribution to OFDM, which was proposed by Peled and Ruiz in 1980 to solve the orthogonality problem [29]. A cyclic prefix, instead of the conventional null band, is added at the beginning of the OFDM symbol after IFFT procedure. The length of the cyclic prefix is chosen to be longer than the channel length such that the interference of multipath components from one symbol cannot affect the next symbol. Meanwhile, if the guard interval contains cyclically extending the OFDM signal, i.e.,

$$\{s(N-1-\mathcal{P}), s(N-\mathcal{P}), \ldots, s(N-1), s(0), s(1), \ldots, s(N-2), s(N-1)\},$$

where $\mathcal{P}$ is the length of CP, the linear circular channel is converted into a cyclic circular

channel, which ensures orthogonality over a time-dispersive channel and eliminates the ISI between subcarriers to a large extent. The only drawback of the CP extension is the reduction in the efficiency of transmissions. After the parallel-to-serial (P/S) conversion, the baseband time-domain OFDM signal $s(n)$ is passed through the digital-to-analog (D/A) converter to generate the analog signals from the digital signals. Then, the baseband OFDM signal is upconverted to the desired centering frequency f_c and amplified for transmission.

The receiver as shown in Fig. 2.1.2 (b) performs the reverse operation of the transmitter. The RF signals is downconverted to baseband for processing and converted to digital signals using an analog-to-digital (A/D) converter. The sampled time signals pass through a S/P converter to generate the parallel streams. Then the CP is discarded from the received composite signal. The received time-domain signal is given by

$$r(n) = \frac{1}{N} \sum_{k=0}^{N-1} H_k S_k e^{\frac{j2\pi nk}{N}} + \omega(n), \tag{2.5}$$

where H_k denotes the channel fading coefficients for the k-th subchannel which is assumed to be a flat fading, and $\omega(n)$ is additive white Gaussian noise. After that, a fast Fourier transform (FFT) is applied to recover the original frequency-domain transmitted data in parallel as

$$\hat{S}_k = \frac{1}{N} \sum_{n=0}^{N-1} r(n) e^{\frac{j2\pi nk}{N}}. \tag{2.6}$$

These parallel data substreams are aggregated into the serial data stream and demodulated to recover the original high speed serial information data stream. At the receiver side, frequency and timing synchronization is an important task to correctly demodulate the OFDM symbol. Channel estimation and equalization techniques are also required depending upon the transmission surroundings and the bit-error-rate requirements of the communication systems.

Figure 2.4: Two-hop relay system

2.2 Basic Concepts for Relay Communication

2.2.1 Fundamental Idea of Relay Communication

Cooperative communication is an alternative technique to provide impressive performance by exploiting spatial diversity in wireless transmission. In fact, relay communication has been seriously considered for cellular, wireless ad hoc and sensor networks [35].

In relay communications, the cooperative diversity is achieved by using relay nodes. The relay nodes receive the source transmission and retransmit the signals to the destination based on some protocols. Relays can be mobile terminals (user terminals) or fixed terminals known as infrastructure relays. When there is only one relay node is assigned to assist the communication between the source and the destination, it is called a single-relay system, while if multiple relays participate in the communications, it is called a multiple-relay system. In a two-hop relaying communication system as shown in Fig. 2.4, the general operation can be divided into two phases. In the first phase, the source S broadcasts the signal to the relay node R and the destination D. During the second phase, the relay forwards the received signal from the source to the destination node through an orthogonal (non-interfering) channel, while the source keeps silent.

When the direct link between the source and the destination is available, the destination node will receive two replicas of the same data transmitted through two different and indepen-

dent channels: the S−R−D channel and the S−D channel. The destination node combines the relayed signals in the second phase and the direct signal in the first phase to improve the S-NR. Since the relay nodes are generally located in different physical locations, a diversity gain can be created by the spatial separation of the relays which would enforce independent fading. In addition to the benefits of increased diversity, cooperative networks also can increase the coverage and lower power consumption compared to the conventional networks [36].

2.2.2 Classification of Relay Schemes

A huge variety of relay schemes have been proposed; [37] provides a good overview. According to the processing functionality of relay node, the cooperative communication scheme can be divided in to two major categories: Amplify-and-Forward (AF) [18] and Decode-and-Forward (DF) [38].

AF Relaying

In AF scheme, the relay simply captures the waveform received from the source, amplifies it, then re-transmits a noisy version of source transmission. Therefore, AF relays can be considered transparent to modulation and coding techniques which are performed at the source and the destination. Since AF relay do not need decoding, it has low-complexity transceivers and low processing power consumption. One of the key parameters in AF relaying design is the amplifying gain. There are two widely used types of amplifying gain, i.e., variable gain which depends on the instantaneous channel fading of the received path to choose the amplification gain [39] and fixed gain which is constant and depends on the fading channel statistics [40]. Variable gain relaying generally outperforms the fixed gain relaying systems. However, the requirement of instantaneous channel information will rise the complexity and cost of the relay. While in fixed gain relaying, the relay uses long term statistics of the inward channel when designing the amplification gain [41]. Therefore, fixed gain relaying does not required the instantaneous channel state information (CSI). This scheme is also known as semi-blind relay. The advantage of fixed gain relaying is that the relay does not need to measure the channel from the source, and hence has less system overhead and complexity. Due to its lower complexity,
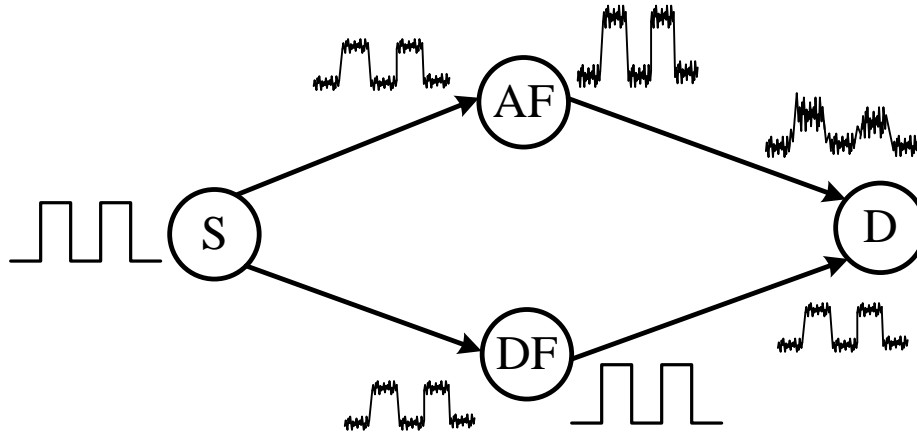
Figure 2.5: Comparison of the signal processing between the AF and the DF relays

the fixed gain AF relaying scheme is preferred in the systems which has a strict requirement of transmission delay.

DF Relaying

In DF scheme, the relay implements a full physical lay transceiver. The relay decodes the signals received from the source, re-encodes the entire received signal, then retransmits to the destination. In order to achieve the maximal diversity order, the relay should be able to know whether or not it has decoded correctly and then adaptively transmit the re-encoded signal based on the obtained knowledge. Usually, error correction codes are utilized for DF relaying to detect and correct the errors at relay node. Under reasonable channel conditions, the regenerated signal can be identical to the source signal when all transmission errors between source and relay are corrected by channel coding.

Fig. 2.5 compares the signal processing in AF and DF relays. As illustrated in this figure, DF relay can generates the clean retransmitted signal which is equal to the signal transmitted by the source. Such an ability can be realized through some sophisticated mechanisms, such as error detecting codes [42] and appropriate SNR thresholds at the relay [43, 44]. However, these mechanisms will increase the complexity of the systems. On the other hand, if the relay forwards the decoded signals blindly, the system performance will be degraded by errors at the relay which are propagated to the destination. Compared to DF relay, the noise and fading of the two-hop channel is accumulated with the desired signals along the transmission path in the

AF relay systems. Although, the AF relay does not suffer from the error propagation problem as the DF relay, since no hard-decision operation is performed on the received signal at the relay.

In addition to AF and DF protocols, other relaying protocols have been proposed in the literature, such as estimate-and-forward [45], and compress-and-forward [46].

2.2.3   One-Way & Two-Way Relay Systems

In One-way relay systems, the information is always transmitted form the source node, and the destination only receive the signal of the source. In two-way scenario, the communication is bidirectional where two users exchange information. Under this scenario, each node is not only a source, but also the intended destination of the other node. Examples of two-way relay systems are when a mobile user communicates with the base station via a dedicated relay in a cellular system, or two mobile users exchange their data in a WLAN via the access point.

The relay scheme used in one-way communication systems can also be used for two-way relay systems, with some modifications. In a typical one-way relay system, the communication is established in two phases. A straightforward approach of a two-way relay system to avoid interference is to deploy two successive one-way relay schemes. Since most of the current wireless devices operate in half-duplex transmission mode, a two-way relaying scheme requires four phases (in time or frequency) to accomplish the exchange of symbols between the two transceivers.

In order to achieve two-way relay transmission in less phases, the relay node requires a more complicated hardware and a higher signal processing capability. The received data from the two transceivers need be combined at the relay. There are different approaches of combining data, such as superposition coding, network coding and Lattice coding. In superposition coding, the relay retransmits the linear sum of the two sets of symbols containing the decoded data of the two transceivers. Each transceivers subtracts its own data first and then decodes the data of the other user [47]. In network coding, the relay combines data from the two terminals exploiting the XOR operation. The combined data is remodulated and retransmitted. The two terminals will find out the desired data by XORing the received data with its own transmitted

data [48, 49]. While, the relay with Lattice coding utilizes nonlinear operations for combining the data [50].

2.3 Literature Review

2.3.1 OFDM-based Cooperative Communications

The concept of cooperative communication can be traced back to the three-terminal communication channel (or the relay channel) in [51] by Van Der Meulen. Upper and lower bounds on the capacity of such channel were also developed in [51]. Shortly after, Cover and El Gamal studied the general relay channel and established an achievable lower bound for data transmission [52]. These two seminal works laid down the foundation for the present-day research on cooperative communication.

Recent interest in OFDM techniques and cooperative communication has resulted in a number of new protocols employing OFDM to improve the system performance of relay networks [53–72].

In [53], OFDM is applied to a simple single-relay-node ST-coded cooperative transmission. The design of an OFDM frame and techniques for synchronization, as well as channel estimation, are considered. In other work, [54–56], the focus is either on other aspects of a cooperative system (such as coding and synchronization problems) or the OFDM signal is treated as a single entity. Mei et al. [57] and Li et al. [58] adopted a distributed OFDM scheme based on the assumption that the relay nodes can perfectly recover the original information. In [59], power allocation scheme over the subcahnnels in frequency and space domain is proposed to maximize the instantaneous rate. The power and bandwidth allocation for an OFDM multihop network with the objective of maximizing the end-to-end rate is considered in [60]. In [61], a soft-decode-and-forward (SDF) relay strategy for asynchronous wireless networks with doubly-selective (both time-selective and frequency selective) was presented which adopt distributed OFDM scheme and employ a block decision feedback equalizer (BDFE) at relay nodes.

In OFDM-based relay systems, the amplification gain can be adaptively changed for each

subchannel to compensate multipath channels. These systems are classified into AF relay systems [61, 67–72], as they avoid decoding and encoding operations. Bit and power loading techniques for OFDM-based AF relay systems was investigated in [67, 68]. The proposed approaches are to minimize the transmit power consumption with the throughput constraint [67] or minimize the bit error rate under power consumption constraint [68]. Bit and power loading techniques were investigated for OFDM-based AF relay systems in [68, 69] to minimize the bit error rate under power consumption constraint or minimize the total transmit power at the relay node.

Th OFDMA systems are considered in [62–66]. In [62], with amplify-and-forward relaying, OFDMA is used to enable a node to transmit both its own information as well as that from another source by partitioning the set of subchannels. The focus of this work is on optimizing the resource assignment problem to determine which nodes help other nodes, how many subchannels are allocated for helping, and how many are allocated for sending their own data. The solutions that are presented come from a complex optimization that requires global knowledge of the channel conditions and the transmit powers. In [63], aiming at maximizing the achievable sum rate from all the sources to the destination, a source, relay, and subchannel allocation problem for an OFDMA relay network is studied. In [64], the choices of relay node, relay strategy, and the allocation of power and bandwidth for each user in a cooperative OFDMA uplink scenario are considered. An optimal resource allocation algorithm is proposed. In [65], joint cooperative diversity and scheduling for multiuser OFDMA relaying systems is addressed. In [66], the cooperative cellular network employs orthogonal frequency-division multiple-access (OFDMA) is considered, and cross-layer resource allocation optimization is design maximize the overall utility.

2.3.2　Relay Techniques for Combating Multipath Channels

In practical systems, channels connecting the source, relay and destination suffer from inter-symbol interference (ISI) caused by frequency-selective fading. A number of related techniques have been investigated in [61, 68–80] to address the frequency selective fading in relay communications.

Relaying schemes for single-carrier transmission over frequency-selective channels are investigated in [73, 74, 76–79, 81]. A cooperative filter-and-forward beamforming (FF-BF) technique [73, 74, 81] was proposed and optimized under the assumptions that there is the destination and full channel state information of all links is available. FF-BF relays are equipped with finite impulse response (FIR) or infinite impulse response (IIR) filters (corresponding to the linear equalization and decision feedback equalization) to compensate for the transmitter-to-relay and relay-to-destination channels. The considered BF problems are to maximize the SNR at the receivers subject to the total and individual relay transmitted power constraints [81] [73], or minimize the total relay transmitted power subject to the destination SNR constraint [73]. Nevertheless, beamforming technique require the relay nodes are close to each other to achieve the performance improvement, which is less economical in the cellular with large coverage. Moreover, beamforming technique needs multiple relay nodes to assist the communication between the source and destination, which additional feedbacks between relay nodes and terminal nodes are required to perform the global optimization. When the number of relay nodes is large, the amount of the control signals lead to a low system efficiency and long processing delay.

Other related work simply focuses on the receiver design at destination nodes to equalize the frequency selective channel [76–80]. The distributed space time-coding techniques at the relays and equalization at the destination proposed in [76] has became a technique for the frequency selective fading. H. Mheidat et al. applied this combination of space time-coding and single carrier frequency domain equalization in cooperative diversity communication in [76] [77]. Block equalization of space-time coding scheme was proposed in [76–78] for the so-called protocol III [78] where the source sends to the relay during the first slot and both the source and relay send to the destination in the second slot. The simulation results they got showed this kind of combination could obtain significant diversity gain and superior symbol error rate (SER) performance. The transmission model protocol III neglected the broadcasting property of the wireless communications. In [79], the authors introduced a maximum ratio combining (MRC)-aided strategy for protocol I [78], i.e., a scheme similar to protocol III except that the destination receives direct signal from the source in the first slot, under the AF mode and operating over a frequency-selective relay channel. Distributed space-time coding does not require full CSI but has a worse performance than FF-BF. However, combating the

accumulated channel effect at destination naturally increases the processing complexity as well as the power consumption of mobile terminals.

2.3.3   Relay Selection in Multiple-Relay Networks

When there exist multiple relays in a cooperative communication, there are many different strategies to exploit multiple relays: distributed space-time coding (DSTC) [76–78], distributed beamforming [82–84], and relay selection.Although it is shown that DSTC achieves full diversity order and has higher spectral efficiency than the repetition-based schemes [76], implementing space-time coding over distributed nodes needs the symbol level synchronization which makes it almost surely impractical. Relay selection is an integral component in performance optimization problems for cooperative communication since proper choice of the relays in the network can have profound impact on the achievable performance of a session. Besides, compared to the distributed STC and distributed beamforming which require ideal frequency/time synchronization across the relays, relay selection can exhibit excellent performance with full diversity while it is simple to implement and it requires only low feedback signaling overhead [85–95].

In [85] and [86], Bletsas et al. proposed opportunistic AF-based relaying in which the best relay is selected based on a quality policy among the available relay nodes, and showed that it was outage-optimal among single relay selection schemes. In [87], the outage probability and throughput of AF-based relaying with and without relay selection are compared which showed that the relay with relay selection provided better performance except in the low SNR regime.

Following the opportunistic relay selection, several other single relay selection schemes emerged in the same spirit as opportunistic relay selection but with different choice of relay selection criteria. In [86–88], the optimal single relay selection scheme that maximizes the end-to-end signal-to-noise ratio (SNR) while achieving full diversity with the highest throughput is examined. In [89–91], the relay selection rule based on the location of the node is demonstrated which is called distributed nearest-neighbor protocol. In this schemes, the user selects a neighboring node as the relay based on its proximity to the source node. In [85, 90], the best worse channel selection is proposed. For two-hop relay system, the worse channel between

the source-to-relay and the relay-to-destination links is recognized as its bottleneck channel. Among all the relays, the one whose bottleneck channel is the best gains the permission to forward. In [85] and [93], a derivative of the best worse selection is used for AF relay systems where the relay with the best harmonic mean of the source-to-relay and the relay-to-destination links is selected.

There are some research work on the performance analysis of relay selection schemes adopt either AF or DF protocols [88, 93–95]. In [88], Jing et al. derived the diversity order of the above single relay selection schemes and proposed several SNR-suboptimal multiple relay selection schemes. It has been shown that the relay selection schemes achieve full diversity under perfect channel state information. The work in [88, 94, 95] provides analysis in term of outage and bit error probability for AF and DF protocol.

The aforementioned RS schemes only focus on the effect of channel fading to improve the transmission reliability and throughput of relay networks. In the specified situation with accumulated multipath fading channels, the relay selection scheme should not only consider the received SNR but also the effect of delay spread and the transmission efficiency.

2.3.4 Resource Allocation in Relay Systems

Adaptive resource allocation (RA) plays a crucial role in relay networks. The main goal of resource allocation for relay systems is to maximize the end-to-end channel capacity or minimize the resource consumption by adaptively allocating the transmission resources, including time slots, frequency bandwidth and power consumption. In order to improve the system performance, many resource allocation schemes have been investigated in the literature for the different scenarios of the relay networks [96–122].

In [96–98], a two-hop relay system is considered in which the channel resource is allocated for maximizing the instantaneous channel capacity, subject to the total power constraints [96, 97] or individual power constraints [98]. The optimal resource allocation to guaranteeing QoS for the users has been investigated in [99, 100]. Several other resource allocation problems have been considered with the objective of minimizing outage probability [104], minimizing transmission power [105, 106], and minimizing average symbol error rate prob-

ability [107]. In the relay network where there exist multiple relay nodes, the performance of the cooperative systems also depends on how the relay nodes are selected to participate in the communications between the source and destination [105, 107, 108]. Therefore, relay selection and resource allocation should be jointly optimized as a combinatorial problem, but this problem is often handled as separate subproblems [104, 105, 107–110]. In most cases, a fixed number of relays are selected first, then resource allocation is performed. However, since the channels are fluctuating all the time, the relay node should be able to adaptively decide to cooperate or not cooperate to avoid certain loss in terms of spectral efficiency or energy efficiency [104, 109–112], for instance, when the source-relay channel is poor. To solve this problem, selective relaying, i.e., relaying only when it is beneficial for the system, can significantly improve the performance [104, 109, 110, 112].

For the OFDM-based relay systems, the resource allocation problem has been studied in [113–117, 123]. In [123], the optimal power allocation over the subchannel at source and relay that maximizes the instantaneous rate is proposed for a two-hop OFDM-based AF relay network. Optimal power allocations at source and relay nodes (regenerative and nonregenerative) are discussed in [113, 114] for the case that source and relay nodes share a total amount of transmission power over the two time slots. In [115], the optimal gain allocation for multiple AF relays is presented which maximizes the instantaneous rate. The power allocation is proposed in [116] for multiple OFDM-based AF relays maximizing the average SNR of the maximum-ratio combiner at the destination node. In [117], the OFDM and OFDMA networks consisting of multiple relays and one source/destination pair was considered. Resource allocation for a multiuser two-way OFDMA relay network is investigated in [124] and [125] to support two-way communication between the base station and each of multiple users.

In [101–103, 126–129], the resource allocation problem combined with the subcarrier selection has been investigated for the OFDM-based relay systems. In [126, 127, 129] the best relay selection and resource allocation for an OFDMA relay network with multiple relays and multiple/single user have been investigated. When both users and relays are multiple, relay selection and resource allocation are complicated because of the interactions among the users. In [128], an isolated relay assignment and power allocation algorithm is proposed for cooperative wireless networks considering homogeneous traffic.

For the multihop relay systems, the resource allocation scheme are investigated in [118–122]. The allocation schemes for AF and DF relay systems were proposed in [118] and [119] respectively. In [120], the time slot and transmission power are optimized for the multihop OFDM-based relay system. In [121, 122], allocation algorithms are proposed for the specific requirements of the multihop relay networks employing cognitive radio or MIMO techniques respectively.

2.3.5 Transmission Efficiency Improvement of Relay Communications

In relay communication systems, multiple time slots or different frequency bands are used to send same information signals to a destination node. This will cause a reduction in the transmission rate or bandwidth and an increase in the transmission delay. Meanwhile, the additive processing delay at relay nodes involves in the extra transmission overhand and lowers the transmission efficiency of the overall systems [130]. To address this problem, some techniques have been prosed in the literature to improve the efficiency of the relay networks with the different scenarios [11, 131–140].

Different adaptive relay schemes are proposed in [131–134] to enhance the transmission efficiency of the cooperative communications. Authors in [131] presented an adaptive relay scheme based on hierarchical constellations to improve the cell capacity of multi-hop networks. In the proposed scheme, a symbol consists of multiple bits with varying degrees of robustness against channel errors, and was retransmitted adaptively according to the channel conditions. Two strategies for performing independent adaptive modulation and coding over dual-hop systems were studied in [132]. A finite-state Markov chain model is used to analyze the proposed strategies over general fading channels, and exact analytical expressions of key performance indicators were obtained in [132], including the average transmission efficiency, the average packet loss rate as well as the average transmission delay. In [133], a relay-caching mechanism was introduced that exploits fixed RSs in cellular networks to improve spectrum efficiency and to reduce energy consumption. In [134], the authors propose an incremental opportunistic DF relay scheme employing orthogonal spacetime block codes to maximize the diversity gain and improve transmission efficiency.

Besides, the cooperative network coding technique was investigated in [135, 136] to reduce the consumption of radio resources and improve the spectrum efficiency. In [135], the performance of network coding based cooperative multicast scheme was analyzed in terms of throughput, delay and average queueing length, and an optimal scheme to maximize throughput subject to delay and queue length constraints was proposed. In [136], the relay transmission using instantaneously-decodable binary network coding is studied, which can minimize decoding delay and achieve low complexity. Although the network coding technique can diminish resource consumption, the additional control signal overhead involved by it will worsen spectrum efficiency [141]. Therefore, it is important and difficult to achieve a good trade-off between system efficiency and control overhead.

The relay station placement schemes for improving the transmission or energy efficiency were also studied in [11, 137–140]. A random selection scheme was proposed in [137] to minimize the deployment cost based on the integer programming technique. [138, 139] proposed relay deployment mechanisms for IEEE 802.16j WiMAX Networks. In [138], the mechanism determines the relay locations so that the bandwidth requirement of mobile stations was satisfied and the network throughput was improved. In [139], the objective of the relay placement problem is to determine the required number of relay nodes and their locations such that the network capacity can be maximized under the deployment budget constraint. The placement strategy in [11] maximized the capacity of the network as well as achieved the minimal traffic demand by each subscriber station. The joint optimization of relay station (RS) placement and RS sleep/active probability was investigated in [140] to enhance the energy efficiency of a one-dimensional cellular network.

2.4   Summary

In this chapter, we briefly introduce the background subjects related to our research and discusses considerations involved in the study of this dissertation. The basic principles of multicarrier modulation and OFDM techniques are presented. The benefits of cooperative communications and the classification of cooperative schemes are also introduced. In Literature Review part, we survey the development and important results in the major issues associated

with cooperative communication from a broad array of related references. The study areas involved in this dissertation are specifically discussed, i.e., OFDM-based cooperative communications, relay techniques for multipath channels, relay selection and resource allocation in relay systems, and transmission efficiency improvement of relay communications.

Chapter 3

Amplify-and-Forward Relay System with Adaptive Guard Interval

3.1   Introduction

An AF relay typically has lower complexity and less processing burden than a DF relay, hence, it is often preferable in the systems with strict latency requirement. However, given that there is no channel compensation techniques at AF relays, multi-hop transmissions over frequency selective fading channels result in an accumulation of delay spread, which could lead to strong intersymbol interference (ISI) at the destination. The length of the end-to-end channel of the relaying link is increased by the sum of channel lengths of each hop. This means that if OFDM with fixed length guard interval (GI) were to be used in this AF system, the duration of the GI has to be extended to the longest possible channel delay spread to avoid ISI.

Although increasing the GI length can alleviate the channel delay spread issue, it comes at the expense of a lower data transmission rates. For instance, in WiMAX [33], the longest GI length is 25% of the OFDM symbol. If the GI length has to be doubled to cover two multipath channels, that means as much as 40% of the signal transmission time becomes GI. In the multi-hop scenario, the GI length has to extend even further. However, using such a long GI lowers the effective data transmission throughput. In practice, considering the mobility of relay and destination nodes, the channel delay spread varies over a wide range during data transmission [142] [143]. Hence, a large fixed GI will reduce the resource utilization rate when

the delay spread is small.

To this end, an adaptive GI technique are proposed to reduce the GI overhead and enhance the transmission efficiency in this chapter for dual-hop signal-relay and multiple-relay AF systems. The proposed adaptive GI technique can dynamically choose the most suitable GI length to cover the accumulated delay spread in AF relay systems as well as reduce the overall transmission overhead.

Compared to the single-relay systems, cooperative multiple-relay systems can further enhance the overall system performance by performing full cooperative diversity. However, the cooperative multiple-relay transmission requires complex operations (e.g. symbol level synchronization in distributed space-time code) and the additional resource consumption (e.g. power and bandwidth in the repetition-based cooperation schemes). In order to achieve the benefits of multiple-relay systems, relay selection (RS) is an efficient alternative transmission scheme which provides all the advantages of the cooperative diversity while minimizing the overhead by avoiding the synchronization across relays. However, considering the challenge of AF relay networks, the multipath channel accumulation, an appropriate RS scheme in cooperative multiple-relay networks should not only enhance the overall transmission reliability but also minimize the relay overhead. Therefore, a novel relay selection scheme is proposed based on the adaptive GI technique which selects the best relay by considering both the end-to-end SNR and the effect of delay spread on the transmission efficiency.

3.2   System Model

In this chapter, we consider an AF relay system as shown in Fig. 3.1, which is composed of a source node S, a destination node D, M relay nodes, $\{R_1, \ldots, R_M\}$. The relay nodes dedicate their resources to relaying the information for the source. It is assumed that there is no direct link between the source and destination nodes. The relaying link is dual-hop, where only one relay is chosen to participate into the communication between the source and the destination by forwarding the signal for the source node. For the multiple-relay system in Sections 3.4, i.e., $M \geq 2$, the best relay node is selected based on some relay selection techniques; while in the single-relay system, i.e., $M = 1$, in Section 3.3, the best relay node becomes the relay node
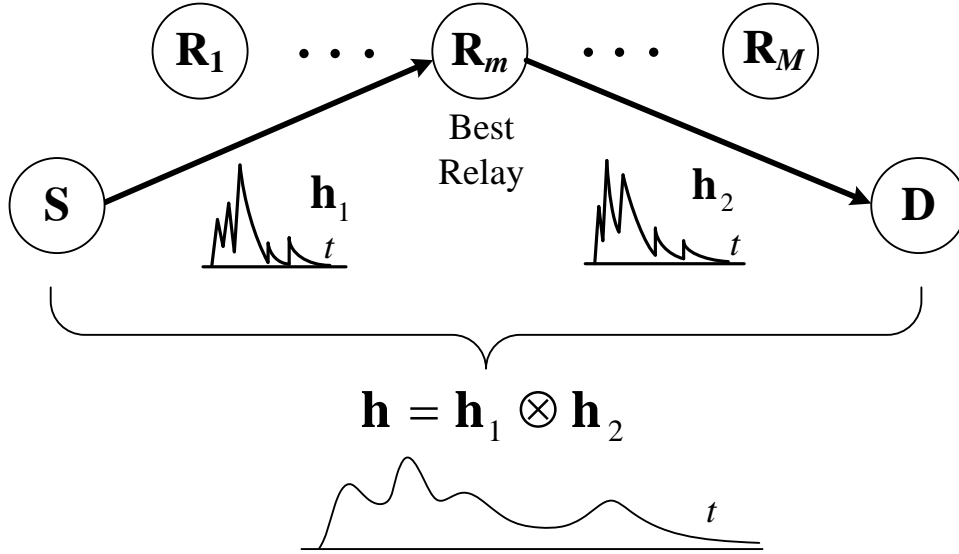
Figure 3.1: A two-hop AF relay system over accumulated multipath channels.

itself.

Each relay node operates in a time-division half-duplex mode. To avoid interference, each hop is assigned an orthogonal channel. The transmission from the source to destination involves two stages. During the first phase, signals are transmitted from source S to relay R. During the second time slot, the relay node forwards the received signal to the destination D while the source node remains silent.

In wireless communications, multipath propagation causes frequency selective fading and delay spread due to the broadband transmission. Here, we consider a baseband-equivalent, discrete-time model of the multipath channels between S and Rs and between Rs and D. Denote that $\mathbf{h}_i = [h_i(0), h_i(1), \ldots, h_i(L_i - 1)]$ is the channel of the i-th hop, where L_i is the channel length of $\mathbf{h}_i$, $\{h_i(l)\}$ is the the baseband channel tap coefficients of the i-th hop, and $i = 1, 2$. It is assumed that $h_i(l)$ are mutually independent complex random variables, and the channel is reciprocal [118, 119], i.e., the uplink and downlink gains are the same. The amplitude of $h_i(l)$ is modeled as a Rayleigh distribution with probability density function (PDF)

$$f_{|h_i(l)|}(x) = \frac{2x}{\Upsilon_{i,l}} \exp(-\frac{x^2}{\Upsilon_{i,l}}), \qquad x \geq 0, \tag{3.1}$$

where $\Upsilon_{i,l} = E[|h_i(l)|^2]$ is the power of the l-th tap of $\mathbf{h}_i$.

In an OFDM system with N subcarriers, the time-domain transmitted signal is defined as $s(n)$, $n = 0, 1, \ldots, N - 1$. During the first stage of the relay communications, the transmitted signal $s(n)$ is distorted by channel $\mathbf{h}_1$, and superimposed by an additive white Gaussian noise (AWGN) term $\omega_1(n)$ with variance σ_1^2. The received signal at relay R is therefore given by

$$r_1(n) = \sum_{l=0}^{L_1-1} h_1(l)s(n - l) + \omega_1(n). \tag{3.2}$$

In order to mitigate ISI, guard interval (GI) is introduced for each OFDM symbol. The CP length should be no less then the channel length to completely eliminate ISI. Consequently, the convolution in time domain in (3.2) becomes a circular one on blocks of size N, i.e.,

$$\mathbf{r}_1 = \mathbf{H}_1\mathbf{s} + \mathbf{w}_1, \tag{3.3}$$

where $\mathbf{H}_1$ is an $N \times N$ matrix given by

$$\begin{bmatrix}
h_1(0) & 0 & \cdots & 0 & h_1(L_1 - 1) & \cdots & \cdots & h_1(1) \\
h_1(1) & h_1(0) & \cdots & 0 & & h(L_1 - 1) & \cdots & h_1(2) \\
\vdots & & \ddots & & & \ddots & \vdots & \vdots \\
h_1(L_1 - 1) & h_1(L_1 - 2) & \cdots & h_1(0) & 0 & \cdots & \cdots & 0 \\
0 & h_1(L_1 - 1) & \cdots & h_1(1) & h_1(0) & \cdots & \cdots & 0 \\
\vdots & & \ddots & & & \ddots & \vdots & \vdots \\
0 & & \cdots & 0 & h_1(L_1 - 1) & \cdots & & h_1(1) & h_1(0)
\end{bmatrix}, \tag{3.4}$$

$\mathbf{r}_1 = [r_1(0), r_1(1), \ldots, r_1(N-1)]^T$, $\mathbf{s} = [s(0), s(1), \ldots, s(N-1)]^T$ and $\mathbf{w}_1 = [\omega_1(0), \omega_1(1), \ldots, \omega_1(N-1)]^T$.

The N-size discrete Fourier transform (DFT) of the received signal $r_1(n)$ and channel impulse response $h_1(l)$ is denoted by

$$R_{1,k} = \sum_{n=0}^{N-1} r_1(n)e^{\frac{-j2\pi nk}{N}}, \tag{3.5}$$

and

$$H_{1,k} = \sum_{l=0}^{L_1-1} h_1(l) e^{\frac{-j2\pi lk}{N}}, \tag{3.6}$$

where $k = 0, 1, \ldots, N - 1$ is the subcarrier index. In frequency domain , the convolution becomes the product as

$$R_{1,k} = H_{1,k} S_k + W_{1,k}, \tag{3.7}$$

where $\{S_k\}$ and $\{W_{1,k}\}$ are the DFT of $\{s(n)\}$ and $\{\omega_1(n)\}$. And, the received signals at the relay node can be expressed by

$$r_1(n) = \frac{1}{N} \sum_{k=0}^{N-1} R_{1,k} H_{1,k} e^{\frac{j2\pi nk}{N}} + \omega_1(n). \tag{3.8}$$

For AF relay protocols, the received signal at relay node is multiplied with a amplification factor and then retransmitted. In the second phase, the selected relay node amplifies the received signal, and forwards it to the destination node. The retransmitted signal at the relay node is

$$y(n) = Gr_1(n) \tag{3.9}$$

where G is the amplifying gain at the AF relay node which can be defined as

$$G = \sqrt{\frac{P_s}{P_s \sigma_{\mathbf{h}_1}^2 + \sigma_1^2}}, \tag{3.10}$$

where P_s is the average symbol power, $\sigma_{\mathbf{h}_1}^2$ and σ_1^2 are the variance of $\mathbf{h}_1$ and Gaussian noise, respectively. After the completion of the all phased, the instantaneous AF received signal at the destination node becomes

$$\mathbf{r}_2 = G\mathbf{h}_2 \otimes \mathbf{h}_1 \otimes \mathbf{s} + G\mathbf{h}_2 \otimes \mathbf{w}_1 + \mathbf{w}_2,$$
$$= G\mathbf{h} \otimes \mathbf{s} + \mathbf{w}, \tag{3.11}$$

where

$$\mathbf{h} = \mathbf{h}_2 \otimes \mathbf{h}_1, \tag{3.12}$$

and

$$\mathbf{w} = G\mathbf{h}_2 \otimes \mathbf{w}_1 + \mathbf{w}_2. \tag{3.13}$$

The time domain received signal is given by

$$r_2(n) = \frac{G}{N} \sum_{k=0}^{N-1} S_k H_{1,k} H_{2,k} e^{\frac{j2\pi nk}{N}} + \frac{G}{N} \sum_{k=0}^{N-1} H_{2,k} W_{1,k} e^{\frac{j2\pi nk}{N}} + \omega_2(n). \tag{3.14}$$

In AF relay systems, one of the major impacts from the accumulation of multipath channels is that the delay spread of the end-to-end channel increases proportionally to the number of relays [22]. Since there is no channel compensation at AF relay node to alleviate the channel accumulation, the end-to-end channel impulse response from to the destination, i.e., $\mathbf{h} = \{h_0, \ldots, h_{L-1}\}$, becomes the convolution of the impulse responses of the multipath channels. When the relay link is a multi-hop one, the end-to-end channel in AF relay systems is given by

$$\mathbf{h} = \mathbf{h}_1 \otimes \mathbf{h}_2 \otimes \cdots \otimes \mathbf{h}_M, \tag{3.15}$$

where M is the number of hops. The time-domain received signal at destination becomes

$$\begin{aligned}
\mathbf{r}_M &= \mathbf{h}_1 \otimes \mathbf{h}_2 \otimes \cdots \otimes \mathbf{h}_M \otimes \mathbf{s} + \mathbf{w} \\
&= \mathbf{h} \otimes \mathbf{s} + \mathbf{w}.
\end{aligned} \tag{3.16}$$

As a result, the end-to-end delay spread increases proportionally to the number of relays [22] as

$$L = L_1 + L_2 + \cdots + L_M - 1. \tag{3.17}$$

Therefore, when the CP length is not long enough, the signal will suffer ISI. On the other hand, the long CP, which is used to avoid ISI from the extended delay spread, comes at the expense of a lower data transmission rates.

From (3.14), the instantaneous end-to-end SNR of the AF relay link can be written as

$$
\begin{aligned}
\gamma_{\mathrm{AF}_k} &= \left| \frac{GH_{1,k}H_{2,k}S_k}{GH_{2,k}W_{1,k} + W_{2,k}} \right|^2 \\
&= \left| \frac{\frac{H_{2,k}S_k}{W_{2,k}} \frac{H_{1,k}S_k}{W_{1,k}}}{\frac{H_{2,k}S_k}{W_{2,k}} + \frac{S_k}{W_{1,k}G}} \right|^2 \\
&= \frac{\gamma_{1,k}\gamma_{2,k}}{\gamma_{2,k} + \frac{S_k}{W_{1,k}G}},
\end{aligned}
\tag{3.18}
$$

where $\gamma_{i,k}$ is the SNR of the k-th subcarrier in i-th hop, $\gamma_{i,k} = \left| \frac{H_{2,k}S_k}{W_{2,k}} \right|^2$, $i = 1, 2$.

3.3   An Efficient Single-Relay Systems with Adaptive Guard Interval

We propose a novel adaptive guard interval (GI) scheme for OFDM-based AF relay networks to cover the extended delay spread and reduce the overall transmission overhead by dynamically choosing the most suitable GI length. The proposed adaptive GI scheme for AF relay networks allows the destination to detect the length of the variable GI without resorting to the transmission of an additional control signal. This is achieved by asking the transmitter to determine the delay spread from the training signal sent by the destination. Then by invoking channel reciprocity, the source selects the code from a pre-determined variable-length orthogonal set that represents that delay spread and used it as the GI. By exploiting the orthogonal property between different GI sequences, the proposed adaptive GI scheme can be implemented without any extra control signal transmitted by the source to notify the destination about the GI used. In contrast, the related work in [144] [145] requires an additional control signal from the source to inform the destination of the GI length used, which introduces extra transmission overhead and reduces system efficiency. Therefore, the proposed adaptive GI scheme can address the accumulation of delay spread in multi-hop transmission without increasing the signaling overhead while improving the overall transmission efficiency.

(a) Transmitter at the source.

(b) Receiver at the destination.
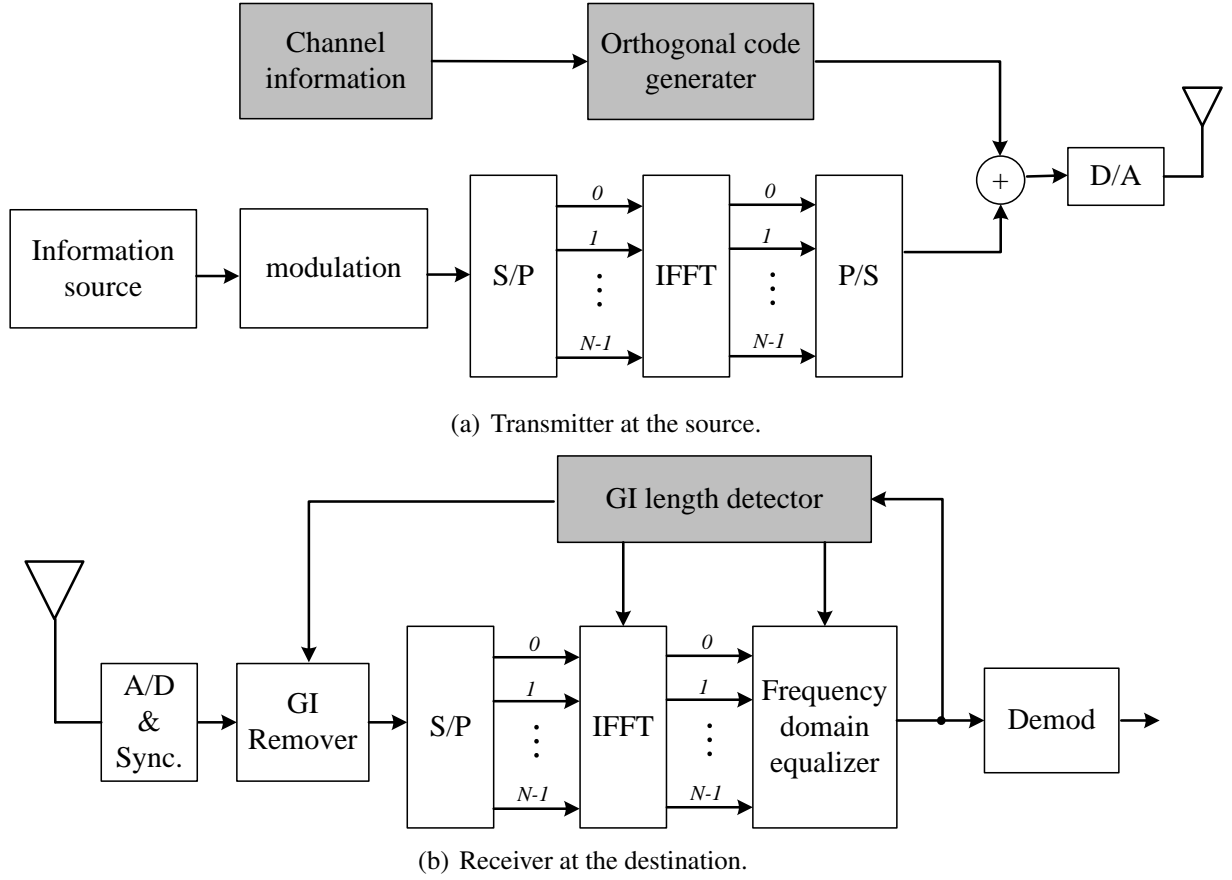
Figure 3.2: Block diagram of adaptive GI relay system.

3.3.1 Adaptive Guard Interval with Variable Length Orthogonal Codes

The transmitter and the receiver of the proposed AF system with OFDM and adaptive GI technique are shown in Fig. 3.2. The OFDM symbol at the source node, $\mathbf{s}$, is obtained by an inverse fast Fourier transform (IFFT) of the complex data vector $\mathbf{S}$ of size N. Each OFDM symbol in time domain can be described as

$$\mathbf{s} = \mathbf{F}_N^{-1}\mathbf{S}, \tag{3.19}$$

where F is a FFT transform matrix

$$\mathbf{F} = \begin{bmatrix} 1 & 1 & \cdots & 1 \\ 1 & e^{-2\pi j/N} & \cdots & e^{-2\pi j(N-1)/N} \\ \vdots & \vdots & \ddots & \vdots \\ 1 & e^{-2\pi j/N} & \cdots & e^{-2\pi j(N-1)(N-1)/N} \end{bmatrix}. \tag{3.20}$$

Before transmission of the OFDM symbol, **s**, a variable-length GI sequence is inserted into **s** as its prefix. The source estimates the length of the overall reverse channel relay from the training symbols transmitted from D to S via R. Exploiting channel reciprocity, S can then determine the GI length of the next frame transmitted to D.

In order to adapt the length of the GI according to the channel without additional control signals, the GI length, $\mathcal{P}$, is quantized into several different lengths as follows

$$\mathcal{P} = \mathcal{P}_q, \qquad \mathcal{P}_{q-1} < L \leq \mathcal{P}_q, \tag{3.21}$$

where L is the end-to-end channel length, and $q = 1, \ldots, Q$ are the quantization levels. Then, the corresponding binary code

$$\mathbf{c}_q = \{c_q(i)\}, \qquad i = 0, 1, \ldots, \mathcal{P}_q - 1, \tag{3.22}$$

is used as the GI sequence. Usually the format of the GI in OFDM systems is zero-padded or cyclic prefix extension of the data symbols [146] [147]. In the proposed scheme though, the GI is chosen from variable length orthogonal codes which are those with different lengths satisfying the orthogonal property [148].

Specifically, variable length Walsh Hadamard codes are employed as the GI sequence in the proposed system. The code generation algorithm is similar to the recursive generation of the Walsh codes by means of the Hadamard matrices. The codes are generated from a orthogonal variable spreading factor code tree as shown in Fig. 3.3 . A code with length 2^k can be generated
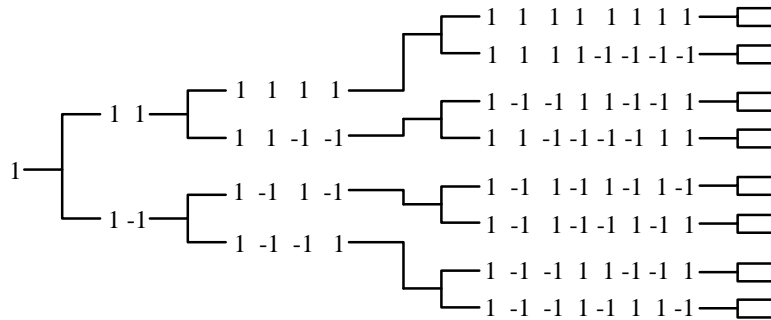
Figure 3.3: Code tree for generation of variable length orthogonal codes.

at the k-th layer using the recursive relation in with an initial condition $\mathbf{c}_0 = \{1\}$. Any two codes in the tree are orthogonal to each other only if:

- The codes are in the same layer; or

- One code is not the mother code of the other.

The code set adopted in the proposed strategy includes Q codes whose lengths are different from each other. The length range is from 2^u to 2^{u+Q}, corresponding to GI lengths of $\{\mathcal{P}_q = 2^{u+q-1}\}$, where u and Q are positive integers. The periodic correlation between any two codes in the code set at shift υ is

$$\sum_{i=0}^{2^{u+q-1}} c_q(i)c_p(i-\upsilon) = 0, \quad q < p \text{ and } q, p \in [u, u+Q]. \tag{3.23}$$

For instance, a code set which includes three different length codes can be given as

$$\begin{bmatrix} 1 & 1 & & & & & & \\ 1 & -1 & 1 & -1 & & & & \\ 1 & 1 & -1 & -1 & 1 & 1 & -1 & -1 \end{bmatrix}. \tag{3.24}$$

If the estimated channel length L equals to 6, the 8-bit code $\{1, 1, -1, -1, 1, 1, -1, -1\}$ will be adopted as the GI.

These orthogonal codes with different lengths allow us to adapt the GI to the channel length. When there is no change in the delay spread of channel, each OFDM symbol is preceded by the same orthogonal code as its GI. This process creates a series of new symbols of length $\mathcal{P} + N$ samples,

$$[c_q(0), \ldots, c_q(\mathcal{P}_q - 1), s(0), \ldots, s(N-1)]^T. \tag{3.25}$$

Figure 3.4: Signal transmission and receiving of two adjacent data symbols.

The received signal at destination can be expressed as

$$\mathbf{r} = \mathbf{H} \begin{bmatrix} \mathbf{c} \\ \mathbf{s} \end{bmatrix} + \mathbf{w}_{N+P+L-1}, \tag{3.26}$$

where

$$\mathbf{s} = [s(0), s(1), \ldots s(N-1)]^T \tag{3.27}$$

$$\mathbf{c}_q = [c_q(0), \ldots c_q(\mathcal{P}-1)]^T, \tag{3.28}$$

and $\mathbf{H}$ is the end-to-end channel matrix with size $(N + \mathcal{P}_q + L - 1) \times (N + \mathcal{P}_q)$,

$$\mathbf{H} = \begin{bmatrix} h_0 & 0 & \cdots & \cdots & \cdots & 0 \\ h_1 & h_0 & 0 & \cdots & & \vdots \\ \vdots & & \ddots & & & \vdots \\ h_{L-1} & \cdots & h_1 & h_0 & \cdots & 0 \\ \vdots & & \ddots & & & \vdots \\ 0 & \cdots & h_{L-1} & \cdots & & h_0 \\ \vdots & \cdots & & h_{L-1} & \cdots & h_1 \\ \vdots & & \ddots & & & \vdots \\ 0 & & \cdots & & 0 & h_{L-1} \end{bmatrix}, \tag{3.29}$$

and $\mathbf{w}$ denotes the Gaussian noise vector with length $(N + \mathcal{P}_q + L - 1)$. Removing the last $(L-1)$ samples which is the delay spread of $\mathbf{s}$, and the first $\mathcal{P}_q$ GI samples which is overlapped by the delay spread from the previous symbol, the desired symbol is given by

$$\tilde{\mathbf{r}} = \mathbf{H}_s \mathbf{s} + \mathbf{H}_g \mathbf{c}_N + \mathbf{w}_N, \tag{3.30}$$

where $\mathbf{c}_N = [\mathbf{0}_{1 \times (N - \mathcal{P}_q)}, c(0), \ldots c(\mathcal{P}_q - 1)]^T$.

$\mathbf{H}_s$ and $\mathbf{H}_g$ are two $N \times N$ matrices,

$$\mathbf{H}_s = \begin{bmatrix} h_0 & 0 & \cdots & 0 & 0 & \cdots & 0 \\ h_1 & h_0 & \cdots & 0 & 0 & \cdots & 0 \\ \vdots & \vdots & \ddots & \vdots & \vdots & \ddots & 0 \\ h_{L-1} & h_{L-2} & \cdots & h_0 & 0 & \cdots & 0 \\ 0 & h_{L-1} & \cdots & h_1 & h_0 & \cdots & 0 \\ \vdots & \vdots & \ddots & \vdots & \vdots & \ddots & \vdots \\ 0 & 0 & \cdots & 0 & h_{L-1} & \cdots & h_0 \end{bmatrix}, \tag{3.31}$$

$$\mathbf{H}_g = \begin{bmatrix} 0 & \cdots & 0 & h_{L-1} & h_{L-2} & \cdots & h_1 \\ 0 & \cdots & & 0 & h_{L-1} & \cdots & h_2 \\ \vdots & \vdots & \ddots & \vdots & \vdots & \ddots & \ddots \\ 0 & \cdots & & \cdots & \cdots & 0 & h_0 \\ 0 & \cdots & & 0 & \cdots & & 0 \\ \vdots & \vdots & \ddots & \vdots & \vdots & \ddots & \vdots \\ 0 & \cdots & & 0 & \cdots & & 0 \end{bmatrix}. \tag{3.32}$$

3.3.2 Detection and Equalization for Adaptive Guard Interval System

In the proposed adaptive GI system, there is no extra control signal for the GI information transmission, hence the GI length is unknown to the receiver. Moreover, from (3.30), the preceding GI sequence overlaps with the received symbols in the current interval. It is therefore of great importance to develop a receiver with ISI cancelation and GI length detection. Fig.3.2(b) shows the block diagram of the receiver.

When the channel length does not change, the same GI sequence precedes and succeeds every data symbol, i.e.,

$$\mathbf{s}' = [c_q(0), \ldots, c_q(\mathcal{P}_q - 1), s(0), \ldots, s(N - 1), c_q(0), \ldots, c_q(\mathcal{P}_q - 1)]^T.$$

It is equivalent to generating a new symbol of $(N + 2\mathcal{P}_q)$ samples with the orthogonal code as its last $\mathcal{P}_q$ samples and the same code as its cyclic prefix in the first $\mathcal{P}_q$ samples [149]. Fig. 3.4

depicts the transmitted and received signal over two data symbols and three adjacent GIs. By exploiting this CP extended structure, we can force the convolution to become a circular one on blocks of size $(N + \mathcal{P}_q)$. The received signals, after the removal of the CP, can be written in the following matrix form

$$\mathbf{r}' = \mathbf{H}_{cyc}\mathbf{s}' + \mathbf{w}_{N+\mathcal{P}_q}, \tag{3.33}$$

where $\mathbf{H}_{cyc}$ is an $(N + \mathcal{P}_q) \times (N + \mathcal{P}_q)$ matrix given by

$$\begin{bmatrix}
h_0 & 0 & \cdots & 0 & h_{L-1} & \cdots & \cdots & h_1 \\
h_1 & h_0 & \cdots & 0 & \cdots & h_{L-1} & \cdots & h_2 \\
\vdots & & \ddots & & & & \ddots & \vdots & \vdots \\
h_{L-1} & h_{L-2} & \cdots & h_0 & 0 & \cdots & \cdots & 0 \\
0 & h_{L-1} & \cdots & h_1 & h_0 & \cdots & \cdots & 0 \\
\vdots & & \ddots & & & & \ddots & \vdots & \vdots \\
0 & \cdots & 0 & h_{L-1} & \cdots & & h_1 & h_0
\end{bmatrix}, \tag{3.34}$$

and $\mathbf{s}' = [s(0), \ldots, s(N-1), c(0), \ldots, c(\mathcal{P}_q - 1)]$. Applying a FFT matrix to the Eq. (5.2) leads to

$$\mathbf{F}_{N+P}\mathbf{r}' = \mathbf{F}_{N+\mathcal{P}_q}\mathbf{H}_{cyc}\mathbf{F}_{N+\mathcal{P}_q}^{-1}\mathbf{S}' = \mathbf{H}_{diag}\mathbf{S}', \tag{3.35}$$

where $\mathbf{H}_{diag}$ is the $(N + P) \times (N + \mathcal{P}_q)$ diagonal matrix with the frequency domain channel response as its diagonal elements, and $\mathbf{S}'$ is the frequency domain vector of $\mathbf{s}'$. At this point, we can employ zero-forcing (ZF) equalization in the frequency domain [150]. The equalized received signal in time domain is

$$\begin{bmatrix} \tilde{\mathbf{s}} \\ \tilde{\mathbf{c}} \end{bmatrix} = \mathbf{F}_{N+\mathcal{P}_q}^{-1}(\mathbf{H}_{diag}^{-1}\mathbf{F}_{N+\mathcal{P}_q}\mathbf{r}'). \tag{3.36}$$

The above discussion is for the scenario which the channel's delay spread (i.e. the GI length) remains constant between two adjacent block of data. When the channel length varies, the transmitter will reset the GI length according to the channel condition. In order to reconstruct the cyclic structure for ISI cancelation, the last symbol before the GI length changing

should be succeeded by an additional GI sequence, i.e.,

$$[c(0), \ldots, c(P_q - 1), s(0), \ldots, s(N - 1), c(0), \ldots, c(P_q - 1)]^T.$$

After equalization, the block $\tilde{\mathbf{c}}$ is collected to perform GI detection. Since the GI length is unknown to the destination, equalization is repeated for each possible P_q to obtain $\tilde{\mathbf{c}}_q$, $q = 1, \ldots, Q$. Then, inner products between the $\tilde{\mathbf{c}}_q$ and the corresponding $\mathbf{c}_q$ are calculated. From the orthogonal property of the codes, when the transmitted code does not equal to $\mathbf{c}_q$, the inner product should be zero. Hence, the code that yields the maximum inner product will be detected as the transmitted GI sequence $\hat{\mathbf{c}}$. Moreover, the orthogonal characteristics between the variable length codes is affected by the equalization error and channel noise. To improve the detection accuracy of proposed adaptive GI technique, we extend the detection range from single symbol to M_d multiple symbols.

$$\hat{\mathbf{c}} = \arg \max_{\mathbf{c}_q} \left\{ \sum_{i=1}^{M_d} \langle \tilde{\mathbf{c}}_q, \mathbf{c}_q \rangle \right\}, \quad q = 1, \ldots, Q. \tag{3.37}$$

where $\langle \cdot \rangle$ is the calculation of inner product. Then, the transmitted GI length is equal to the length of $\hat{\mathbf{c}}$.

3.3.3 Simulation Results

In this section, the performance of the proposed adaptive GI strategy for OFDM-based AF relay systems is evaluated by simulation. In the simulation, uncoded QPSK scheme with 1024

Table 3.1: The channel models used in simulations

	$\mathbf{h}_{m,1}$		$\mathbf{h}_{m,2}$	
Tap	Delay τ	Average power (dB)	Delay τ	Average power (dB)
1	0.0783	-2.2204	0.0498	-2.6682
2	0.0550	-1.7184	0.0221	-6.2147
3	0.2259	-5.1896	0.1420	-10.4132
4	0.5938	-9.0516	0.4887	-16.4735
5	1.0000	-12.5013	1.0000	-22.1898
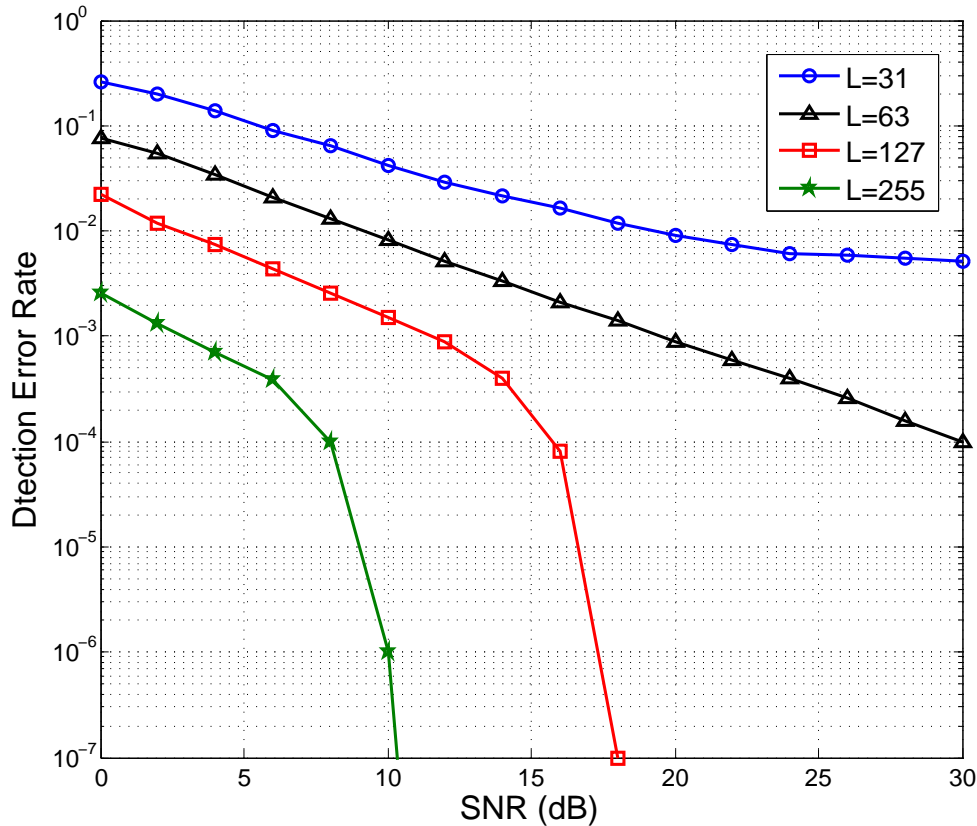
Figure 3.5: Detection error rates of the proposed adaptive GI technique over fixed channel lengths, $L = 31, 63, 127, 255$. The corresponding length of GI sequence is $32, 64, 128, 256$. The detection range is one symbol, $M_d = 1$.

OFDM subcarriers is employed.

$\mathbf{h}_1$ and $\mathbf{h}_2$ are the channels from S to R and from R to D which are multipath channels with Rayleigh fading in each path. The parameters of each path are listed in Table 3.1 [151]. The channel length of $\mathbf{h}_1$ and $\mathbf{h}_2$, L_1 and L_2 are independent and identically distributed (i.i.d.) random variables which follow the same truncated log-normal distribution with expected value μ' and variance σ'^2 i.e.,

$$L_i = \begin{cases} 5 & L_i \leq 5 \\ \lceil L_i \sim \ln \mathcal{N}(\mu, \sigma^2) \rceil & 5 < L_i < 128 \\ 128 & L_i \geq 128 \end{cases} \quad . \tag{3.38}$$
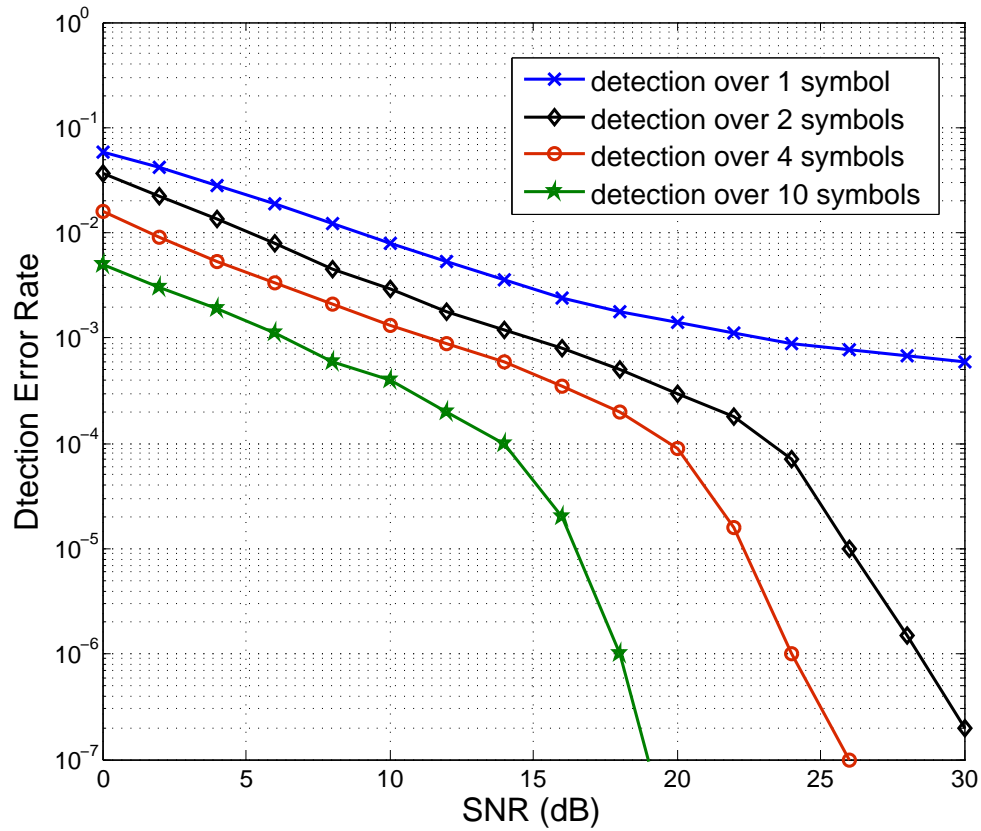
Figure 3.6: Detection error rates of the proposed adaptive GI technique with different detection ranges. The channel lengths is variable and follows the log-normal distribution, $\mu' = 64$ and $\sigma'^2 = 32$. $M_d = 1, 2, 4, 10$.

where

$$\mu = \ln\left(\frac{\mu'^2}{\sqrt{\sigma' + \mu'^2}}\right) \tag{3.39}$$

and

$$\sigma^2 = \ln\left(\frac{\sigma'}{\mu'^2} + 1\right). \tag{3.40}$$

The delay spread of each tap equals to $\lceil L_i \times \tau \rceil$. Four different GI lengths are chosen, $\{\frac{1}{32}, \frac{1}{16}, \frac{1}{8}, \frac{1}{4}\} \times N$. The length of corresponding codes, or GIs, are $\{32, 64, 128, 256\}$. The average SNRs of each hop are equal and defined as

$$\text{SNR} = \frac{\mathbb{E}[|H_{k,1}|^2]}{N_{0_1}} = \frac{\mathbb{E}[|H_{k,2}|^2]}{N_{0_2}}. \tag{3.41}$$

To evaluate the proposed adaptive GI scheme, the detection error rate is simulated and
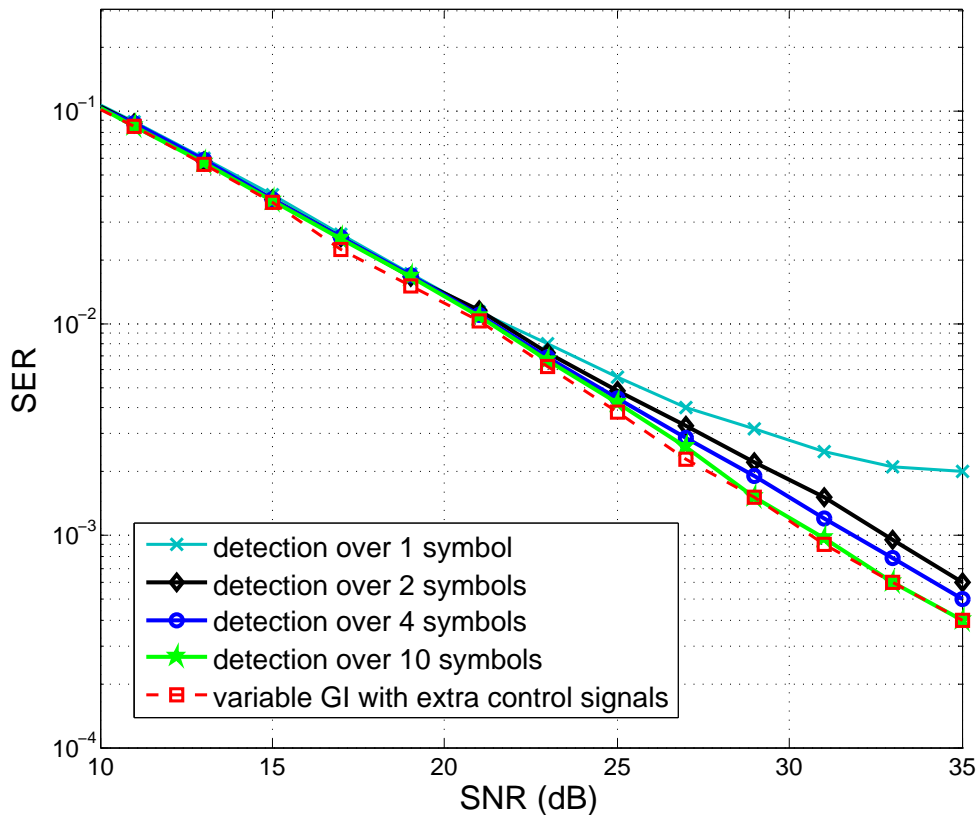
Figure 3.7: Symbol error rates of the proposed adaptive GI with different detection ranges and variable GI which required extra control signals. $M_d = 1, 2, 4, 10$. The channel lengths is variable and follows the log-normal distribution, $\mu' = 64$ and $\sigma'^2 = 32$.

plotted in Fig. 3.5 and Fig. 3.6. Fig. 3.5 shows the detection error rate of the proposed adaptive GI scheme over the fixed length channel, i.e., $L = 31, 63, 127, 255$, $L = L_1 + L_2 - 1$. The corresponding lengths of the GI sequence are 32, 64, 128, 256. The detection is operated over one symbol, i.e., $M_d = 1$. It is observed that the detection error is reduced when long GI sequences are used.

The detection error rate of over variable channel lengths is shown in Fig. 3.6. Here, the channel length follows the distribution in (3.38), and the detection operation is over multiple symbols, i.e., $M_d = 1, 2, 4, 10$. The detection error significantly decrease as the detection range extend to multiple symbols. With single symbol detection, detection error is 10^{-3} at the SNR of 18dB. However, this number can be reduce to 10^{-7} when the detection is performed over 10 symbols. Therefore, the detection accuracy can be guaranteed by using more received symbols when the system suffers low SNR.
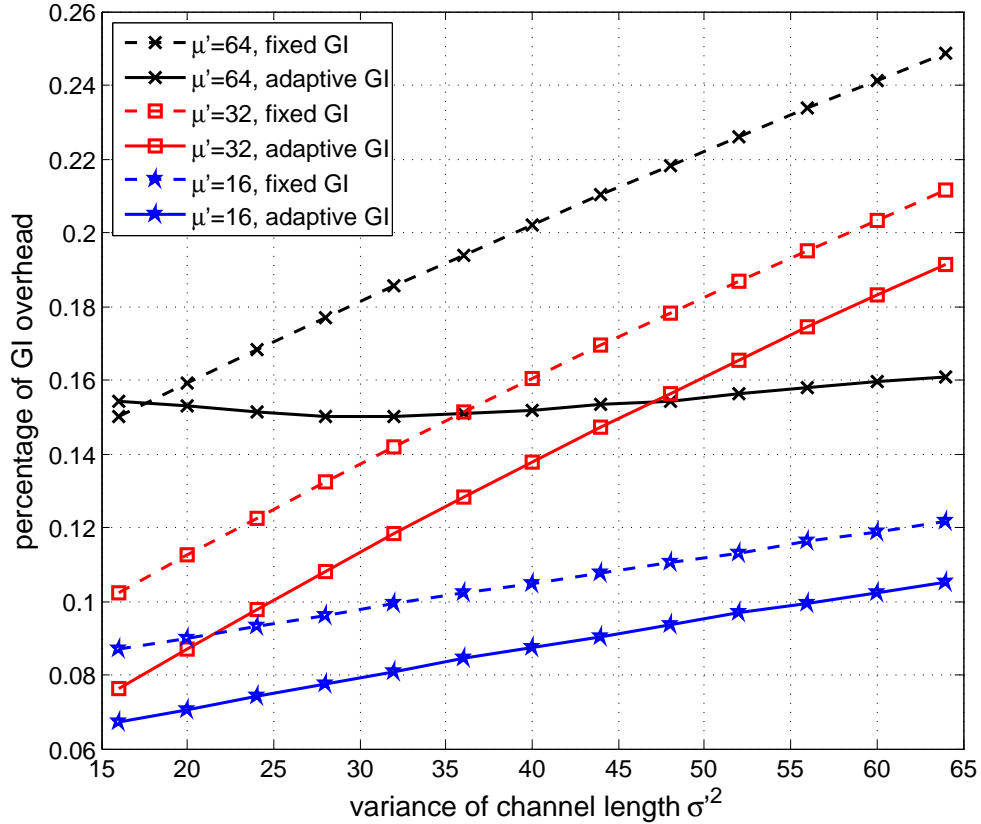
Figure 3.8: Average percentages of GI overhead of the proposed adaptive GI and the fixed GI systems. The channel lengths is variable and follows the log-normal distribution, $\mu' = 16, 32, 64$.

Fig. 3.7 presents the symbol error rate (SER) at the destination for the proposed adaptive GI OFDM systems over variable length channels. From the figure, the SER performance of the proposed scheme is improved when the GI length and detection range are extended, which is expected as seen form the detection error property. Besides, the performance of the conventional variable GI scheme, which requires extra control signals, and the proposed variable orthogonal GI schemes are compared under the same modulation and equalization scheme. In the conventional variable GI scheme, receiver has the GI knowledge notified by transmitter. With low SNR, the proposed scheme with different detection ranges provides the same SER with variable GI scheme which requires extra control signals. It means that although the detection error rate is high when SNR is low, the effect on the SER performance is not significant because

Fig.3.8 compares average GI overhead percentages of the proposed adaptive GI and the

fixed GI systems over different distributions of the channel length, which is defined as

$$\text{Percentage of GI overhead} = \frac{\mathcal{P}}{\mathcal{P} + N}. \tag{3.42}$$

The fixed GI length is chosen to satisfy $P_{\text{fix}} \geq \ln \mathcal{N}^{-1}(0.95|\mu', \sigma')$. The mean value of the channel length, μ', equals to 16,32,64 respectively. When the average channel length is relatively low, the overhead percentages of the fixed GI system and the proposed adaptive GI system both increase with the variance of the channel length. It implies that when channel length is varying strongly, the average overhead becomes high. Compared to the fixed GI system, the overhead of the proposed adaptive GI system always provides a lower overhead percentage. When the average channel length is 64, the overhead percentage of the fixed GI system still grows with the variance of the channel length, while, the adaptive GI system only exhibits little overhead increasing. Especially, when the variance is large, i.e., $\sigma^2 = 64$, the overhead percentage of the proposed scheme remarkably reduces, i.e., the fixed GI system have to used 25% of symbol as GI, while the adaptive GI only occupies average less than 16% of symbol.

3.4 Relay Selection Scheme for Multiple-Relay Systems with Adaptive GI

In order to reduce the overhead as well as improve the transmission reliability for the multiple-relay cooperative networks, we propose a novel RS scheme based on the adaptive CP technique. Most of the previous RS schemes [85–88, 90, 152–154] only focus on the effect of channel fading to improve the transmission reliability and throughput of relay networks, while the transmission overhead of the multi-hop link and its effect on the overall system performance are largely ignored.

To achieve high transmission efficiency, the RS schemes for AF relay networks should not only consider the channel gain or SNR but also the effect of the accumulated channel delay spread. In multiple-relay systems, the relay link with shortest delay spread and requiring the minimum CP length is trended to be chosen to reduce the transmission overhead; on the other hand, the relay link with highest channel gain should be selected to enhance the transmission reliability. Therefore, we defined the normalized effective throughput as the selection criterion which depends on both the accumulated channel delay spread and end-to-end SNR. With this criterion, the best relay link and the corresponding CP length are selected at source to achieve the trade-off between the transmission reliability and overhead.

3.4.1 Relay Selection Scheme with Adaptive GI

We consider a dual-hop relay system with one source terminal S, M relay nodes $\{R_1, \ldots, R_M\}$ and one destination terminal D as shown in Fig. 3.9.

In this section, define that

$$\mathbf{h}_{1,m} = [h_{1,m,0}, h_{1,m,1}, \ldots, h_{1,m,L_{1,m}-1}] \tag{3.43}$$

and

$$\mathbf{h}_{2,m} = [h_{2,m,0}, h_{2,m,1}, \ldots, h_{2,m,L_{2,m}-1}] \tag{3.44}$$

are the baseband channels of the first and second hop respectively, where $L_{i,m}$ is the channel
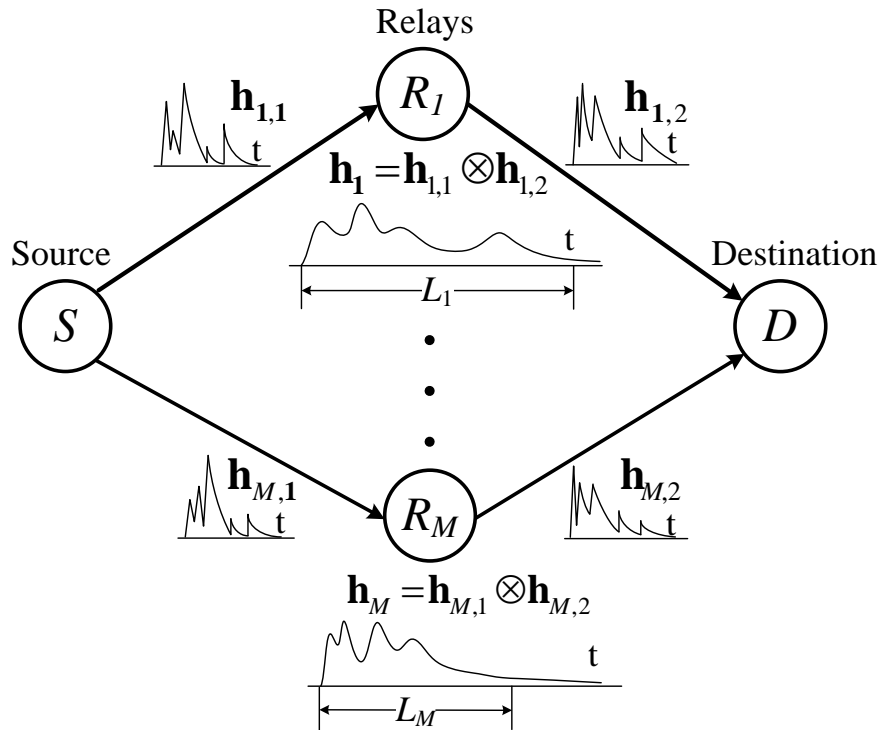
Figure 3.9: Cooperative multiple-relay system over accumulated multipath channels.

length of $\mathbf{h}_{i,m}$, $m = 1, \ldots, M$, $i = 1, 2$.

We assume that the source estimates the length of the overall reverse channel from the training symbols transmitted from D to S via R. Exploiting channel reciprocity, the source can then determine required GI length of the next frame transmitted to D and notices the destination with control signals. With the adaptive CP scheme, the CP length is dynamically chosen according to the end-to-end delay spread, i.e., $\mathcal{P} = (L_{m,1} + L_{m,2})$.

In OFDM systems, when the number of subchannels is sufficiently large, the signal in each subchannel is exposed to flat fading rather than frequency selective fading. Then, the frequency-domain received signal can be written as

$$R_k = H_{2,m,k}GH_{1,m,k}S_k + H_{2,m,k}GW_{1,m,k} + W_{2,m,k}, \tag{3.45}$$

where G is given by (3.10). Based on the availability of instantaneous channel state information, approximate bit error rate (BER) expression with the Rayleigh fading channel is given

by [2]

$$P_{b_m} \approx d \sum_{k=1}^{N} Q(\sqrt{a\gamma_{m,k}}), \tag{3.46}$$

where Q(·) represents the Gaussian Q function,

$$Q(x) = \frac{1}{\sqrt{2\pi}} \int_x^{\infty} e^{-t^2/2} dt, \tag{3.47}$$

$$a = \begin{cases} \frac{2}{\sigma^2} \sin^2\left(\frac{\pi}{\mathcal{M}}\right) & \text{for } \mathcal{M}\text{-PSK} \\ \frac{3}{\sigma^2(\mathcal{M}-1)} & \text{for } \mathcal{M}\text{-QAM} \end{cases}, \tag{3.48}$$

$$d = \begin{cases} \frac{\mathcal{M}-1}{\sum_{k=1}^{N} \log_2 \mathcal{M}} & \text{for } \mathcal{M}\text{-PSK} \\ \frac{4}{\sum_{k=1}^{N} \log_2 \mathcal{M}} \left(\frac{\sqrt{\mathcal{M}}-1}{\sqrt{\mathcal{M}}}\right) & \text{for } \mathcal{M}\text{-QAM} \end{cases}, \tag{3.49}$$

and $\gamma_{m,k}$ is the end-to-end SNR of the each subcarrier at the destination,

$$\begin{aligned} \gamma_{m,k} &= \mathbb{E}\left[\left|\frac{H_{m,2,k}GH_{m,1,k}S_k}{H_{2,m,k}GW_{1,m,k} + W_{2,m,k}}\right|^2\right] \\ &= \mathbb{E}\left[\frac{|H_{m,2,k}GH_{m,1,k}|^2 P_s}{(|H_{m,2,k}G|^2 + 1)\sigma_\omega^2}\right] \\ &= \frac{\gamma_{1,m,k}\gamma_{2,m,k}}{\gamma_{2,m,k} + C}, \end{aligned} \tag{3.50}$$

where $\sigma_\omega^2 = \sigma_1^2 = \sigma_2^2$, $\gamma_{i,m,k} = |H_{i,m,k}|^2 P_s/\sigma_\omega^2$, and $C = P_s/(|G|^2\sigma_\omega^2)$.

The performance of the relay system is not only affected by the end-to-end channel gain but also the transmission overhead. If a long CP is adopted, the effective data throughput at destination will decrease. To improved the system performance by considering both channel fading and delay spread, we defined a *normalized effective throughput* as the relay selection criterion. The effective normalized throughput is given as

$$\eta = \frac{N}{\mathcal{P} + N}(1 - P_b), \tag{3.51}$$

which represents the percentage of the effective data received correctly at destination in the total data (including effective data and overhead) transmitted by source.

When the delay spread increases, the CP length grows, therefore the throughput degrades; on the other hand, when the channel gain is severe, BER at destination will raise, then the throughput also degrades. In order to achieve the trade-off between the transmission reliability and efficiency, the best relay node, R_b is the one with maximum η, which can be formulated as

$$
\begin{aligned}
b &= \underset{m\in\{1,\ldots,M\}}{\arg\max} \quad \eta_m \\
&= \underset{m\in\{1,\ldots,M\}}{\arg\max} \quad \frac{N}{\mathcal{P}_m + N}(1 - P_{b_m}).
\end{aligned}
\tag{3.52}
$$

In Eq. (3.52), η_m depends on the overall subchannel conditions of the two-hop link via the mth relay. For OFDM systems, since the overall performance is limited by the subcarrier with the worst error probability, therefore, using the fact that

$$
P_b(\gamma_k) = dQ(\sqrt{a\gamma_k}) \propto \frac{1}{\gamma_k},
\tag{3.53}
$$

we obtain the following RS strategy

$$
b = \underset{m\in\{1,\ldots,M\}}{\arg\max} \quad \frac{N}{\mathcal{P}_m + N} \left(1 - P_b(\underset{k\in\{1,\ldots,N\}}{\min} \gamma_{m,k})\right).
\tag{3.54}
$$

After the best relay node b is determined, the GI length can be set corresponding to $(L_{1,b} + L_{2,b})$.

3.4.2 Performance Analysis

Assume that the b-th relay has the maximum effective throughput, $\eta_{\max} = \max\{\eta_1,\ldots,\eta_M\}$. Since each relaying link in the networks is independent, the cumulative distribution function (CDF) of $\eta_{\max}$ is given by

$$
P(\eta_{\max} \leq \eta) = \prod_{m=1}^{M} P(\eta_m \leq \eta).
\tag{3.55}
$$

From Eq. (3.54), we clearly have

$$
P_{b_m} \approx c \sum_{k=1}^{N} Q(\sqrt{a\gamma_{m,k}}) \geq c \sum_{k=1}^{N} Q\left(\sqrt{a \underset{k\in\{1,\ldots,N\}}{\min} \gamma_{m,k}}\right).
\tag{3.56}
$$

Therefore, the CDF of $\eta_{\max}$ can be written as

$$P(\eta_{\max} \leq \eta) \geq \prod_{m=1}^{M} P\left(\frac{N}{\mathcal{P}_m + N}(1 - P_{b_m}) \leq \eta\right). \tag{3.57}$$

We suppose that the end-to-end delay spread of relay channels, $\{L_1, \ldots, L_M\}$, are independent and identically distributed (i.i.d.) random variables which follow a log-normal distribution, i.e.,

$$\mathcal{P}_m = L_m \sim \frac{1}{x\sqrt{2\pi\sigma^2}} \exp\left(-\frac{(\ln x - \mu)^2}{2\sigma^2}\right), \tag{3.58}$$

where μ is the expectation of $\ln x$, and $\sigma^2 > 0$ is the variance of $\ln x$, then

$$\frac{\mathcal{P}_m + N}{N} \sim \frac{1}{x\sqrt{2\pi\sigma'^2}} \exp\left(-\frac{(\ln x - \mu')^2}{2\sigma'^2}\right), \tag{3.59}$$

where μ' and σ' satisfy the following equations,

$$\begin{cases} \frac{1}{N}e^{\mu + \frac{\sigma^2}{2}} + N = e^{\mu' + \frac{\sigma'^2}{2}} \\ \frac{1}{N^2}(e^{\sigma^2} - 1)e^{2\mu + \sigma^2} = (e^{\sigma'^2} - 1)e^{2\mu' + \sigma'^2} \end{cases}. \tag{3.60}$$

The CDF of $(\mathcal{P}_m + N)/N$ is given by

$$P\left(\frac{\mathcal{P}_m + N}{N} \leq x\right) = \frac{1}{2}\mathrm{erfc}\left(-\frac{(\ln x - \mu')^2}{2\sigma'^2}\right). \tag{3.61}$$

Since both $\frac{N}{\mathcal{P}_m+N}$ and $\frac{\eta}{1-P_{b_m}}$ are positive, Eq. (3.57) can be rewritten as

$$P(\eta_{\max} \leq \eta) \geq \left(P(\frac{\mathcal{P}_m + N}{N} \geq \frac{1 - P_{b_m}}{\eta})\right)^M. \tag{3.62}$$

We have

$$
\begin{aligned}
P\left(\frac{\mathcal{P}_m + N}{N} \geq \frac{1 - P_{b_m}}{\eta}\right) &= 1 - P\left(\frac{\mathcal{P}_m + N}{N} \leq D(\eta)\right) \\
&= 1 - \frac{1}{2}\text{erfc}\left(-\frac{(\ln D(\eta) - \mu')^2}{2\sigma'^2}\right) \\
&= 1 - Q\left(-\frac{(\ln D(\eta) - \mu')^2}{\sqrt{2}\sigma'^2}\right).
\end{aligned}
\tag{3.63}
$$

where $D(\eta) = \frac{1 - P_{b_m}}{\eta}$. The lower bonder of $P(\eta_{\max} \leq \eta)$ can be obtained as

$$
P(\eta_{\max} \leq \eta) \geq \left(1 - Q\left(-\frac{(\ln D(\eta) - \mu')^2}{\sqrt{2}\sigma'^2}\right)\right)^M.
\tag{3.64}
$$

With that $0 < Q(x) < 1$,

$$
0 < 1 - Q\left(-\frac{(\ln D(\eta) - \mu')^2}{\sqrt{2}\sigma'^2}\right) < 1.
\tag{3.65}
$$

From Eq. (3.64) and (3.65), when the number of available relay nodes M increases, the lower bonder of $P(\eta_{\max} \leq \eta)$ decreases, which impacts that the effective throughput improves.

Consider the following three cases:

1. σ^2 is large, i.e., $\sqrt{2}\sigma'^2 > 1$;

   If $\sqrt{2}\sigma'^2 > 1$, the value of $\left(1 - Q(-\frac{(\ln D(\eta) - \mu')^2}{\sqrt{2}\sigma'^2})\right)$ keeps low, because $\left(-\frac{(\ln D(\eta) - \mu')^2}{\sqrt{2}\sigma'^2}\right)$ approaches zero slowly. Therefore, the lower bonder of the effective throughput will drop quickly when M rises, and the improvement of the throughput is significant.

2. σ^2 is small, i.e., $\sqrt{2}\sigma'^2 \leq 1$;

   When $\sqrt{2}\sigma'^2 \leq 1$, $\left(-\frac{(\ln D(\eta) - \mu')^2}{\sqrt{2}\sigma'^2}\right)$ approaches zero quicker than that with $\sqrt{2}\sigma'^2 > 1$. Then the throughput gain will reduce.

3. σ^2 is tiny, i.e., $\sqrt{2}\sigma'^2 \to 0$.

   In the case with $\sqrt{2}\sigma'^2 \to 0$, the channel delay spread can be considered as a constant, hence the proposed RS scheme provides the same performance as the maximum end-to-end SNR RS scheme, i.e.,

$$
b = \arg\max_{m \in \{1,\dots,M\}} \min_{k \in \{1,\dots,N\}} \gamma_{m,k}.
\tag{3.66}
$$
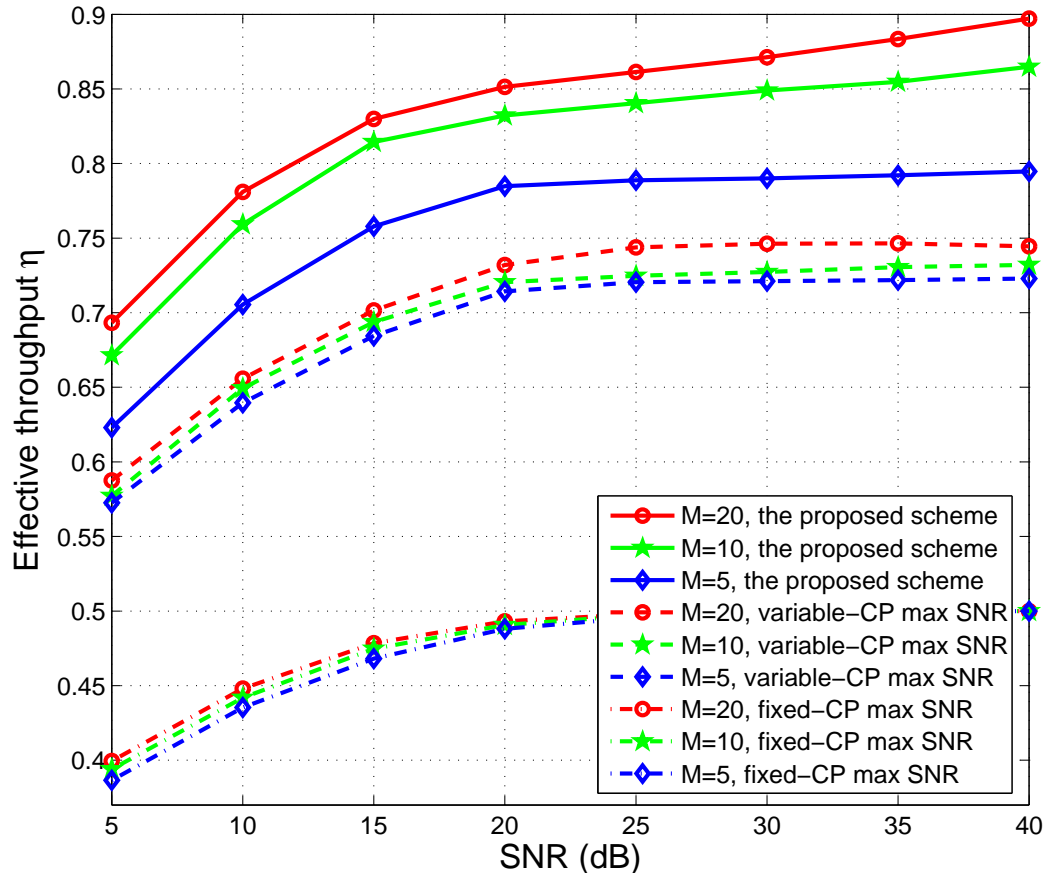
Figure 3.10: The average normalized effective throughput of different RS schemes for AF relay networks with variable channel length. The channel lengths is variable and follows the log-normal distribution, $\mu' = 4.5$ and $1/\sqrt{2} < \sigma^2$.

3.4.3 Simulation Results

In the simulations, we assume that the length of each channel, $L_{i,m}$, $i = 1, 2$, $m = 1, \ldots, M$, follows the same distribution given by (3.38). The CP length, $\mathcal{P}_m$, is adapted to $(L_{1,m} + L_{2,m})$. At destination, the zero forcing channel equalization with ideal channel response is performed.

We evaluate the normalized effective throughput of the proposed RS scheme, and compare it with that of the maximum end-to-end SNR selection schemes with variable/fixed-CP given by (3.66). The fixed CP length is decided to satisfy $CP_{\text{fix}} \geq \ln \mathcal{N}^{-1}(0.9|\mu, \sigma)$. Three different cases are considered: the variance of channel length is large, small and close to zero. The corresponding values of σ are $\sigma^2 > \frac{1}{\sqrt{2}}$, $0 < \sigma^2 < \frac{1}{\sqrt{2}}$ and $\sigma^2 \to 0$ respectively. In the three cases, we keep the same value of μ, i.e., $\mu \approx 4.5$.
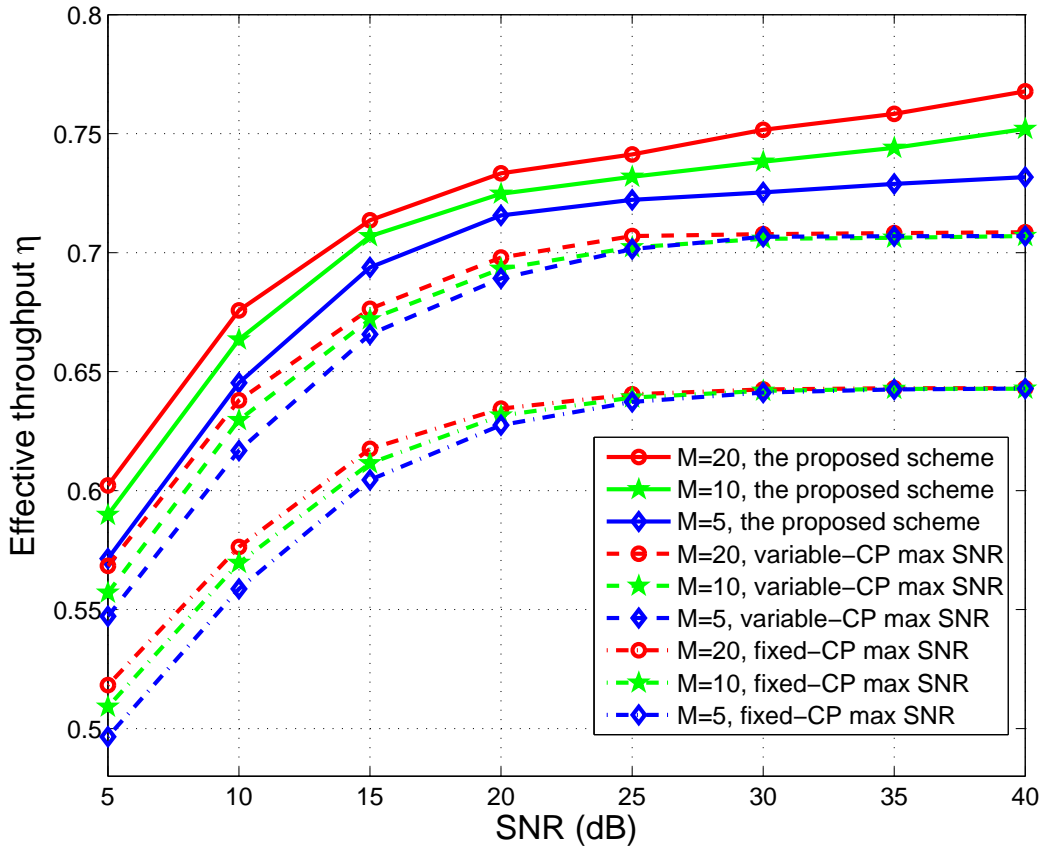
Figure 3.11: he average normalized effective throughput of different RS schemes for AF relay networks with variable channel length. The channel lengths is variable and follows the log-normal distribution, $\mu' = 4.5$ and $0 < \sigma^2 < 1/\sqrt{2}$.

For the case that the variance of channel length is large, we set $\frac{1}{\sqrt{2}} < \sigma^2 \approx 1$. Fig. 3.10 presents the normalized effective throughput of the proposed selection scheme and maximum end-to-end SNR scheme with variable/fixed CP. The throughput of the maximum SNR and proposed RS scheme grows when the number of available relay nodes increases because of the improvement of the end-to-end SNR. Compared to the maximum SNR RS scheme with variable CP, the proposed scheme provides a higher effective throughput by considering channel length as well as the end-to-end SNR. For the maximum SNR scheme with fixed CP, a large CP duration has to be chosen due to the wide variation range of the channel length. Therefore, the effective throughput of the fixed-CP maximum SNR scheme is significantly limited even with a high SNR. Moreover, the performance gain of the proposed scheme significantly increases when the available relay nodes become more. While the maximum end-to-end S-
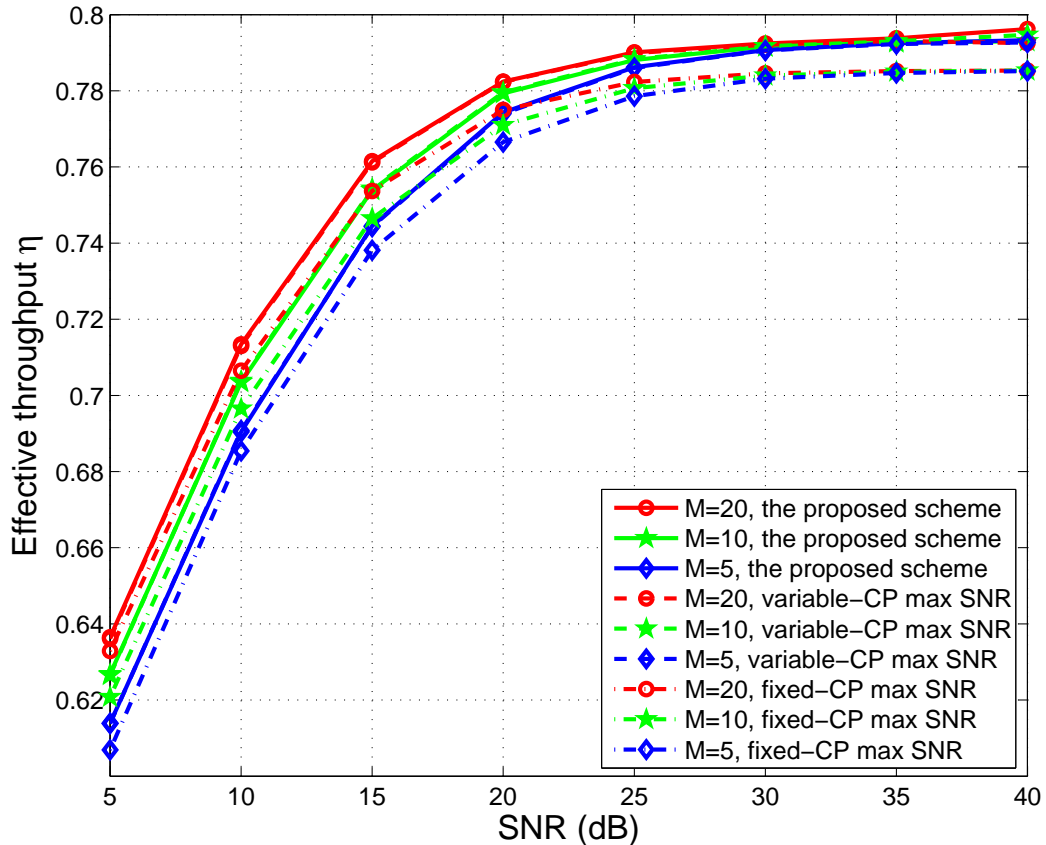
Figure 3.12: he average normalized effective throughput of different RS schemes for AF relay networks with variable channel length. The channel lengths is variable and follows the log-normal distribution, $\mu' = 4.5$ and $\sigma^2 \to 0$.

NR scheme with variable/fixed CP whose selection criterion only depends on SNR provides a slight improvement.

For the case that the variance of channel length is small, i.e., $0 < \sigma^2 < \frac{1}{\sqrt{2}}$, the channel length is varying in a smaller range than the case $\frac{1}{\sqrt{2}} < \sigma^2$. We set $\sigma = 0.28$. From the results in Fig. 3.11, the proposed scheme can achieve a higher throughput gain than the maximum end-to-end SNR scheme in this case. With the narrow variation range of channel length, the fixed-CP RS scheme can adopt a shorter CP duration, and consequently has a higher effective throughput than in the case with $\sigma^2 > \frac{1}{\sqrt{2}}$. However, the throughput of the maximum end-to-end SNR scheme with variable/fixed CP approaches to a constant when SNR increases, which implies that the maximum SNR scheme cannot obtain the throughput gain from the large SNR. While the throughput performance of the proposed scheme can keep growing with

SNR. Compared to the case with $\sigma^2 > \frac{1}{\sqrt{2}}$, the performance gain of the proposed RS strategy becomes lower, because the smaller variable range of channel length affects the activity of the proposed scheme.

For the third case that the variance of channel length $\psi = (e^{\sigma^2} - 1)e^{2\mu + \sigma^2} \rightarrow 0$, we have $\sigma^2 \rightarrow 0$. In this case, the channel length is little variable, and the proposed scheme become the maximum end-to-end SNR scheme. In the simulation, we set $\sigma' = 0.03$. Fig. 3.12 presents the effective throughput of the different relay selection schemes. As expected, the performances of the maximum end-to-end SNR and proposed schemes are the same. In this case, the fixed-CP maximum SNR scheme also exhibits similar throughput performance by choosing a relatively short CP duration. The performance gain provided by these schemes only shows in terms of the error probability rather than the throughput when the number of available relay nodes increases.

3.5   Summary

In this chapter, we have proposed two adaptive cooperative schemes for amplify-and-forward relay systems, i,e., the efficient adaptive guard interval scheme for single-relay systems and the relay selection scheme for multiple-relay systems with adaptive guard interval.

The novel adaptive guard interval (GI) scheme was proposed to solve the accumulation of multipath delay spread caused by multi-hop transmissions in AF relay systems. The GI was adapted to channel conditions and was replaced by a variable length orthogonal codes which can carry the GI length information. By exploiting the orthogonal property between different GI sequences, the destination detects GI length independently without an extra control signal. The corresponding receiver for the proposed system was designed by combining the GI length detection and equalization. The detection error is reduced by operating the detection over multiple symbols. The proposed adaptive GI scheme can achieve the same symbol error rate performance as the variable GI scheme with additional control signals. The adaptive GI scheme can address the variable delay spread in multi-hop AF relay systems, meanwhile compared to the fixed GI scheme, the transmission overhead was reduced.

For multiple-relay systems, the novel relay selection scheme was proposed to minimize the

overhead as well as enhance the overall transmission reliability. This scheme maximizes the end-to-end transmission efficiency by dynamically choosing the most suitable relay node and adapting the corresponding cyclic prefix length over variable-length multipath channels. We defined a normalized effective throughput as the selection criterion in the proposed strategy which depends on both the end-to-end channel gain and the accumulated delay spread. The performance of the proposed scheme is evaluated with different variances of the end-to-end channel lengths. When the variance is large, the effective throughput of the proposed scheme achieves increases significantly with the growing of the number of available relay nodes and signal-to-noise ratio (SNR). When the channel length is invariant, the proposed scheme provides the same performance as the maximum end-to-end SNR selection scheme.

The works in this chapter can be found in published research papers [155, 156].

Chapter 4

Resource Allocation for Two-Way Decode-and-Forward Relay Systems

4.1   Introduction

In two-way relay systems, the communication is bidirectional where the two terminals exchange information assisted by the relay node. Examples of two-way relay systems are when a mobile user communicates with the base station via a dedicated relay in a cellular system, or two mobile users exchange their data in a wireless local area networks (WLAN) via the access point. The relay scheme used in one-way communication systems can also be used for two-way relay systems, with some modifications [157]. A straightforward approach of a two-way relay system is to deploy two successive one-way relay schemes.

Practical relay systems typically avoid the interference between the received and retransmitted signals at any relay node by orthogonalizing these signals. Two common methods for orthogonal relay transmission are frequency division (FD) and time division (TD) where the available bandwidth or time frame, respectively, are shared. A simple way to perform FD or TD is to share the channel resource equally among hops. However, due to the path loss and fading effects, the capacity of these orthogonal channels are considerably different. Also, taking the mobility of the relay and terminal nodes into account, the channel fading is time-variant. Therefore, allocating transmission resources to the hops equally and statically will lead to the overall system capacity reduction.

The main goal of resource allocation for multihop relay systems is to maximize the end-to-end channel capacity or minimize the resource consumption by adaptively allocating the transmission resources, including time slots, frequency bandwidth and power consumption. In order to improve the system performance, many resource allocation schemes have been investigated in the literature, for the different scenarios of the relay networks [99, 101, 157–166]. However, the allocation schemes in previous work only aim to maximize the total end-to-end channel capacity, which implies the assumption that the traffic loads from the source to the destination and from the destination to the source are the same. However, this assumption is not practical at all. For different application, the traffic loads of down-link and up-link are asymmetric in most practical systems. For instance, the web browsing and online video service have dominant traffic volume in downlink direction [167–169]. The results of measured traffic statistics also shows that the traffic of down-link and up-link is significantly different in most practical cases [23–25]. Therefore, in two-way systems, the resource allocation algorithm without considering the asymmetric traffic loads leads to the fairness issue. Simply maximizing the total end-to-end capacity will result in the lopsided allocation of the resource, i.e., light traffic flows would obtain relatively excessive resource. On the other hand, forcing the two terminals with different traffic loads achieve the same capacity only according to the channel condition causes a problem such that the heavy traffic flows is deprived of resources and suffers low data rate. Meanwhile, the allocation scheme to achieve the equal capacity of two terminals does not take into account the notion that the two terminals might have different data rate requirements, eg., in the systems with service level differentiation or flexible billing mechanisms for different classes of users. Therefore, ignoring the asymmetric traffic in resource allocation lowers the overall quality of service of the relay network. For the bidirectional asymmetric traffic scenario, the traffic-load ratio between the two terminals should also be one of the factor to determine the resource allocation algorithm.

To this end, we propose two adaptive resource allocation schemes for two-way communications to improve the performance of the dual-hop relay systems. In the two allocation algorithms, transmission time, power and subcarriers are optimally allocated to maximize the end-to-end capacity of the two-way system under the capacity ratio constraint. In order to consider both the requirements of total end-to-end capacity and the capacity ratio between the
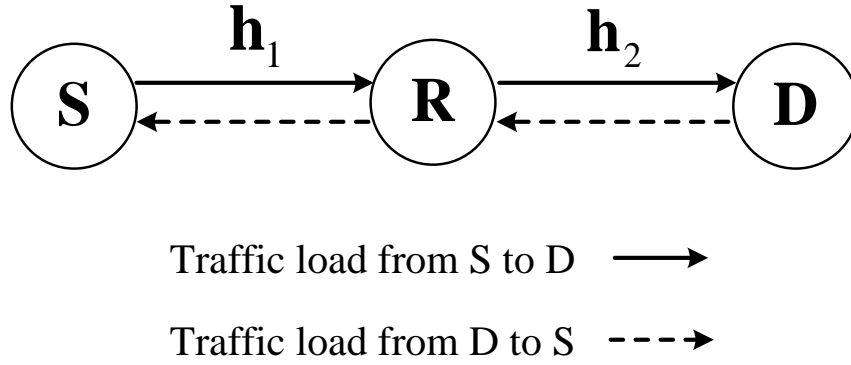
Figure 4.1: A two-way relay system.

forward and reverse links, a balanced end-to-end capacity is defined as the performance met-
ric. In these two schemes, the two-way communication is performed by time division and
frequency division respectively.

For the time division relay system, the total end-to-end capacity is maximized by optimiz-
ing the transmission time and power allocation subject to the capacity ratio and total transmis-
sion time/power constraints. For the frequency division system, which exploits the orthogo-
nality of the subcarriers, we optimize the subcarrier allocation, subcarrier power or time slot
to achieve the maximum balanced capacity. Since the allocation algorithm for the frequency
division scenario combines the subcarrier and power allocation together, the optimal solution
is extremely computationally complex to obtain and probibit it form practical implementation.
Therefore, we develop a low-complexity suboptimal approach which considers the fairness of
resource allocation, system efficiency as well as complexity. The suboptimal scheme separates
subcarrier allocation and time/power allocation to reduce the complexity. Simulation results
compare the performance of the suboptimal algorithm with the optimal one.

4.2   System Model

In this chapter, we consider a two-way relay system as shown in Fig. 4.1, which is composed
of a source node S, a destination node D and a relay node. It is assumed that there is no direct
link between the source and destination nodes. The communication between the source and the
destination is the two-way scenario. In one-way systems, the data signals are transmitted from

the source to the destination through the dual-hop link. While, in a two-way relay system, the source and the destination want to exchange information with each other with the help of a relay node. The two-way relaying models the communication scenario where the destination node also has some data to send to source node e.g. downlink and uplink in cellular communication, or packet acknowledgments in a wireless network.

The relay node operates in a half-duplex mode. To avoid interference, each hop is assigned an orthogonal channel. A straightforward approach to achieve two-way relaying is to deploy two successive one-way relaying schemes. Frequency division and time division are two common methods for orthogonal relay transmission. For the time division model, it requires four stages to accomplish the exchange of and symbols between the source and destination nodes in the same frequency bandwidth. And for the frequency division, two stages and two different frequency bandwidths are needed to execute the two-way transmission.

Denote that the traffic load from S to D is $\mathcal{L}_S$, and the traffic load from D to S is $\mathcal{L}_D$. The traffic load ratio between the forward and reverse transmission is defined as

$$\ell = \frac{\mathcal{L}_S}{\mathcal{L}_D}. \tag{4.1}$$

The multipath channels between S and R is denoted as $\mathbf{h}_1 = [h_1(0), h_1(1), \ldots, h_1(L_1 - 1)]$ and the channel between R and D is $\mathbf{h}_2 = [h_2(0), h_2(1), \ldots, h_2(L_2 - 1)]$, where L_i, $i = 1, 2$, is the channel length of $\mathbf{h}_i$. It is assumed that $h_i(l)$ are mutually independent complex random variables whose amplitude follow the same Rayleigh distribution, and the channels are reciprocal. The amplitude of $h_i(l)$ is modeled as a Rayleigh distribution with PDF

$$f_{|h_i(l)|}(x) = \frac{2x}{\Upsilon_{i,l}} \exp(-\frac{x^2}{\Upsilon_{i,l}}), \qquad x \geq 0, \tag{4.2}$$

where $\Upsilon_{i,l} = E[|h_i(l)|^2]$ is the power of the l-th tap of $\mathbf{h}_i$. The application of DFT represents a linear transformation of jointly Gaussian random variables and yields jointly Gaussian random variables [170]. Thus, the frequency response of each subchannel also has a Rayleigh fading distribution [171], i.e.,

$$f_{|H_{m,k}|}(y) = \frac{y}{2\Upsilon_{L_i}} \exp(-\frac{y^2}{4\Upsilon_{L_i}}), \qquad y \geq 0, \tag{4.3}$$

where $H_{i,k}$ is the frequency domain channel gain of k-th subchannel, $i = 1, 2$, and $\Upsilon_{L_i} = \sum_{l=0}^{L_i-1} \Upsilon_{i,l}$.

Since the DF relay scheme can provide flexible and adaptive communications for the source-relay and relay-destination links, we use the DF scheme at the relay node for retransmission. In the one-way DF relay protocol, the transmission starts with sending a source information to the selected relay node in the first phase. The received signals at the relay node can be expressed by

$$r_1(n) = \frac{1}{N} \sum_{k=0}^{N-1} R_{1,k} H_{1,k} e^{\frac{j2\pi nk}{N}} + \omega_1(n), \tag{4.4}$$

where $R_{1,k}$ is the frequency domain received signal at the relay node and $\omega_1(n)$ the AWGN term with variance N_{0_1}.

Unlike the AF relay, the DF mode can eliminate the additive noise and channel fading that accumulated in the relays. The relay node with the DF protocols is equipped with error detection and correction techniques. Therefore, in the second phase, the selected relay node detects, encodes, and retransmits the received signal to the destination node. The retransmitted signal at the relay node can be written as

$$y(n) = \hat{s}(n), \tag{4.5}$$

where $\hat{s}(n)$ is the regenerated signal at the relay node. $\hat{s}(n)$ will be the original source signal $s(n)$ with reasonable channel conditions under which all transmission errors between the source and relay are corrected by the error protection coding. Then, the received signal at the destination node can be written as

$$\mathbf{r}_2 = \mathbf{h}_2 \otimes \hat{\mathbf{s}} + \mathbf{w}_2, \tag{4.6}$$

where $\mathbf{r}_2 = \{r_2(n)\}$ is the time-domain received signals at the destination, $n = 0, 1, \ldots, N-1$, and

$$r_2(n) = \frac{1}{N} \sum_{k=0}^{N-1} \hat{S}_k H_{2,k} e^{\frac{j2\pi nk}{N}} + +\omega_2(n). \tag{4.7}$$

In a DF relay system, errors at the destination occur either when the S$\rightarrow$R transmission is received correctly and the R$\rightarrow$D transmission is received in error, or when the S$\rightarrow$R transmission is received in error and the R$\rightarrow$D transmission is received correctly. Hence, the end-to-end
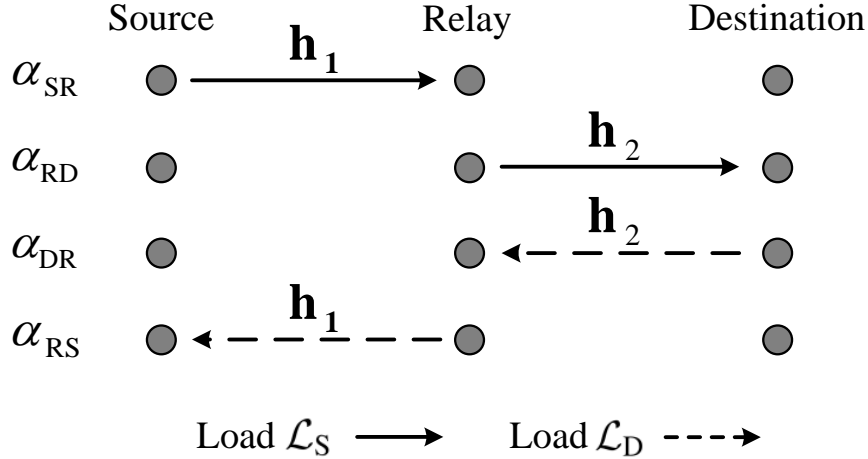
Figure 4.2: A two-way relay system with time-division model.

error probability of DF relay is given by

$$
\begin{aligned}
P_{\gamma_{DF}}&(\gamma|\bar{\gamma}_1, \bar{\gamma}_2) \\
&= (1 - P_{\rm e}(\gamma|\bar{\gamma}_1))P_{\rm e}(\gamma|\bar{\gamma}_2) + (1 - P_{\rm e}(\gamma|\bar{\gamma}_2))P_{\rm e}(\gamma|\bar{\gamma}_1) \\
&= P_{\rm e}(\gamma|\bar{\gamma}_1) + P_{\rm e}(\gamma|\bar{\gamma}_2) - 2P_{\rm e}(\gamma|\bar{\gamma}_1)P_{\rm e}(\gamma|\bar{\gamma}_2),
\end{aligned}
\tag{4.8}
$$

where $P_e(\gamma)$ is the error probability with SNR γ, and $\bar{\gamma}_i$ is the average SNR of the ith hop.

4.3 Resource Allocation for Two-Way Time-Division Relay Systems with Asymmetric Traffic

In this section, we consider a dual-hop two-way relay system as illustrated in Fig. 4.2 in which the two-way communication is accomplished by time-division model. All the nodes in the system are half-duplex in the same channel (within the same frequency bandwidth or the same time slot). To avoid interference without applying the network coding, the total transmission time are split into four time slots to perform two-way communications. Each hop is assigned a different time slot, and in each time slot all subcarriers of the OFDM system are used to transmit signals. In the first two time slots, S transmits its data to D with the participation of the relay node. During the third and forth time slot, the destination sends the data signals to the

source through the dual-hop relay link.

Denote the normalized time slot dedicated to each hop as

$$\vec{\alpha} = [\alpha_{SR}, \alpha_{RD}, \alpha_{DR}, \alpha_{RS}],$$

and

$$\alpha_{SR} + \alpha_{RD} + \alpha_{DR} + \alpha_{RS} = 1. \tag{4.9}$$

The instantaneous signal-to-noise ratio (SNR) of the k-th subcarrier of the hop between S and R in the first time slot is given by

$$\gamma_{SR,k} = \frac{P_{SR,k}|H_{1,k}|^2}{N_{0_1}}, \tag{4.10}$$

where $P_{SR,k}$ and N_{0_1} are the transmission power and the variance of the additive white Gaussian noise (AWGN) of the k-th subcarrier, respectively. The corresponding instantaneous Shannon's channel capacity in bit/second/Herz, c_{SR}, can be obtain as

$$c_{SR} = \frac{1}{N} \sum_{k=0}^{N-1} \log_2(1 + \gamma_{SR,k}). \tag{4.11}$$

The channel capacity of the links R→D, D→R and R→S in the other time slots, i.e., c_{RD}, c_{DR} and c_{RS}, can be similarly defined respectively. With DF protocol, the end-to-end capacity from S to D and from D to S are limited by the minimum per hop capacity, and they are given by

$$C_{SD} = \min(\alpha_{SR}c_{SR}, \alpha_{RD}c_{RD}), \tag{4.12}$$

and

$$C_{DS} = \min(\alpha_{DR}c_{DR}, \alpha_{RS}c_{RS}) \tag{4.13}$$

In related work, the resource allocation optimizes the total end-to-end capacity, i.e., (C_{SD} + C_{DS}), with the assumption that the traffic loads from S to D and from D to S are equal, i.e., $\mathcal{L}_S = \mathcal{L}_D$. However, for the two-way systems with asymmetric traffic loads, the transmission resources assigned to the forward and reverse links should be constrained by traffic load ratio

between S and D. Given the total transmission time and power, the optimal resource allocation of the time-dividing two-way relay systems is to dynamically determine the time slot and the subcarrier power for each hop adaptively to the instantaneous channel condition and the traffic loads. Hence, the allocation problem becomes

$$
\begin{aligned}
\max_{\{\vec{\alpha}, \underline{P_t}\}} \quad & C_{\mathrm{SD}} + C_{\mathrm{DS}} \\
\text{subject to} \quad & \frac{C_{\mathrm{SD}}}{C_{\mathrm{DS}}} = \ell \\
& \alpha_{\mathrm{SR}} + \alpha_{\mathrm{RD}} + \alpha_{\mathrm{DR}} + \alpha_{\mathrm{RS}} = 1, \\
& 0 \geq \alpha_{\mathrm{SR}}, \alpha_{\mathrm{RD}}, \alpha_{\mathrm{DR}}, \alpha_{\mathrm{RS}} \geq 1, \\
& \sum_{k=0}^{N-1} P_{\mathrm{SR},k} + \sum_{k=0}^{N-1} P_{\mathrm{RD},k} + \sum_{k=0}^{N-1} P_{\mathrm{DR},k} + \sum_{k=0}^{N-1} P_{\mathrm{RS},k} = P_{\mathrm{tot}}.
\end{aligned}
\tag{4.14}
$$

where $\underline{P_t} = \{P_{\mathrm{SR},k}, P_{\mathrm{DR},k}, P_{\mathrm{RD},k}, P_{\mathrm{RS},k}\}$, P_{tot} is the total transmission power used for one two-way relay communication, and $\frac{C_{\mathrm{SD}}}{C_{\mathrm{DS}}} = \ell$ is the capacity ratio constraint which guarantees the fair data rates of the two terminals.

To achieve the maximum total end-to-end capacity, both the time slot and subcarrier power need to be optimally allocated. Since the joint transmission time and power allocation is convex, which means that several combination of time slot and power allocations can provide the maximum total end-to-end capacity. Therefore, in the following sections, we will discuss the time slot and power allocation for the time-division two-way scenario respectively.

4.3.1 Time Slot Allocation for Two-Way TD Relay Systems

The time slot allocation is first investigated in this section. When the value of $\underline{P_t}$ is given, $\vec{\alpha}$ is optimized such that the total channel capacity from S to D and from D to S is maximized, i.e.,

$$
\begin{aligned}
\max_{\vec{\alpha}} \quad & C_{\mathrm{SD}} + C_{\mathrm{DS}} \\
\text{subject to} \quad & \frac{C_{\mathrm{SD}}}{C_{\mathrm{DS}}} = \ell, \\
& \alpha_{\mathrm{SR}} + \alpha_{\mathrm{RD}} + \alpha_{\mathrm{DR}} + \alpha_{\mathrm{RS}} = 1, \\
& 0 \leq \alpha_{\mathrm{SR}}, \alpha_{\mathrm{RD}}, \alpha_{\mathrm{DR}}, \alpha_{\mathrm{RS}} \leq 1.
\end{aligned}
\tag{4.15}
$$

In order to achieve the optimal total channel capacity, the end-to-end channel capacity from S to D and from D to S, i.e., C_{SD} and C_{DS}, need to be maximized respectively. Hence, we have

$$
\begin{cases}
\max\limits_{\{\alpha_{SR}, \alpha_{RD}\}} C_{SD} = \max\limits_{\{\alpha_{SR}, \alpha_{RD}\}} \min(\alpha_{SR} c_{SR}, \alpha_{RD} c_{RD}), \\
\max\limits_{\{\alpha_{DR}, \alpha_{RS}\}} C_{DS} = \max\limits_{\{\alpha_{DR}, \alpha_{RS}\}} \min(\alpha_{DR} c_{DR}, \alpha_{RS} c_{RS}).
\end{cases}
\tag{4.16}
$$

The solution of the *min-max* problems in (4.16) is that

$$
\begin{cases}
\alpha_{SR} c_{SR} = \alpha_{RD} c_{RD}, \\
\alpha_{DR} c_{DR} = \alpha_{RS} c_{RS}.
\end{cases}
\tag{4.17}
$$

Using (4.17) in the total time slot constraint, we have

$$
\frac{\alpha_{SR} c_{RD}}{c_{SR}} + \alpha_{RD} + \alpha_{DR} + \frac{\alpha_{DR} c_{DR}}{c_{RS}} = 1.
\tag{4.18}
$$

From (4.18), we can obtain that

$$
\alpha_{RD} = \frac{1 - \alpha_{RD}(1 + \frac{c_{DR}}{c_{RS}})}{1 + \frac{c_{RD}}{c_{SR}}}.
\tag{4.19}
$$

Moreover, according to the capacity ratio constrains, i.e.,

$$
\frac{C_{SD}}{C_{DS}} = \ell,
\tag{4.20}
$$

when (4.17) is satisfied, the capacity ratio constrain becomes that

$$
\frac{\alpha_{SR} c_{SR}}{\alpha_{RS} c_{RS}} = \frac{\alpha_{RD} c_{RD}}{\alpha_{DR} c_{DR}} = \ell.
\tag{4.21}
$$

Substituting (4.19) into (4.21), the value of α_{DR} can be figured out as

$$
\alpha_{DR} = \frac{1}{c_{DR}(\frac{\ell}{c_{SR}} + \frac{\ell}{c_{RD}} + \frac{1}{c_{RS}}) + 1},
\tag{4.22}
$$

and consequently, α_{SR}, α_{RD} and α_{RS} can be solved using (4.17),(4.18), and (4.21). The solution

of the optimization problem stated in (4.15) is

$$
\vec{\alpha} = \begin{bmatrix} \alpha_{\text{SR}} \\ \alpha_{\text{RD}} \\ \alpha_{\text{DR}} \\ \alpha_{\text{RS}} \end{bmatrix} = \begin{bmatrix} \dfrac{\ell}{c_{\text{SR}}(\frac{\ell}{c_{\text{RD}}} + \frac{1}{c_{\text{DR}}} + \frac{1}{c_{\text{RS}}}) + \ell} \\ \dfrac{\ell}{c_{\text{RD}}(\frac{\ell}{c_{\text{SR}}} + \frac{1}{c_{\text{DR}}} + \frac{1}{c_{\text{RS}}}) + \ell} \\ \dfrac{1}{c_{\text{DR}}(\frac{\ell}{c_{\text{SR}}} + \frac{\ell}{c_{\text{RD}}} + \frac{1}{c_{\text{RS}}}) + 1} \\ \dfrac{1}{c_{\text{RS}}(\frac{\ell}{c_{\text{SR}}} + \frac{\ell}{c_{\text{RD}}} + \frac{1}{c_{\text{DR}}}) + 1} \end{bmatrix}.
\tag{4.23}
$$

4.3.2 Power Allocation for Two-Way TD Relay Systems

In this section, the power allocation is considered for the two-way relay systems with asymmetric traffic loads. Here, it is assumed that the vector $\vec{\alpha}$ is given. Thus, $\underline{P_{\text{t}}} = \{P_{\text{SR},k}, P_{\text{DR},k}, P_{\text{RD},k}, P_{\text{RS},k}\}$ is optimized to maximize the total instantaneous end-to-end channel capacity under the capacity ratio ℓ and total transmission power P_{tot} constraints, i.e.,

$$
\begin{aligned}
\max_{\underline{P_{\text{t}}}} \quad & C_{\text{SD}} + C_{\text{DS}} \\
\text{subject to} \quad & \frac{C_{\text{SD}}}{C_{\text{DS}}} = \ell \\
& P_{\text{SR},k}, P_{\text{RD},k}, P_{\text{DR},k}, P_{\text{RS},k} \geq 0, \\
& \sum_{k=0}^{N-1} P_{\text{SR},k} + \sum_{k=0}^{N-1} P_{\text{RD},k} + \sum_{k=0}^{N-1} P_{\text{DR},k} + \sum_{k=0}^{N-1} P_{\text{RS},k} = P_{\text{tot}}.
\end{aligned}
\tag{4.24}
$$

Denote the total transmission power in each time slot as

$$
\sum_{k=0}^{N-1} P_{\text{SR},k} = \bar{P}_{\text{SR}},
$$

$$
\sum_{k=0}^{N-1} P_{\text{DR},k} = \bar{P}_{\text{DR}},
$$

$$
\sum_{k=0}^{N-1} P_{\text{RD},k} = \bar{P}_{\text{RD}},
$$

$$
\sum_{k=0}^{N-1} P_{\text{RS},k} = \bar{P}_{\text{RS}}.
$$

The optimization problem in (4.24) can be expressed by two optimization problems. One is to

allocates the subtotal power for each time slot , $\{\bar{P}_{SR}, \bar{P}_{RD}, \bar{P}_{DR}, \bar{P}_{RS}\}$, i.e.,

$$
\max_{\{\bar{P}_{SR}, \bar{P}_{DR}, \bar{P}_{RD}, \bar{P}_{RS}\}} \quad C_{SD} + C_{DS}
$$

$$
\text{subject to} \quad \frac{C_{SD}}{C_{DS}} = \ell,
$$

$$
\bar{P}_{SR}, \bar{P}_{DR}, \bar{P}_{RD}, \bar{P}_{RS} \geq 0,
$$

$$
\bar{P}_{SR} + \bar{P}_{DR} + \bar{P}_{RD} + \bar{P}_{RS} = P_{\text{tot}},
$$

(4.25)

Then, when the optimal allocation of the subtotal powers is figured out, the subcarrier power allocation is derived to maximized the instantaneous channel capacity of each hop, as

$$
\max_{P_{X,k}} \quad c_X = \frac{1}{N} \sum_{k=0}^{N-1} \log_2 \left(1 + \frac{P_{X,k} |H_{i,k}|^2}{N_{0_i}} \right)
$$

$$
\text{subject to} \quad P_{X,k} \geq 0,
$$

(4.26)

$$
\sum_{k=0}^{N-1} P_{X,k} = \bar{P}_X,
$$

where c_X is c_{SR}, c_{DR}, c_{RD} or c_{RS}, the $P_{X,k}$ and $\rho_{X,k}$ are the corresponding power and selection indicator of the k-th subcarrier, $\bar{P}_X$ is the subtotal power of $P_{X,k}$, and $i = 1, 2$.

The optimization problem in (4.26) is equivalent to finding the maximum of the following cost function

$$
\mathcal{L}(P_{X,k}, \lambda_X) = \sum_{k=0}^{N-1} \log_2 \left(1 + \frac{P_{X,k} |H_{i,k}|^2}{N_{0_i}} \right) + \lambda_X \left(\sum_{k=0}^{N-1} P_{X,k} - \bar{P}_X \right),
$$

(4.27)

where λ_X is the Lagrangian multipliers. Differentiate with respect to $P_{X,k}$ and set each derivative to zero to obtain

$$
\frac{\partial \mathcal{L}}{\partial P_{X,k}} = \frac{1}{\ln 2} \frac{1}{1 + \frac{P_{X,k} |H_{i,k}|^2}{N_{0_1}}} \frac{|H_{i,k}|^2}{N_{0_i}} + \lambda_X
$$

$$
= \frac{1}{\ln 2} \frac{|H_{i,k}|^2}{N_{0_1} + P_{X,k} |H_{1,k}|^2} + \lambda_X
$$

$$
= 0.
$$

(4.28)

Denote that $|H_{X,\min}|$ is the minimum channel gain, and $P_{X,\min}$ is the corresponding power of the subchannel $H_{X,\min}$. Then, we can be obtained that

$$\frac{\partial \mathcal{L}}{\partial P_{X,k}} = \frac{\partial \mathcal{L}}{\partial P_{X,\min}} = 0, \quad k = 0, \ldots, N-1. \tag{4.29}$$

Therefore, the relationship between $P_{X,k}$ and $P_{X,\min}$ can be found out as

$$\frac{1}{N \ln 2} \frac{1}{1 + \frac{P_{X,k}|H_{i,k}|^2}{N_{0_1}}} \frac{|H_{i,k}|^2}{N_{0_i}} + \lambda_X = \frac{1}{N \ln 2} \frac{1}{1 + \frac{P_{X,\min}|H_{i,k}|^2}{N_{0_1}}} \frac{|H_{i,k}|^2}{N_{0_i}} + \lambda_X. \tag{4.30}$$

From (4.30), we have

$$P_{X,k} = P_{X,\min} + N_{0_i} \frac{|H_{i,k}|^2 - |H_{i,\min}|^2}{|H_{i,k}|^2 |H_{i,\min}|^2}. \tag{4.31}$$

The equation (4.31) shows that every subcarrier power in $\{P_{X,k}\}$, expect $P_{X,\min}$, can be descripted by $P_{X,\min}$, $H_{i,\min}$ and $H_{i,k}$. Based on this, $\bar{P}_X$ can be expressed as

$$\begin{aligned}
\bar{P}_X &= \sum_{k=0}^{N-1} P_{X,k} \\
&= N P_{X,\min} + N_{0_i} \sum_{k \neq \min} \frac{|H_{i,k}|^2 - |H_{i,\min}|^2}{|H_{i,k}|^2 |H_{i,\min}|^2},
\end{aligned} \tag{4.32}$$

and the channel capacity of each time slot can be rewritten as

$$\begin{aligned}
c_X &= \frac{1}{N} \sum_{k=0}^{N-1} \log_2 \left(1 + \frac{P_{X,k}|H_{i,k}|^2}{N_{0_i}} \right) \\
&= \frac{1}{N} \log_2 \prod_{k=0}^{N-1} \left(1 + \frac{P_{X,k}|H_{i,k}|^2}{N_{0_i}} \right) \\
&= \frac{1}{N} \log_2 \left(\left(1 + \frac{P_{X,\min}|H_{i,\min}|^2}{N_{0_i}} \right) \prod_{k \neq \min} \left(1 + \frac{P_{X,k}|H_{i,k}|^2}{N_{0_i}} \right) \right).
\end{aligned} \tag{4.33}$$

Using $P_{X,\min}$ to express $P_{X,k}$ from (4.31), we can obtained that

$$
\begin{aligned}
1 + \frac{P_{X,k}|H_{i,k}|^2}{N_{0_i}} &= 1 + P_{X,\min}\frac{|H_{i,k}|^2}{N_{0_i}} + \frac{|H_{X,k}|^2 - |H_{X,\min}|^2}{|H_{X,\min}|^2} \\
&= \frac{P_{X,\min}|H_{i,k}|^2}{N_{0_i}} + \frac{|H_{i,k}|^2}{|H_{i,\min}|^2} \\
&= \left(\frac{P_{X,\min}|H_{i,k}|^2}{N_{0_i}} + 1\right)\frac{|H_{i,k}|^2}{|H_{i,\min}|^2}.
\end{aligned}
\tag{4.34}
$$

Then, (4.33) can be given by

$$
\begin{aligned}
c_X &= \frac{1}{N}\log_2\left(\left(1 + \frac{P_{X,\min}|H_{i,\min}|^2}{N_{0_i}}\right)\prod_{k\neq\min}\left(1 + \frac{P_{X,k}|H_{i,k}|^2}{N_{0_i}}\right)\right) \\
&= \frac{1}{N}\log_2\left(\left(1 + \frac{P_{X,\min}|H_{i,\min}|^2}{N_{0_i}}\right)\prod_{k\neq\min}\left(\left(1 + \frac{P_{X,\min}|H_{i,k}|^2}{N_{0_i}}\right)\frac{|H_{i,k}|^2}{|H_{i,\min}|^2}\right)\right) \\
&= \frac{1}{N}\log_2\left(\left(1 + \frac{P_{X,\min}|H_{i,\min}|^2}{N_{0_i}}\right)^N\prod_{k\neq\min}\frac{|H_{i,k}|^2}{|H_{i,\min}|^2}\right) \\
&= \log_2\left(1 + \frac{P_{X,\min}|H_{i,\min}|^2}{N_{0_i}}\right) + \frac{1}{N}\sum_{k\neq\min}\log_2\frac{|H_{i,k}|^2}{|H_{i,\min}|^2}.
\end{aligned}
\tag{4.35}
$$

Moreover, using the relationship between $\bar{P}_X$ and $P_{X,\min}$ in (4.32), we have that

$$
\begin{aligned}
1 + \frac{P_{X,\min}|H_{i,\min}|^2}{N_{0_i}} &= 1 + \frac{1}{N}\left(\bar{P}_X - N_{0_i}\sum_{k\neq\min}\frac{|H_{i,k}|^2 - |H_{i,\min}|^2}{|H_{i,k}|^2|H_{i,\min}|^2}\right)\frac{|H_{i,\min}|^2}{N_{0_i}} \\
&= 1 + \frac{\bar{P}_X|H_{i,\min}|^2}{NN_{0_i}} - \sum_{k\neq\min}\frac{|H_{i,k}|^2 - |H_{i,\min}|^2}{N|H_{i,k}|^2}
\end{aligned}
\tag{4.36}
$$

By substituting (4.36) into (4.35), the channel capacity of each time slot can be expressed as

$$
c_X = \log_2\left(1 + \frac{\bar{P}_X|H_{i,\min}|^2}{NN_{0_i}} - \sum_{k\neq\min}\frac{|H_{i,k}|^2 - |H_{i,\min}|^2}{N|H_{i,k}|^2}\right) + \frac{1}{N}\sum_{k\neq\min}\log_2\frac{|H_{i,k}|^2}{|H_{i,\min}|^2}
\tag{4.37}
$$

To optimize the subtotal power in each time slot, $\{\bar{P}_{SR}, \bar{P}_{RD}, \bar{P}_{DR}, \bar{P}_{RS}\}$, we have

$$
\begin{aligned}
\max_{\{\bar{P}_{SR}, \bar{P}_{DR}, \bar{P}_{RD}, \bar{P}_{RS}\}} \quad & \min(c_{SR}, c_{RD}) + \min(c_{DR}, c_{RS}) \\
\text{subject to} \quad & \frac{\min(c_{SR}, c_{RD})}{\min(c_{DR}, c_{RS})} = \ell, \\
& \bar{P}_{SR}, \bar{P}_{DR}, \bar{P}_{RD}, \bar{P}_{RS} \geq 0, \\
& \bar{P}_{SR} + \bar{P}_{DR} + \bar{P}_{RD} + \bar{P}_{RS} = P_{\text{tot}}.
\end{aligned}
\tag{4.38}
$$

The optimal solution of the max-min problem in (4.38) can be given by

$$
\begin{cases}
c_{SR} = c_{RD}, \\
c_{DR} = c_{RS}.
\end{cases}
\tag{4.39}
$$

Rewrite (4.39) by using (4.37) as

$$
\begin{aligned}
& \log_2\left(1 + \frac{\bar{P}_{SR}|H_{1,\min}|^2}{NN_{0_1}} - \sum_{k\neq\min} \frac{|H_{1,k}|^2 - |H_{1,\min}|^2}{N|H_{1,k}|^2}\right) + \frac{1}{N}\sum_{k\neq\min} \log_2 \frac{|H_{1,k}|^2}{|H_{1,\min}|^2} \\
& = \log_2\left(1 + \frac{\bar{P}_{RD}|H_{2,\min}|^2}{NN_{0_2}} - \sum_{k\neq\min} \frac{|H_{2,k}|^2 - |H_{2,\min}|^2}{N|H_{2,k}|^2}\right) + \frac{1}{N}\sum_{k\neq\min} \log_2 \frac{|H_{2,k}|^2}{|H_{2,\min}|^2}
\end{aligned}
\tag{4.40}
$$

and

$$
\begin{aligned}
& \log_2\left(1 + \frac{\bar{P}_{DR}|H_{2,\min}|^2}{NN_{0_2}} - \sum_{k\neq\min} \frac{|H_{2,k}|^2 - |H_{2,\min}|^2}{N|H_{2,k}|^2}\right) + \frac{1}{N}\sum_{k\neq\min} \log_2 \frac{|H_{2,k}|^2}{|H_{2,\min}|^2} \\
& = \log_2\left(1 + \frac{\bar{P}_{RS}|H_{1,\min}|^2}{NN_{0_1}} - \sum_{k\neq\min} \frac{|H_{1,k}|^2 - |H_{1,\min}|^2}{N|H_{1,k}|^2}\right) + \frac{1}{N}\sum_{k\neq\min} \log_2 \frac{|H_{1,k}|^2}{|H_{1,\min}|^2}
\end{aligned}
\tag{4.41}
$$

Adding the capacity ratio and total transmission power constraints

$$
\frac{c_{SR}}{c_{RS}} = \frac{c_{RD}}{c_{DR}} = \ell,
\tag{4.42}
$$

$$
\bar{P}_{SR} + \bar{P}_{DR} + \bar{P}_{RD} + \bar{P}_{RS} = P_{\text{tot}},
\tag{4.43}
$$

the optimal $\{\bar{P}_{SR}, \bar{P}_{RD}, \bar{P}_{DR}, \bar{P}_{RS}\}$ then can be solved from (4.40),(4.41),(4.42) and (4.43).

Once the subtotal power for each hop, $\{\bar{P}_{SR}, \bar{P}_{DR}, \bar{P}_{RS}, \bar{P}_{RD}\}$, is figured out, the power allo-

cated to the subchannel with the lowest channel gain of each hop can be determined by

$$\frac{\partial \mathcal{L}}{\partial P_{X,\min}} = \frac{1}{\ln 2} \frac{1}{1 + \rho_{X,k} \frac{P_{X,k}|H_{i,k}|^2}{N_{0_i}}} \frac{|H_{i,k}|^2}{N_{0_i}} + \lambda_X$$
$$= 0. \tag{4.44}$$

The solution is given by

$$P_{X,\min} = \left[\frac{1}{\lambda_X} - \frac{N_{0_i}}{|H_{i,\min}|^2}, \right]^\dagger \tag{4.45}$$

where $[\cdot]^\dagger = \max(\cdot, 0)$. Then, the rest subcarrier power allocation in each hop can be calculated by

$$P_{X,k} = P_{X,\min} + N_{0_i} \frac{|H_{i,k}|^2 - |H_{i,\min}|^2}{|H_{i,k}|^2 |H_{i,\min}|^2}. \tag{4.46}$$

Equation (4.46) which gives the power distribution on the k-th subchannel for each the hop shows that more power will be put into the subchannels with higher channel-to-noise ratio. This is the water-filling algorithm [172] in frequency domain.

4.3.3   Simulation Results

In this section, we verify the proposed resource allocation schemes by computer simulations and compare their performance with various allocation schemes, for different scenarios. One of performance metrics adopted here is the balanced end-to-end capacity, which is defined as

$$C_b = \min(C_{SD}, \ell C_{DS}). \tag{4.47}$$

We adopt this metric instead of the total end-to-end capacity, $C_{SD} + C_{DS}$, for the two-way relay system with asymmetric loads, because this parameter not only shows how large the total end-to-end capacity is, but also shows how close the capacity ratio is to the required one. Therefore, the balanced end-to-end capacity reflects both the requirements of maximizing the total end-to-end channel capacity and minimizing the difference between the actual and the required capacity ratio. The other metric defined to evaluated the performance of resource allocation
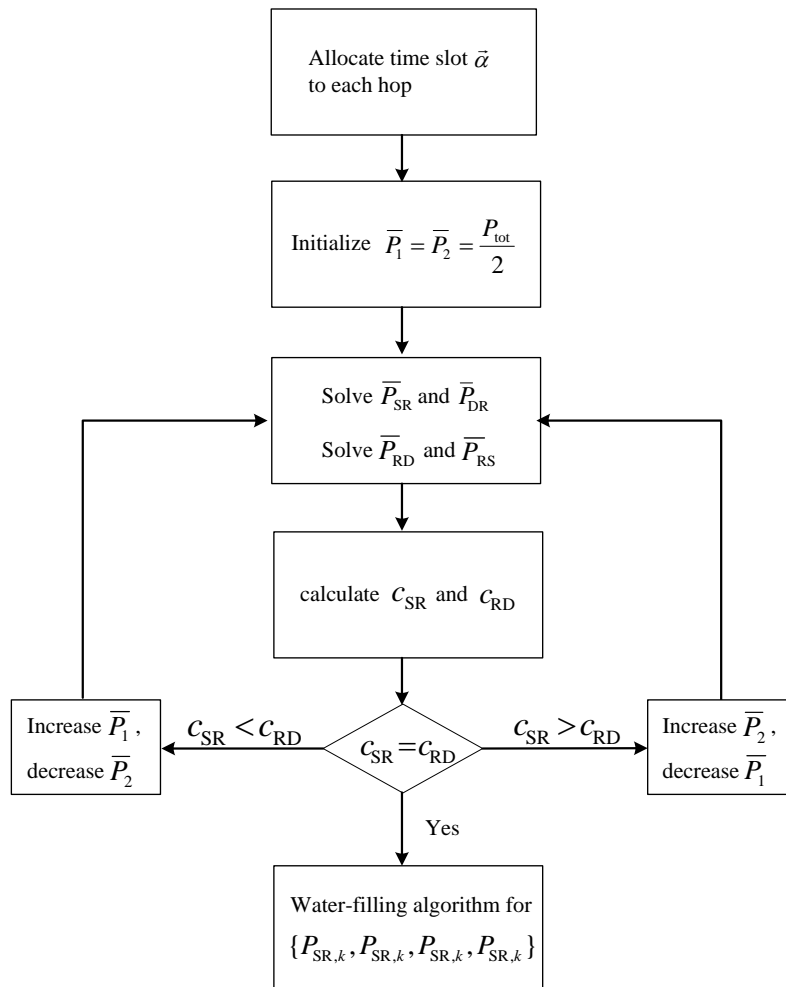
Figure 4.3: Illustration of the proposed time slot and power allocation algorithm.

algorithms is the capacity gain, which is defined as

$$\mathcal{G} = \frac{C_{\text{opt}} - C}{C}, \tag{4.48}$$

where C_{opt} is the optimal achievable end-to-end capacity of the system, and C is the practical end-to-end capacity based on a certain resource allocation scheme. This parameter shows how the proposed optimal allocation algorithm outperforms other allocation schemes.

Denote that the average SNRs of each hop are

$$\bar{\gamma}_1 = \frac{\mathbb{E}[|H_{k,1}|^2]}{N_{0_1}}, \qquad (4.49)$$

$$\bar{\gamma}_2 = \frac{\mathbb{E}[|H_{k,2}|^2]}{N_{0_2}}. \qquad (4.50)$$

The optimal allocation algorithm is calculated numerically which is implemented as the flow shown in Fig. 4.3. The computer simulation results are obtained by $100,000$ independent Monte Carlo runs of the network.

Time slot allocation

In this part, we assume that the subcarrier power of each hop is given, i.e., $P_{SR,k} = P_{RD,k} = P_{DR,k} = P_{RS,k} = 1$, then with the channel reciprocity, we have

$$c_1 = c_{SR} = c_{RS} = \frac{1}{N}\sum_{k=1}^{N}\log_2\left(1 + \frac{|H_{1,k}|^2}{N_{0_1}}\right), \qquad (4.51)$$

$$c_2 = c_{RD} = c_{DR} = \frac{1}{N}\sum_{k=1}^{N}\log_2\left(1 + \frac{|H_{2,k}|^2}{N_{0_2}}\right). \qquad (4.52)$$

In order to evaluate the performance of the proposed time slot allocation scheme, we compare it with two different allocation schemes. A simple method to perform two-way relay communications is equally sharing the transmission time in each hop. The end-to-end channel capacity from S to D and from D to S are then given by

$$C_{SD} = C_{DS} = \frac{1}{4}\min(c_1, c_2). \qquad (4.53)$$

Another allocation scheme we considered here is the random allocation scheme, where the normalized time slot of each hop, $\{\alpha_{SR}, \alpha_{RD}, \alpha_{DR}, \alpha_{RS}\}$, is random selected.

The average balanced end-to-end capacity of the proposed optimal time slot allocation scheme is compared with that of equal and random schemes in Fig. 4.4, where the average SNRs of the hops S−−R and R−−D are equal, i.e., $\bar{\gamma} = \bar{\gamma}_1 = \bar{\gamma}_2 =15$, 25dB. In this figure, the balanced capacity of the equal allocation keeps constant when the capacity ratio is varying,

Figure 4.4: Average balanced end-to-end capacities of different time slot allocation schemes vs. ℓ. $\bar{\gamma} = \bar{\gamma}_1 = \bar{\gamma}_2 = 15, 25$dB.

because the time slot assigning in this scheme is fixed without considering the instantaneous channel condition and traffic loads. Compared to the optimal allocation, when the traffic loads are equal, i.e., $\ell = 1$, the equal and optimal allocation have a very similar balanced capacity, but when ℓ grows, the optimal one significantly outperforms the equal one. Moreover, the balanced capacities of the optimal and random allocation algorithms are increasing when the capacity ratio rises. However, the proposed optimal scheme can provide a much higher balanced capacity than the random one under different average SNRs, because the required capacity ratio can not be satisfied all the time in the random algorithm. On the other hand, the proposed scheme considers both the channel condition and the asymmetric traffic loads at the same time, therefore, it exhibits the best performance in the three algorithms.

Figure 4.5: Average balanced end-to-end capacities of different time slot allocation schemes vs. ℓ. $\bar{\gamma}_1 + \bar{\gamma}_2 =$30dB.

In Fig. 4.5, The average balanced end-to-end capacities of different allocation schemes are compared under the scenario that the average SNR of each hop is different. Tow cases are considered, i.e., $\bar{\gamma}_1 = 2\bar{\gamma}_2 = 20$dB and $\bar{\gamma}_1 = 4\bar{\gamma}_2 = 24$dB. Similarly to the results in Fig. 4.4, the balanced capacity of equal allocation is constant, while that of the optimal and random schemes grows with the increasing of the capacity ratio. Besides, the random allocation suffers the similar low balanced capacity in both scenarios due to the blind selection of the time slot for each hop. The performances of optimal and equal algorithms are affected by different average SNRs of the two-hop channels. When the difference between $\bar{\gamma}_1$ and $\bar{\gamma}_2$ increases, i.e., $\frac{\bar{\gamma}_1}{\bar{\gamma}_2}$ becomes large, the balanced end-to-end capacities of optimal and equal allocations decrease.
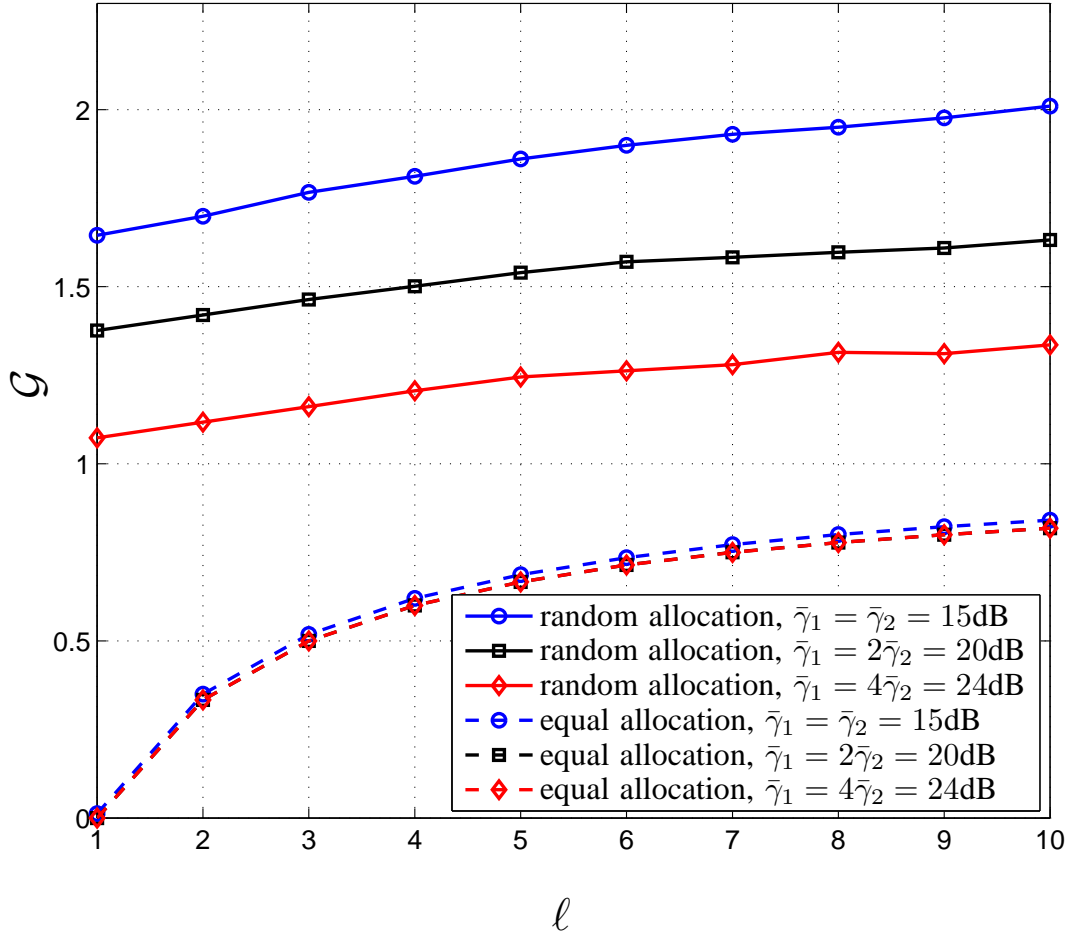
Figure 4.6: Average capacity gain of the optimal time slot allocation compared to different schemes vs. ℓ. $\bar{\gamma}_1 + \bar{\gamma}_2 = 30$dB.

It happens because the end-to-end capacity is limited by the worse channel in the two hops when only the time slot can be adaptively assigned. Although, the proposed optimal algorithm provides the significant performance gains compared to the equal and random schemes in both scenarios.

In Fig. 4.6, we present the capacity gains between the optimal and the other algorithms with different required capacity ratios and average SNRs. Comparing the random allocation scheme to the optimal one, the capacity gain is always higher than 1, which means the balanced capacity of the optimal allocation is at least twice as large as that of the random one. When the average SNRs of the hops are equal, i.e., $\bar{\gamma}_1 = \bar{\gamma}_2 = 15$dB , the performance gain of the optimal algorithm compared to the random time slot allocation is highest. While, compared to

the equal one, the capacity gains of different scenario are very similar, and are lower than that of random allocation. In additional, in all cases, the capacity gains grow when ℓ increases. It implies that the proposed allocation scheme can provide higher balanced end-to-end capacity than both the equal and random schemes when the traffic loads in two-way relay systems are asymmetric.

Power allocation

We then evaluate the performance of the proposed power allocation scheme by comparing it with random and equal power allocation schemes. Here, we assume that the time slot of each hop is the same and normalizes to 1, and the total available transmit power, P_{tot} is 1W. For the equal power allocation algorithm, the subtotal power of each hop is equal, i.e.,

$$\bar{P}_{\text{SR}} = \bar{P}_{\text{RD}} = \bar{P}_{\text{DR}} = \bar{P}_{\text{RS}} = \frac{1}{4} P_{\text{tot}}, \tag{4.54}$$

and the subcarrier power is calculated by using waterfilling algorithm as

$$P_{\text{X},k} = \left[\frac{1}{\lambda_{\text{X}}} - \frac{N_0}{|H_{i,k}|^2} \right]^{\dagger}, \tag{4.55}$$

where λ_{X} is a constant which satisfied that $\sum_{k=0}^{N-1} P_{\text{X},k} = \bar{P}_{\text{X}}$. In random power allocation scheme, $\{\bar{P}_{\text{SR}}, \bar{P}_{\text{RD}}, \bar{P}_{\text{DR}}, \bar{P}_{\text{RS}}\}$, are random value and satisfy the total power constrain, i.e.

$$\bar{P}_{\text{SR}} + \bar{P}_{\text{RD}} + \bar{P}_{\text{DR}} + \bar{P}_{\text{RS}} = P_{\text{tot}}. \tag{4.56}$$

Fig. 4.7 shows the average balanced end-to-end capacities of the proposed optimal, equal and random power allocation schemes, where the average SNRs of the hops S−−R and R−−D are equal, i.e., $\bar{\gamma} = \bar{\gamma}_1 = \bar{\gamma}_2 = 15, 25$dB. In both cases, the balanced capacity of the optimal power allocation increases when the capacity ratio ℓ is growing, while the capacity of equal power allocations keep constant. With $\bar{\gamma} = 15$dB, the random scheme has the same constant capacity with the equal one. With $\bar{\gamma} = 25$dB, the capacity of random algorithm is slight lower than that of equal scheme, and the difference is relatively large when $\ell < 3$. Moreover, the optimal allocation significantly outperforms the equal and random one with both $\bar{\gamma} = 15$ and
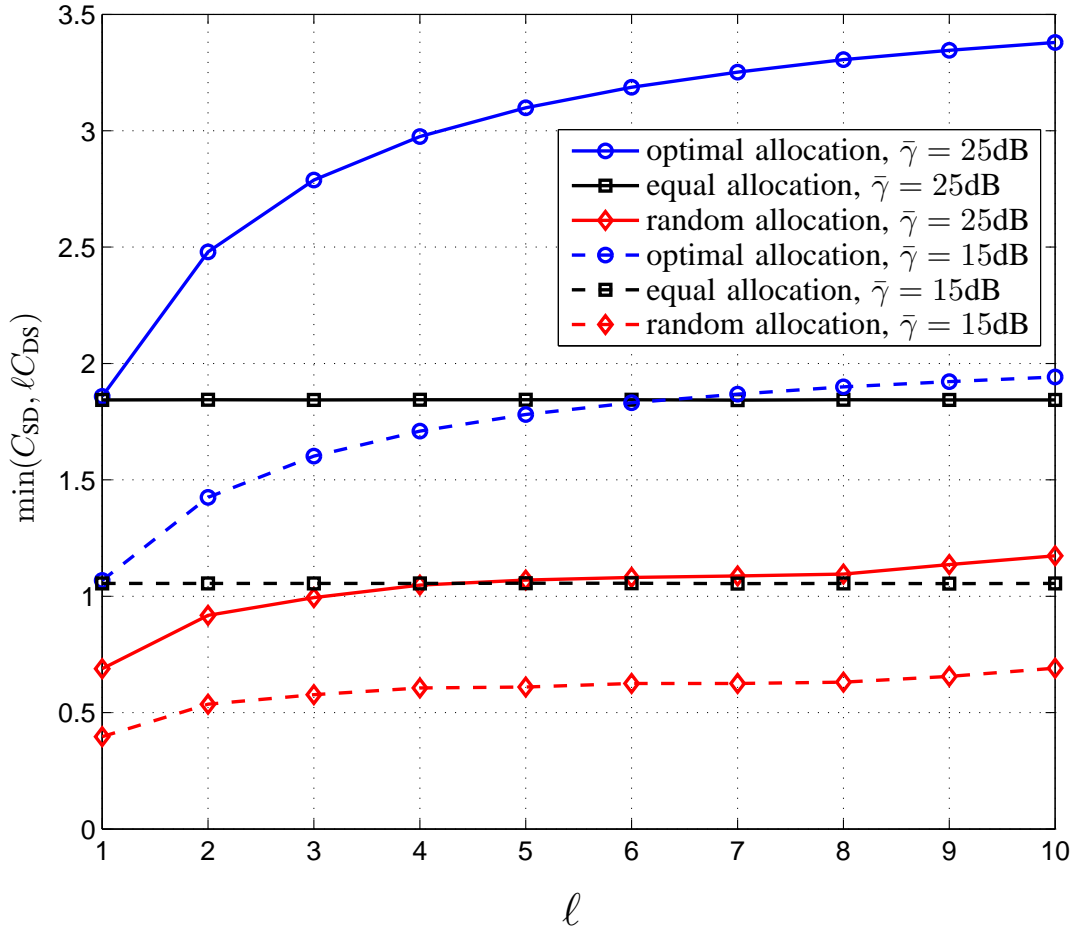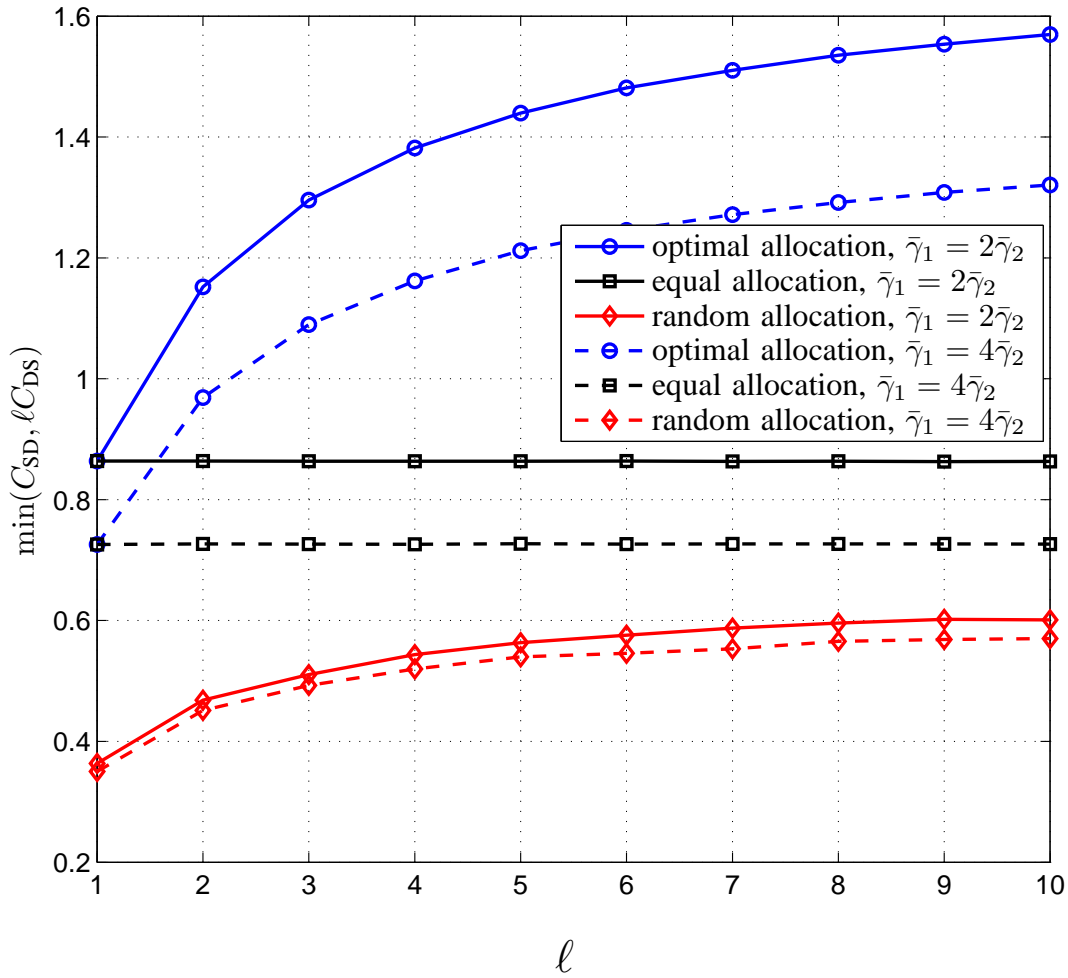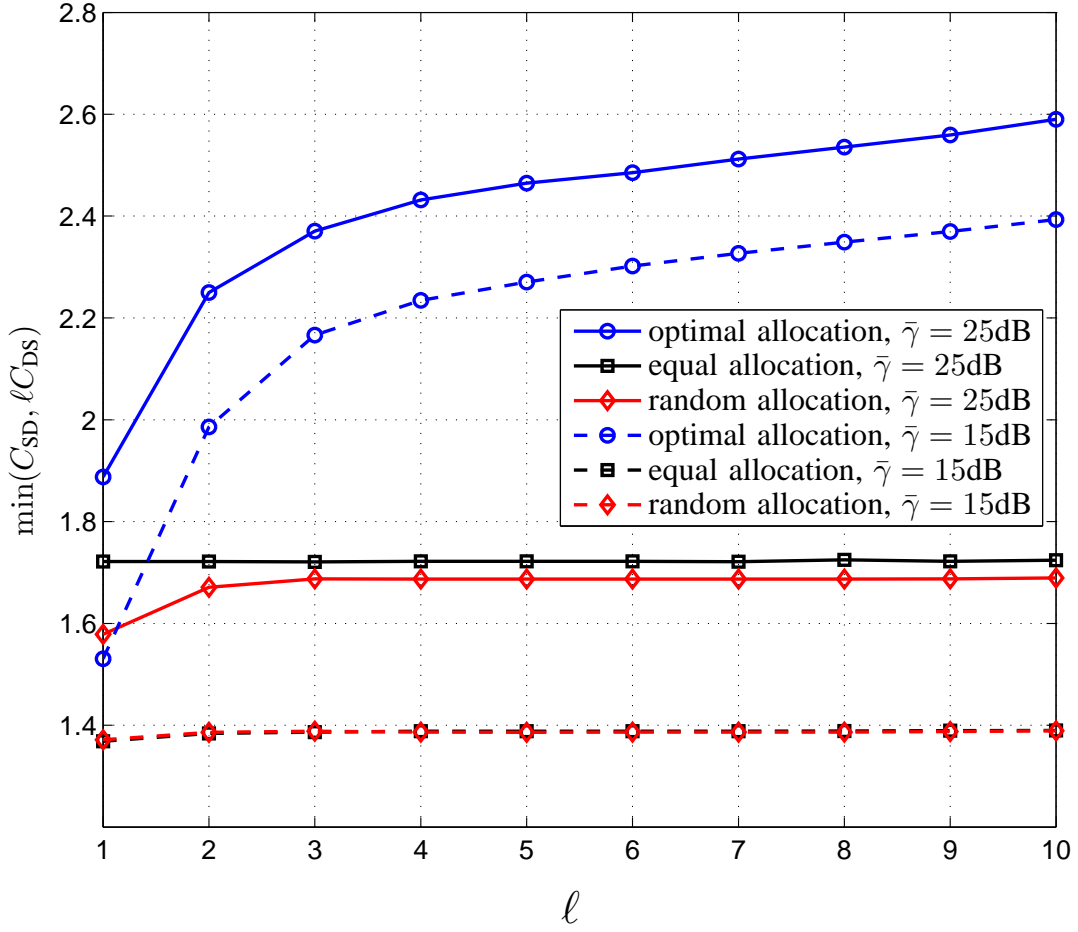
Figure 4.7: Average balanced end-to-end capacities of different power allocation schemes vs. ℓ. $\bar{\gamma} = \bar{\gamma}_1 = \bar{\gamma}_2 = 15, 25$dB.

25dB, because the transmission power assigning in the proposed scheme considers both the instantaneously channel condition and asymmetric traffic loads.

The average balanced end-to-end capacity of the optimal power allocation is compared with the equal and random ones in Fig. 4.8 under the scenario that the average SNRs of hops are different, i.e., $\bar{\gamma}_1 = 2\bar{\gamma}_2 = 20$dB and $\bar{\gamma}_1 = 4\bar{\gamma}_2 = 24$dB. When the traffic loads from S to D and from D to S are equal, i.e., $\ell = 1$, these three algorithm have similar capacity for both scenarios. However, when ℓ rises, the capacity of the optimal scheme increases with ℓ, while those of the equal and random schemes do not change much. Besides, when the SNR difference between $\bar{\gamma}_1$ and $\bar{\gamma}_2$, i.e., $\frac{\bar{\gamma}_1}{\bar{\gamma}_1}$, become large, the optimal algorithm provides similar results, but the capacities of the equal and random allocation slightly increase. This result is different with the one which
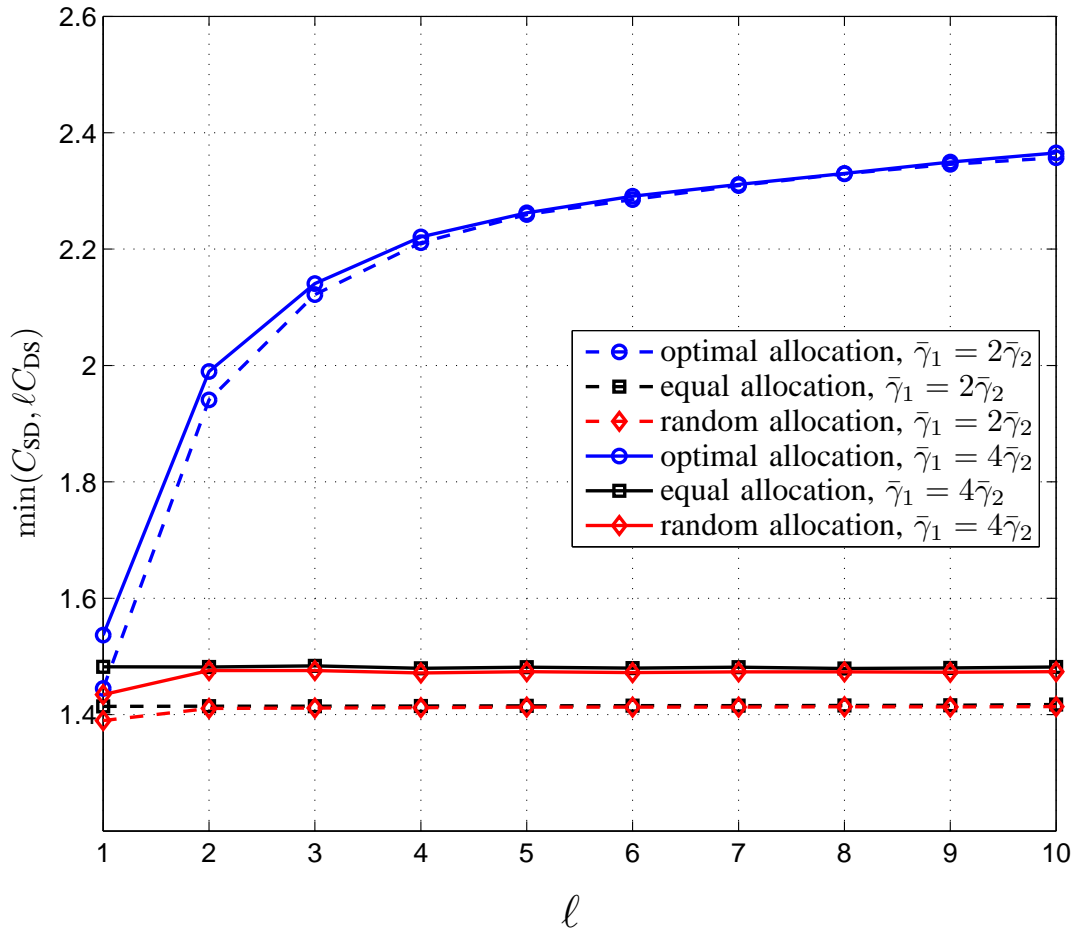
Figure 4.8: Average balanced end-to-end capacities of different power allocation schemes vs. ℓ. $\bar{\gamma}_1 + \bar{\gamma}_2 =$30dB.

only allocates the time slot for each hop. When the time slot is the only parameter to optimize, the end-to-end channel condition is limited by the worse hop, however adaptively assigning the power for each hop can improve the channel condition of the worse hop and balance the end-to-end channel, therefore the overall capacity of the optimal power allocation does not vary a lot under the same total power constraint. From Fig. 4.7 and 4.8, the end-to-end capacities of the equal and random scheme are similar in different scenarios. It implies that the performance of these two allocations only depends on the channel condition and the total available transmitted power.

In Fig. 4.9, the capacity gains between the optimal and the other algorithms are presented with different required capacity ratios and average SNRs. As expected from the results in Fig.
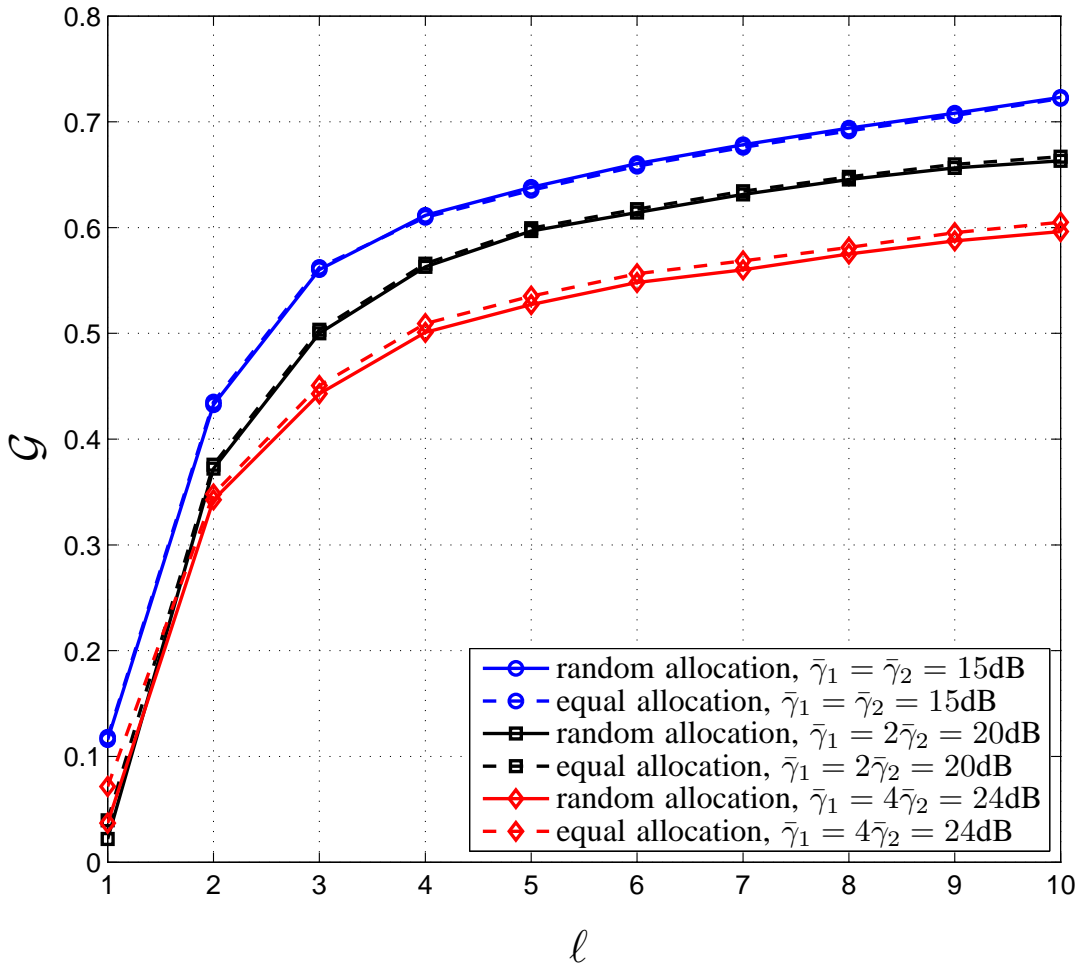
Figure 4.9: Average capacity gain of the optimal power allocation compared to different schemes vs. ℓ. $\bar{\gamma}_1 + \bar{\gamma}_2$ =30dB.

4.7 and 4.8, the capacity gain of the equal and random power allocations are very similar. When ℓ grows, the balanced capacity gain significantly increases, since the proposed scheme can maximize the capacity of each hop and achieves the required capacity ratio at the same time. Moreover, when $\frac{\bar{\gamma}_1}{\bar{\gamma}_2}$ grows, the capacity gain become lower. Although the optimal allocation can improve the channel condition of the worse hop, the end-to-end capacity is still limited by the worse hop, therefore, balancing the two-hop channel capacity becomes difficult when $\frac{\bar{\gamma}_1}{\bar{\gamma}_2}$ is large.
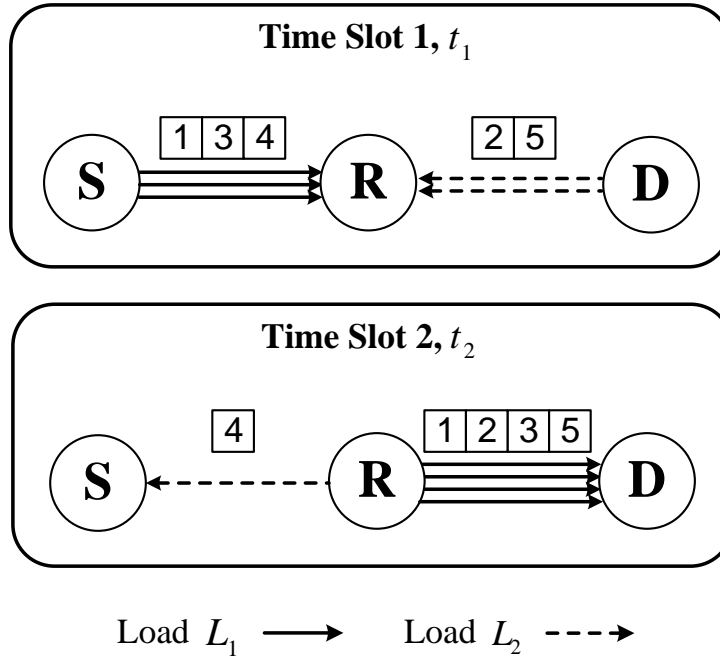
Figure 4.10: An OFDM-based two-way relay system with frequency-division model.

4.4   Resource Allocation for Two-Way Frequency-Division Relay Systems with Asymmetric Traffic

In this section, an OFDM-based two-way relay systems as illustrated in Fig. 4.10 is considered, where the frequency-division model is adopted. In OFDM systems, every subchannel is orthogonal to each other, hence, the transmission between S and R and between D and R can be perform simultaneously by using different subchannels. The frequency-division two-way communications between the source and destination nodes consists of two time slots. In each time slot, all the subcarriers are separated into two sets to be exploited as S–R and R–D links. In the first time slot, S and D simultaneously transmit their data to the relay node through channel $\mathbf{h}_1$ and $\mathbf{h}_2$ respectively. To avoid interference among S and D, the signals from S and D are transmitted on different subcarrier sets. Each subcarrier is only assigned to one hop. For the fairness, each hop at least occupies one subcarrier. During the second time slot, the relay node forwards the received signals to S and D over different subcarrier sets respectively. The subcarrier sets in the second time slot may not be the same as that used in the first time slot.

In the first time slot, denote

$$\vec{\rho}_{\text{SR}} = [\rho_{\text{SR},0}, \rho_{\text{SR},2}, \cdots, \rho_{\text{SR},N-1}]^{\text{T}} \tag{4.57}$$

and

$$\vec{\rho}_{\text{DR}} = [\rho_{\text{DR},0}, \rho_{\text{DR},2}, \cdots, \rho_{\text{DR},N-1}]^{\text{T}} \tag{4.58}$$

as the indicator vectors of subcarrier selection for the transmission from S to R and from D to R respectively, where $\rho_{\text{SR},k}, \rho_{\text{DR},k} \in \{0, 1\}$. When $\rho_k = 1$ means that the k-th subcarrier is selected. Otherwise, $\rho_k = 0$. Since each subcarrier can be selected by one and only one hop, the binary variables $\rho_{\text{SR},k}$ and $\rho_{\text{DR},k}$ must satisfy

$$\sum_{k=1}^{N} \rho_{\text{SR},k}\rho_{\text{DR},k} = 0. \tag{4.59}$$

The instantaneous SNR of the k-th subcarrier of the hop between S and R in the first time slot is given by

$$\gamma_{\text{SR},k} = \frac{P_{\text{SR},k}|H_{1,k}|^2}{N_{0_1}}, \tag{4.60}$$

where $P_{\text{SR},k}$ and N_{0_1} are the transmission power and the variance of AWGN of the k-th subcarrier, respectively. The corresponding instantaneous Shannon's channel capacity in bit/second/Herz, c_{SR}, can be obtain as

$$c_{\text{SR}} = \sum_{k=1}^{N} \log_2(1 + \rho_{\text{SR},k}\gamma_{\text{SR},k}). \tag{4.61}$$

The SNR of the k-th subcarrier and the channel capacity of the hop between D and R in the first time slot are

$$\gamma_{\text{DR}} = \frac{P_{\text{DR},k}|H_{2,k}|^2}{N_{0_2}}, \tag{4.62}$$

and

$$c_{\text{DR}} = \sum_{k=1}^{N} \log_2(1 + \rho_{\text{DR},k}\gamma_{\text{DR},k}). \tag{4.63}$$

Similarly, for the second time slot, the channel capacity of the hops between R and S and

between R and D are respectively given by

$$
\begin{aligned}
c_{\text{RD}} &= \sum_{k=1}^{N} \log_2\left(1 + \rho_{\text{RD},k}\frac{P_{\text{RD},k}|H_{2,k}|^2}{N_{0_1}}\right) \\
&= \sum_{k=1}^{N} \log_2(1 + \rho_{\text{RD},k}\gamma_{\text{RD},k}).
\end{aligned}
\tag{4.64}
$$

and

$$
\begin{aligned}
c_{\text{RS}} &= \sum_{k=1}^{N} \log_2\left(1 + \rho_{\text{RS},k}\frac{P_{\text{RS},k}|H_{1,k}|^2}{N_{0_1}}\right) \\
&= \sum_{k=1}^{N} \log_2(1 + \rho_{\text{RS},k}\gamma_{\text{RS},k}),
\end{aligned}
\tag{4.65}
$$

where $\{\rho_{\text{RD},k}\}$, $\{\rho_{\text{RS},k}\}$ are the indicators vector of subcarrier selection for the transmission R→D and R→S, and $P_{\text{RD},k}$ and $P_{\text{RS},k}$ are the subcarrier powers. The end-to-end capacities from S to D and from D to S are limited by the respective minimum hops, which are given by

$$
C_{\text{SD}} = \min\left(\alpha c_{\text{SR}}, (1-\alpha)c_{\text{RD}}\right),
\tag{4.66}
$$

and

$$
C_{\text{DS}} = \min\left(\alpha c_{\text{DR}}, (1-\alpha)c_{\text{RS}}\right),
\tag{4.67}
$$

where α is the normalized transmission time allocated to the first time slot.

When the traffic loads in the two-way relay system are unbalanced, the channel capacity assigned to the source and the destination should satisfies the capacity ratio that

$$
\frac{c_{\text{SR}}}{c_{\text{DR}}} = \frac{c_{\text{RD}}}{c_{\text{RS}}} = \ell.
\tag{4.68}
$$

In this specific scenario, there are two objectives for the resource allocation of the relay system, i.e., to minimize the difference between the channel capacity ratio $\frac{C_{\text{SD}}}{C_{\text{DS}}}$ and the required ratio ℓ, and to maximize the total end-to-end capacity of the two-way relay transmission. Therefore, considering the two requirements of the allocation algorithm, we choose the balanced end-to-

end capacity as the objective function of the optima problem, i.e.,

$$\min(C_{\mathrm{SD}}, \ell C_{\mathrm{DS}}), \tag{4.69}$$

and then the optimal problem can be formulated as

$$
\begin{aligned}
&\max_{\{\underline{\rho_1}, \underline{\rho_2}, \underline{P_t}, \alpha\}} && \min(C_{\mathrm{SD}}, \ell C_{\mathrm{DS}}) \\
&\text{subject to} && 0 < \alpha < 1, \\
& && \underline{\rho_1} \mathbb{I}_{2\times 1} = \underline{\rho_2} \mathbb{I}_{2\times 1} = \mathbb{I}_{N\times 1}, \\
& && \underline{\rho_1}^{\mathrm{T}} \mathbb{I}_{N\times 1} = \underline{\rho_2}^{\mathrm{T}} \mathbb{I}_{N\times 1} = N\mathbb{I}_{2\times 1}, \\
& && P_{\mathrm{SR},k}, P_{\mathrm{DR},k}, P_{\mathrm{RD},k}, P_{\mathrm{RS},k} \geqslant 0, \\
& && \sum_{k=1}^{N} P_{\mathrm{SR},k} + \sum_{k=1}^{N} P_{\mathrm{DR},k} + \sum_{k=1}^{N} P_{\mathrm{RD},k} + \sum_{k=1}^{N} P_{\mathrm{RS},k} = P_{\mathrm{tot}}.
\end{aligned}
\tag{4.70}
$$

where $\mathbb{I}_{i\times j}$ is an $(i\times j)$ identity matrix, $\underline{\rho_1} = [\vec{\rho}_{\mathrm{SR}}\ \vec{\rho}_{\mathrm{DR}}]$, $\underline{\rho_2} = [\vec{\rho}_{\mathrm{RD}}\ \vec{\rho}_{\mathrm{RS}}]$, $\underline{P_t} = \{P_{\mathrm{SR},k}, P_{\mathrm{DR},k}, P_{\mathrm{RD},k}, P_{\mathrm{RS},k}\}$, and P_{tot} is the total transmission power used to finish one two-way relay communication. The second constraint describes that each subcarrier is only allocated to one hop in one time slot, and the third constraint requires that all subcarrier must be used in any time slot.

Unfortunately, since the subcarrier allocation in the optimal problem (4.70) is the discrete optimization problem, to solve this optimal problem, the complexity is $O(2^{2N})$. When the number of subcarrier, N, is larger, this high complexity will significantly increase the processing latency in practical systems. Therefore, we proposed a suboptimal algorithm with reduced complexity for this problem. In the proposed algorithm, the optimization problem is separated into two problems: the subcarrier allocation and the time slot/power allocation.
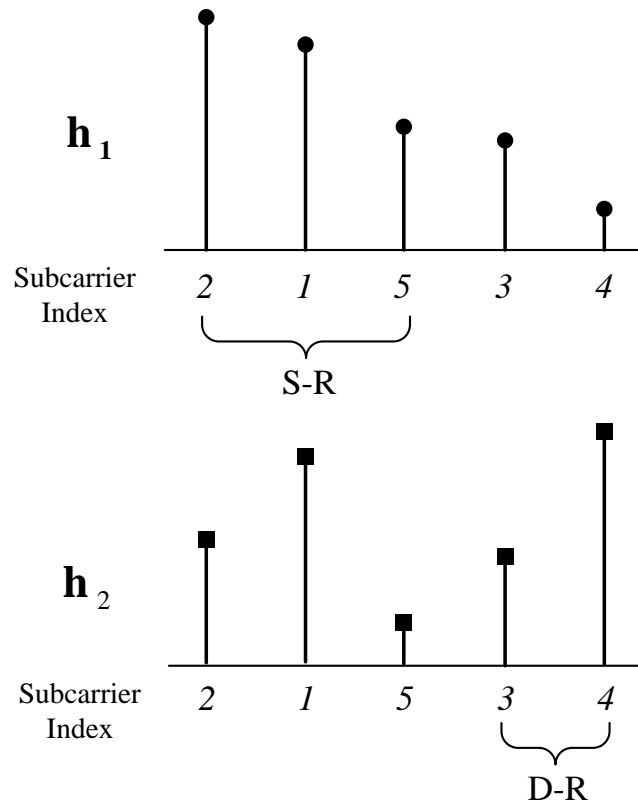
Figure 4.11: Illustration of the proposed subcarrier allocation algorithm.

4.4.1   Subcarrier Allocation for Two-Way FD Relay Systems

In this section, we consider the subcarrier allocation problem for the two-way relay system with unbalanced traffic loads. Here, we assume that the power and time slot allocation is known, then the optimization problem in (4.70) becomes

$$
\begin{aligned}
\max_{\{\underline{\rho_1}, \underline{\rho_2}\}} \quad & \min(C_{\text{SD}}, \ell C_{\text{DS}}) \\
\text{subject to} \quad & \underline{\rho_1}, \underline{\rho_2} \in \{0, 1\}, \\
& \underline{\rho_1} \mathbb{I}_{2 \times 1} = \underline{\rho_2} \mathbb{I}_{2 \times 1} = \mathbb{I}_{N \times 1}, \\
& \underline{\rho_1}^{\text{T}} \mathbb{I}_{N \times 1} = \underline{\rho_2}^{\text{T}} \mathbb{I}_{N \times 1} = N \mathbb{I}_{2 \times 1}.
\end{aligned}
\tag{4.71}
$$

which is discrete optimization problem and the complexity of the exhaustive searching is $O(2^{2N})$.

A suboptimal subcarrier allocation algorithm with low complexity is introduced, in which

the subcarrier allocation is performed for each time slot. In each time slot, the searching for the subcarrier sets is achieved by two individual searching which required the computation complexity $O(N)$ as shown in Fig. 4.11. The principle of the subchannel allocation algorithm is to use the subchannel with high SNR as much as possible. At each iteration, one more subcarrier is selected by the i-th hop till the difference between the capacity ratio and the required ratio value is minimized. For the first time slot which including the transmissions from S to R and from D to R, the assigning procedures starts by searching in $\{H_{1,k}\}$, as follows

1. Initialize the vectors $\vec{\rho}_{SR}$ and $\vec{\rho}_{SR}$ as

$$\vec{\rho}_{SR} = [0, 0, \ldots, 0],$$
$$\vec{\rho}_{DR} = [1, 1, \ldots, 1];$$

set the capacity-ratio difference R_c as

$$R_c = \left| \sum_{k=0}^{N-1} \log_2(1 + \rho_{DR,k}\gamma_{DR,k}) - \ell \right|; \tag{4.72}$$

and set the candidate subcarrier set of the hop between S and R to include all the nonassigned subcarrier, i.e.,

$$\mathcal{H}_{SR} = \{H_{1,k}\}, \quad k = 0, \ldots, N-1. \tag{4.73}$$

2. Select the subchannel with the largest instantaneous capacity for the hop between S and R from $\mathcal{H}_{SR}$, i.e.,

$$H_{SR,\kappa} = \max \left\{ \frac{P_{1,k}|H_{1,k}|^2}{N_{0_1}} \right\}, \quad H_{1,k} \in \mathcal{H}_{SR}; \tag{4.74}$$

find out the corresponding index of this subchannel, κ; and set that

$$\rho_{SR,\kappa} = 1$$
$$\rho_{DR,\kappa} = 0,$$

3. Calculate the new capacity-ratio difference of the two hops

$$R'_c = \left| \frac{\sum_{k=0}^{N-1} \log_2(1 + \rho_{SR,k}\gamma_{SR,k})}{\sum_{k=0}^{N-1} \log_2(1 + \rho_{DR,k}\gamma_{DR,k})} - \ell \right|; \tag{4.75}$$

4. If $R'_c < R_c$, remove the subcarriers κ from the set $\mathcal{H}_{SR}$, which means the κ-th subcarrier is allocated to the hop between S and R, then go back to Step 2, repeat the procedures from Step 2 to Step 5 until the set $\mathcal{H}_{SR}$ is empty, i.e., $\mathcal{H}_{SR} = \emptyset$;

   if $R'_c \geq R_c$, set that

$$\rho_{SR,\kappa} = 0$$

$$\rho_{DR,\kappa} = 1,$$

and let $\vec{\rho}'_{SR} = \vec{\rho}_{SR}$ and $\vec{\rho}'_{DR} = \vec{\rho}_{DR}$.

These procedures are repeated for the hop between D and R to search the subcarrier assigning vectors $\vec{\rho}''_{SR}$ and $\vec{\rho}''_{DR}$. In that case, the initial vextor $\vec{\rho}_{SR}$ and $\vec{\rho}_{SR}$ becomes

$$\vec{\rho}_{SR} = [1, 1, \ldots, 1],$$

$$\vec{\rho}_{DR} = [0, 0, \ldots, 0],$$

and the initial candidate subcarrier set is $\mathcal{H}_{DR} = \{H_{2,k}\}$, $k = 0, \ldots, N - 1$. Then, we have that

$$\vec{\rho}_{SR} \in \{\vec{\rho}'_{SR}, \vec{\rho}''_{SR}\}, \text{ and } \vec{\rho}_{DR} \in \{\vec{\rho}'_{DR}, \vec{\rho}''_{DR}\}. \tag{4.76}$$

Similarly, for the second time slot, the candidate assigning sets are obtained by using the same algorithm

$$\vec{\rho}_{RD} \in \{\vec{\rho}'_{RD}, \vec{\rho}''_{RD}\}, \text{ and } \vec{\rho}_{RS} \in \{\vec{\rho}'_{RS}, \vec{\rho}''_{RS}\}. \tag{4.77}$$

Finally, the vector combination which provider the highest total capacity will be selected from the candicate sets and be used in subcarrier assigning, i.e.,

$$\underline{\rho_1}, \underline{\rho_2} = \underset{\vec{\rho}_{SR}, \vec{\rho}_{DR}, \vec{\rho}_{RD}, \vec{\rho}_{RS}}{\arg\max} \ \min\left(C_{SD}, \ell C_{DS}\right). \tag{4.78}$$

4.4.2 Time Slot Allocation for Two-Way FD Relay Systems

When the subcarrier allocation is determined, the transmission time assigned to the first and second time slot will be optimized such that the instantaneous end-to-end channel capacity is maximized. Denote that normalized transmission time allocated to the first slot is α, and then $(1 - \alpha)$ is the transmission time for the second slot. The optimization problem becomes

$$\max_{\alpha} \quad C_{\text{SD}} + C_{\text{DS}}$$
$$\text{subject to} \quad \frac{C_{\text{SD}}}{C_{\text{DS}}} = \ell,$$
$$0 < \alpha < 1. \tag{4.79}$$

Using the similar algorithm in Section 4.3.1, the capacity ratio of the hop between S and R and between R and D in a time slot satisfies the channel capacity ratio constraint, i.e.,

$$\frac{c_{\text{SR}}}{c_{\text{DR}}} = \frac{c_{\text{RD}}}{c_{\text{RS}}} = \ell. \tag{4.80}$$

Therefore, the first constraint in (4.79) can be guaranteed. Then we have

$$\min\left(\alpha c_{\text{SR}}, (1 - \alpha)c_{\text{RD}}\right) + \min\left(\alpha c_{\text{DR}}, (1 - \alpha)c_{\text{RS}}\right)$$
$$= \min\left(\alpha c_{\text{SR}}, (1 - \alpha)c_{\text{RD}}\right) + \min\left(\alpha \frac{1}{\ell}c_{\text{SR}}, (1 - \alpha)\frac{1}{\ell}c_{\text{RD}}\right) \tag{4.81}$$
$$= \left(1 + \frac{1}{\ell}\right)\min\left(\alpha c_{\text{SR}}, (1 - \alpha)c_{\text{RD}}\right).$$

The optimization problem is simplified as

$$\max_{\{\alpha\}} \quad \min\left(\alpha c_{\text{SR}}, (1 - \alpha)c_{\text{RD}}\right)$$
$$\text{subject to} \quad 0 < \alpha < 1. \tag{4.82}$$

The solution of the problems in (4.82) is given by

$$\alpha = \frac{c_{\text{RD}}}{c_{\text{SR}} + c_{\text{RD}}} \quad \text{or} \quad \frac{c_{\text{DR}}}{c_{\text{DR}} + c_{\text{RS}}}. \tag{4.83}$$

4.4.3   Power Allocation for Two-Way FD Relay Systems

When the time slot allocation is known, to a certain determined subcarrier allocation, the optimization problem of power allocation can be formulated as

$$
\begin{aligned}
\max_{\{\underline{P_t}\}} \quad & \min(C_{SD}, \ell C_{DS}) \\
\text{subject to} \quad & P_{SR,k}, P_{DR,k}, P_{RD,k}, P_{RS,k} \geqslant 0, \\
& \sum_{k=0}^{N-1} P_{SR,k} + \sum_{k=0}^{N-1} P_{DR,k} + \sum_{k=0}^{N-1} P_{RD,k} + \sum_{k=0}^{N-1} P_{RS,k} = P_{tot}.
\end{aligned}
\tag{4.84}
$$

Different with the subchannel allocation which is a discrete optimization problem, the power allocation problem is a continues one, therefore, this optimization problem in (4.84) can be formulated by two optimization problems. One is to allocate the total power to each hop in each time slot as

$$
\begin{aligned}
\max_{\{\bar{P}_{SR}, \bar{P}_{DR}, \bar{P}_{RD}, \bar{P}_{RS}\}} \quad & C_{SD} + C_{DS} \\
\text{subject to} \quad & \frac{c_{SR}}{c_{DR}} = \frac{c_{RD}}{c_{RS}} = \ell, \\
& \bar{P}_{SR}, \bar{P}_{DR}, \bar{P}_{RD}, \bar{P}_{RS} \geq 0, \\
& \bar{P}_{SR} + \bar{P}_{DR} + \bar{P}_{RD} + \bar{P}_{RS} = P_{tot},
\end{aligned}
\tag{4.85}
$$

where the subtotal power of each hop in each time slot is $\bar{P}_{SR}, \bar{P}_{DR}, \bar{P}_{RD}$ and $\bar{P}_{RS}$ respectively. When the subtotal power of each hop is given, the subcarrier power allocation for each hop can be derived to maximized the total channel capacity of this hop as

$$
\begin{aligned}
\max_{\{P_{X,k}\}} \quad & c_X = \sum_{k=0}^{N-1} \log_2 \left(1 + \rho_{X,k} \frac{P_{X,k}|H_{i,k}|^2}{N_{0_i}} \right) \\
\text{subject to} \quad & P_{X,k} \geq 0, \\
& \sum_{k=0}^{N-1} P_{X,k} = \bar{P}_X,
\end{aligned}
\tag{4.86}
$$

where $\rho_{X,k}$ is the corresponding selection indicator of the k-th subcarrier.

   Similar to (4.27), the optimization problem in (4.86) can be derived to finding the maximum

of the cost function

$$\mathcal{L}(P_{X,k}, \lambda_X) = \sum_{k=0}^{N-1} \log_2\left(1 + \rho_{X,k}\frac{P_{X,k}|H_{i,k}|^2}{N_{0_i}}\right) + \lambda_X\left(\sum_{k=0}^{N-1} P_{X,k} - \bar{P}_X\right). \tag{4.87}$$

Taking the gradient in terms of $P_{X,k}$ and equating it to zero

$$\frac{\partial\mathcal{L}}{\partial P_{X,k}} = \frac{1}{\ln 2}\frac{1}{1 + \rho_{X,k}\frac{P_{X,k}|H_{1,k}|^2}{N_{0_1}}}\frac{\rho_{X,k}|H_{i,k}|^2}{N_{0_i}} + \lambda_X$$

$$= 0. \tag{4.88}$$

Denote that Λ_X is the subcarrier set which is given by

$$\Lambda_X = \{k \mid \rho_{X,k} = 1\}, \tag{4.89}$$

N_X is the number of subcarriers in Λ_X, $|H_{i,\min}|$ is the minimum channel gain, $k \in \Lambda_X$, and $P_{X,\min}$ is the power of the subchannel $H_{i,\min}$. Then, for $k \in \Lambda_X$, it can be obtained that

$$\frac{\partial\mathcal{L}}{\partial P_{X,k}} = \frac{\partial\mathcal{L}}{\partial P_{X,\min}} = 0. \tag{4.90}$$

The relationship between $P_{X,k}$ and $P_{X,\min}$ can be found out as

$$P_{X,k} = P_{X,\min} + N_{0_i}\frac{|H_{X,k}|^2 - |H_{X,\min}|^2}{|H_{X,k}|^2|H_{X,\min}|^2}, \quad k \in \Lambda_X, \tag{4.91}$$

and consequently, $\bar{P}_X$ can be expressed as

$$\bar{P}_X = N_X P_{X,\min} + N_{0_i}\sum_{k\in\Lambda_X, k\neq\min}\frac{|H_{X,k}|^2 - |H_{X,\min}|^2}{|H_{X,k}|^2|H_{X,\min}|^2}. \tag{4.92}$$

Then, the channel capacity of each hop is written as

$$c_X = N_X \log_2\left(1 + \frac{\bar{P}_X|H_{i,\min}|^2}{N_X N_{0_i}} - \sum_{k\in\Lambda_X, k\neq\min}\frac{|H_{i,k}|^2 - |H_{i,\min}|^2}{N_X|H_{i,k}|^2}\right) + \sum_{k\in\Lambda_X, k\neq\min}\log_2\frac{|H_{i,k}|^2}{|H_{i,\min}|^2} \tag{4.93}$$

According to the capacity ratio constraints in (4.85),

$$\frac{c_{\mathrm{SR}}}{c_{\mathrm{DR}}} = \frac{c_{\mathrm{RD}}}{c_{\mathrm{RS}}} = \ell, \tag{4.94}$$

substituting (4.93) into (4.94), we have

$$\begin{aligned}
&N_{\mathrm{SR}} \log_2\left(1 + \frac{\bar{P}_{\mathrm{SR}}|H_{1,\min}|^2}{N_{\mathrm{SR}}N_{0_1}} - \sum_{k \in \Lambda_{\mathrm{SR}}, k \neq \min} \frac{|H_{1,k}|^2 - |H_{1,\min}|^2}{N_{\mathrm{SR}}|H_{1,k}|^2}\right) + \sum_{k \in \Lambda_{\mathrm{SR}}, k \neq \min} \log_2 \frac{|H_{1,k}|^2}{|H_{1,\min}|^2} \\
&= \ell N_{\mathrm{DR}} \log_2\left(1 + \frac{\bar{P}_{\mathrm{DR}}|H_{2,\min}|^2}{N_{\mathrm{DR}}N_{0_2}} - \sum_{k \in \Lambda_{\mathrm{DR}}, k \neq \min} \frac{|H_{2,k}|^2 - |H_{2,\min}|^2}{N_{\mathrm{DR}}|H_{2,k}|^2}\right) + \sum_{k \in \Lambda_{\mathrm{DR}}, k \neq \min} \log_2 \frac{|H_{2,k}|^2}{|H_{2,\min}|^2}
\end{aligned} \tag{4.95}$$

and

$$\begin{aligned}
&N_{\mathrm{RD}} \log_2\left(1 + \frac{\bar{P}_{\mathrm{RD}}|H_{2,\min}|^2}{N_{\mathrm{RD}}N_{0_2}} - \sum_{k \in \Lambda_{\mathrm{SR}}, k \neq \min} \frac{|H_{2,k}|^2 - |H_{2,\min}|^2}{N_{\mathrm{RD}}|H_{2,k}|^2}\right) + \sum_{k \in \Lambda_{\mathrm{RD}}, k \neq \min} \log_2 \frac{|H_{2,k}|^2}{|H_{2,\min}|^2} \\
&= \ell N_{\mathrm{RS}} \log_2\left(1 + \frac{\bar{P}_{\mathrm{RS}}|H_{1,\min}|^2}{N_{\mathrm{RS}}N_{0_1}} - \sum_{k \in \Lambda_{\mathrm{RS}}, k \neq \min} \frac{|H_{1,k}|^2 - |H_{1,\min}|^2}{N_{\mathrm{DR}}|H_{1,k}|^2}\right) + \sum_{k \in \Lambda_{\mathrm{RS}}, k \neq \min} \log_2 \frac{|H_{1,k}|^2}{|H_{1,\min}|^2}.
\end{aligned} \tag{4.96}$$

When the capacity ratio constraint is satisfied, the problem in (4.85) will be equivalent to

$$\begin{aligned}
\max_{\{\underline{P}_{\mathrm{t}}\}} \quad & \min\left(c_{\mathrm{SR}}, c_{\mathrm{RD}}\right) + \min\left(c_{\mathrm{DR}}, c_{\mathrm{RS}}\right) \\
\text{subject to} \quad & P_{\mathrm{SR},k}, P_{\mathrm{DR},k}, P_{\mathrm{RD},k}, P_{\mathrm{RS},k} \geq 0, \\
& \sum_{k=0}^{N-1} P_{\mathrm{SR},k} + \sum_{k=0}^{N-1} P_{\mathrm{DR},k} + \sum_{k=0}^{N-1} P_{\mathrm{RD},k} + \sum_{k=0}^{N-1} P_{\mathrm{RS},k} = P_{\mathrm{tot}}.
\end{aligned} \tag{4.97}$$

The optimal solution of the max-min problem in (4.97) is

$$\begin{cases} c_{\mathrm{SR}} = c_{\mathrm{RD}}, \\ c_{\mathrm{DR}} = c_{\mathrm{RS}}. \end{cases} \tag{4.98}$$

Therefore, we have

$$
\begin{aligned}
&N_{\text{SR}} \log_2 \left(1 + \frac{\bar{P}_{\text{SR}}|H_{1,\text{min}}|^2}{N_{\text{SR}}N_{0_1}} - \sum_{k \in \Lambda_{\text{SR}}, k \neq \text{min}} \frac{|H_{1,k}|^2 - |H_{1,\text{min}}|^2}{N_{\text{SR}}|H_{1,k}|^2}\right) + \sum_{k \in \Lambda_{\text{SR}}, k \neq \text{min}} \log_2 \frac{|H_{1,k}|^2}{|H_{1,\text{min}}|^2} \\
&= N_{\text{RD}} \log_2 \left(1 + \frac{\bar{P}_{\text{RD}}|H_{2,\text{min}}|^2}{N_{\text{RD}}N_{0_2}} - \sum_{k \in \Lambda_{\text{RD}}, k \neq \text{min}} \frac{|H_{2,k}|^2 - |H_{2,\text{min}}|^2}{N_{\text{RD}}|H_{2,k}|^2}\right) + \sum_{k \in \Lambda_{\text{RD}}, k \neq \text{min}} \log_2 \frac{|H_{2,k}|^2}{|H_{2,\text{min}}|^2}
\end{aligned}
\tag{4.99}
$$

and

$$
\begin{aligned}
&N_{\text{DR}} \log_2 \left(1 + \frac{\bar{P}_{\text{DR}}|H_{2,\text{min}}|^2}{N_{\text{DR}}N_{0_2}} - \sum_{k \in \Lambda_{\text{DR}}, k \neq \text{min}} \frac{|H_{2,k}|^2 - |H_{2,\text{min}}|^2}{N_{\text{DR}}|H_{2,k}|^2}\right) + \sum_{k \in \Lambda_{\text{DR}}, k \neq \text{min}} \log_2 \frac{|H_{2,k}|^2}{|H_{2,\text{min}}|^2} \\
&= N_{\text{RS}} \log_2 \left(1 + \frac{\bar{P}_{\text{RS}}|H_{1,\text{min}}|^2}{N_{\text{RS}}N_{0_1}} - \sum_{k \in \Lambda_{\text{RS}}, k \neq \text{min}} \frac{|H_{1,k}|^2 - |H_{1,\text{min}}|^2}{N_{\text{RS}}|H_{1,k}|^2}\right) + \sum_{k \in \Lambda_{\text{RS}}, k \neq \text{min}} \log_2 \frac{|H_{1,k}|^2}{|H_{1,\text{min}}|^2}
\end{aligned}
\tag{4.100}
$$

Adding the total power constraint

$$
\bar{P}_{\text{SR}} + \bar{P}_{\text{DR}} + \bar{P}_{\text{RD}} + \bar{P}_{\text{RS}} = P_{\text{tot}},
\tag{4.101}
$$

the optimal subtotal power of each hop in each time slot can be solved from (4.95), (4.96), (4.99), (4.100) and (4.101).

Once the total power for each hop, $\{\bar{P}_{\text{SR}}, \bar{P}_{\text{DR}}, \bar{P}_{\text{RS}}, \bar{P}_{\text{RD}}\}$, is known, the power allocated to the subchannel with the lowest channel gain of each hop can be determined by

$$
P_{\text{X,min}} = \left[\frac{1}{\lambda_{\text{X}}} - \frac{N_{0_i}}{|H_{i,\text{min}}|^2}\right]^{\dagger}.
\tag{4.102}
$$

and then the other subcarrier power can be figured out as

$$
P_{\text{X},k} = P_{\text{X,min}} + N_{0_i} \frac{|H_{i,k}|^2 - |H_{i,\text{min}}|^2}{|H_{i,k}|^2|H_{i,\text{min}}|^2}.
\tag{4.103}
$$

The complexity of the optimal solution which only can obtained by exhaustive searching is $O(2^{2N})$, while the complexity of suboptimal allocation algorithm is $O(N)$ in each iteration, and the number of iterations is limited.

The proposed power allocation algorithm can be implemented as follows

1. Initialize the power allocated to the first and second time slot $\bar{P}_1$ and $\bar{P}_2$ as

$$\bar{P}_1 = \bar{P}_2 = \frac{P_{\text{tot}}}{2} \tag{4.104}$$

   where

$$\bar{P}_1 = \bar{P}_{\text{SR}} + \bar{P}_{\text{DR}} \tag{4.105}$$

   and

$$\bar{P}_2 = \bar{P}_{\text{RD}} + \bar{P}_{\text{RS}}; \tag{4.106}$$

2. Solve $\bar{P}_{\text{SR}}$ and $\bar{P}_{\text{DR}}$ from (4.95) and (4.99);

   solve $\bar{P}_{\text{SR}}$ and $\bar{P}_{\text{DR}}$ from (4.96) and (4.100);

3. Calculate c_{SR} and c_{RD} using (4.93)

4. If $c_{\text{SR}} = c_{\text{RD}}$, go to the next step; if $c_{\text{SR}} \neq c_{\text{RD}}$, adjust $\bar{P}_1$ and $\bar{P}_2$, then go back to Step 2, repeat the procedures from Step 2 to Step 4 until $c_{\text{SR}} = c_{\text{RD}}$.

5. Allocate the power to each subcarrier based on the water filling algorithm.

Allocated subcarriers for Time slot 1, i.e., $\vec{\rho}_{\text{SR}}$ and $\vec{\rho}_{\text{DR}}$, with algorithm in 5.3.1

Allocated subcarriers for Time slot 2, i.e., $\vec{\rho}_{\text{RS}}$ and $\vec{\rho}_{\text{RD}}$, with algorithm in 5.3.1

Select the suboptimal allocation set according to
$$\{\vec{\rho}_{\text{RD}}, \vec{\rho}_{\text{RD}}\} = \arg\max \ \min(C_{\text{SD}}, \ell C_{\text{SD}})$$

Initialize $\overline{P}_1 = \overline{P}_2 = \dfrac{P_{\text{tot}}}{2}$

Solve $\overline{P}_{\text{SR}}$ and $\overline{P}_{\text{DR}}$ from Eq. (5.78) and (5.87);
Solve $\overline{P}_{\text{RD}}$ and $\overline{P}_{\text{RS}}$ from Eq. (5.79) and (5.88)

calculate c_{SR} and c_{RD} using Eq. (5.76)

Increase $\overline{P}_1$, decrease $\overline{P}_2$

$c_{\text{SR}} < c_{\text{RD}}$

$c_{\text{SR}} = c_{\text{RD}}$

$c_{\text{SR}} > c_{\text{RD}}$

Increase $\overline{P}_2$, decrease $\overline{P}_1$

Yes

Water-filling algorithm for
$$\{P_{\text{SR},k}, P_{\text{SR},k}, P_{\text{SR},k}, P_{\text{SR},k}\}$$
by Eq. (5.84) and (5.85)

4.4.4   Simulation Results

In this section, we verify the proposed allocation schemes by computer simulations and compare its performance with different allocation schemes for different scenarios. To investigate the performance of the proposed suboptimal scheme, two metric are adopted, i.e., the balanced end-to-end capapcity, $\min(C_{\text{SD}}, \ell C_{\text{DS}})$, and the relative error, which is defined as

$$e_{\text{b}} = \frac{C_{\text{opt}} - C}{C_{\text{opt}}} \tag{4.107}$$

where C_{opt} is the optimal achievable end-to-end capacity of the system, and C is the practical end-to-end capacity based on a certain resource allocation scheme. The average relative error is the average of the relative error given by (4.107) over a large number of realizations. Here, the optimal end-to-end capacity is obtained by exhaustive searching. The average SNRs of each hop are denoted as

$$\bar{\gamma}_1 = \frac{\mathbb{E}[|H_{k,1}|^2]}{N_{0_1}},$$
$$\bar{\gamma}_2 = \frac{\mathbb{E}[|H_{k,2}|^2]}{N_{0_2}}.$$

All simulation results in this section are based on 10 million independent realizations of the system.

Subcarrier Allocation

In order to evaluate the performance of the proposed subcarrier allocation scheme, we compare it with three different allocation schemes. A simple method to assign subchannels to each hop is random allocation. In this scheme, the total number of subcarriers occupied by each hop in a time slot, N_{X}, is randomly selected. Then, the hop will randomly choose the subcarrier set according the given total number of subcarriers. Another allocation scheme is equal allocation, in which the overall subcarriers are equally shared by the hops in the same time slot, i.e.

$$N_{\text{SR}} = N_{\text{DR}} = N_{\text{RD}} = N_{\text{RS}} = \frac{N}{2}. \tag{4.108}$$
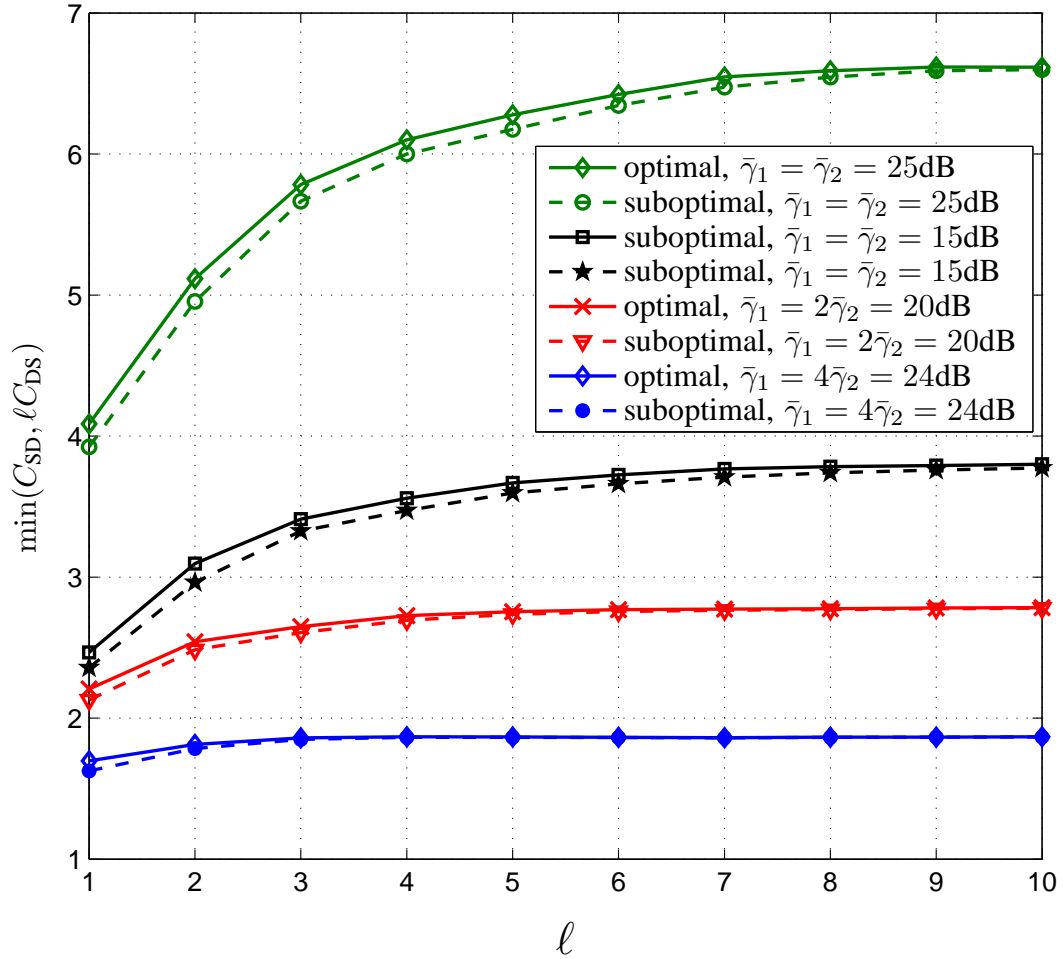
Figure 4.12: Average balanced end-to-end capacities of the optimal and suboptimal subcarrier allocation schemes vs. ℓ.

Then, each hop will randomly select the subcarriers. These schemes do not require the channel information, therefore, the capacity of each hop is also random. The third scheme we compared here is that the total number of the subcarriers allocated to each hop is based on the required capacity ratio, i.e.,

$$\frac{N_{\text{SR}}}{N_{\text{DR}}} = \frac{N_{\text{RD}}}{N_{\text{RS}}} = \ell, \tag{4.109}$$

where $N_{\text{SR}} + N_{\text{DR}} = N_{\text{RD}} + N_{\text{RS}} = N$. In this scheme, the hop with the high traffic load will have more subcarriers for transmission. However, since this allocation do not consider the channel condition of each subchannel, it cannot guarantee that the hop with the high traffic load has a high capacity.

The average balanced end-to-end capacities of the optimal and the proposed suboptimal
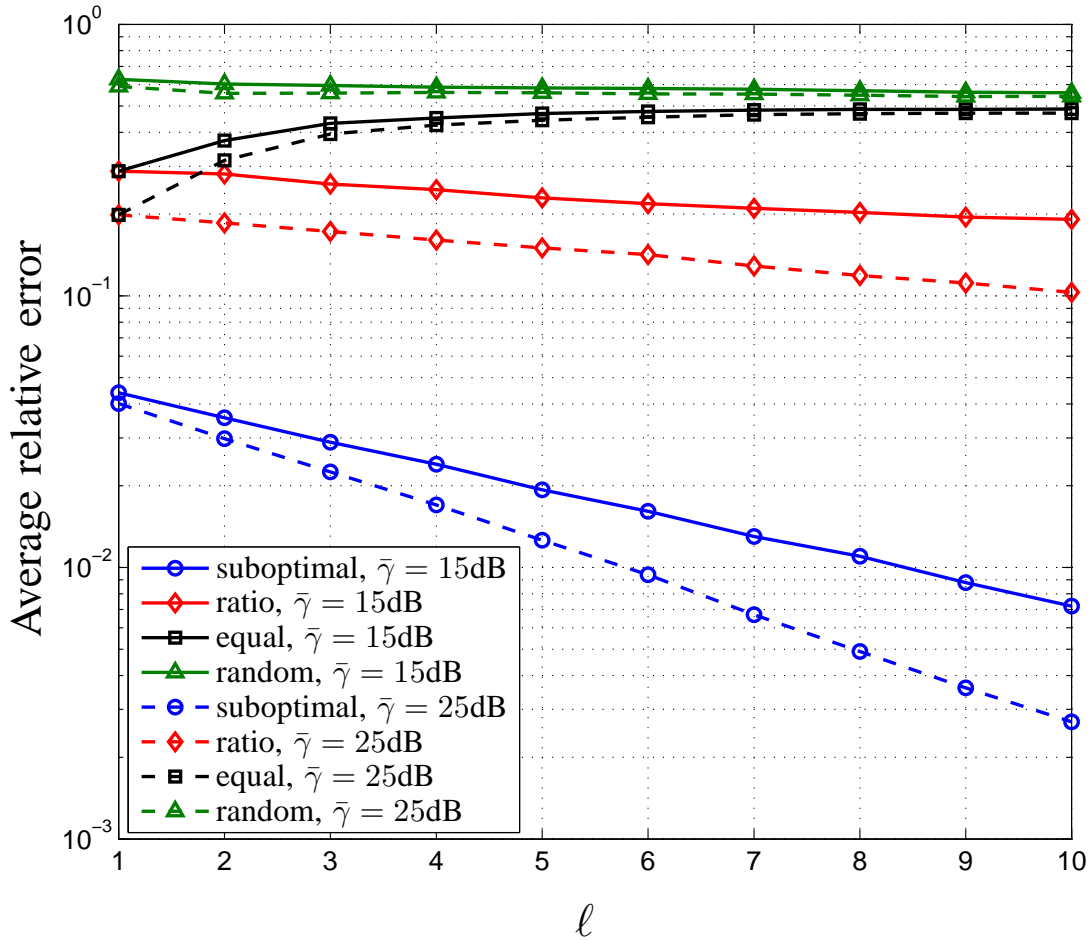
Figure 4.13: Average relative error of different subcarrier allocation schemes vs. ℓ. $\bar{\gamma} = \bar{\gamma}_1 = \bar{\gamma}_2 =$15,25dB.

allocation schemes are compared in Fig. 4.12 with different the average SNR of the hops S–R and R–D. In this figure, the balanced capacity of the suboptimal scheme is very close to the optimal one especially with different values of ℓ, $\bar{\gamma}_1$ and $\bar{\gamma}_2$, especially when the value of ℓ is large. This implies that the proposed algorithm can achieve similar performance with the optimal one with a significantly lower complexity. The balanced capacities of the optimal and suboptimal schemes are increasing when the capacity ratio rises. This feature becomes obvious when the average SNR is high or the ratio between $\bar{\gamma}_1$ and $\bar{\gamma}_2$ is small, e.g., when $\bar{\gamma}_1 = \bar{\gamma}_2$. When $\bar{\gamma}_1 = 4\bar{\gamma}_2$, the capacity tends to constant with different ℓ. It happens because when the difference of the channel condition of the two hops is larger, it becomes more difficult to perform the balanced allocation. Moreover, since the end-to-end capacity is limited by the
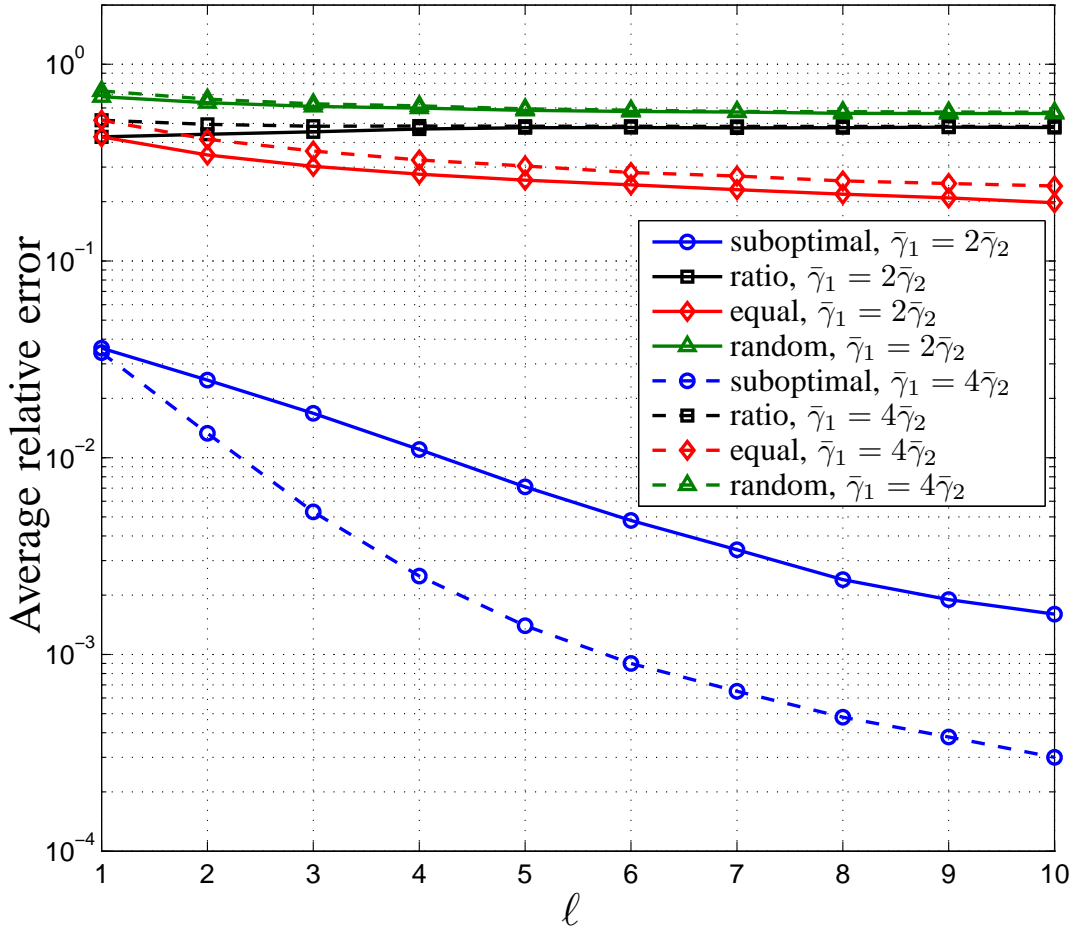
Figure 4.14: Average relative error of different subcarrier allocation schemes with different average SNRs. $\bar{\gamma}_1 + \bar{\gamma}_2 =$30dB.

hop with the worse channel condition, the increasing of the ratio between $\bar{\gamma}_1$ and $\bar{\gamma}_2$, i.e., $\bar{\gamma}_1/\bar{\gamma}_2$, results in the reduction of the balanced capacity.

The average relative error of different allocation schemes is compared in Fig. 4.13 with $\bar{\gamma} = \bar{\gamma}_1 = \bar{\gamma}_2 =$15, 25dB. From the results, when the traffic loads ratio is varying, the average error of the random allocation keeps constant without considering the instantaneously channel condition and traffic loads. When $\ell = 1$, the equal and ratio-based algorithm has the same relative error. When ℓ increases, equally sharing the subcarrier leads to low balanced capacity and high relative error, while the error of the proposed suboptimal and the ratio-based schemes decrease. Among the four algorithms, the proposed suboptimal one exhibits the lowest relative error, i.e., $e_{\text{b,subopt}} < 0.05$, while the error of the other schemes is always higher than 0.1.

Especially, when $\bar{\gamma} = 25$dB, the relative error of the suboptimal scheme can reach 0.003 with $\ell = 10$. When the average SNR is large, i.e., $\bar{\gamma} = 25$dB, the proposed scheme can achieve a lower average error than that when the SNR is small, because when the SNR approaches to infinite, the subcarrier allocation will have less effect on the end-to-end capacity.

In Fig. 4.14, we present the average relative error of different subcarrier allocation algo-rithms with the different average SNRs of each hop. Tow cases are considered, i.e., $\bar{\gamma}_1 = 2\bar{\gamma}_2 = 20$dB and $\bar{\gamma}_1 = 4\bar{\gamma}_2 = 24$dB. In this figure, when $\frac{\bar{\gamma}_1}{\bar{\gamma}_2}$ raises, the relative errors of random, equal and ratio-based schemes almost keep the same value, while the one of the suboptimal scheme reduces. The proposed scheme achieves the significantly low relative error compared the other schemes under the two scenarios. Besides, similarly with the results in Fig. 4.13, when the value of ℓ increases, the balanced capacity of suboptimal scheme become close to the optimal one. These results verifies that the proposed suboptimal subcarrier allocation can ex-hibit similar balanced end-to-end capacity with the optimal algorithm under different channel conditions.

Subcarrier & Time Slot Allocation

In this part, we evaluate the allocation scheme which combines the subcarrier allocation pro-posed in 4.4.1 and time slot allocation proposed in 4.4.2.

The proposed allocation scheme is compared with two different allocation schemes to veri-fy the performance of it. One method to assign the subchannels and time slots for the two-way relay systems is random allocation. In this scheme, the subcarrier is randomly allocated follow the random subcarrier scheme in last part, then, the transmission time also randomly assigns to each time slot. The other allocation scheme is equal allocation, in which the overall subcarriers is equally shared by the hops, and the transmission time of each time slot is equal, i.e.

$$N_{\text{SR}} = N_{\text{DR}} = N_{\text{RD}} = N_{\text{RS}} = \frac{N}{2}, \tag{4.110}$$
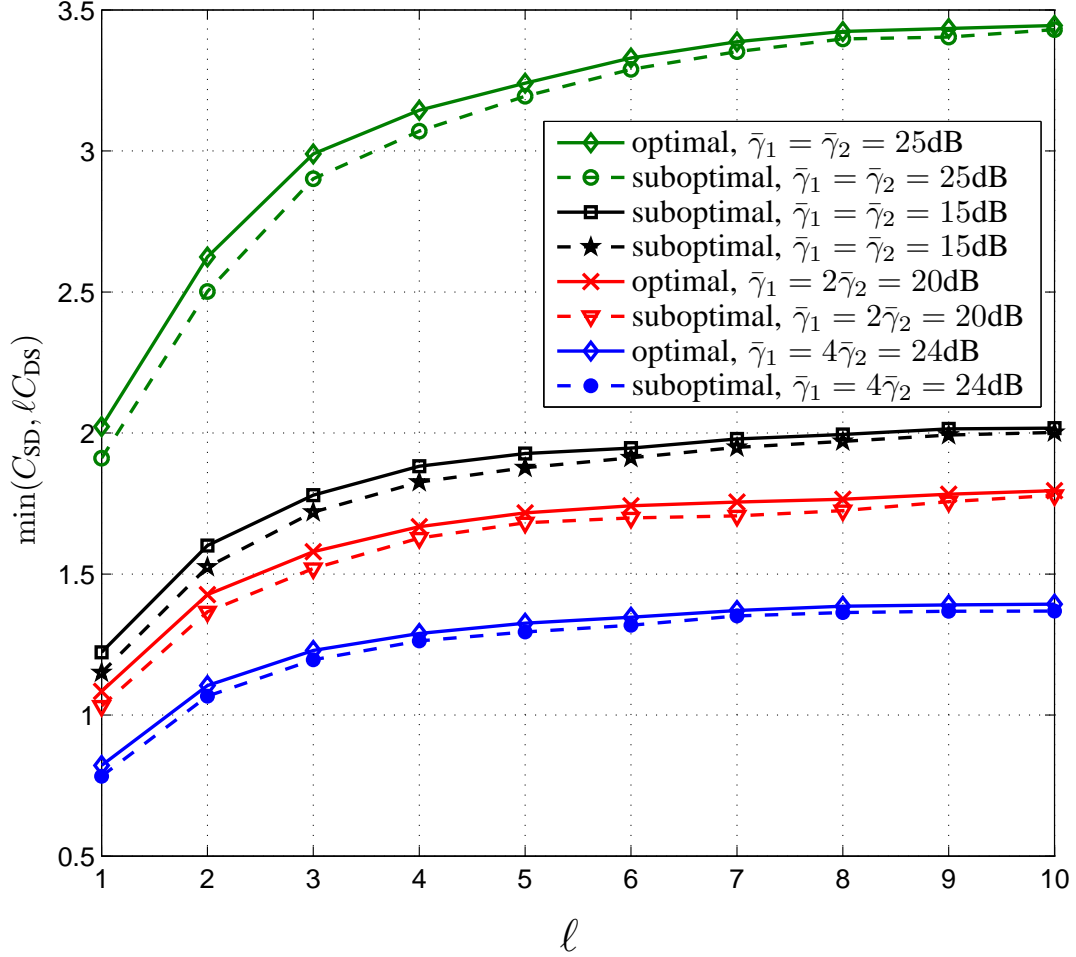
Figure 4.15: Average balanced end-to-end capacities of the optimal and suboptimal resource allocation (subcarrier & time slot allocation) vs. ℓ.

and

$$C_{\text{SD}} = \frac{1}{2} \min(c_{\text{SR}}, c_{\text{RD}}), \tag{4.111}$$

$$C_{\text{DS}} = \frac{1}{2} \min(c_{\text{DR}}, c_{\text{RS}}). \tag{4.112}$$

Fig. 4.15 compares the average balanced end-to-end capacities of the optimal and the proposed suboptimal allocation schemes with different value of ℓ and average SNRs. In this figure, the balanced capacity of the suboptimal scheme is always close to the optimal one with different values of ℓ, $\bar{\gamma}_1$ and $\bar{\gamma}_2$, especially when the value of ℓ is large. It proves that the proposed algorithm can achieve a significantly lower complexity without the capacity loose. The bal-
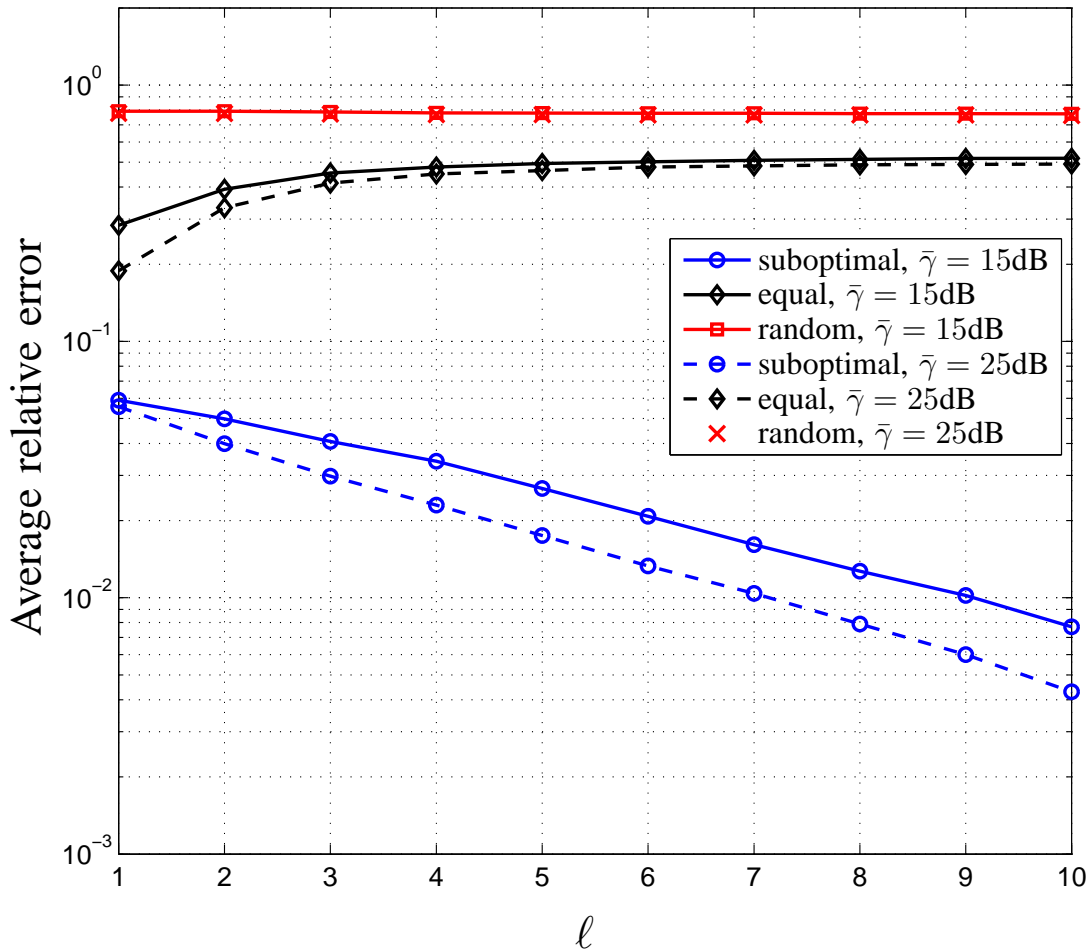
Figure 4.16: Average relative error of different resource allocation schemes (subcarrier & time slot allocation) vs. ℓ. $\bar{\gamma} = \bar{\gamma}_1 = \bar{\gamma}_2$=15, 25dB.

anced capacity of the optimal and suboptimal schemes becomes large with the increasing of the traffic-load ratio. When $\bar{\gamma}_1 = \bar{\gamma}_2 = 25$dB, the balanced capacity of the two schemes increase most obviously in all cases. Moreover, when the ratio between $\bar{\gamma}_1$ and $\bar{\gamma}_2$, i.e., $\bar{\gamma}_1/\bar{\gamma}_2$, rises, the values of balanced capacity become low because of the limitation of the hop with the worse channel condition on the end-to-end capacity.

In Fig. 4.16, we present the average relative error of different allocation algorithms with $\bar{\gamma} = \bar{\gamma}_1 = \bar{\gamma}_2$ =15, 25dB. Without considering the instantaneously channel condition and traffic loads, the relative error of the random allocation keeps constant when the traffic loads ratio and average SNR are varying. The relative error of the equal algorithm grows with the increasing of ℓ, because when $\ell > 1$, equally sharing the subcarrier and transmission time results in the
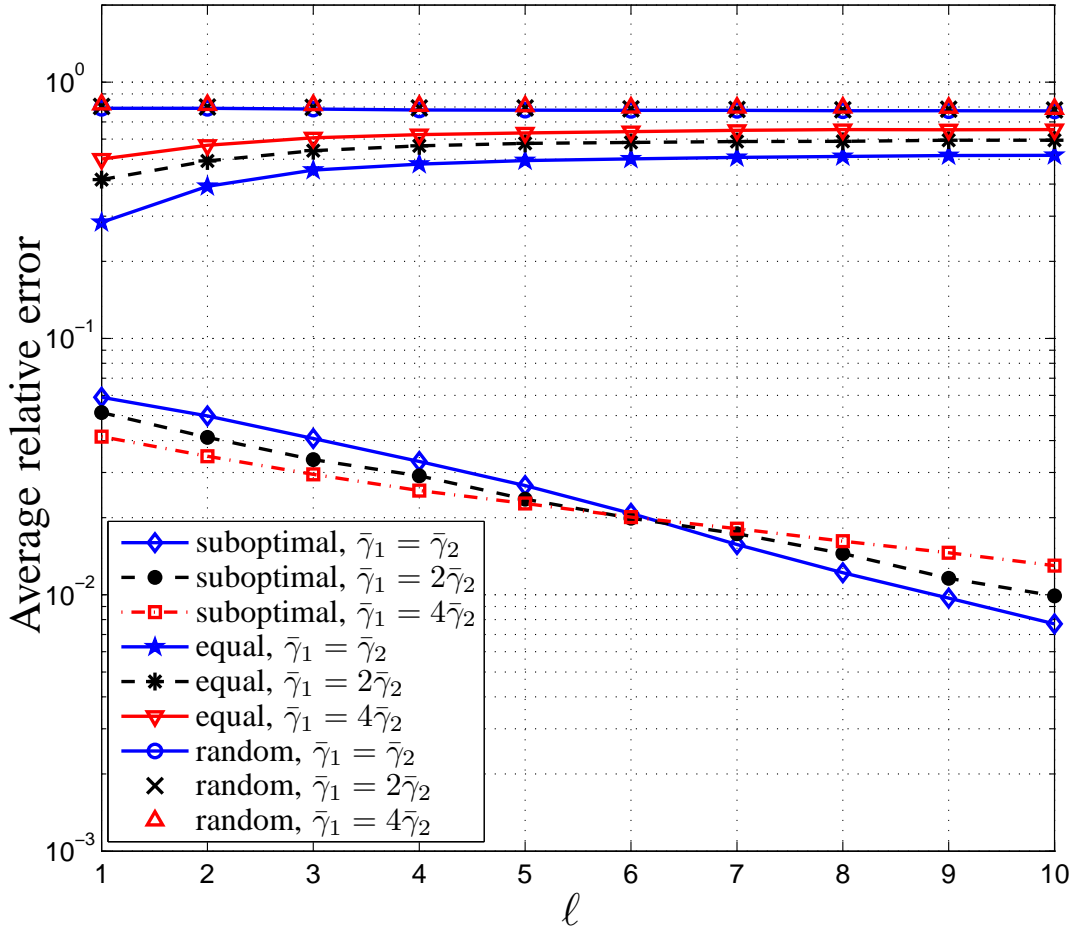
Figure 4.17: Average relative error of different resource allocation schemes (subcarrier & time slot allocation) with different average SNRs. $\bar{\gamma}_1 + \bar{\gamma}_2$ =30dB.

reduction of the end-to-end capacity. By contrast, the error of the proposed suboptimal scheme decreases when the value of ℓ rises, which implies that the proposed scheme can achieve better performance when ℓ is large. Moreover, among the three algorithms, the suboptimal one exhibits the lowest relative error. When $\ell \geq 9$, the error of the suboptimal scheme is lower than 0.001, while the one of the equal and random schemes is higher than 0.4.

The average relative error of the optimal power allocation is compared with the suboptimal, equal and random ones in Fig. 4.17 under different average SNRs of hops, i.e., $\bar{\gamma}_1 = \bar{\gamma}_2 = 15$dB, $\bar{\gamma}_1 = 2\bar{\gamma}_2 = 20$dB and $\bar{\gamma}_1 = 4\bar{\gamma}_2 = 24$dB. Similarly to the results in Fig. 4.16, the average relative error of the random allocation is constant under different scenarios. The error of the equal scheme slightly raises when $\bar{\gamma}_1/\bar{\gamma}_2$ increases. With different scenarios, the relative errors

of the proposed suboptimal scheme do not vary obviously. With the increasing of $\bar{\gamma}_1/\bar{\gamma}_2$, the error of suboptimal algorithm become low when $\ell < 6$; while when $\ell > 6$, the relative error slightly grows. In other words, when $\bar{\gamma}_1/\bar{\gamma}_2$ becomes large, the relative error of the suboptimal scheme approaches to constant with different ℓ.

Subcarrier & Power Allocation

In this part, the proposed allocation scheme which combines the subcarrier allocation in 4.4.1 and power allocation in 4.4.3 is evaluated. The total available transmit power, P_{tot}, is 1W. The time slot of each hop is the same and normalized to 1.

We compare the proposed suboptimal allocation scheme with two different allocation schemes to investigate the performance of it. One scheme is random allocation in which the subchannels and the subtotal power for each hop is assigned randomly. In this scheme, the subcarrier is first allocated using the random subcarrier scheme, then the subtotal transmission power also randomly assigns to each hop, i.e., $0 < \bar{P}_{\text{SR}}, \bar{P}_{\text{DR}}, \bar{P}_{\text{RD}}, \bar{P}_{\text{RS}} < P_{\text{tot}}$, and after that the power of each subcarrier is calculated by using waterfilling algorithm.

The other allocation scheme is equal allocation, in which both the overall subcarriers and transmission power are equally shared by the hops, i.e.

$$N_{\text{SR}} = N_{\text{DR}} = N_{\text{RD}} = N_{\text{RS}} = \frac{N}{2}, \tag{4.113}$$

and

$$\bar{P}_{\text{SR}} = \bar{P}_{\text{DR}} = \bar{P}_{\text{RD}} = \bar{P}_{\text{RS}} = \frac{1}{4}P_{\text{tot}}, \tag{4.114}$$

then the power of each subcarrier is also calculated by using waterfilling algorithm.

Fig. 4.18 compares the average balanced end-to-end capacities of the optimal and the suboptimal allocation scheme with different value of ℓ and average SNRs. From the figure, the balanced capacities of the optimal and suboptimal schemes grow with the increasing of the capacity ratio. In all cases, this feature is most obvious when $\bar{\gamma}_1 = \bar{\gamma}_2 = 25\text{dB}$. Moreover, when $\bar{\gamma}_1/\bar{\gamma}_2$ rises, the balanced capacity of both schemes becomes low, because the worse hop has to
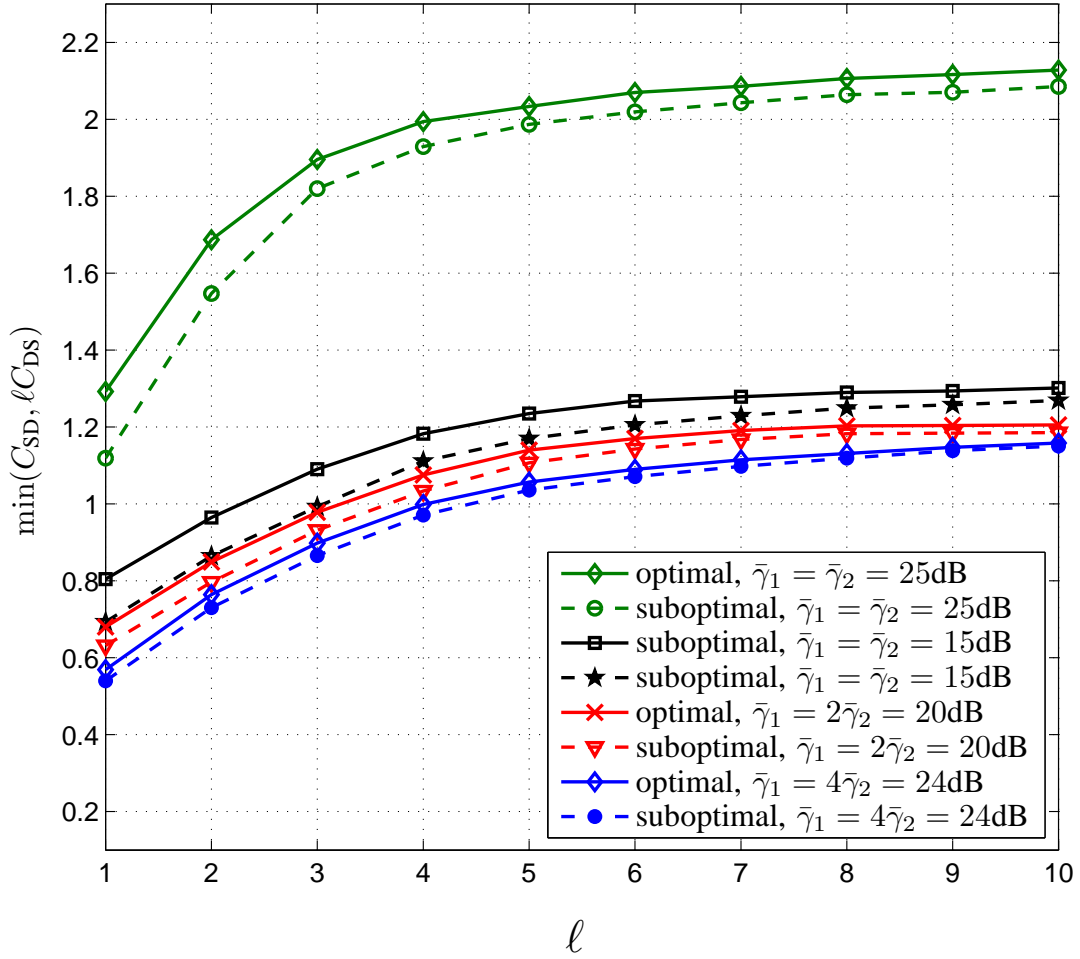
Figure 4.18: Average balanced end-to-end capacities of the optimal and suboptimal resource allocation (subcarrier & power allocation) vs. ℓ.

consume more resource to achieve the capacity balance. Furthermore, the balanced capacity of the suboptimal scheme is close to that of the optimal one with different values of ℓ, $\bar{\gamma}_1$ and $\bar{\gamma}_2$. It proves that the proposed suboptimal resource allocation algorithm can provider the similar performance with the optimal one with reduced complexity.

We present the average relative error of various allocation algorithms with different SNR in Fig. 4.19. The random allocation has the same average error with different value of $\bar{\gamma}$. And when ℓ increases, the error of the random scheme only has a slightly reduction. Similarly with the results of the subcarrier and time slot allocation in Fig. 4.16, the equal power allocation scheme also suffers the growth of the relative error when ℓ becomes large. Among the three algorithms, only the proposed suboptimal one provides a decreasing relative error with the in-
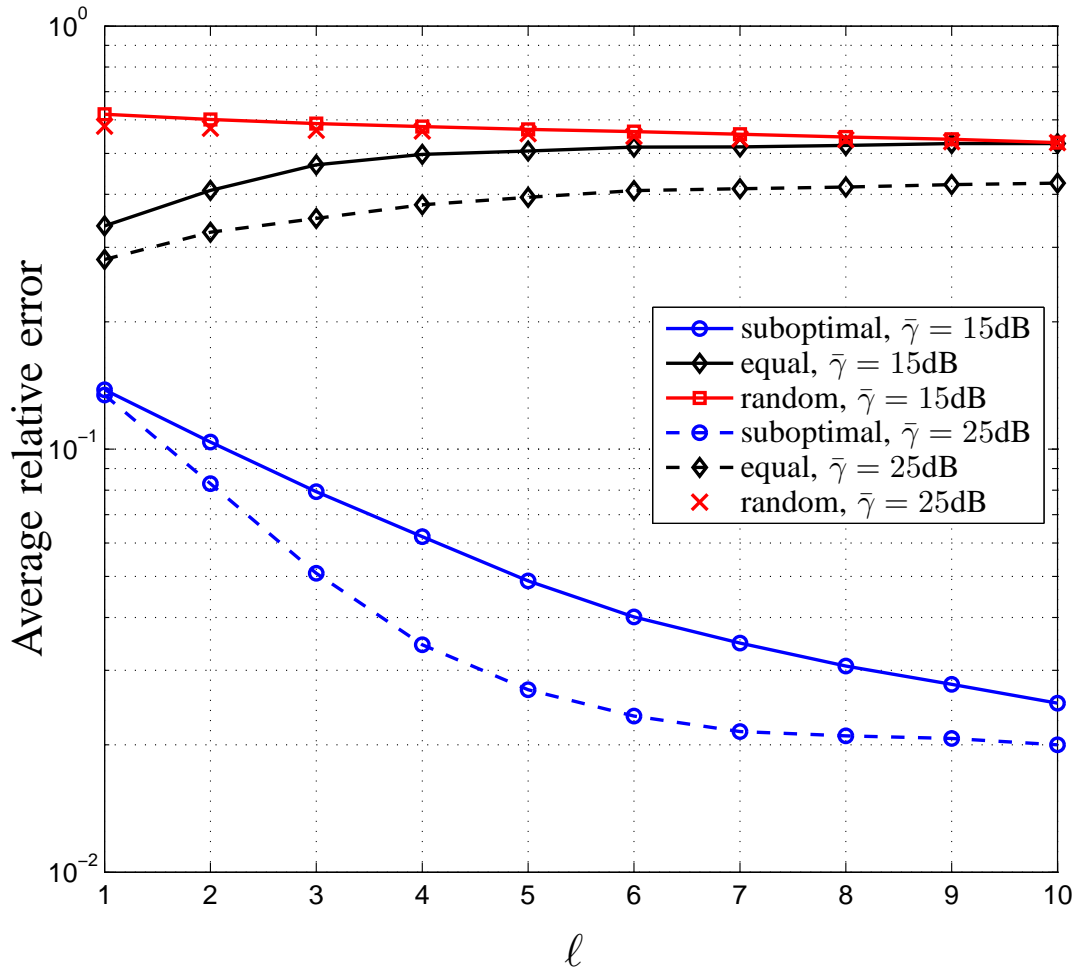
Figure 4.19: Average relative error of different resource allocation schemes (subcarrier & power allocation) vs. ℓ. $\bar{\gamma} = \bar{\gamma}_1 = \bar{\gamma}_2$=15, 25dB.

creasing of ℓ. Moreover, both equal and suboptimal algorithms can achieve a lower average error when $\bar{\gamma}$ raises. The suboptimal one exhibits the lowest relative error in the three algorithms which is always lower than 0.1 when $\ell > 2$, while the error of the equal and random schemes reach 0.4 when ℓ is large.

In Fig. 4.20, the average relative errors of different subcarrier allocation algorithms are compared under the scenario that the average SNR of each hop is different. Three cases are considered, i.e., $\bar{\gamma}_1 = \bar{\gamma}_2$ =15dB, $\bar{\gamma}_1 = 2\bar{\gamma}_2$ =20dB and $\bar{\gamma}_1 = 4\bar{\gamma}_4$ =24dB. In this figure, we can see that the balanced capacity of the random allocation scheme is the lowest in the three algorithms, and is not sensitive to the traffic load ratio and the channel condition of the two hops. On the other hand, the errors of the equal and the suboptimal algorithms rise when
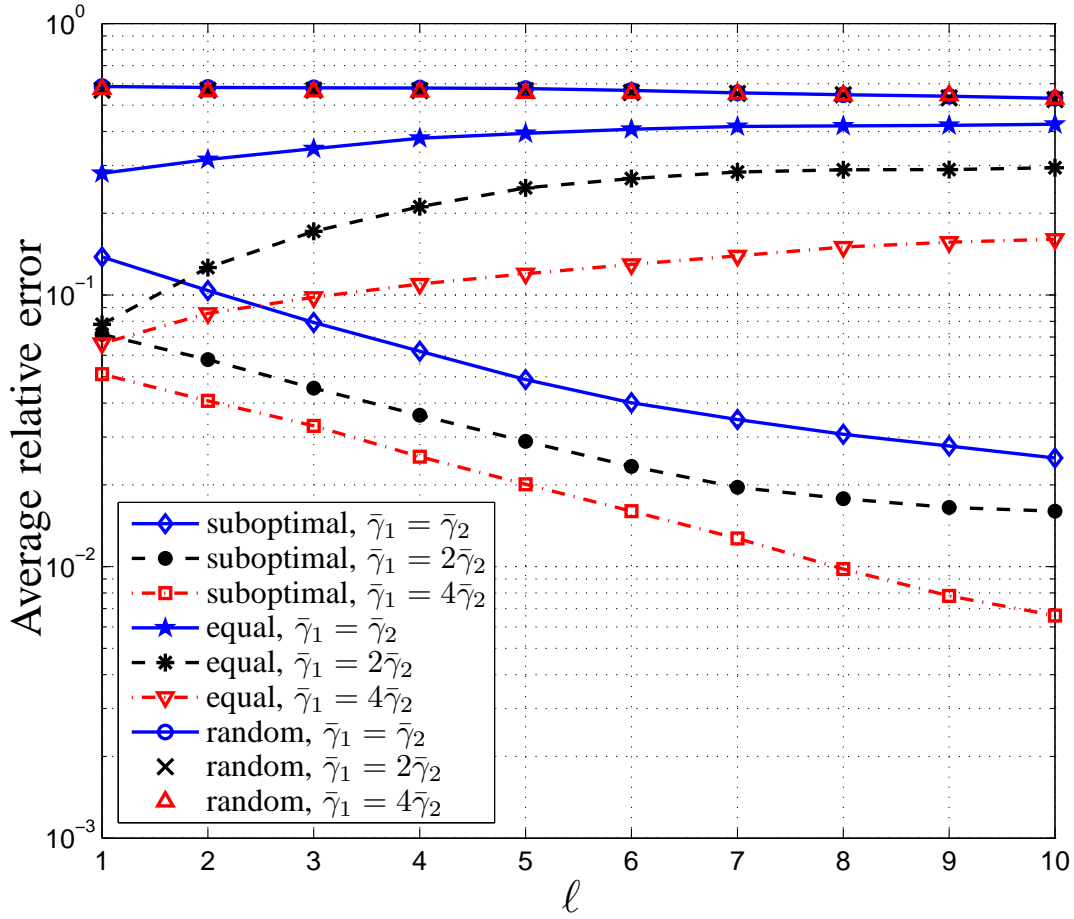
Figure 4.20: Average relative error of different resource allocation schemes (subcarrier & power allocation) with different average SNRs. $\bar{\gamma}_1 + \bar{\gamma}_2 =$30dB.

$\bar{\gamma}_1/\bar{\gamma}_2$ grows. When $\ell = 1$, the suboptimal and equal algorithms has similar average error with $\bar{\gamma}_1 = 2\bar{\gamma}_2$ and $\bar{\gamma}_1 = 4\bar{\gamma}_4$. However, when ℓ grows, the proposed suboptimal can provide the lower error, e.g., $e_{b,subopt} < 0.03$ with $\ell = 10$.

4.5 Summary

In this chapter, we have proposed two resource allocation scheme for two-way decode-and-forward relay systems with asymmetric traffic loads.

For the time-division two-way relay systems, the optimal resource allocation algorithm is introduced to maximize the total end-to-end capacity with the capacity constraint which de-

pends on the bidirectional asymmetric traffics. Both the time slot and the subcarrier power are optimized where the total transmission time and power is given. The performance of the proposed optimal allocation scheme is compared with different allocation schemes, including the random and equal allocations, by computer simulations. In order to combine the requirements of maximizing the end-to-end capacity and achieving the given capacity ratio, we defined a balanced end-to-end capacity as the performance metric. From the simulation results, the proposed allocation algorithm remarkably outperform the other schemes in different scenarios in terms of the balanced capacity, which verified the proposed one can significantly improve the system performance for the time-division two-way relay network with asymmetric traffic loads.

In the frequency-division two-way relay systems, where the two-way communication is performed by exploiting the orthogonality of the subcarriers in OFDM system. In this scenario, the S and D can simultaneously transmit signals to R by using different subcarriers. Three transmission resources are adaptively assigned, i.e., the subchannels, time slot and subcarrier power. However, since the subcarrier allocation is the discrete optimization problem, the complexity to solve this problem is extremely high, especially when the number of the subcarriers is large. Therefore, we proposed a suboptimal allocation scheme with low complexity, which separates the subcarrier and time/power allocation. The performance of the proposed scheme is evaluated and compared to the optimal and some other allocation schemes under different channel conditions. The results shows that the suboptimal scheme can provide better balanced end-to-end capacity then the random and equal allocations. Meanwhile, the proposed algorithm achieve the similar performance with optimal one. In some cases, the relative error of the suboptimal scheme can reach as low as 10^{-2}. It implies that the proposed suboptimal scheme can significantly reduce the complexity of adaptive resource allocation for two-way relay systems without the performance loss.

Chapter 5

Equalize-and-Forward Relay System

5.1   Introduction

In the related work on relay systems, most of attentions focus on the two most popular relay techniques, i.e., AF and DF protocols. The AF relay typically has lower complexity and less processing burden than a DF relay, while the DF relay can provide a higher quality of retransmission over fading channels and makes it possible to have flexible and adaptive communications for the source-relay and relay-destination links. However, both of them have obvious drawbacks, i.e. the low transmission reliability for AF and large relay latency for DF schemes.

Although the AF relay has a short processing delay, the channel condition of the AF relay link is rough because there is no channel compensation techniques at relay nodes. In traditional AF relay systems, the end-to-end channel condition of relaying links deteriorates substantially in broadband wireless systems using OFDM, where the aggregation of multipath propagation environment leads to accumulated frequency selectivity and delay spread. Since there is no channel compensation at AF relay node to alleviate the channel accumulation, the system performance of relay networks becomes a challenge. For OFDM systems, the end-to-end frequency-domain channel response becomes the product of the two-hop channels. Therefore the dynamic range of frequency-selective fading is significantly increased. This deteriorated channel condition caused the reduction of the transmission reliability of the relay link in the OFDM systems with the traditional AF relay. On the other hand, the overall channel impulse response from the source via the relay to the destination is the convolution of the impulse re-
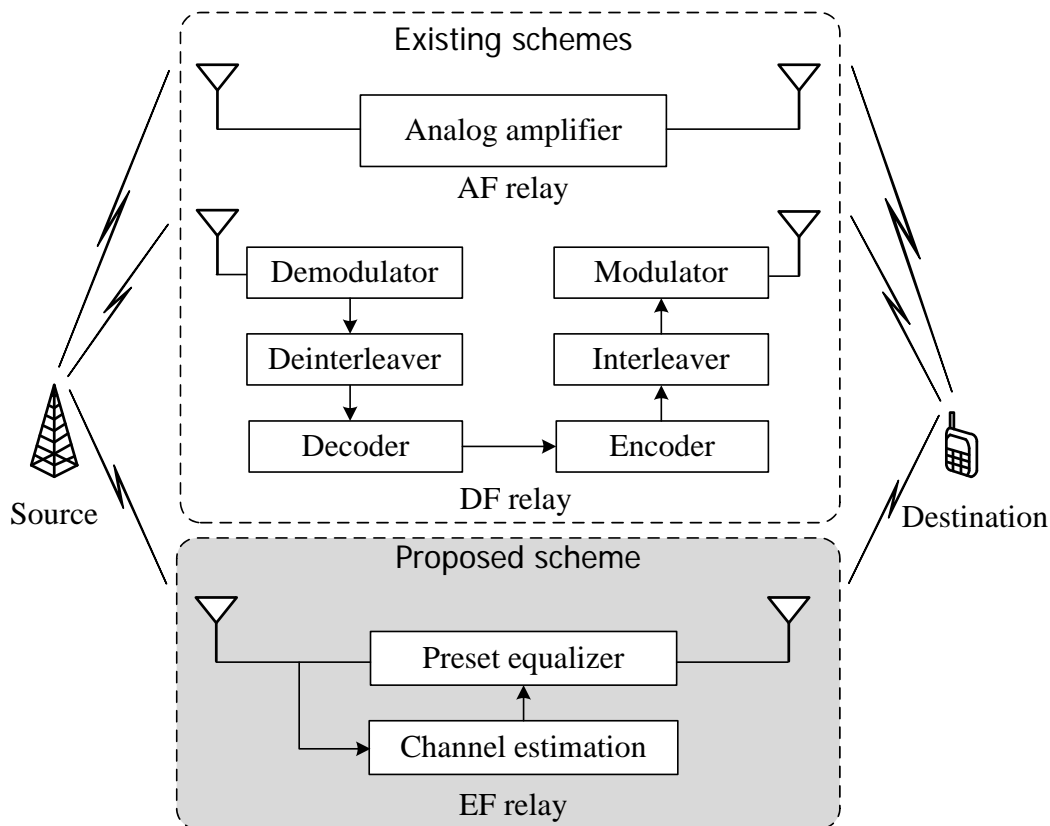
Figure 5.1: Illustration of AF, DF and the proposed EF structures.

sponses of the two-hop multipath channels in AF relay systems. As a result, the end-to-end delay spread increases proportionally to the number of relays [22], which results in further performance degradation when the overall channel delay spread is longer than the duration of cyclic prefix (CP) of OFDM signal.

Although the DF relay scheme can eliminate the accumulation effect of frequency selective fading, it requires a long additional processing delay from the required signal demodulation, decoding and regenerating at the relay node. For instance, the FFT/IFFT in OFDM-based systems will take over $15\mu s$ delay [26], and de/interleaving and de/encoding need even longer processing time. Furthermore, the relay has to retrieve all coded packets in an interleaved block before decoding in order to achieve the expected performance. This means that the aggregated processing time at the DF relay node cannot be neglected in the relay communications at all. The large delay overhead in DF scheme reduces the end-to-end transmission time utilization rate particularly in packet and interactive communications. Moreover, the stringent latency

requirement in the realtime and delay sensitive applications cannot tolerate high-complexity operations and long processing time of the multi-hop DF relay scheme.

In order to further improve the transmission reliability and minimal processing latency in relay communications, we propose a novel equalize-and-forward (EF) relay scheme. The structural differences among AF, DF and EF relays are illustrated in Figure 5.1. Compared to the traditional AF relay with an amplifier at relay node, the proposed EF relay scheme involves the equalization procedure to eliminate the multipath distortion between source and relay nodes. Meanwhile, the proposed EF relay achieves reduced processing latency at the relay node in comparison to the DF relay by avoiding the highly complex operations, e.g., demodulation, decoding, encoding and modulation. Furthermore, the proposed EF relay scheme has an efficient parallel structure, which can provide accurate equalization as well as limit the relay latency to accomplish the reduction of the overhead and multipath channel effect accumulation.

Some related work also adopted equalization techniques at the relay node [173–176]. A time-domain channel estimation scheme was proposed for the relay node in [173]. In [174–176], the equalizer exploited at relay node is designed for two-hop multiple-input multiple-output (MIMO) relay systems. Compared to AF relay scheme, these EF schemes also suffers the long processing delay, because they have to involve high-complexity operations for equalization and resource allocation algorithms. Moreover, the aforementioned techniques only consider improving the transmission reliability or rate, while the processing delay at the relay node caused by the highly complex processing and its effect on the overall system performance are largely ignored.

More specifically, the proposed EF relay estimates and equalizes the channel between source and relay to address the accumulation effect of frequency selective channels. To reduce the processing delay at relay nodes, channel estimation and equalization are performed in parallel. In the proposed EF scheme, the equalization efficiency is improved by passing data symbols through an equalizer preset with the current channel response, which is predicted by using multiple previous channel responses. The equalization is performed in time-domain to avoid the FFT/IFFT operations and minimize the processing time of the main path. Moreover, the equalization accuracy is enhanced by exploiting the model-based channel estimation and prediction to reduce the impact of background Gaussian noise and further improve the quality
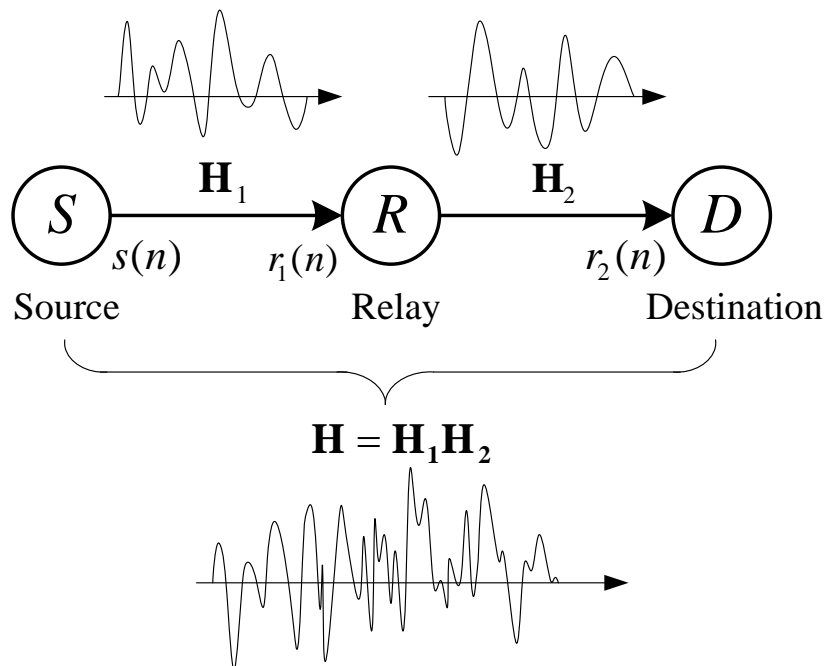
Figure 5.2: A two-hop relay system with accumulated multipath channels.

of retransmitted signals. Compared to the related work, the proposed scheme can

- exactly equalize the S−R channel with the accurate channel information to eliminate the accumulation of the multipath distortion, which can not be achieve by the traditional AF relay with a simple amplifier at relay node;

- accomplish reduced processing the processing latency at relay node in comparison to the DF relay by avoiding some highly complex operations and employing the novel parallel structure;

- increase the estimation accuracy and limit the processing delay of equalization under time-varying channels by adopting the parallel structure and the model-based channel prediction.

5.2   System Model

In this chapter, we consider a two-hop relay system as shown in Fig. 5.2 in which the source terminal S communicates with the destination terminal D via a single relay R. It is assumed that there is no direct link between the source and destination nodes. The transmission from

the source to destination involves two stages: S−R and R−D.

Denote that the channel S−R is $\mathbf{h}_1$ and the channel R−D is $\mathbf{h}_2$. The received signal at relay R is given by

$$r_1(n) = \sum_{l=0}^{L_1-1} h_1(l)s(n-l) + \omega_1(n), \tag{5.1}$$

where $\omega_1(n)$ is the AWGN term with variance σ_1^2. When the CP is long enough, the received signal at relay node can be written as

$$\mathbf{r}_1 = \mathbf{H}_1\mathbf{s} + \mathbf{w}_1, \tag{5.2}$$

where $\mathbf{H}_1$ is an $N \times N$ matrix given by

$$\begin{bmatrix} h_1(0) & \cdots & 0 & h_1(L_1-1) & \cdots & \cdots & h_1(1) \\ h_1(1) & \cdots & 0 & & h(L_1-1) & \cdots & h_1(2) \\ \vdots & \ddots & & & \ddots & \vdots & \vdots \\ h_1(L_1-1) & \cdots & h_1(0) & 0 & \cdots & \cdots & 0 \\ 0 & \cdots & h_1(1) & h_1(0) & \cdots & \cdots & 0 \\ \vdots & & \ddots & & \ddots & & \vdots \\ 0 & 0 & h_1(L_1-1) & \cdots & & h_1(1) & h_1(0) \end{bmatrix}, \tag{5.3}$$

$\mathbf{r}_1 = [r_1(0), r_1(1), \ldots, r_1(N-1)]^\mathrm{T}$, $\mathbf{s} = [s(0), s(1), \ldots, s(N-1)]^\mathrm{T}$ and $\mathbf{w}_1 = [\omega_1(0), \omega_1(1), \ldots, \omega_1(N-1)]^\mathrm{T}$.

In frequency domain, the N-size discrete Fourier transform (DFT) of the received signal $r_1(n)$ and channel impulse response $h_1(l)$ is denoted by

$$R_{1,k} = \sum_{n=0}^{N-1} r_1(n)e^{\frac{-j2\pi nk}{N}}, \tag{5.4}$$

and

$$H_{1,k} = \sum_{l=0}^{L_1-1} h_1(l)e^{\frac{-j2\pi lk}{N}}, \tag{5.5}$$

where $k = 0, 1, \ldots, N-1$ is the subcarrier index. The frequency-domain received signal at

relay is

$$R_{1,k} = H_{1,k}S_k + W_{1,k}, \tag{5.6}$$

where $\{S_k\}$ and $\{W_{1,k}\}$ are the DFT of $\{s(n)\}$ and $\{\omega_1(n)\}$.

If there is no channel compensation at the relay node, the frequency-domain received signal $R_{2,k}$ at destination D can be expressed by

$$\begin{aligned} R_{2,k} &= H_{2,k}H_{1,k}S_k + H_{2,k}W_{1,k} + W_{2,k} \\ &= H_{2,k}H_{1,k}S_k + W_k, \end{aligned} \tag{5.7}$$

where $\{R_{2,k}\}$ and $\{H_{2,k}\}$ are the DFT of $\{r_2(n)\}$ and channel $\mathbf{h}_2$ respectively; and $\{W_{2,k}\}$ is the DFT of white Gaussian noise $\{\omega_2(n)\}$ with variance $\sigma_2{}^2$. $W_k = H_{2,k}W_{1,k} + W_{2,k}$ is the overall noise with zero mean and variance $\sigma^2 = \sigma_1^2\sigma_{\mathbf{h}_1}^2 + \sigma_2^2$, where $\sigma_{\mathbf{h}_1}^2$ is the variance of channel $\mathbf{h}_1$.

In order to eliminate the accumulation of multipath channels as well as maintain a short relay latency, the proposed equalize-and-forward (EF) relay scheme whose block diagram is shown in Fig. 5.3 estimates and equalizes the channel between S and R. The proposed relay provides a transparent operation to assist the transmission between S and D, which means it does not requires any extra control signal or feedback from S and D. Denote that $\mathbf{G}$ is the relay amplification factor matrix with size $(N \times N)$. In the proposed EF relay, the time domain received signal at destination becomes

$$\mathbf{r}_2 = \mathbf{H}_2\mathbf{G}\mathbf{H}_1\mathbf{s} + \mathbf{H}_2\mathbf{G}\mathbf{w}_1 + \mathbf{w}_2 \tag{5.8}$$

where $\mathbf{H}_2$ with the same format of $\mathbf{H}_1$ is the channel matrix between R and D, and $\mathbf{w}_2$ is the noise vector. For the relay node, the channel $\mathbf{H}_1$ can be estimated from the pilot symbol transmitted by S, while the channel $\mathbf{H}_2$ is unknown because the relay node is transparent to the source and destination, thus there is not feedback from D to notice the channel information of $\mathbf{H}_2$.

To reduce the relay overhead, the structure of EF relay is designed with two parallel signal paths, i.e., main path and ancillary parallel path. The main signal path only includes minimum operations for the time-domain equalization, while parallel path performs the high complexity
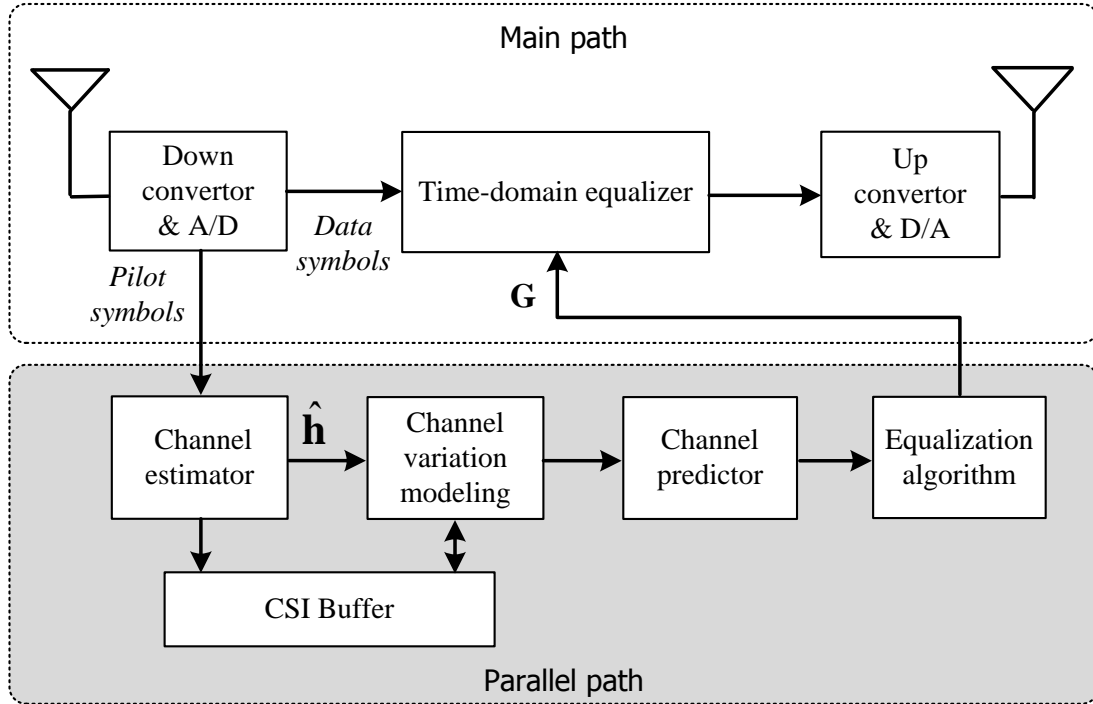
Figure 5.3: Block diagram of the proposed equalize-and-forward relay with the delay-efficient parallel structure .

operations which require long processing time, i.e., the channel estimation, prediction and equalizer coefficient generation. Pilot symbols are processed in the parallel path to estimate the channel $\mathbf{h}_1$. The current channel response is used to calculate the equalizer coefficients, which are sent to the main path to set the equalizer. In the main path, the received OFDM signals at the relay node pass through a time-domain equalizer which is preset by parallel path. The frequency-domain equalization is often applied in OFDM systems, however it requires FFT/IFFT operations which involve the extra processing time in the main path. Therefore, the proposed EF relay scheme adopts a time-domain equalizer to avoid the processing overhead of FFT/IFFT. After that, the equalized signals are forwarded to destination. The design of each block in the proposed relay is shown in Section 5.4.

5.3 Performance Impacts of Multi-hop Transmissions

The communication between the source and destination through the relaying link involve multi-hop transmission, which has fundamental impacts on the system performance in terms of trans-

(a) Accumulated frequency selectivity vs. the number of hops

(b) Symbol error probability vs. SNR
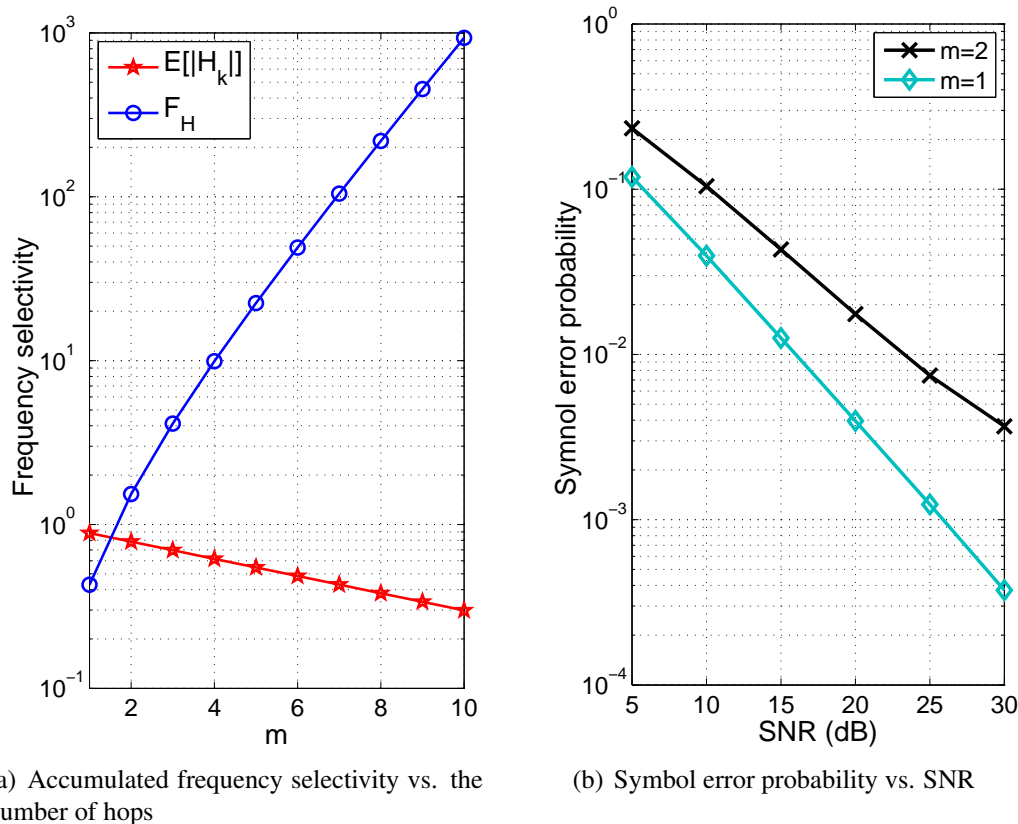
Figure 5.4: Effect of multi-hop transmissions on the channel characteristics and error probability.

mission reliability and efficiency. In the traditional AF scheme, the transmission reliability is impacted by the accumulated multipath channel in the multi-hop relaying, since there is no proper channel equalization scheme to mitigate the accumulation of multipath channels at relay nodes. In the DF relay scheme, the transmission efficiency (utilization rate of transmission time) of the end-to-end link is impaired by the multi-hop relay due to the additional processing delay involved at relay nodes.

5.3.1 Channel Accumulation

One of the major impacts from the accumulation of multipath channels is that the dynamic range of the frequency selectivity significantly increases. Without channel compensation techniques at the relay node, the end-to-end frequency response H_k becomes the product of the

channel of each hop when the CP length is sufficient, i.e.,

$$H_k = H_{1,k}H_{2,k}\ldots H_{M+1,k}, \qquad M = 1, 2, 3, \ldots, \tag{5.9}$$

where M is the number of relay nodes. We define the *frequency selectivity* of channel $|H_k|$ as the variance of $|H_k|$, i.e.,

$$F_H = \mathbb{E}[(|H_k| - \mathbb{E}[|H_k|])^2], \tag{5.10}$$

where $\mathbb{E}[\cdot]$ is the expectation.

We assume that the baseband channel tap coefficients $\{h_m(l)\}$, are mutually independent complex random variables whose amplitude follow the same Rayleigh distribution [2], $m = 1, 2, \ldots, M + 1$. The probability density function (PDF) of $|h_m(l)|$ is

$$f_{|h_m(l)|}(x) = \frac{2x}{\Upsilon_{m,l}} \exp(-\frac{x^2}{\Upsilon_{m,l}}), \qquad x \geq 0, \tag{5.11}$$

where $\Upsilon_{m,l} = \mathbb{E}[|h_m(l)|^2]$ is the power of the lth tap of $\mathbf{h}_m$. The application of DFT represents a linear transformation of jointly Gaussian random variables and yields jointly Gaussian random variables [170]. Thus, the frequency response of each subchannel also has a Rayleigh fading distribution [171], i.e.,

$$f_{|H_{m,k}|}(y) = \frac{y}{2\Upsilon_{L_m}} \exp(-\frac{y^2}{4\Upsilon_{L_m}}), \qquad y \geq 0, \tag{5.12}$$

where $\Upsilon_{L_m} = \sum_{l=0}^{L_m-1} \Upsilon_{m,l}$. The i-th moment of $|H_{m,k}|$ is

$$\begin{aligned} \mathbb{E}[|H_{m,k}^i|] &= \int_0^\infty \frac{y^{i+1}}{2\Upsilon_{L_m}} \exp(-\frac{y^2}{4\Upsilon_{L_m}})dy \\ &= \Upsilon_{L_m}^{i/2}\Gamma\left(\frac{i}{2} + 1\right), \end{aligned} \tag{5.13}$$

where $\Gamma(t) = \int_0^\infty x^{(t-1)}e^{(-x)}dx$.

Since the channel response of each hop is statistically independent, the expectation of $|H_k|$

can be given as

$$
\begin{aligned}
\mathbb{E}[|H_k|] &= \mathbb{E}[|H_{1,k}H_{2,k}\ldots H_{M+1,k}|] \\
&= \mathbb{E}[|H_{1,k}|]\mathbb{E}[|H_{2,k}|]\ldots\mathbb{E}[|H_{M+1,k}|] \\
&= (\Upsilon_{L_1}\ldots\Upsilon_{L_{M+1}})^{1/2}\Gamma^{M+1}(\frac{3}{2}),
\end{aligned}
\tag{5.14}
$$

where

$$
\Gamma(t) = \int_0^\infty x^{(t-1)}e^{(-x)}dx.
\tag{5.15}
$$

The frequency selectivity of the accumulated channel can be determined using

$$
\begin{aligned}
F_H &= \mathbb{E}[|H_k|^2] - \mathbb{E}^2[|H_k|] \\
&= \prod_{m=1}^{M+1}\mathbb{E}[|H_{m,k}|^2] - \prod_{m=1}^{M+1}\mathbb{E}^2[|H_{m,k}|] \\
&= (\Upsilon_{L_1}\ldots\Upsilon_{L_{M+1}})\left(\Gamma^{M+1}(2) - \Gamma^{2(M+1)}(\frac{3}{2})\right).
\end{aligned}
\tag{5.16}
$$

When the channel of each hop has the same power, i.e.

$$
\Upsilon_L = \Upsilon_{L_1} = \ldots = \Upsilon_{L_{M+1}},
$$

the expectation and frequency selectivity of the accumulated channel can be given by

$$
\mathbb{E}[|H_k|] = \Upsilon_L^{(M+1)/2}(\frac{\sqrt{\pi}}{2})^{(M+1)},
\tag{5.17}
$$

and

$$
F_H = 2^{(M+1)}\Upsilon_L^{(M+1)}[1 - (\frac{\pi}{4})^{(M+1)}].
\tag{5.18}
$$

From (5.16), it is implied that the frequency selectivity of the accumulated channel grows with the increased number of hops. Fig. 5.4(a) shows the effect of the accumulated multipath channel on the channel characteristics.

As shown in (5.7), the end-to-end frequency response H_k from source to destination becomes the combination of S → R and R → D channels. When the CP length is sufficient, the

end-to-end channel response is the product of M_h channels in frequency domain, i.e.,

$$H_k = H_{1,k}H_{2,k}\ldots H_{M+1,k}. \tag{5.19}$$

Hence, the distribution of $|H_k|$ is no longer Rayleigh distribution. When the number of cascaded channels equals to 2, the distribution of $|H_k|$ becomes a double-Rayleigh distribution [177]

$$f_{|H_k|}(y) = \frac{y}{4\Upsilon_{L_1}\Upsilon_{L_2}}K_0(\frac{y}{2\sqrt{\Upsilon_{L_1}\Upsilon_{L_2}}}), \tag{5.20}$$

where $K_i(\cdot)$ is the ith-order modified Bessel function of the second kind [178]. For $m \geq 3$, the distribution function can be generated by using the Meijer $\mathcal{G}$-function as [179]

$$f_{|H_k|}(y) = 2(\prod_{m=1}^{(M+1)} \Upsilon_{L_m})^{1/2}\mathcal{G}_{0,(M+1)}^{(M+1),0}\left((\prod_{m=1}^{(M+1)} \Upsilon_{L_m})^{-1}y^2 \mid_{\frac{1}{2},\cdots,\frac{1}{2}}^{-}\right). \tag{5.21}$$

The definition of the Meijer $\mathcal{G}$-function is given in [180].

Since the frequency selectivity of the end-to-end link is expanded by multi-hop transmissions, the system performance at destination deteriorates. Although the OFDM technique can combat the frequency-selective fading channel by achieving flat fading at each subchannel, the enlarged frequency selectivity still increases the probability that the deep fading occurs at each subchannel. Therefore, the large frequency selectivity degrades the reception performance at the destination. In order to gain insight into the impact from the accumulated channel impairments, the error probability over multi-hop channels is evaluated by averaging the conditional symbol error probability in AWGN channel over the fading distribution, as

$$P_e = \int_0^{\infty} P_e(\gamma)f_{|H_k|}(\gamma)d\gamma, \tag{5.22}$$

where $P_e(\gamma)$ is the error probability in AWGN.

Fig. 5.4(b) compares the error probabilities of single-hop and two-hop channels. From this figure, we can see that the transmission reliability of the two-hop links substantially degrades. Although the OFDM technique can combat the frequency-selective fading channel by achieving flat fading at each subchannel, the enlarged frequency selectivity still increases the
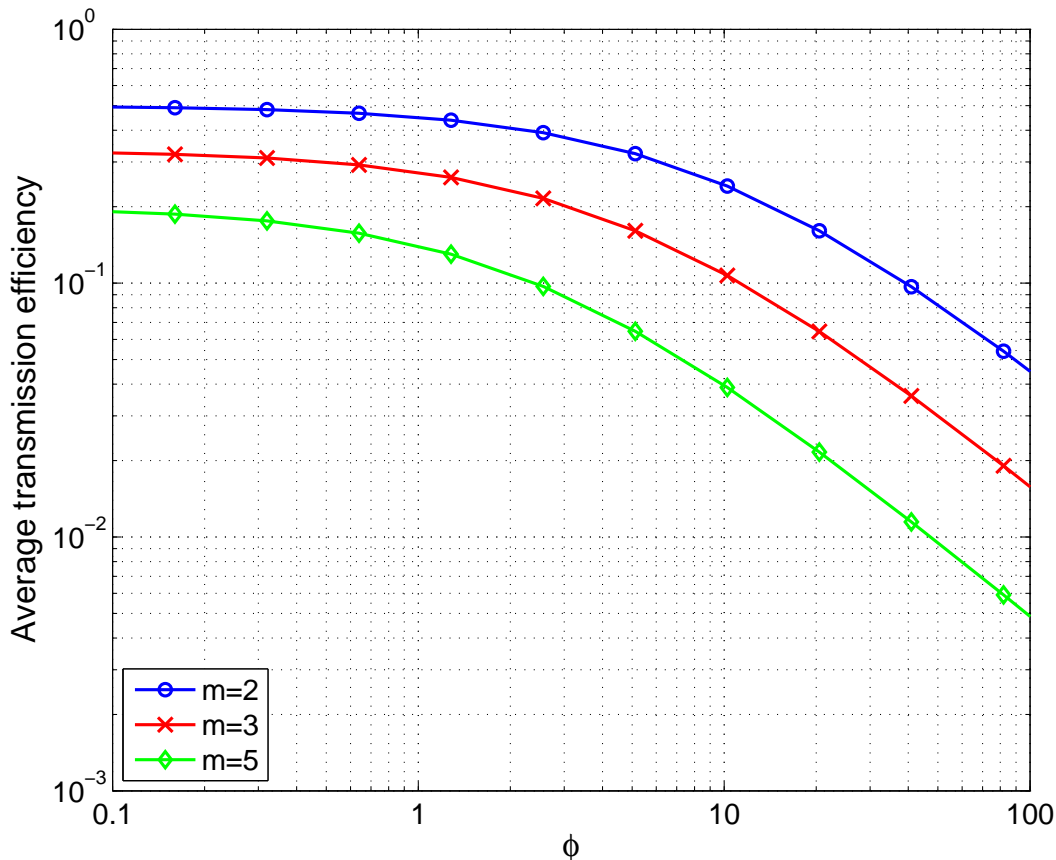
Figure 5.5: Average transmission efficiency vs. different relaying delay. The number of hop, *m*, is 2,3,5.

probability that the deep fading occurs at each subchannel. Therefore, the large frequency s-electivity degrades the reception performance at the destination, such as in the traditional AF scheme.

5.3.2   Transmission Efficiency

On the other hand, the transmission efficiency (utilization rate of transmission time) of the end-to-end link is also impaired by the multi-hop relay due to the additional processing delay involved at relay nodes. The large overhead at relay nodes causes a low efficiency of the overall transmission time utilization, especially for packet or burst transmissions [181] [182]. Moreover, the long processing delay introduces additional challenge in achieving stringent latency requirement in the delay sensitive communications, such as interactive and realtime communications.
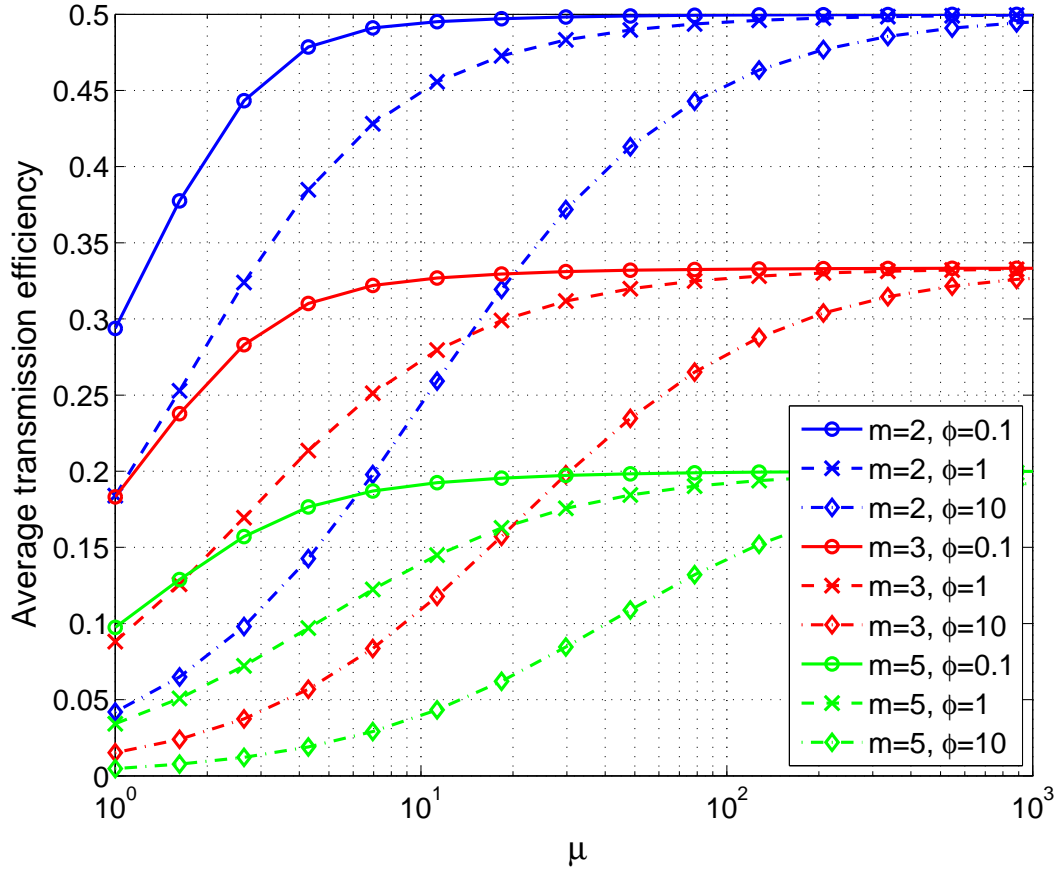
Figure 5.6: Average transmission efficiency vs. different average packet sizes. The number of hop, m, is 2,3,5. The relay delay T_d equals to $\{0.1, 1, 10\} \times T_s$.

Denote that the total end-to-end transmission time is T_{total}, which includes the data symbol transmission time of each hop and processing delay T_{d} of each relay. The end-to-end transmission efficiency can be defined as

$$\eta_{\text{T}} = \frac{qT_{\text{s}}}{T_{\text{total}}} = \frac{qT_{\text{s}}}{mqT_{\text{s}} + (m-1)T_{\text{d}}}, \quad (5.23)$$

where T_{s} is the symbol duration, and q is the number of symbols in a packet, $q = 0, 1, 2, \ldots$. With $T_{\text{d}} = \phi T_{\text{s}}$, the transmission efficiency becomes

$$\eta_{\text{T}} = \frac{q}{m(q + \phi) - \phi}, \quad (5.24)$$

where ϕ is a real number and $\phi > 0$.

For a general scenario, we assume that q is a random variable with Poisson distribution. Consequently, the average transmission efficiency becomes

$$\bar{\eta}_T = e^{-\mu} \sum_{q=0}^{\infty} \left(\frac{q}{m(q+\phi)-\phi} \right) \frac{\mu^q}{q!}, \tag{5.25}$$

where $q!$ is the factorial of q, and μ is the mean value of the number of symbols in a packet, $\mu > 0$.

In Fig. 5.5 and 5.6, the impact of the different relay delay and transmission packet size on the system efficiency respectively is elaborated. Fig. 5.5 shows that the transmission efficiency decreases as the relay delay increases. In particular, the efficiency sharply drops when $\phi > 1$, which means that high complexity and long processing time at relay node lead to the significant degradation of the efficiency, such as in DF relay. Fig. 5.6 shows the transmission efficiency vs. different transmission packet size. From this figure, it is clear that in continuous communications, i.e., $\mu \to \infty$, the efficiency $\bar{\eta}_T \to \frac{1}{m}$; and relay schemes with different delay provide the same performance. However, the relay nodes with long delay overhead, i.e., $\phi = 10$, incurs a poor efficiency performance in small packet communications, which usually happens in the burst and interactive communications.

Based on the discussions above, it becomes clear that the performance of a relay system is affected by both accumulated multipath channels and the processing delay of relay nodes. Therefore, two requirements of the relay scheme design, i.e., the multipath distortion compensation and reasonable processing delay, have to be addressed to overcome the current difficulties of AF and DF schemes.

5.4   Equalize-and-Forward Relays Design

The major design objectives of the proposed equalize-and-forward relay scheme is to eliminate the accumulation of multipath channels as well as maintain a short relay latency.

The processing delay of relay nodes is caused by the high complexity operations which require long processing time, i.e., the channel estimation, prediction and equalizer coefficient generation. If the frequency-domain equalization is performed, the FFT/IFFT operations will

involve the extra processing time. Therefore, the structure of the propose EF relay scheme is separated into two two parallel signal paths to reduce the relay overhead. As shown in Fig. 5.3, parallel path includes the operations which lead to long processing latency, while the main path only includes minimum operations for equalization. Moreover, the proposed EF relay scheme adopts a time domain equalizer to avoid the processing overhead of FFT/IFFT. This new parallel structure can minimize the relaying delay for each relay slot, and therefore shorten the relay overhead.

The other design challenge addressed in the proposed relay scheme is the equalizer performance in the main path due to the channel estimation noise in the parallel path. Denote that $\mathbf{G}$ is the relay amplification factor matrix with size $(N \times N)$, $\mathbf{r}_2$ is the received signal vector at the destination, $\mathbf{H}_2$ is the channel matrix between the relay and destination with the same format of $\mathbf{H}_1$, and $\mathbf{w}_2$ is the noise vector. For the relay node, the channel $\mathbf{H}_1$ can be estimated from the pilot symbol transmitted by S, while the channel $\mathbf{H}_2$ is unknown because the relay node is transparent to the source and destination, thus there is not feedback from D to notice the channel information of $\mathbf{H}_2$. In the proposed EF relay, $\mathbf{G}$ is optimized to remove the multipath channel S $\rightarrow$ R, i.e.,

$$
\begin{aligned}
\mathbf{r}_2 &= \mathbf{H}_2 \mathbf{G} \mathbf{H}_1 \mathbf{s} + \mathbf{H}_2 \mathbf{G} \mathbf{w}_1 + \mathbf{w}_2 \\
&\approx \mathbf{H}_2 \mathbf{s} + \mathbf{w}_{\text{total}}.
\end{aligned}
\tag{5.26}
$$

In (5.26), the total noise $\mathbf{w}_{\text{total}}$ mainly comes from signal propagation environments and equalization errors. The EF relay environmental noise includes the white Gaussian noise in wireless channels and thermal noise from analog front-ends which both can be controlled in a reasonable low range in practical devices. While the channel equalization and estimation error introduce the major challenge to overcome in relay scheme design especially under time-varying channels. To enhance the estimation accuracy, a channel variation model is utilized to exploit multiple past channel estimations. This model is also used to predict the current channel response to compensate the processing delay of the parallel path.
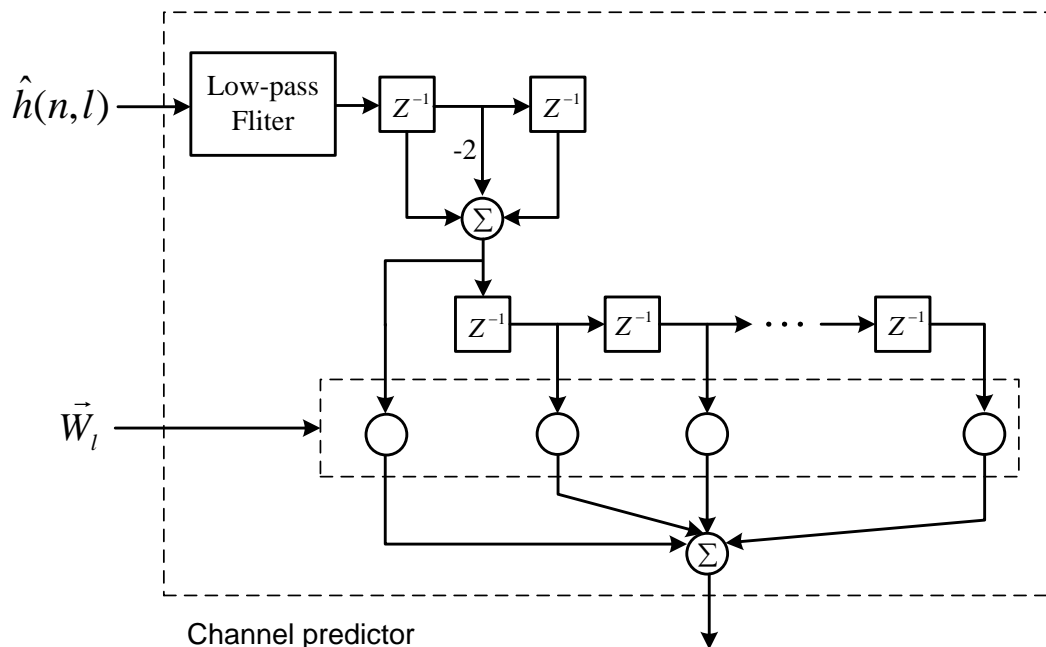
Figure 5.7: Predictor Structure.

5.4.1   Channel Estimation and Prediction for the EF Relay

As mentioned, the performance of the proposed EF relay is sensitive to the equalization error caused by channel estimation error and noise. The channel estimation from a single pilot symbol cannot guarantee high estimation accuracy due to channel variation and background noise. Therefore, the modeled-based channel estimation and prediction procedure are exploited here to improve the performance of the EF relay. Although the channel response is time-varying, it has been observed in [183] that the model for channel variation remains stable for a sufficiently long time. This property can be exploited to improve the accuracy of channel estimation based on multiple pilot symbols. The channel variation model also can be used to predict the channel response in the absence of pilot symbols.

Although existing channel estimators are performed in the frequency-domain in OFDM systems [184, 185], time-domain techniques in channel estimation and prediction have shown to be an attractive alternative to frequency-domain ones [183, 186]. The time-domain technique adopted in this paper requires estimation of fewer parameters than in frequency domain, which significantly decreases the complexity of signal processing at relay node.

The complex baseband representation of the time-varying multipath channel is given as

$$h(t, \tau) = \sum_{l=0}^{L-1} a_l(t)\delta(\tau - \tau_l(t)), \tag{5.27}$$

where $\tau_l(t)$ is the delay spread, $a_l(t)$ is the complex amplitude of the lth multipath tap, and L is the number of propagation paths. We consider a Wide Sense Stationary - Uncorrelated Scattering (WSSUS) channel, which implies that the channel correlation is dependent only on the time difference Δt in the time domain and the multipath components are uncorrelated in the delay domain [187]. Therefore, the Doppler shift and the channel variation of different multipath taps are uncorrelated. In time domain, the variation of a given multipath component, that experiences a Doppler shift of f_d Hz, is:

$$h(n, l) = h(l)e^{j2\pi f_d(l)n}, \tag{5.28}$$

where n is the discrete-time index, and the channel envelope $h(l)$ remains invariant over a number of symbols. The current channel can be generated by a linear filter as shown in Fig. 5.7, which linearly combines the past channel impulse responses as follows,

$$h(n, l) = \sum_{q=1}^{Q_p} W_p(q, l)h(n - q, l), \tag{5.29}$$

where $\overrightarrow{W}_l = \{W_p(q, l)\}$ is the coefficient set, and Q_p is the modeling order. To further eliminate the effect of noise, the channel variation rate is used in the predictor instead of the channel impulse responses to built the channel variation model [183], which is defined as

$$\Delta^2 h(n, l) = h(n + 2, l) - 2h(n + 1, l) + h(n, l). \tag{5.30}$$

The coefficient set $\overrightarrow{W}_l$ is determined to minimize the mean square error (MSE) between the estimated channel $\hat{h}$ and the actual channel, i.e.,

$$\text{MSE} = \mathbb{E}[|h(n) - \hat{h}(n)|^2], \tag{5.31}$$

as [188]:

$$\mathbf{c}_l = R_{\Delta^2}^{-1} r_{\Delta^2}, \tag{5.32}$$

where

$$R_{\Delta^2}(i, j) = E[\Delta^2 \hat{h}(n - 1 - i, l)\Delta^2 \hat{h}^*(n - 1 - j, l)] \tag{5.33}$$

is the correlation matrix, calculated for the lth multipath component, and

$$r_{hh}(i) = E[\Delta^2 \hat{h}(n - i, l)\Delta^2 \hat{h}^*(n, l)] \tag{5.34}$$

is the cross-correlation vector between past and current channel variation rate.

To reduce the equalization induced latency, the equalizer coefficients are preset by the parallel path before the data symbol is received. Therefore, the equalizer coefficients are calculated based on the past CSI instead of the current one. When the channel coherence time is short (fast-varying channels), the channel response may vary between two available pilot symbols for channel estimations. In addition, the processing delay in the parallel path also needs to be compensated during the equalizer presetting in order to improve the equalization accuracy. Hence, a predictor is exploited to update the channel response according to the processing delay of parallel path. The channel response $\hat{\mathbf{h}}(t + \Delta t)$ is predicted from the past channel response $\hat{\mathbf{h}}(t)$ in the absence of latest pilot symbols, where Δt includes the signal propagation time difference t_p between the main path and the parallel path and the prediction range t_r, i.e., $\Delta t = t_p + t_r$. The processing time difference t_p can be self determined since it is a constant for a given device.

The current channel response can then be given by

$$\hat{h}(n + \Delta t, l) = \sum_{q=1}^{Q} c_l(q)\hat{h}(n + \Delta t - q, l). \tag{5.35}$$

When the channel varies slowly, the model can be simplified as

$$\hat{h}(n, l) = \frac{1}{Q} \sum_{q=1}^{Q} \hat{h}(n - q, l). \tag{5.36}$$

5.4.2   Equalization Algorithm with Power Constraint for the EF Relay

With the model-based estimation and predication, we can obtain the current channel impulse response $\hat{\mathbf{h}}_1$. The estimated channel response is exploited to create the equalizer coefficients based on an equalization algorithm. Unlike the traditional equalizer at destination, a relay as a transceiver is usually under a power constraint. Therefore, we consider the equalization algorithm subject to a power constraint for the EF relay.

Denote that the retransmitted signal vector at relay is $\mathbf{y} = [y(0), y(1), \ldots, y(N-1)]^{\mathrm{T}}$. Then the retransmitted signal can be written in the following matrix form

$$\mathbf{y} = \mathbf{GH}_1\mathbf{s} + \mathbf{Gw}_1, \tag{5.37}$$

The retransmitted power can be determined by

$$P_{\text{tot}} = \mathbb{E}[\mathbf{y}^{\mathrm{H}}\mathbf{y}], \tag{5.38}$$

where $(\cdot)^{\mathrm{H}}$ denotes the conjugate transpose operation.

The coefficients of the equalizer are adjusted to minimize the error between the transmitted signal by source and retransmitted signal by relay, i.e., $\mathbf{e} = \mathbf{y} - \mathbf{s}$. The minimum mean squared error (MMSE) algorithm with a power constraint is defined as

$$\mathbf{G}_{\text{opt}} = \arg\min_{\mathbf{G}} \ \mathbb{E}[|\mathbf{y} - \mathbf{s}|^2]$$
$$\text{subject to } \mathbb{E}[\mathbf{y}^{\mathrm{H}}\mathbf{y}] = P_{\text{tot}}. \tag{5.39}$$

Since the problem in (5.39) is convex [189], we can formulate the Lagrangian problem as

$$
\begin{aligned}
\mathcal{L}(\mathbf{G}, \lambda) =& \mathbb{E}[|\mathbf{y} - \mathbf{s}|^2] + \lambda(\mathbb{E}[\mathbf{y}^\mathrm{H}\mathbf{y}] - P_{\text{tot}}) \\
=& \mathbb{E}[(\mathbf{GH}_1\mathbf{s} + \mathbf{w}_1 - \mathbf{s})^\mathrm{H}(\mathbf{GH}_1\mathbf{s} + \mathbf{w}_1 - \mathbf{s})] \\
& + \lambda(\mathbb{E}[(\mathbf{GH}_1\mathbf{s} + \mathbf{w}_1)^\mathrm{H}(\mathbf{GH}_1\mathbf{s} + \mathbf{w}_1)] - P_{\text{tot}}) \\
=& \mathrm{tr}(\sigma_s^2\mathbf{H_1}^\mathrm{H}\mathbf{G}^\mathrm{H}\mathbf{GH}_1 - \sigma_s^2\mathbf{G}^\mathrm{H}\mathbf{H}_1^\mathrm{H} \\
& + \sigma_1^2\mathbf{G}^\mathrm{H}\mathbf{G} - \sigma_s^2\mathbf{H}_1\mathbf{G}) - \sigma_s^2 + \sigma_1^2 \\
& + \lambda(\mathrm{tr}(\sigma_s^2\mathbf{H}_1^\mathrm{H}\mathbf{G}^\mathrm{H}\mathbf{GH}_1 + \sigma_1^2\mathbf{G}^\mathrm{H}\mathbf{G}) - P_{\text{tot}}),
\end{aligned}
\tag{5.40}
$$

where σ_s^2 is the average symbol energy transmitted by source, λ is a Lagrangian multiplier, and $\mathrm{tr}(\cdot)$ is the trace operation. Taking the gradient of (5.40) in terms of $\mathbf{G}$ and equating it to zero

$$
\nabla_\mathbf{G}\mathcal{L}(\mathbf{G}, \lambda) = 0,
\tag{5.41}
$$

we obtain

$$
\mathbf{G} = \frac{1}{(1 + \lambda)}\sigma_s^2\mathbf{H}_1^\mathrm{H}(\sigma_s^2\mathbf{H}_1^\mathrm{H}\mathbf{H}_1 + \sigma_1^2)^{-1}.
\tag{5.42}
$$

The value of λ is found out by substituting (5.42) into the power constraint equation, i.e., $\mathbb{E}[\mathbf{y}^\mathrm{H}\mathbf{y}] = P_{\text{tot}}$. Then we have

$$
\lambda = \frac{\pm\sigma_s^2\sqrt{\sigma_1^2\|\mathbf{H}_1\|_\mathrm{F}^2 + \sigma_s^2\|\mathbf{H}_1^\mathrm{H}\mathbf{H}_1\|_\mathrm{F}^2}}{\sqrt{P_{\text{tot}}}(\sigma_s^2\|\mathbf{H}_1\|_\mathrm{F}^2 + \sigma_1^2)} - 1,
\tag{5.43}
$$

where $\|\cdot\|_\mathrm{F}$ denotes the Frobenius norm of the matrix. By substituting (5.43) in (5.42), the optimal coefficient matrix $\mathbf{G}_{\text{opt}}$ can be solved as

$$
\mathbf{G}_{\text{opt}} = \frac{\sqrt{P_{\text{tot}}}(\sigma_s^2\|\mathbf{H}_1\|_\mathrm{F}^2 + \sigma_1^2)\mathbf{H}_1^\mathrm{H}}{\sqrt{\sigma_1^2\|\mathbf{H}_1^\mathrm{H}\|_\mathrm{F}^2 + \sigma_s^2\|\mathbf{H}_1^\mathrm{H}\mathbf{H}_1\|_\mathrm{F}^2}}(\sigma_s^2\mathbf{H}_1^\mathrm{H}\mathbf{H}_1 + \sigma_1^2)^{-1}.
\tag{5.44}
$$

The overall equalization algorithm can be described as follow,

1. The channel impulse response $\hat{\mathbf{h}}_1(n)$ is estimated through the cross correlation of the received signal $\mathbf{r}_1$ and the pilot, and send to channel information buffer.

2. The time-domain equalizer is set with the coefficients trained by the proposed equalization algorithm.

3. The current channel is estimated according to the past channel impulse response in the buffer, i.e., $\hat{\mathbf{h}}(n), \hat{\mathbf{h}}(n-1), \ldots, \hat{\mathbf{h}}(n-Q_p)$.

4. The accommodated channel impulse response $\tilde{\mathbf{h}}(n)$ is calculated by the time-domain predictor with the value of time delay parameter Δt.

5. If the channel variation is $\Delta\mathbf{h} = \frac{|\tilde{\mathbf{h}}(n)-\hat{\mathbf{h}}(n)|}{\hat{\mathbf{h}}(n)}$ is smaller than a certain threshold value for judging channel variation, regenerate equalization coefficients with the update channel impulse response $\tilde{\mathbf{h}}(n)$. Otherwise, regenerate the coefficients with the average of past channel impulse response. Then return to Step 2 to reset the equalizer.

The complexity and processing delay of the proposed EF relay scheme are higher than the traditional AF relay due to the involvement of the equalization operation. However, the elimination of decoding and signal regeneration through encoding and modulation significantly reduces the relay processing delay in the EF scheme, when compared with conventional DF system. In addition, the delay of the EF relay is further minimized by exploiting the parallel structure to a reasonable range compared to the relatively long delay of OFDM-based AF relay in [68, 69] which adjusts the amplification gain for each subchannel. Moreover, the improvement of the end-to-end SNR with the proposed relay scheme can support a higher data rate which compensates the effect of relaying delay.

5.5 Performance Evaluation

In this section, the performance of the proposed EF relay is analysed and compared with AF and DF schemes.

As we analysed in Section 5.3, the overall performance of a relay network is not only impacted by error probability at destination, but also the transmission efficiency which depends on the relaying delay. We therefore adopt the outage probability with effective data rate as the metric to comprehensively compare the performance of various relay schemes. Denote that the

size of the packet send from source to destination is L_p bit, and the transmission data rate R_d bit per second is

$$R_d = \frac{L_p}{T_{total}}, \tag{5.45}$$

where the end-to-end transmission time T_{total} includes the data symbol transmission time and the relay delay T_d. Obviously, with a constant T_{total}, the growing of the delay T_d will affect the available data transmission time. Hence, we define an *effective data rate* as

$$R_e = \frac{L_p}{T_{total} - T_d}. \tag{5.46}$$

The analysis of the outage probability with the effective data rate can provide a comprehensive evaluation of the performance of the relay schemes with different retransmission quality and relaying delay.

From (5.26), we can drive the end-to-end SNR of kth subchannel from source via relay to destination as

$$
\begin{aligned}
\gamma_k &= E\left[\left|\frac{H_{2,k}G_kH_{1,k}S_k}{H_{2,k}G_kW_{1,k} + W_{2,k}}\right|^2\right] \\
&= E\left[\left|\frac{\frac{H_{2,k}S_k}{W_{2,k}}\frac{H_{1,k}S_k}{W_{1,k}}}{\frac{H_{2,k}S_k}{W_{2,k}} + \frac{S_k}{W_{1,k}G_k}}\right|^2\right],
\end{aligned}
\tag{5.47}
$$

where G_k is the equivalent equalization coefficient of each subchannel in frequency domain. For a fair comparison between various relay schemes, we assume that the ideal instantaneous CSI of $\mathbf{h}_1$ is available at the relay node.

With the ideal channel information, the EF relay node can completely remove the multipath channel S→ R. Thus, the equalizer weight G_k can be simplified as $G_k = \frac{1}{H_{1,k}}$. The end-to-end SNR of the EF relay link becomes

$$
\gamma_{EF_k} = E\left[\left|\frac{\frac{H_{2,k}S_k}{W_{2,k}}\frac{H_{1,k}S_k}{W_{1,k}}}{\frac{H_{1,k}S_k}{W_{1,k}} + \frac{H_{2,k}S_k}{W_{2,k}}}\right|^2\right] = \frac{\gamma_{1,k}\gamma_{2,k}}{\gamma_{1,k} + \gamma_{2,k}},
\tag{5.48}
$$

where $\gamma_{i,k} = |H_{i,k}|^2\sigma_s^2/\sigma_i^2$, $i = 1, 2$.

In the fixed-gain AF relay scheme, the amplification factor G keeps the same for all sub-

channels, which is defined as

$$G = \sqrt{\frac{\sigma_s^2}{\sigma_s^2 \sum_{l=0}^{L_1-1} E[|h_1(l)|^2] + \sigma_1^2}}. \tag{5.49}$$

The end-to-end SNR of the AF relay link can be written as

$$\gamma_{\text{AF}_k} = E\left[\left|\frac{\frac{H_{2,k}S_k}{W_{2,k}} \frac{H_{1,k}S_k}{W_{1,k}}}{\frac{H_{2,k}S_k}{W_{2,k}} + \frac{S_k}{W_{1,k}G}}\right|^2\right] = \frac{\gamma_{1,k}\gamma_{2,k}}{\gamma_{2,k} + C_{\text{AF}}}, \tag{5.50}$$

where C_{AF} is a constant, $C_{\text{AF}} = \sigma_s^2/(|G|^2\sigma_1^2)$.

Since the frequency response of each subchannel $|H_{i,k}|$ is a Rayleigh random variable, $|H_{i,k}|^2$ has a chi-squared probability distribution with two degrees of freedom. Consequently, $\gamma_{i,k}$ also is chi-square distributed, i.e.,

$$p_{\gamma_{i,k}}(\gamma) = \frac{1}{\bar{\gamma}_i} e^{-\gamma/\bar{\gamma}_i}, \qquad \gamma > 0, \tag{5.51}$$

where $\bar{\gamma}_i$ is the average SNR of the ith hop.

If the S→R and R→D links are identical, i.e., $\bar{\gamma}_1 = \bar{\gamma}_2 = \bar{\gamma}$, the PDF, $p_{\gamma_{\text{EF}}}(\gamma)$, and moment generating function (MGF), $M_{\gamma_{\text{EF}}}(\alpha)$, of γ_{EF_k} are expressed by [190]

$$p_{\gamma_{\text{EF}}}(\gamma) = \frac{2}{\bar{\gamma}^2}\gamma e^{-\frac{2\gamma}{\bar{\gamma}}}[2K_1(\frac{2\gamma}{\bar{\gamma}}) + 2K_0(\frac{2\gamma}{\bar{\gamma}})], \qquad \gamma > 0, \tag{5.52}$$

and

$$M_{\gamma_{\text{EF}}}(\alpha) = \frac{\sqrt{\frac{\bar{\gamma}}{4}\alpha(\frac{\bar{\gamma}}{4} + 1)} + \arcsin(\sqrt{\frac{\bar{\gamma}}{4}\alpha})}{2\sqrt{\frac{\bar{\gamma}}{4}\alpha}(\frac{\bar{\gamma}}{4}\alpha + 1)^{3/2}}. \tag{5.53}$$

The OFDM-based AF relay which applies a different amplification factor for each subchannel has the same end-to-end SNR with the proposed EF relay scheme, therefore it drives the same PDF and MGF with the EF relay scheme.

For AF relay, the PDF and MGF of γ_{AF_k} can be given by [191]

$$p_{\gamma_{\text{AF}}}(\gamma) = \frac{2}{\bar{\gamma}^2}e^{-\frac{2\gamma}{\bar{\gamma}}}[\frac{\sqrt{C_{\text{AF}}\gamma}}{\bar{\gamma}}K_1(\frac{\sqrt{C_{\text{AF}}\gamma}}{\bar{\gamma}}) + \frac{C_{\text{AF}}}{\bar{\gamma}}K_0(\frac{\sqrt{C_{\text{AF}}\gamma}}{\bar{\gamma}})], \tag{5.54}$$

and

$$M_{\gamma_{AF}}(\alpha) = \frac{1}{(\bar{\gamma}\alpha + 1)} + \frac{C_{AF}\bar{\gamma}\alpha \exp(C_{AF}/(\bar{\gamma}^2\alpha + 1))}{\bar{\gamma}(\bar{\gamma}\alpha + 1)^2}\mathcal{E}_1(\frac{C_{AF}}{\bar{\gamma}^2\alpha + \bar{\gamma}}),\qquad(5.55)$$

where $\mathcal{E}_1(\cdot)$ is the exponential integral function.

In a DF relay system, errors at the destination occur either when the S→R transmission is received correctly and the R→D transmission is received in error, or when the S→R transmission is received in error and the R→D transmission is received correctly. Hence, the end-to-end error probability of DF relay is given by

$$\begin{aligned}P_{\gamma_{DF}}&(\gamma|\bar{\gamma}_1, \bar{\gamma}_2)\\&= (1 - P_e(\gamma|\bar{\gamma}_1))P_e(\gamma|\bar{\gamma}_2) + (1 - P_e(\gamma|\bar{\gamma}_2))P_e(\gamma|\bar{\gamma}_1)\\&= P_e(\gamma|\bar{\gamma}_1) + P_e(\gamma|\bar{\gamma}_2) - 2P_e(\gamma|\bar{\gamma}_1)P_e(\gamma|\bar{\gamma}_2).\end{aligned}\qquad(5.56)$$

Using the cumulative distribution function (CDF) of chi-squared distribution

$$P_e(\gamma|\bar{\gamma}_i) = 1 - e^{(-\frac{\gamma}{\bar{\gamma}_i})},\qquad i = 1, 2,\qquad(5.57)$$

the CDF of γ_{DF_k} can be written as

$$P_{\gamma_{DF}} = e^{-\frac{\gamma}{\bar{\gamma}_1}} + e^{-\frac{\gamma}{\bar{\gamma}_2}} - 2e^{-(\frac{1}{\bar{\gamma}_1} + \frac{1}{\bar{\gamma}_2})\gamma},\qquad(5.58)$$

and the PDF of γ_{DF_k} is derived by

$$\begin{aligned}p_{\gamma_{DF}} &= \frac{\partial P_{\gamma_{DF}}}{\partial \gamma}\\&= 2\frac{\bar{\gamma}_1\bar{\gamma}_2}{\bar{\gamma}_1 + \bar{\gamma}_2}e^{-(\frac{1}{\bar{\gamma}_1} + \frac{1}{\bar{\gamma}_2})\gamma} - \frac{1}{\bar{\gamma}_1}e^{-\gamma/\bar{\gamma}_1} - \frac{1}{\bar{\gamma}_2}e^{-\gamma/\bar{\gamma}_2}.\end{aligned}\qquad(5.59)$$

With $\bar{\gamma}_1 = \bar{\gamma}_2 = \bar{\gamma}$, $p_{\gamma_{DF}}$ is simplified as

$$p_{\gamma_{DF}} = \frac{1}{\bar{\gamma}}(e^{-2\gamma/\bar{\gamma}} - 2e^{-\gamma/\bar{\gamma}}).\qquad(5.60)$$

Using the definition of MGF, the MGF of γ_{DF_k} can be expressed by

$$
\begin{aligned}
M_{\gamma_{\mathrm{DF}}}(\alpha) &= \int_{-\infty}^{\infty} e^{\alpha\gamma} p_{\gamma_{\mathrm{DF}}}(\gamma) d\gamma \\
&= \frac{4}{2 + \bar{\gamma}\alpha} - \frac{2}{1 + \bar{\gamma}\alpha}.
\end{aligned}
\tag{5.61}
$$

In order to consider the effect of the relaying delay on the system performance, the outage probability is evaluated with the effective data rate R_e as

$$
P_\mathrm{out} = P(\log_2(1 + \gamma) < R_\mathrm{e}),
\tag{5.62}
$$

where B is the bandwidth in Hz. When the received SNR at the destination and the total transmission time T_total are not changed, a long relaying delay leads to a high R_e, therefore the outage probability will increase. On the other hand, when the relayding delay and T_total are not changed, the outage probability will be raised by a low received SNR at the destination. Therefore, the outage probability with the effective data rate, which is chosen as the metric, combines both the effect of the relaying delay and retransmission quality.

Using the closed-form expressions of MGF for the relay schemes, the outage probability of them can be evaluated by [192]

$$
P_\mathrm{out} = \mathfrak{L}^{-1}\left(\frac{M_\gamma(\alpha)}{\alpha}\right)\bigg|_{\gamma_\mathrm{th}},
\tag{5.63}
$$

where $\mathfrak{L}^{-1}(\cdot)$ denotes the inverse Laplace transform, and $\gamma_\mathrm{th} = 2^{R_\mathrm{e}} - 1$. The inversion of Laplace transform can be calculated using numerical techniques as in [193, 194].

5.6 Simulation Results

The performance of the proposed EF relay scheme is evaluated and compared with AF and DF relay schemes through computer simulations. MATLAB was used to plot all simulation results. Numerical results are obtained by averaging over 10^5 independent Monte Carlo runs.

In the simulations, we consider an OFDM system with QPSK modulation in each subcarrier. The total number of subcarriers in the OFDM system is $N = 512$, and the CP length is

64, CP$\geq$ ($L_1 + L_2$). The OFDM symbol duration, T_s, is 94μs. The S$\rightarrow$R and R$\rightarrow$ D chan-
nels considered in the simulations are the multipath model with Rayleigh fading in each path
whose parameters are listed in Table 3.3.3. The channel length $L_1 = L_2 = 31$. The least square
(LS) channel estimation algorithm is used at relay and destination nodes, which is given by
$\hat{\mathbf{h}}_{LS} = (\mathbf{s}^H\mathbf{s})^{-1}\mathbf{s}^H\mathbf{r}_i$, $i = 1, 2$. The received signal at destination is equalized in frequency domain
by a zero-forcing (ZF) equalizer which is to minimize the parameter $(\mathbf{r}_2 - \mathbf{Hs})^H(\mathbf{r}_2 - \mathbf{Hs})$. The
equalization coefficient $\mathbf{U}$ is the pseudoinverse of $\hat{\mathbf{H}}_{\text{diag}} = \text{diag}(H_0, H_1, \ldots, H_{N-1})$, i.e.,

$$\mathbf{U} = (\mathbf{H}_{\text{diag}}^H\mathbf{H}_{\text{diag}})^{-1}\mathbf{H}_{\text{diag}}^H. \tag{5.64}$$

We use a rate 1/2 convolutional code. The relay node decodes signals using the Viterbi algo-
rithm, and the traceback depth is equal to 7 times of the constraint length.

For the EF relay, the power constraint at relay node is normalized $P_{\text{tot}} = 1$. The length of
channel state information (CSI) buffer is 50, which means that 50 previous channel responses
are used to generate the channel variation model. The modeling order Q_p equals to 5, which
implies the current channel impulse response is estimated from 5 past channel responses. The
channel variation threshold $\Delta\mathbf{h}$=0.01.

5.6.1   Error Probability

We first elaborate the performance of the EF relay with the proposed parallel structure in terms
of the normalized mean square error (NMSE) at the relay nodes and average symbol error rate
(SER) at destination. The NMSE of the EF relay is compared with that of AF (fixed-gain and
OFDM-based) and DF schemes in Fig. 5.8. In this figure, the fixed-gain AF relay scheme
suffers from an error floor due to the lack of channel and noise compensation techniques. The
DF relay scheme performs better NMSE at high SNR (SNR> 15dB) by completely removing
the effect of channel and noise between source and relay. But the DF relay exhibits high
NMSE at low SNR as a result of involving additional decoding error. The EF and OFDM-
based AF relay have the similar low NMSE when SNR< 14dB over the time-invariant channel.
In additional, the NMSE of the EF relay with the proposed model-based estimation is better
then the OFDM-based AF scheme. In the case with the time-varying channel, the normalized
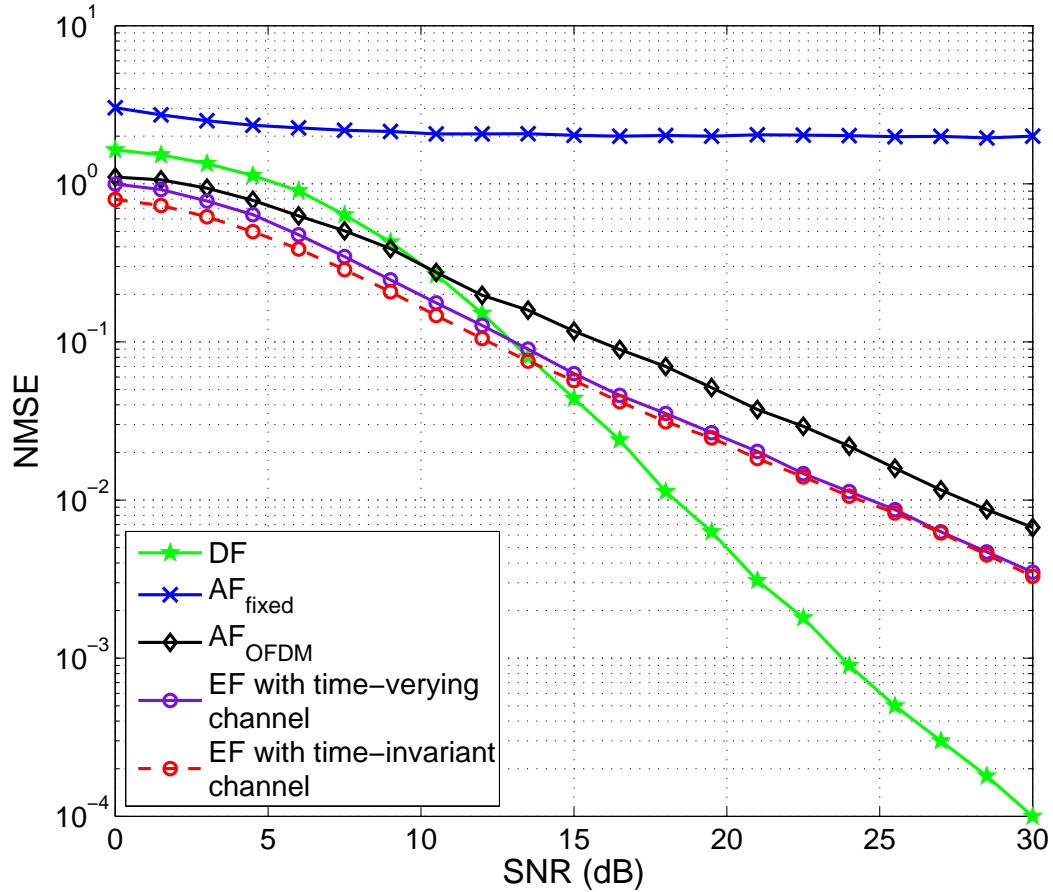
Figure 5.8: Normalized mean square errors of retransmitted signals at relay nodes with different relay schemes.

Doppler frequency is $f_d T = 0.05$. When the model-based prediction is used at the EF relay node, the proposed scheme over time-varying channel can keep the similar NMSE performance to that under the time-invariant channel by predicting and equalizing the channel accurately.

Fig. 5.9 compares the average SER at destination of different relay schemes. The fixed-gain AF relay scheme provides the worst SER performance resulting from the accumulation of multipath channels and noise. Under the time-invariant channel, the EF relay exhibits the same SER performance with DF and OFDM-based AF relay. Furthermore, the proposed EF relay still achieves a low SER, when the channel is time-varying, i.e., $f_d T = 0.05$. It implies that the EF relay can perform the same error probability as the DF relay with a reduced processing delay.
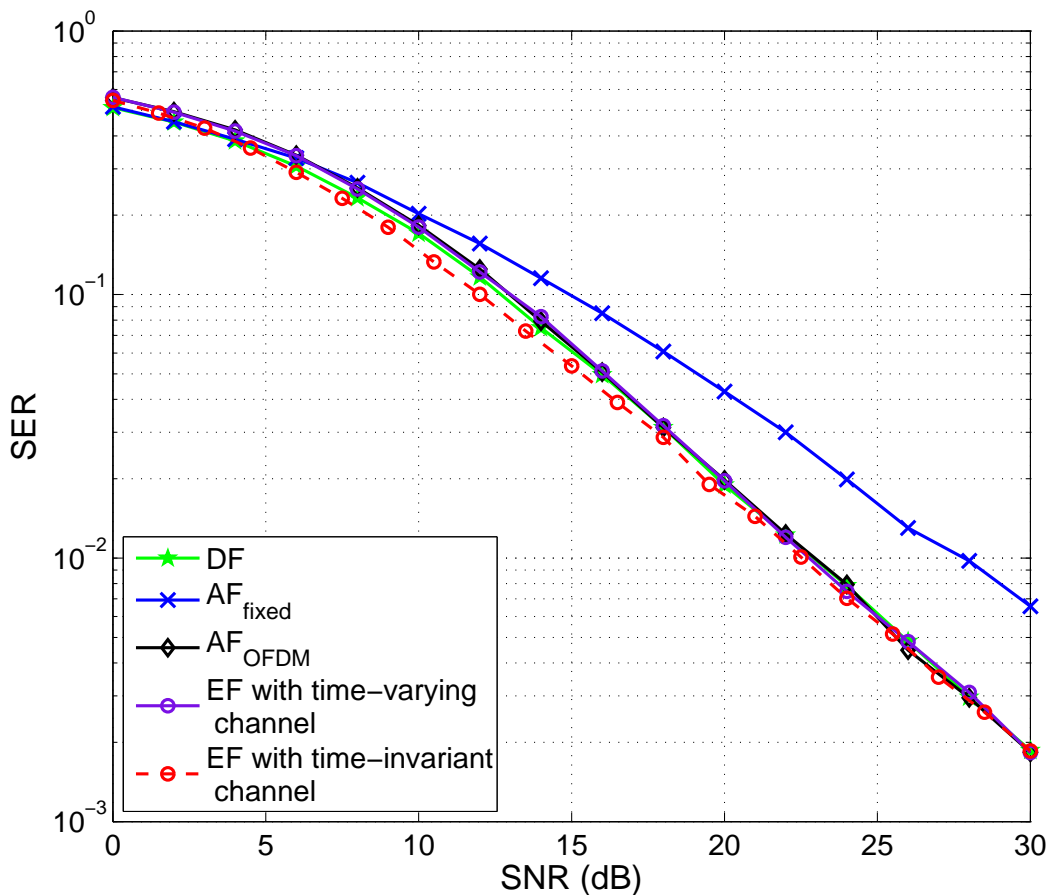
Figure 5.9: Average end-to-end SERs of different relay schemes under time-invariant and time-varying channels.

5.6.2   Outage Probability

We then consider the outage probabilities at destination of AF (fixed-gain and OFDM-based), DF and EF relay schemes. Here we assume that the equalizer structure and algorithm used in EF, OFDM-based AF and DF relays is the same. We set the total transmission time $T_{\text{total}} = 3qT_s$ during the simulations. T_s is the same constant in all simulations of outage probability. When $\mathcal{M}$-ary modulation is adopted,

$$q = \frac{L_p}{N \log_2 \mathcal{M}}. \tag{5.65}$$
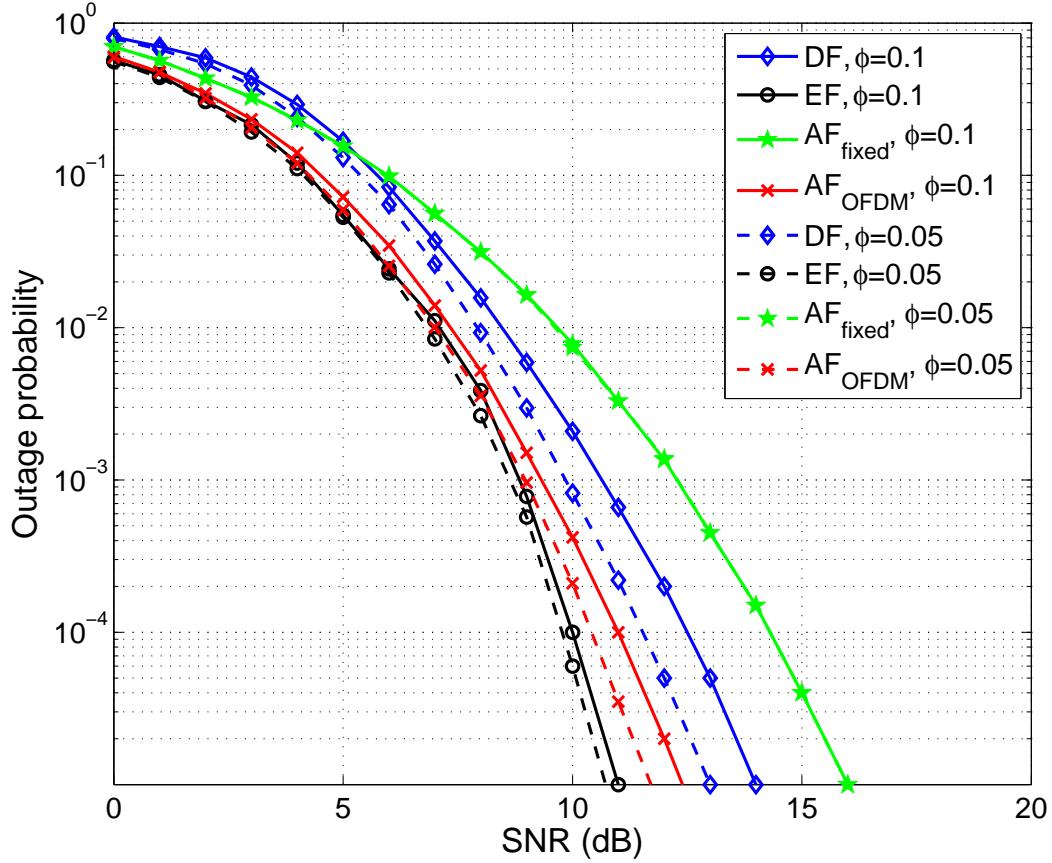
Figure 5.10: Average end-to-end outage probabilities of different relay schemes vs. SNR. $L_p = 2^{14}$. ϕ=0.1 and 0.5.

The effective date rate then can be obtained as

$$R_e = \frac{L_p}{3qT_s - T_d}$$
$$= \frac{bL_p}{(3L_p - \phi b)T_s},$$

(5.66)

where $b = N \log_2 \mathcal{M}$. When QPSK modulation with 512 subcarriers is applied, $b = 1024$. The fixed-gain AF relay has the shortest processing delay of only several microseconds; the proposed EF relay has a longer delay than AF scheme caused by involving equalization operations; the processing delay of the OFDM-based AF relay is longer than that of the proposed scheme because the FFT/IFFT and high-complexity algorithms are performed in series; while the delay of DF scheme (including de/modulation, de/interleaving, and de/encoding delay) is much longer than the ones of AF and EF. Consequently, we set $\phi_{\text{AF}_{\text{fixed}}} = \phi$, $\phi_{\text{EF}} = 5\phi$, $\phi_{\text{AF}_{\text{OFDM}}} = 15\phi$,
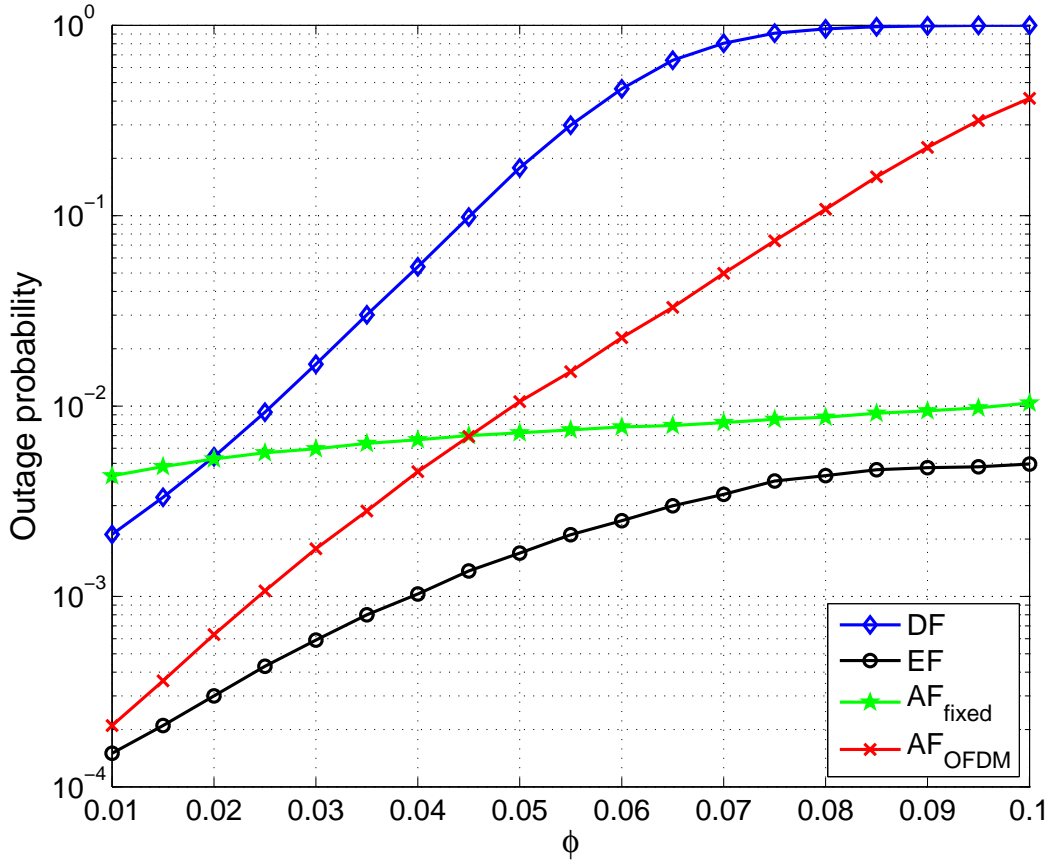
Figure 5.11: Average end-to-end outage probabilities of different relay schemes vs. relaying delay. $L_p = 2^{10}$ and SNR= 10dB.

and $\phi_{DF} = 25\phi$.

Obviously, one of the main factors which affect the outage probability performance of relay systems is the relaying delay. In Fig. 5.10, we show the average outage probabilities at destination of different relay schemes vs. SNR. Two different delay is considered, i.e., $\phi = 0.1$ and $\phi = 0.05$. We can see from the plots that the outage probability of EF, DF and OFDM-based AF relays becomes lower when the delay decreases from $\phi = 0.1$ to $\phi = 0.05$; while the performance of fixed-gain AF relay scheme remains the same. It implies that the effect of the delay on the outage probability is more appreciable in EF, DF and OFDM-based AF schemes than in fixed-gain AF relay, because the percentage of relaying delay in the total transmission time for the three relays are larger compared to that in fixed-gain AF scheme. Moreover, for both $\phi = 0.1$ and $\phi = 0.05$, the proposed EF relay exhibits the lowest outage probability by achieving channel compensation with a relatively short delay. In contrast, the

outage probability of OFDM-based AF relay is higher than the proposed scheme as the result of the inefficient structure. Meanwhile, both the fixed-gain AF and DF relays suffer high outage probabilities due to the accumulated channel fading and the long relaying delay respectively.

The outage probability performance vs. relaying delay of the various relay schemes is further investigated in Fig. 5.11. When the processing delay of the relay nodes increases, the outage probabilities of these four schemes all rise. More specifically, the fixed-gain AF relay incurs high outage probability even if ϕ is small due to the inferior retransmission. The DF relay, which has the longest precessing delay in these schemes, only outperforms the fixed-gain AF scheme when $\phi < 0.02$. Compared to the fixed-gain AF scheme, the proposed EF relay has higher complexity and longer processing delay by involving equalization operations; however it achieves sufficiently low outage probabilities by improving the end-to-end SNR. Although the OFDM-based AF scheme has the similar retransmission quality with the proposed scheme, the processing latency of the FFT and channel compensation algorithms leads to high outage probability when $\phi > 0.05$. The EF relay has the best outage probability performance with variable values of ϕ. It means that the proposed EF relay can guarantee the low outage probability under different SNR and delay.

The outage probability performance of relay schemes is also affected by the transmitted packet size. In continuous communications, i.e., $L_{\mathrm{p}} \rightarrow \infty$, the percentage of the relay delay time approaches zero in the total transmission time, therefore the performance only depends on SNR. When the packet size is small, the outage probability is determined by both SNR and relay delay. Average outage probabilities at destination of various relay schemes vs. SNR are depicted in Figure 5.12. In the case of $L_{\mathrm{p}} = 2^{10}$, the fixed-gain AF relay achieves the lowest outage probability, and the EF relay scheme can obtain similar outage probability with fixed-gain AF relay when SNR>15dB. The EF relay provides the best outage probability when $L_{\mathrm{p}} = 2^{14}$ at different SNR by achieving the trade-off between the transmission reliability and efficiency. The DF and OFDM-based AF relays only experience low outage probability when $L_{\mathrm{p}} = 2^{14}$, while it suffers the poor performance when the package size is short.

In Fig. 5.13, we evaluate the impact of packet size L_{p} on the performance of the four relay schemes for SNR=10dB. As expected, the outage probabilities of these three schemes reduce with the growing of packet size L_{p}. When the packet size increases, the performance
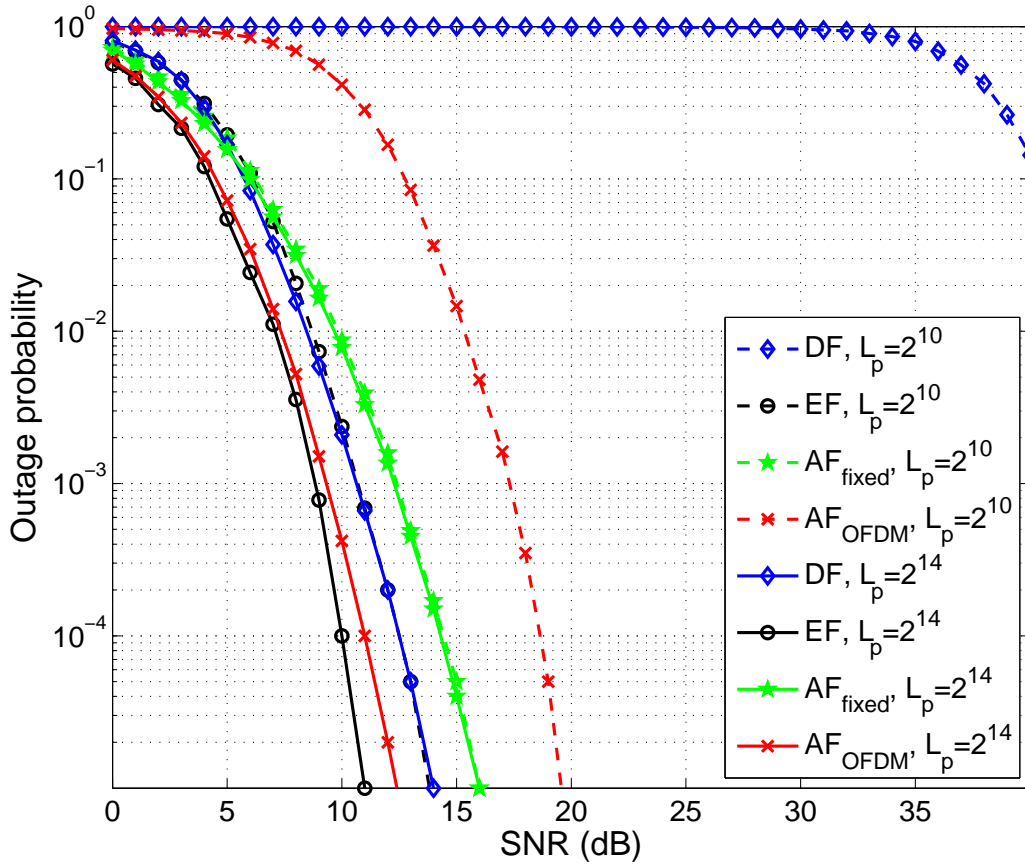
Figure 5.12: Average end-to-end outage probabilities of different relay schemes vs. SNR. $\phi = 0.1$. The packet size is 2^{10} and 2^{14}.

of fixed-gain AF relay cannot benefit form its short latency. Instead, its disadvantage in the end-to-end SNR becomes obvious. The effect of L_p is remarkable on the performance of EF, DF and OFDM-based AF schemes compared to fixed-gain AF relay. Particularly, the DF relay exhibits high outage probability due to its long latency when $L_p < 1500$. This factor limits the performance gain of DF relay substantially in burst and interactive communications. The OFDM-based AF scheme outperforms the DF scheme, however, its outage probability is still relatively high especially when $L_p < 2000$. On the other hand the proposed EF relay can achieve the lowest outage probability with different packet sizes, which implies that the proposed relay strategy can provide reliable retransmissions in both the continuous and interactive communications.
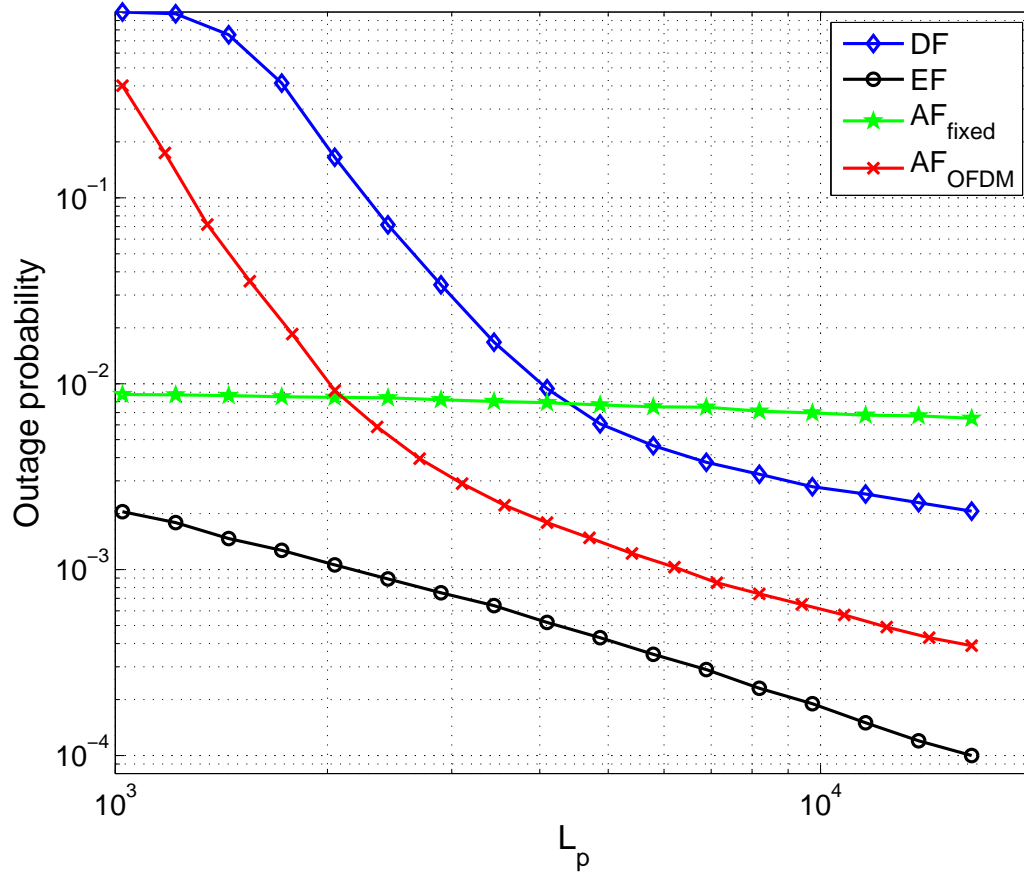
Figure 5.13: Average end-to-end outage probabilities of different relay schemes vs. packet size. $\phi = 0.1$ and SNR= 10dB.

5.7   Summary

In this chapter, a novel equalize-and-forward (EF) relay is proposed in this paper to provide reliable relay communications with the eliminated multipath channel accumulation effect and reduced processing delay at the relay node. The proposed EF relay scheme involves two parallel paths for channel equalization and estimation, i.e., main path and ancillary parallel path. In the main path, the delay minimization for signal relay is achieved by equalizer presetting mechanism without decoding and signal regeneration. The parallel path performs the model-based channel estimation and prediction and equalizer coefficient calculation to compensate the parallel path processing delay. Numerical results show that the proposed relay scheme exhibits comparable symbol error rate (SER) performance as the DF relay with much shorter delay. Compared to the traditional AF relay schemes, the EF relay scheme provides lower

outage probability with minimal processing delay. Moreover, with increasing packet sizes and SNR, the EF relay could achieve lower outage probability than both AF and DF approaches.

Chapter 6

Conclusions and Future Work

In this chapter, the contributions of this dissertation are summarized with some concluding remarks, and the future research directions are discussed.

6.1 Conclusions and Contributions

Cooperative communications as a physical layer technology can be used to achieve spatial diversity and cope fading without requiring multiple antennas on the same node. In cooperative system, the diversity is created via cooperation among neighboring wireless relay nodes. Through such cooperations, relay systems provide significant improvement in coverage and energy efficiency in wireless networks. The engagement of cooperative systems with OFDM transmission has been extensively used in many advanced wireless communications systems, however, there remains many technical challenges due to the more complex communication scenario. This thesis carries out a comprehensive study on relay techniques which mainly explored some important aspects of cooperative OFDM systems: the transmission reliability under accumulated multipath channels, and the transmission efficiency with extra relaying overhead and resource assumption. We developed a number of effective and efficiency schemes for these problems via various forms of OFDM-based relay systems.

The contributions that have been made in this thesis and the conclusions drawn from these contributions can be summarized as follows:

- *Adaptive guard interval scheme for amplify-and-forward relay systems*

In Chapter 3, two adaptive relay schemes with dynamical guard interval (GI) are proposed to minimize the relaying overhead and improve the transmission efficiency for the amplify-and-forward (AF) cooperative system. For the single-relay systems, we propose a novel adaptive GI scheme in which the GI length is adapted to channel conditions and is replaced by a variable length orthogonal codes to carry the GI length information. Numerical results show that the destination can detect the GI length accurately by exploiting the orthogonal property between different GI sequences. Moreover, the proposed adaptive scheme (without additional control signal) can achieve the same symbol error rate (SER) performance as the conventional adaptive GI approaches (with control signal). This implies that the proposed scheme can further save the control signaling overhead without any SER performance loss. Meanwhile, the adaptive GI scheme can cover the variable delay spread in multi-hop AF relay systems with the reduced transmission overhead compared to the fixed GI scheme.

Extending the adaptive GI scheme to multiple-relay systems, a relay selection (RS) scheme is proposed to minimize the overhead as well as enhance the overall transmission reliability. In the proposed strategy, an effective throughput (the data bits which are received correctly by the destination) is defined as the selection criterion which depends on both the end-to-end channel gain and the accumulated delay spread. With this criterion, the best relay link and the corresponding GI length are selected at source to maximize the effective throughput. The performance of the proposed scheme are evaluated through numerical simulations. Both the theoretical analysis and simulation results show that in the case that the channel delay spread is variable, the proposed scheme can dramatically improve the effective data transmission throughput.

- *Adaptive resource allocation for decode-and-forward two-way relay systems with unbalanced traffic loads*

In Chapter 4, we present the two adaptive resource allocation schemes for the two-way DF relay systems. The resource allocation algorithms are proposed to optimize the end-to-end capacity of the two-way system under the capacity ratio constraint which is based on the asymmetric traffic loads between the bidirectional transmissions. The capacity ratio is added as a fairness constraint, which are imposed to assure the quality of service for two terminal nodes. In order to combine the requirements of maximizing the end-to-end capacity and achieving the

given capacity ratio, we defined a balanced end-to-end capacity as the performance metric.

For the time-division two-way relay systems, the total end-to-end capacity is maximized by optimizing the transmission time and power allocations under the capacity ratio and total transmission time/power constraints. The performance of this scheme is compared with different allocation schemes through simulations. The results show that the proposed optimal allocation can significantly improve the balanced capacity compared to the random and equal allocation schemes.

The other resource allocation algorithm is investigated for the frequency-division relay systems where two-way transmission is performed by exploiting the orthogonality of the subchannels in OFDM systems. In this scenario, subcarriers, subcarrier power and time slot are optimized to achieve the maximum balanced end-to-end capacity. Since the optimal solution is extremely computationally complex to obtain, we propose a low-complexity suboptimal allocation algorithm which separates subcarrier allocation and time/power allocation. Simulation results verify that the suboptimal algorithm can provide the similar performance with the optimal one under different channel conditions. It means that the proposed suboptimal scheme can significantly reduce the complexity of resource allocation without the performance loss. Meanwhile, the performance of the proposed scheme is compared to some other allocation schemes. The results shows that the suboptimal scheme exhibits better balanced end-to-end capacity then the random and equal allocations.

- *Adaptive equalize-and-forward relay scheme for accumulated multipath channels*

The investigation of the trade-off between transmission reliability and efficiency in relay networks leads to our work on a novel relay scheme. An equalize-and-forward (EF) relay strategy is proposed in Chapter 5 which compensates the accumulation of frequency selective fading as well as delay spread. First, we investigate the performance impact of the multihop transmission in relay systems. We then provide the EF relay design, which adopted an efficient parallel structure to shorten the processing time and to achieve both transmission reliability and low processing delay. To reduce the processing delay at relay nodes, channel estimation and equalization for the channel between the source and relay are performed in parallel. In the proposed EF scheme, the equalization efficiency is improved by passing data symbols through a time-domain equalizer preset with the current channel response. Moreover, the equaliza-

tion accuracy is enhanced by exploiting the model-based channel estimation and prediction to reduce the impact of background Gaussian noise and further improve the quality of retransmitted signals. Numerical results show that the proposed relay scheme exhibits comparable symbol error rate (SER) performance as the DF relay with much shorter delay. Besides, the outage probability with a given effective data rate is adopted as the metric to comprehensively compare the performance of various relay schemes under different scenarios. Compared to the traditional AF relay schemes, the EF relay scheme provides lower outage probability with minimal processing delay. Meanwhile, with increasing packet sizes and SNR, the EF relay could achieve lower outage probability than both AF and DF approaches.

6.2 Future Work

The contributions presented in this dissertation for relay communication systems can be extended or used to explore new research topics:

- *Synchronization issue in multiple-relay networks*

   In this thesis and most of the previous research work in cooperative systems, it assumed that ideal frequency and time synchronization among nodes. Although this assumption is widely adopted in the literature and seems unavoidable for mathematical tractability, when studying the design and the performance of the practical wireless networks, it is not very realistic. In a large-scale network with a large number of mobile users, perfect synchronization among all the nodes is difficult to achieve. Time offset and frequency offset will deteriorate the performance of the relay networks, especially in an OFDM system. Hence, to model and analyze the relay system performance, both the channel estimation error and the symbol level synchronization error should be considered. When multiple distributed relay nodes transmit to the destination simultaneously, different transmission delays occur due to the different locations of the relay nodes, and each relay link has a different frequency offset. To eliminate the detrimental effects of the multiple frequency offsets, some technique is required at the relay and the destination to compensate the multiple frequency offsets. How to achieve the accurate symbol level synchronization and minimize these synchronization errors are also challenging problems.

- *Multiple-source multi-hop resource allocation for one/two-way relay systems*

In this thesis, we focused on the dual-hop relay system, where one source wishes to communicate with a destination, via a single relay. In realistic wireless networks, a large number of relay nodes could participate in the relay communications, which would involve the multi-hop relay transmissions. Although the allocation schemes in the previous works can enhance the achievable rate of the system or save the power consumption, a centralized controller as well as additional feedbacks are required to perform the global optimization for the network adopting these schemes. When the number of relaying hops is large, the number of controlling signals between terminal nodes and relay nodes increases, which leads to a low system efficiency. Besides, the processing delay caused by receiving the channel state information of the relay nodes, executing the optimization algorithm and feeding the resource allocation parameters back to the relays, results in outdated and non-optimal performance of the system. To this end a distributed resource allocation scheme with low-complexity should be investigated for multihop relay systems.

On the other hand, considering the scenario that the relay node simultaneously forwards the signals for multiple sources, a critical element of the design for such networks is an efficient cooperative strategy in conjunction with the OFDM system. One promising solution for this scenario is to transmit a multicarrier signal with different users' data on different subchannels. The relay node can dynamically allocates the subcarriers to each user according to the channel condition between them. Meanwhile, the transmission resource is optimally assigned to each link to maximize the total end-to-end capacity or data rate under the fairness constraint.

- *Hybrid relay scheme design with latency constraints*

General speaking, to improve the retransmission quality of the relay node, more high-complexity operation or high-complexity relay scheme need to be applied at the relay node, while the relay schemes with low burden tend to suffer the performance loss under the deteriorated channel condition. For the relay systems without a stringent latency requirement, e.g., continuous communications, the high-complexity operations can be adopted at relay node to enhance the performance. However, in the realtime and delay sensitive applications, such as the safety applications in vehicular communications, the high-complexity operations and long processing time at relay node cannot be tolerated, and the relay techniques with low latency will be preferred. Hence, a hybrid relay scheme need to be studied, which can dynamical-

ly select the relay technique performed by the relay node and the corresponding operations adaptive to the given latency constraints and the performance requirement. This strategy can be implemented by centralized or distribute controlling. In the centralized method, the source node decide and notice the relay and destination nodes the relay technique adopted for the current communication based on the specific requirement of the certain content forms and the overall channel condition. The distributed method can be executed by the relay nodes, where each relay independently selects the proper technique to process the received signals from the source. The adaptive relay scheme with latency constraints can be applied for the communication networks which includes different content forms and different requirements on quality of service.

Bibliography

[1] "Cisco visual networking index: Forecast and methodology 2009-2014," Cisco White Paper, Tech. Rep., June 2010.

[2] J. G. Proakis, *Digital Communication*, 5th ed. New York: McGraw-Hill, 2008.

[3] T. Rappaport, S. Sun, R. Mayzus, H. Zhao, Y. Azar, K. Wang, G. Wong, J. Schulz, M. Samimi, and F. Gutierrez, "Millimeter wave mobile communications for 5G cellular: It will work!" *IEEE Access (Invited)*, vol. 1, no. 1, pp. 335–349, May 2013.

[4] C. Wang, F. Haider, X. Gao, X. You, Y. Yang, D. Yuan, H. Aggoune, H. Haas, S. Fletcher, and E. Hepsaydir, "Cellular architecture and key technologies for 5G wireless communication networks," *IEEE Commun. Mag.*, vol. 52, no. 2, pp. 122–130, Feb. 2014.

[5] S. Zhang, "Cooperative relay in the next generation wireless networks," Ph.D. dissertation, The Hong Kong University of Science and Technology, Aug. 2009.

[6] D. Lister, "An operator's view on green radio," in *Proc. IEEE Int. Workshop on Green Communications*, 2009.

[7] Y. Chen, S. Zhang, S. Xu, and G. Li, "Fundamental trade-offs on green wireless networks," *IEEE Commun. Mag.*, vol. 49, no. 6, pp. 30–37, June 2011.

[8] *Air Interface for Fixed and Mobile Broadband Wireless Access Systems*, IEEE Standerd 802.16j, 2006.

[9] A. Goldsmith, S. Jafar, N. Jindal, and S. Vishwanath, "Capacity limits of MIMO channels," *IEEE J. Sel. Areas Commun.*, vol. 21, no. 5, pp. 684–702, June 2003.

[10] W. Zhang, X. Xiang-Gen, and K. B. Letaief, "Space-time/frequency coding for mimo-ofdm in next generation broadband wireless systems," *IEEE Trans. Wireless Commun.*, vol. 14, no. 2, pp. 32–43, June 2007.

[11] B. Lin, P. Ho, L. Xie, X. Shen, and J. Tapolcai, "Optimal relay station placement in broadband wireless access networks," *IEEE Trans. Mobile Comput.*, vol. 9, no. 2, pp. 259–269, Feb. 2010.

[12] E. Dahlman, S. Parkvall, and J. Skold, *4G LTE/LTE-Advanced for mobile broadband*. Academic Press, 2011.

[13] Y. Yang, H. Hu, J. Xu, and G. Mao, "Relay technologies for wimax and lte-advanced mobile systems," *IEEE Commun. Mag.*, vol. 47, no. 10, pp. 100–105, 2009.

[14] *Wireless LAN Medium Access Control (MAC) and Physical Layer (PHY) specifications Amendment 10: Mesh Networking*, IEEE Standard 802.11s, 2011.

[15] S. Chia, T. Gill, L. Ibbetson, D. Lister, A. Pollard, R. Irmer, D. Almodovar, N. Holmes, and S. Pike, "3G evolution," *IEEE Microw. Mag.*, vol. 9, no. 4, pp. 52–63, Aug. 2008.

[16] K. Loa, C. Wu, S. Sheu, Y. Yuan, M. Chion, D. Huo, and L. Xu, "IMT-advanced relay standards [WiMAX/LTE Update]," *IEEE Commun. Mag.*, vol. 48, no. 8, pp. 40–48, 2010.

[17] V. Chandrasekhar, J. Andrews, and A. Gatherer, "Femtocell networks: a survey," *IEEE Commun. Mag.*, vol. 46, no. 9, pp. 59–67, 2008.

[18] J. N. Laneman, D. Tse, and G. Wornell, "Cooperative diversity in wireless networks: Efficient protocls and outage behaiviour," *IEEE Trans. Inf. Theory*, vol. 50, no. 12, pp. 3062–3080, Dec. 2004.

[19] E. E. A. Sendonaris and B. Aazhang, "User cooperation diversity, part I, II," *IEEE Trans. Commun.*, vol. 51, pp. 1927–1948, Nov. 2003.

[20] J. N. Laneman and G. W. Wornell, "Distributed space-time-coded protocols for exploiting cooperative diversity in wireless networks," *IEEE Trans. Inf. Theory*, vol. 49, pp. 2415–2445, Oct. 2003.

[21] R. Pabst, B. Walke, D. Schultz, P. Herhold, H. Yanikomeroglu, S. Mukherjee, H. Viswanathan, M. Lott, W. Zirwas, M. Dohler, H. Aghvami, D. Falconer, and G. Fettweis, "Relay-based deployment concepts for wireless and mobile broadband radio," *IEEE Commun. Mag.*, vol. 42, no. 9, pp. 80–89, Sept. 2004.

[22] T. Riihonen, S. Werner, and R. Wichman, "Hypoexponential power delay profile and performance of multihop OFDM relay links," *IEEE Trans. Wireless Commun.*, vol. 9, no. 12, pp. 3878–3888, Oct. 2010.

[23] C. Na and T. Rappaport, "Measured wireless LAN public hotspot traffic statistics," *Electronics Letters*, vol. 40, no. 19, pp. 1202–1203, Sept. 2004.

[24] C. Na, J. K. Chen, and T. S. Rappaport, "Hotspot traffic statistics and throughput models for several applications," in *Proc. IEEE GLOBECOM*, 2004, pp. 3257–3263.

[25] ——, "Measured traffic statistics and throughput of IEEE 802.11b public WLAN hotspots with three different applications," *IEEE Trans. Wireless Commun.*, vol. 5, no. 11, pp. 3296–3305, Nov. 2006.

[26] Y. Chen, Y.-W. Lin, and C.-Y. Lee, "A block scaling FFT/IFFT processor for WiMAX applications," in *IEEE Asian Solid-State Circuits Conference*, Nov. 2006, pp. 203–206.

[27] A. Goldsmith, *Wireless Communication.*   Cambridge University Press, 2008.

[28] *Carrier sense multiple access with collision detection (CMSA/CD) access method and physical layer specifications*, IEEE Standard 802.20, 2008.

[29] A. Peled and A. Ruiz, "Frequency domain data transmission using reduced computational complexity algorithms," in *Acoustics, Speech, and Signal Processing, IEEE International Conference on ICASSP '80*, vol. 5, Apr. 1980, pp. 964–967.

[30] *Wireless LAN medium access control (MAC) and physical layer (PHY) specifications: High speed physical layer in 5 GHz band*, IEEE Standard 802.11a, 1999.

[31] *Wireless LAN medium access control (MAC) and physical layer (PHY) specifications: Further higher-speed physical layer extension in 2.4 GHz band*, IEEE Standard 802.11g, 2003.

[32] *IEEE Draft STANDARD for Information TechnologyTelecommunications and information exchange between systems-Local and metropolitan area networks-Specific requirements Part 11*, IEEE Draft Standerd P802.11n/D9.0, 2009.

[33] *Air Interface for Fixed Broadband Wireless Access Systems*, IEEE Standerd 802.16, 2004.

[34] R. Prasad, *OFDM for Wireless Communications Systems.*   Artech House, Inc., 2004.

[35] J. N. Laneman, D. Tse, and G. Wornell, "Cooperative diversity in wireless networks: Efficient protocls and outage behaiviour," *IEEE Trans. Inf. Theory*, vol. 50, no. 12, pp. 3062–3080, Dec. 2004.

[36] A. Nosratinia, T. Hunter, and A. Hedayat, "Cooperative communication in wireless networks," *IEEE Commun. Mag.*, vol. 42, no. 10, pp. 74–80, 2004.

[37] I. M. G. Kramer and R. Yates, "Cooperative communications," *Foundations and Trends in Networking*, vol. 1, no. 3, 2006.

[38] C. B. Norman and H. Jeremiah, "A closed-form expression for the outage probability of decode-and-forward relaying in dissimilar rayleigh fading channels," *IEEE Commun. Lett.*, vol. 12, no. 10, pp. 813–815, Dec. 2006.

[39] P. Anghel and M. Kaveh, "Exact symbol error probability of a cooperative network in a rayleigh-fading environment," *IEEE Trans. Wireless Commun.*, vol. 3, no. 5, pp. 1416–1421, 2004.

[40] C. S. Patel and G. L. Stuber, "Channel estimation for amplify and forward relay based cooperation diversity systems," *IEEE Trans. Wireless Commun.*, vol. 6, no. 6, pp. 2348–2356, 2007.

[41] M. Hasna and M.-S. Alouini, "A performance study of dual-hop transmissions with fixed gain relays," *IEEE Trans. Wireless Commun.*, vol. 3, no. 6, pp. 1963–1968, 2004.

[42] T. Wang, A. Cano, G. B. Giannakis, and J. N. Laneman, "High-performance cooperative demodulation with decode-and-forward relays," *IEEE Trans. Commun.*, vol. 55, pp. 1427–1438, 2007.

[43] T. Himsoon, W. P. Siriwongpairat, W. Su, and K. J. R. Liu, "Differential modulation with thresholdbased decision combining for cooperative communications," *IEEE Trans. Signal Process.*, vol. 55, pp. 3905–3923, 2007.

[44] F. Onat, A. Adinoyi, Y. Fan, H. Yanikomeroglu, J. Thompson, and I. Marsland, "Threshold selection for snr-based selective digital relaying in cooperative wireless networks," *IEEE Trans. Wireless Commun.*, vol. 7, 2008.

[45] R. Dabora and S. Servetto, "On the role of estimate-and-forward with time sharing in cooperative communication," *IEEE Trans. Inf. Theory*, vol. 54, no. 10, pp. 440–4431, Oct. 2008.

[46] B. Akhbari, M. Mirmohseni, and M. Aref, "Compress-and-forward strategy for relay channel with causal and non-causal channel state information," *IET Communications*, vol. 4, no. 10, pp. 1174–1186, July 2010.

[47] B. Rankov and A.Wittneben, "Spectral efficient protocols for half-duplex fading relay channels," *IEEE J. Sel. Areas Commun.*, vol. 25, no. 2, pp. 379–389, 2007.

[48] P. Larsson, N. Johansson, and K. Sunell, "Coded bi-directional relaying," in *Proc. IEEE VTC Spring*, vol. 2, 2006, pp. 851–855.

[49] R. Ahlswede, N. Cai, S. Li, and R. Yeung, "Network information flow," *IEEE Trans. Inf. Theory*, vol. 46, no. 4, p. 12041216, 2000.

[50] I. Baik and S. Chung, "Network coding for two-way relay channels using lattices," in *Proc. IEEE ICC*, 2008, pp. 3898–3902.

[51] E. van der Meulen, "Three terminal communication channels," *Advances in Applied Probability*, vol. 3, pp. 120–154, 1971.

[52] T. Cover and A. E. Gamal, "Capacity theorems for the relay channel," *IEEE Trans. Inf. Theory*, vol. 25, no. 5, pp. 572–584, 1979.

[53] O. S. Shin, A. Chan, H. T. Kung, and V. Tarokh, "Design of an OFDM cooperative space-time diversity system," *IEEE Trans. Veh. Technol.*, vol. 56, no. 4, pp. 2203–2251, July 2007.

[54] J. Qi and L. Cao, "Channel mean forwarded regenerative cooperative demodulation in OFDM systems," in *Proc. IEEE WCNC*, Mar. 2008.

[55] B. Can, H. Yomo, and E. D. Carvalho, "Hybrid forwarding scheme for cooperative relaying in OFDM based networks," in *Proc. IEEE ICC*, vol. 10, May 2006, pp. 4520–4525.

[56] D. Wang and U. Tureli, "Cooperative MIMO-OFDM and MAC design for broadband ad hoc networks," in *Proc. Milcom*, vol. 2, Oct. 2005, pp. 630–634.

[57] Y. Mei, Y. Hua, A. Swami, and B. Daneshrad, "Combating synchronization errors in cooperative relays," in *Proc. IEEE ICASSP*, vol. 3, March 2005, pp. 369 – 372.

[58] Z. Li and X.-G. Xia, "A simple alamouti space-time transmission scheme for asynchronous cooperative systems," *IEEE Signal Process. Lett.*, vol. 14, pp. 804 – 807, Nov. 2007.

[59] I. Hammerstrom and A. Wittneben, "Power allocation schemes for amplify-and-forward MIMO-OFDM relay links," *IEEE Trans. Wireless Commun.*, vol. 6, no. 8, pp. 2798–2802, August 2007.

[60] D. Chen and J. N. Laneman, "Joint power and bandwidth allocation in multihop wireless networks," in *Proc. IEEE WCNC*, Mar. 2008.

[61] J. Wu, "Soft-decode-and-forward for asynchronous wireless networks with doubly-selective fading," in *Proc. Globecom*, 2009, pp. 1–5.

[62] Z. Han, T. Himsoon, W. P. Siriwongpairat, and K. J. R. Liu, "Resource allocation for multiuser cooperative OFDM networks: Who helps whom and how to cooperate," *IEEE Trans. Veh. Technol.*, vol. 58, no. 5, pp. 2378–2391, Jun. 2009.

[63] G. Li and H. Liu, "Resource allocation for OFDMA relay networks with fairness constraints," *IEEE J. Sel. Areas Commun.*, vol. 24, no. 11, pp. 2061–2069, Nov. 2006.

[64] T. C. Ng and W. Yu, "Joint optimization of relay strategies and resource allocations in a cooperative cellular network," *IEEE J. Sel. Areas Commun.*, vol. 25, no. 2, pp. 328–339, Feb. 2007.

[65] P. Tarasak and Y. H. Lee, "Joint cooperative diversity and scheduling in ofdma relay systems," in *Proc. IEEE WCNC*, Mar. 2007, pp. 980–984.

[66] T. Ng and W. Yu, "Joint optimization of relay strategies and resource allocations in cooperative cellular networks," *IEEE J. Sel. Areas Commun.*, vol. 25, no. 2, pp. 328–339, February 2007.

[67] N. Y. Y. Ma and R. Tafazolli, "Bit and power loading for OFDM-based three-node relaying communications," *IEEE Trans. Signal Process.*, vol. 56, no. 7, pp. 3236–3247, July 2008.

[68] O. Amin and M. Uysal, "Optimal bit and power loading for amplify-and-forward cooperative OFDM systems," *IEEE Trans. Wireless Commun.*, vol. 10, no. 3, pp. 772–781, March 2011.

[69] T. T. Pham, H. H. Nguyen, and H. D. Tuan, "Power allocation in MMSE relaying over frequency-selective rayleigh fading channels," *IEEE Trans. Commun.*, vol. 58, no. 11, pp. 3330–3343, Nov. 2010.

[70] H. Eghbali and S. Muhaidat, "Single-carrier frequency-domain equalization for multi-relay cooperative systems with relay selection," in *Proc. Globecom Workshops*, 2011, pp. 1353–1358.

[71] O. Amin, S. Ikki, and M. Uysal, "Adaptive bit loading for multi-relay cooperative orthogonal frequency division multiple with imperfect channel estimation," *IET Communications*, vol. 6, no. 12, pp. 1821–1828, Aug. 2012.

[72] Y. Ding and M. Uysal, "Achievable data rates and power allocation for frequency-selective fading relay channels with imperfect channel estimation," *EURASIP Journal on Wireless Communications and Networking*, vol. 2012, no. 1, pp. 1–10, 2012.

[73] Y. Liang, A. Ikhlef, W. Gerstacker, and R.Schober, "Cooperative filter-and-forward beamforming for frequency-selective channels with equalization," *IEEE Trans. Wireless Commun.*, vol. 10, no. 1, pp. 228–239, Jan. 2011.

[74] H. Chen, S. ShahbazPanahi, and A. Gershman, "Filter-and-forward distributed beamforming for two-way relay networks with frequency selective channels," *IEEE Trans. Signal Process.*, vol. 60, no. 4, pp. 1927–1941, April 2012.

[75] T. Wang, B. P. Ng, and M. H. Er, "Frequency-domain approach to relay beamforming with adaptive decision delay for frequency-selective channels," *IEEE Trans. Signal Process.*, vol. 61, no. 22, pp. 5563–5577, Nov. 2013.

[76] H. Mheidat, M. Uysal, and N. Al-Dhahir, "Equalization techniques for distributed space-time block codes with amplify-and-forward relaying," *IEEE Trans. Signal Process.*, vol. 55, no. 5, pp. 1839–1852, May 2007.

[77] ——, "Single-carrier frequency domain equalization for broadband cooperative communications," in *IEEE WCNC*, Las Vegas, April 2006.

[78] R. U.Nabar, F. W.Kneubiihler, and H. Boelcskei, "Performance limits of amplify-and-forward based fading relay channels," in *IEEE ICASSP*, Montreal, May 2004.

[79] Q. Jia, T. Lv, and G. Ping, "An efficient scheme for joint equalization and interference cancellation in distributed cooperative diversity networks," in *Proc. IEEE CNSR*, Halifax, May 2008.

[80] H. Eghbali, S. Muhaidat, and N.Al-Dhahir, "A novel receiver design for single-carrier frequency domain equalization in broadband wireless networks with amplify-and-forward relaying," *IEEE Trans. Wireless Commun.*, vol. 10, no. 3, pp. 721–727, March 2011.

[81] H. Chen, A. Gershman, and S. Shahbazpanahi, "Filter-and-forward distributed beamforming in relay networks with frequency selective fading," *IEEE Trans. Signal Process.*, vol. 58, no. 3, pp. 1251–1262, March 2010.

[82] Z. Yi and I.-M. Kim, "Optimum beamforming in the broadcasting phase of bidirectional cooperative communication with multiple decode-and-forward relays," *IEEE Trans. Wireless Commun.*, vol. 8, pp. 5806–5812, 2009.

[83] I. Hammerstom and A. Wittneben, "Impact of relay gain allocation on the performance of cooperative diversity networks," in *Proc. IEEE VTC*, Sept. 2004, pp. 1815–1819.

[84] Z. Yi and I.-M. Kim, "Joint optimization of relay-precoders and decoders with partial channel side information in cooperative networks," *IEEE J. Sel. Areas Commun.*, vol. 25, pp. 447–458, Feb. 2007.

[85] A. Bletsas, A. Khisti, D. P. Reed, and A. Lippman, "A simple cooperative diversity method based on network path selection," *IEEE J. Sel. Areas Commun.*, vol. 24, pp. 659–672, Mar. 2006.

[86] A. Bletsas, H. Shin, and M. Z. Win, "Cooperative communications with outage-optimal opportunistic relaying," *IEEE Trans. Wireless Commun.*, vol. 6, pp. 3450–3460, Sept. 2007.

[87] Y. Zhao, R. Adve, and T. J. Lim, "Improving amplify-and-forward relay networks: optimal power allocation versus selection," *IEEE Trans. Wireless Commun.*, vol. 6, pp. 3114–3123, Aug. 2007.

[88] Y. Jing and H. Jafarkhani, "Single and multiple relay selection schemes and their achievable diversity order," *IEEE Trans. Wireless Commun.*, vol. 7, pp. 1414–1423, Mar. 2009.

[89] A. K. Sadek, Z. Han, and K. Liu, "A distributed relay-assignment algorithm for cooperative communications in wireless networks," in *Proc. IEEE ICC*, vol. 2, June 2006, pp. 1592–1597.

[90] V. Sreng, H. Yanikomeroglu, and D. Falconer, "Relayer selection strategies in cellular networks with peer-to-peer relaying," in *Proc. IEEE VTC Fall*, vol. 3, Oct. 2003, pp. 1949–1953.

[91] Y. Zou, J. Zhu, B. Zheng, and Y.-D. Yao, "An adaptive cooperation diversity scheme with best-relay selection in cognitive radio networks," *IEEE Trans. Signal Process.*, vol. 58, no. 10, pp. 5438–5445, Oct. 2010.

[92] D. Gunduz and E. Erkip, "Opportunistic cooperation by dynamic resource allocation," *IEEE Trans. Wireless Commun.*, vol. 6, pp. 1446–1454, Apr. 2007.

[93] A. Ribeiro, X. Cai, and G. Giannakis, "Symbol error probabilities for general cooperative links," *IEEE Trans. Wireless Commun.*, vol. 4, no. 3, pp. 1264–1273, May 2005.

[94] Y. Zou, B. Zheng, and W.-P. Zhu, "An opportunistic cooperation scheme and its BER analysis," *IEEE Trans. Wireless Commun.*, vol. 8, pp. 4492–4497, Sept. 2009.

[95] Q. Zhang, Q. Chen, F. Yang, X. Shen, and Z. Niu, "Cooperative and opportunistic transmission for wireless ad hoc networks," *IEEE Network*, vol. 21, pp. 14–20, Jan./Feb. 2007.

[96] A. Høst-Madsen and J. Zhang, "Capacity bounds and power allocation for wireless relay channels," *IEEE Trans. Inf. Theory*, vol. 51, no. 6, pp. 2020–2040, June 2005.

[97] D. Gündüz and E. Erkip, "Opportunistic cooperation by dynamic resource allocation," *IEEE Trans. Wireless Commun.*, vol. 6, no. 4, pp. 1446–1454, April 2007.

[98] Y. Liang, V. V. Veeravalliand, and H. V. Poor, "Resource allocation for wireless fading relay channels: Max-min solution," *IEEE Trans. Inf. Theory*, vol. 53, no. 10, pp. 3432–3453, Oct. 2007.

[99] S. Mallick, R. Devarajan, M. M. Rashid, and V. K. Bhargava, "Resource allocation for selective relaying based cellular wireless system with imperfect CSI," *IEEE Trans. Commun.*, vol. 61, no. 5, pp. 1822–1834, May 2013.

[100] M. Huemer, L. Reindl, A. Springer, and R. Weigel, "Frequency domain equalization of linear polyphase channels," in *Proc. IEEE VTC*, vol. 3, May 2000, pp. 1698–1700.

[101] M. S. Alam, J. W. Mark, and X. Shen, "Relay selection and resource allocation for multi-user cooperative OFDMA networks," *IEEE Trans. Wireless Commun.*, vol. 12, no. 5, pp. 2193–2205, May 2013.

[102] Y.-B. Lin, H. Taiwan, W.-H. Wu, and S. Yu.T., "Optimal and suboptimal resource allocations for multi-hop MIMO-OFDMA networks," in *Proc. IEEE PIMRC*, Sept. 2012, pp. 502–506.

[103] N. Zhou, X. Zhu, Y. Huang, and H. Lin, "Optimal resource allocation for orthogonal frequency division multiplexing-based multi-destination relay systems," *IET Communications*, vol. 5, no. 14, pp. 2075–2081, Sept. 2011.

[104] A. Bletsas, A. Khisti, D. P. Reed, and A. Lippman, "A simple cooperative diversity method based on network path selection," *IEEE J. Sel. Areas Commun.*, vol. 24, no. 3, pp. 659–672, 2006.

[105] K. Vardhe, D. Reynolds, and B. Woerner, "Joint power allocation and relay selection for multiuser cooperative communication," *IEEE Trans. Wireless Commun.*, vol. 9, no. 4, pp. 1255–1260, 2010.

[106] S. Mallick, K. Kandhway, M. M. Rashid, and V. K. Bhargava, "Power allocation for decode-and-forward cellular relay network with channel uncertainty," in *Proc. IEEE ICC*, 2011, pp. 1–5.

[107] A. Khabbazibasmenj and S. A. Vorobyov, "Power allocation based on sep minimization in two-hop decode-and-forward relay networks," *IEEE Trans. Commun.*, vol. 59, no. 8, pp. 3954–3963, 2011.

[108] S. Kadloor and R. Adve, "Relay selection and power allocation in cooperative cellular networks," *IEEE Trans. Wireless Commun.*, vol. 9, no. 5, pp. 1676–1685, 2010.

[109] S. Talwar, Y. Jing, and S. Shahbazpanahi, "Joint relay selection and power allocation for two-way relay networks," *IEEE Signal Process. Lett.*, vol. 18, no. 2, pp. 91–94, 2011.

[110] Z. H. B. Wang and K. J. R. Liu, "Distributed relay selection and power control for multiuser cooperative communication networks using stackelberg game," *IEEE Trans. Mobile Comput.*, vol. 8, no. 7, pp. 975–990, 2009.

[111] Y. W. Hong, W. J. Huang, F. H. Chiu, and C. C. J. Kuo, "Cooperative communications in resource-constrained wireless networks," *IEEE Signal Process. Mag.*, vol. 24, no. 3, pp. 47–57, 2007.

[112] K.-S. Hwang, Y.-C. Ko, and M.-S. Alouini, "Performance analysis of incremental opportunistic relaying over identically and non-identically distributed cooperative paths," *IEEE Trans. Wireless Commun.*, vol. 8, no. 4, pp. 1953–1961, 2009.

[113] Q. Zhang, J. Zhang, C. Shao, Y. Wang, P. Zhang, and R. Hu, "Power allocation for regenerative relay channels with rayleigh fading," in *Proc. IEEE VTC Fall*, Sep. 2004, pp. 26–29.

[114] M. O. Hasna and M.-S. Alouini, "Optimal power allocation for relayed transmissions over rayleigh-fading channels," *IEEE Trans. Wireless Commun.*, vol. 3, pp. 1999–2004, 2004.

[115] I. Hammerstroem, M. Kuhn, and A. Wittneben, "Impact of relay gain allocation on the performance of cooperative diversity networks," in *IEEE VTC Fall*, vol. 3, Sep. 2004, pp. 1815–1819.

[116] I. Maric and R. Yates, "Bandwidth and power allocation for cooperative strategies in gaussian relay networks," in *Asilomar Conf. Signals, Syst., Comput.*, Nov. 2004, pp. 1907–1911.

[117] G. Li and H. Liu, "On the capacity of the broadband relay networks," in *Asilomar Conf. Signals, Syst., Comput.*, 2004.

[118] Z. Zhou, S. Zhou, S. Cui, and J.-H. Cui, "Energy-effcient cooperative communication in a clustered wireless sensor network," *IEEE Trans. Veh. Technol.*, vol. 57, no. 6, pp. 3618–3628, Nov. 2008.

[119] G. Lebrun, J. Gao, and M. Faulkner, "MIMO transmission over a time-varying channel using SVD," *IEEE Trans. Wireless Commun.*, vol. 4, no. 2, pp. 757–764, Mar. 2005.

[120] X. Zhang, W. Jiao, and M. Tao, "End-to-end resource allocation in OFDM based linear multi-hop networks," in *Proc. IEEE Infocom*, April 2008.

[121] L. Lai, J. Wang, A. Huang, and H. Shan, "Routing and resource allocation with collision constraint in multi-hop cognitive radio networks," in *Proc. IEEE Globecome Workshop*, Dec. 2012, pp. 974–979.

[122] F. Li and H. Jafarkhani, "Resource allocation algorithms with reduced complexity in MIMO multi-hop fading channels," in *Proc. IEEE WCNW*, April 2009, pp. 1–6.

[123] I. Hammerström and A. Wittneben, "On the optimal power allocation for nonregenerative OFDM relay links," in *Proc. IEEE ICC*, vol. 10, 2006, pp. 4463–4468.

[124] K. Jitvanichphaibool, R. Zhang, and Y. C. Liang, "Optimal resource allocation for two-way relay-assisted OFDMA," *IEEE Trans. Veh. Technol.*, vol. 58, no. 7, pp. 3311–3321, Sep. 2009.

[125] H. Shin and J. H. Lee, "Joint resource allocation for multiuser two-way OFDMA relay networks with proportional fairness," in *Proc. IEEE VTC Fall*, 2011, pp. 1–5.

[126] W. Dang, M. Tao, H. Mu, and J. Huang, "Subcarrier-pair based resource allocation for cooperative multi-relay OFDM systems," vol. 9, no. 5, pp. 1640–1649, May 2010.

[127] J. Cai, X. Shen, J. Mark, and A. Alfa, "Semi-distributed user relaying algorithm for amplify-and-forward wireless relay networks," *IEEE Trans. Wireless Commun.*, vol. 7, no. 4, pp. 1348–1357, Apr. 2008.

[128] S. Kadloor and R. Adve, "Relay selection and power allocation in cooperative cellular networks," *IEEE Trans. Wireless Commun.*, vol. 9, no. 5, pp. 1676–1685, May 2010.

[129] T. C.-Y. Ng and W. Yu, "Joint optimization of relay strategies and resource allocations in cooperative cellular networks," *IEEE J. Sel. Areas Commun.*, vol. 25, no. 2, pp. 328–339, 2007.

[130] B. Can, H. L. M. Portalski, S. Frattasi, and H. Suraweera, "Implementation issues for OFDM-based multihop cellular networks," *IEEE Commun. Mag.*, vol. 45, no. 9, pp. 74–81, Sept. 2007.

[131] K. Lee and D. Cho, "Hierarchical constellation based adaptive relay scheme in multi-hop networks," *IEEE Commun. Lett.*, vol. 11, no. 3, pp. 225–227, Mar. 2007.

[132] A. Müller and H. Yang, "Dual-hop adaptive packet transmission systems with regenerative relaying," *IEEE Trans. Wireless Commun.*, vol. 9, no. 1, pp. 234–244, Jan. 2010.

[133] X. Wang, Y. Bao, X. Liu, and Z. Niu, "On the design of relay caching in cellular networks for energy efficiency," in *Proc. IEEE Infocom Workshop*, Apr. 2011, pp. 259–264.

[134] C. Yang, W. Wang, S. Chen, and M. Peng, "Outage performance of orthogonal space-time block codes transmission in opportunistic decode-and-forward cooperative networks with incremental relaying," *IET Communications*, vol. 5, no. 1, pp. 61–70, 2011.

[135] P. Fan, C. Zhi, C. Wei, and K. B. Letaief, "Reliable relay assisted wireless multicast using network coding," *IEEE J. Sel. Areas Commun.*, vol. 27, no. 5, pp. 749–762, June 2009.

[136] L. Lu, M. Xiao, and L. Rasmussen, "Design and analysis of relay-aided broadcast using binary network codes," *Journal of Communications*, vol. 6, no. 8, pp. 610–617, Nov. 2011.

[137] L. Wang, W. Su, J. Huang, A. Chen, and C. Chang, "Optimal relay location in multi-hop cellular systems," in *Proc. IEEE WCNC*, Mar. 2008, pp. 1306–1310.

[138] C. Y. Chang, C. T. Chang, M. Li, and C. H. Chang, "A novel relay placement mechanism for capacity enhancement in IEEE 802.16j WiMAX networks," in *Proc. IEEE ICC*, 2009, pp. 1–5.

[139] H. Lu, W. Liao, and F. Lin, "Relay station placement strategy in IEEE 802.16j WiMAX networks," *IEEE Trans. Commun.*, vol. 59, no. 1, pp. 151–158, Jan. 2011.

[140] S. Zhou, A. Goldsmith, and Z. Niu, "On optimal relay placement and sleep control to improve energy efficiency in cellular networks," in *Proc. IEEE ICC*, 2011, pp. 1–6.

[141] M. Peng, C. Yang, Z. Zhao, W. Wang, and H. Chen, "Cooperative network coding in relay-based IMT-advanced systems," *IEEE Commun. Mag.*, pp. 76–84, Apr. 2012.

[142] V. E. et. al., "A model for the multipath delay profile of fixed wireless channels," *IEEE J. Sel. Areas Commun.*, vol. 17, no. 3, pp. 399–410, March 1999.

[143] W. Mohr, "Radio propagation for local loop applications at 2 GHz," in *Proc. 3rd Annual International Universal Personal Communications*, 1994, pp. 119–123.

[144] S. Das, E. Carvalho, and R.Prasad, "Variable guard interval orthogonal frequency division multiplexing in dynamic channel condition," in *Proc. IEEE PIMRC*, Sept. 2006, pp. 1–5.

[145] K. Yan, H. Wu, S. Chang, and Y. Wu, "A novel adaptive prefix interval scheme for MIMO OFDM systems," in *Proc. IEEE ISCS*, May 2009, pp. 2798–2801.

[146] M. Muck, M. Courville, M. Debbah, and P. Duhamel, "A pseudo random postfix OFDM modulator and inherent channel estimation techniques," in *Proc. Globecom*, 2003, pp. 2380–2384.

[147] B. Muquet, Z. Wang, G. B. Giannakis, M. Courville, and P. Duhamel, "Cyclic prefixing or zero padding for wireless multicarrier transmissions?" *IEEE Trans. Commun.*, vol. 50, no. 12, pp. 2136–2148, Dec. 2002.

[148] E. H. Dinan and B. Jabbari, "Spreading codes for direct sequence CDMA and wideband CDMA cellular networks," *IEEE Commun. Mag.*, vol. 36, no. 4, pp. 48–54, Sept. 1998.

[149] W. X, H. Li, and H. Lin, "A new adaptive OFDM system with precoded cyclic prefix for dynamic cognitive radio communications," *IEEE J. Sel. Areas Commun.*, vol. 29, no. 2, pp. 431–442, Feb. 2011.

[150] D. Falconer, S. Ariyavisitakul, A. Benyamin-Seeyar, and B. Eidson, "Frequency domain equalization for single-carrier broadband wireless systems," *IEEE Commun. Mag.*, vol. 40, no. 4, pp. 58–66, 2002.

[151] D. Baum, J. Hansen, and J. Salo, "An interim channel model for beyond-3G systems: extending the 3GPP spatial channel model (SCM)," in *IEEE VTC Spring*, vol. 5, June 2005, pp. 3132–3136.

[152] E. Altubaishi and X. Shen, "Variable-rate based relay selection scheme for decode-and-forward cooperative networks," in *Proc. IEEE WCNC*, Mar. 2011, pp. 1887–1891.

[153] R. Alejandro, X. Cai, and B. G. Giannakis, "Symbol error probabilities for general cooperative links," *IEEE Trans. Wireless Commun.*, vol. 4, no. 3, pp. 1264–1273, May 2005.

[154] Q. Zhang, F. Shu, M. Wang, and J. Sun, "Relay selection schemes for precoded cooperative OFDM and their achievable diversity orders," *IEEE Signal Process. Lett.*, vol. 18, no. 4, pp. 231–234, April 2011.

[155] X. Gao, X. Wang, Y. Zou, and P. Ho, "An efficient ofdm with adaptive guard interval for amplify and forward relay systems," in *Proc. IEEE VTC Fall*, 2013, pp. 1–5.

[156] X. Gao, X. Wang, and Y. Zou, "Relay selection scheme with adaptive cyclic prefix for cooperative amplify-and-forward relay," in *Proc IEEE Globecom*, 2013, pp. 1939–1943.

[157] V. Havary-Nassab, S. ShahbazPanahi, and A. Grami, "Optimal distributed beamforming for two-way relay networks," *IEEE Trans. Signal Process.*, vol. 58, no. 3, pp. 1238–1250, March 2010.

[158] F. He, Y. Sun, L. Xiao, X. Chen, C.-Y. Chi, and S. Zhou, "Capacity region bounds and resource allocation for two-way OFDM relay channels," *IEEE Trans. Wireless Commun.*, vol. 12, no. 6, pp. 2904–2918, June 2013.

[159] Y. Liu and M. Tao, "Optimal channel and relay assignment in OFDM-based multi-relay multi-pair two-way communication networks," *IEEE Trans. Commun.*, vol. 60, no. 2, pp. 317–322, Feb. 2012.

[160] H. Zhang, Y. Liu, and M. Tao, "Resource allocation with subcarrier pairing in ofdma two-way relay networks," *IEEE Wireless Commun. Lett.*, vol. 1, no. 2, pp. 61–65, Apr. 2012.

[161] M. Pischella and D. L. Ruyet, "Optimal power allocation for the two-way relay channel with data rate fairness," *IEEE Commun. Lett.*, vol. 15, no. 9, pp. 959–961, Sep. 2011.

[162] K. Xiong, Q. Shi, P. Fan, and K. B. Letaief, "Resource allocation for two-way relay networks with symmetric data rates: An information theoretic approach," in *Proc. IEEE ICC*, 2013, pp. 6060–6064.

[163] T. C.-Y. Ng and W. Yu, "Joint optimization of relay strategies and resource allocations in cooperative cellular networks," *IEEE J. Sel. Areas Commun.*, vol. 25, no. 2, pp. 328–339, Feb. 2007.

[164] M. Zhou, Q. Cui, R. Jäntti, and X. Tao, "Energy-efficient relay selection and power allocation for two-way relay channel with analog network coding," *IEEE Commun. Lett.*, vol. 16, no. 6, pp. 816–819, June 2012.

[165] X. Liang, S. Jin, X. Gao, and K.-K. Wong, "Outage performance for decode-and-forward two-way relay network with multiple interferers and noisy relay," *IEEE Trans. Commun.*, vol. 61, no. 2, pp. 521–531, Feb. 2013.

[166] Z. Chen, T. J. Lim, and M. Motani, "Two-way relay networks optimized for Rayleigh fading channels," in *IEEE Globecom*, Dec. 2013, pp. 3843–3848.

[167] P. Upadhyay and S. Prakriya, "Performance of analog network coding with asymmetric traffic requirements," *IEEE Commun. Lett.*, vol. 15, no. 6, pp. 647–649, 2011.

[168] X. Ji, B. Zheng, Y. Cai, and L. Zou, "On the study of half-duplex asymmetric two-way relay transmission using an amplify-and-forward relay," *IEEE Trans. Veh. Technol.*, vol. 61, no. 4, pp. 1649–1664, 2012.

[169] Z. Ni, X. Zhang, and D. Yang, "Outage performance of two-way fixed gain amplify-and-forward relaying systems with asymmetric traffic requirements," *IEEE Commun. Lett.*, vol. 18, no. 1, pp. 78–81, 2014.

[170] A. Papoulis, *Probability, Random Variables, and Stochastic Processes*, 3rd ed. New York: McGraw-Hill, 1991.

[171] Z. Du, J. Cheng, and N. Beaulieu, "Accurate error-rate performance analysis of OFDM on frequency-selective nakagami-m fading channels," *IEEE Trans. Commun.*, vol. 54, no. 2, pp. 319–328, Feb. 2006.

[172] T. M. Cover and J. A. Thomas, *Elements of Information Theory*. New York: Wiley, 1991.

[173] D. Neves, C. Ribeiro, A. Silva, and A. Gameiro, "A time domain channel estimation scheme for equalize-and-forward relay-assisted systems," in *Proc. IEEE VTC Fall*, Sep. 2010, pp. 1–5.

[174] S. Devar, K. KS, B. Ramamurthi, and R. D. Koilpillai, "Downlink throughput enhancement of a cellular network using two-hop user-deployable indoor relays," *IEEE J. Select. Areas Commun.*, vol. 31, no. 8, pp. 1607–1617, Aug. 2013.

[175] K. Singh, M.-L. Ku, and J.-C. Lin, "An optimal temporal-and-spatial equalizer for two-hop mimo relay networks with backward csis," in *Proc. IEEE WCNC*, Apr. 2013, pp. 3242–3247.

[176] ——, "A two-dimensional mmse equalizer for mimo relay networks in multipath fading channels," in *Proc. IEEE WCNC*, Sept. 2010, pp. 1–5.

[177] V. Erceg, S. Fortune, J. Ling, J. R. A.J., and R. Valenzuela, "Comparisons of a computer-based propagation prediction tool with experimental data collected in urban microcellular environments," *IEEE J. Sel. Areas Commun.*, vol. 15, no. 4, pp. 677–684, May 1997.

[178] M. Abramowitz and I. A. Stegun, *Handbook of Mathematical Functions With Formulas, Graphs, and Mathematical Tables*, 9th ed. New York: Dover, 1970.

[179] J. Salo, H. El-Sallabi, and P. Vainikainen, "The distribution of the product of independent Rayleigh random variables," *IEEE Trans. Antennas Propag.*, vol. 54, no. 2, pp. 639–643, Feb. 2006.

[180] Y. luke, *Special Function and Their Approximations*.   Academix Press, 1969, vol. 1.

[181] M. Kornfeld and G. May, "DVB-H and IP datacast broadcast to handheld devices," *IEEE Trans. on Broadcast.*, vol. 53, no. 1, pp. 161–170, Mar 2007.

[182] J. Hu, G. Min, and M. E. Woodward, "Performance analysis of the txop burst transmission scheme in single-hop ad hoc networks with unbalanced stations," *Computer Communications*, 2010.

[183] V.-H. Pham, X. Wang, J. Nadeau, and J.-Y. Chouinard, "Cluster-based time-domain channel prediction for dynamic wireless communications," in *Proc. IEEE Globecom Workshops*, Dec. 2010, pp. 59–63.

[184] Y. Zheng and C. Xiao, "Frequency-domain channel estimation and equalization for broadband wireless communications," in *Proc. IEEE ICC*, June 2007, pp. 4475–4480.

[185] N. Benvenuto and S. Tomasin, "Iterative design and detection of a DFE in the frequency domain," *IEEE Trans. Commun.*, vol. 53, pp. 1867–1875, Nov. 2005.

[186] X. Wang, Y. Wu, J.-Y. Chouinard, S. Lu, and B. Caron, "A channel characterization technique using frequency domain pilot time domain correlation method for DVB-T systems," *IEEE Trans. Consum. Electron.*, vol. 49, no. 4, pp. 949–957, Nov 2003.

[187] S. Bug, C. Wengerter, I. Gaspard, and R. Jakoby, "WSSUS - channel models for broadband mobile communication systems," in *IEEE VTC Spring*, vol. 2, May 2002, pp. 894–898.

[188] S. Haykin, *Neural Networks and Learning Machines*, 3rd ed.   Prentice Hall, 2008.

[189] J. Wang and D. P. Palomar, "Robust mmse precoding in mimo channels with pre-fixed receivers," *IEEE Trans. on Signal Processing*, vol. 58, no. 11, pp. 5802–5818, Nov. 2010.

[190] M. Hasna and M.-S. Alouini, "End-to-end performance of transmission systems with relays over rayleigh-fading channels," *IEEE Trans. Wireless Commun.*, vol. 2, pp. 1126–1131, Nov. 2003.

[191] ——, "A performance study of dual-hop transmissions with fixed gain relays," *IEEE Trans. Wireless Commun.*, vol. 3, no. 6, pp. 1965–1968, Nov. 2004.

[192] S. Ikki and M. H. Ahmed, "Performance analysis of cooperative diversity wireless networks over Nakagami-m fading channel," *IEEE Commun. Letters*, vol. 11, no. 4, pp. 334–336, Apr. 2007.

[193] Y. C. Ko, M. S. Alouini, and M. K. Simon, "Outage probability of diversity systems over generalized fading channels," *IEEE Trans. Commun.*, vol. 48, no. 11, pp. 1783–1787, Nov. 2000.

[194] J. Abate, "Numerical inversion of laplace transforms of probability distributions," *ORSA J. Computing*, vol. 7, no. 1, pp. 36–43, 1995.

Curriculum Vitae

Name:	Xin Gao
Post-Secondary Education and Degrees:	2003 - 2007: Jilin University, Changchun, China Bachelor Degree 2007 - 2009: Lakehead University, Thunder Bay, ON, Canada Master Degree 2010 - 2014: Western University, London, ON, Canada Ph.D. Degree
Related Work Experience:	2008 - 2009: Teaching Assistant, Lakehead University 2009 - 2010: Research Assistant, Lakehead University 2010 - 2014: Teaching Assistant, Western University

Publications:

J. Yang, X. Wang, X. Gao, S. I. Park and H. M. Kim, "Optimal Reliable Data Feedback Selection Based Iterative Decision-Directed Channel Estimation for OFDM System," in *Proc. IEEE 24th CCECE*, May 2011, pp. 597-602.

X. Gao, X. Wang and J. Rahman, "Latency-Reduced Equalizer with Model-Based Channel Estimation for Vehicle-to-Vehicle Communications," in *Proc. IEEE VTC Fall Workshop*, Sept. 2012, pp. 1-5.

X. Gao, X. Wang, Y. Zou and P. Ho, "An Efficient OFDM with Adaptive Guard Interval for Amplify and Forward Relay Systems," in *Proc. IEEE VTC Fall*, Sept. 2013, pp. 1-5.

X. Gao, X. Wang and Y. Zou, "Relay Selection Scheme with Adaptive Cyclic Prefix for Cooperative Amplify-and-Forward Relay," in *Proc IEEE Globecom*, Dec. 2013, pp 1939-1943.

X. Gao, A. Behnad and X. Wang, "Performance Analysis of Decode-and-Forward Dual-Hop Opportunistic Relaying With Power Control," in *Proc IEEE ICC*, June. 2014.

X. Gao, X. Wang and V. Leung, "A Two-Hop Equalize-and-Forward Relay Scheme in OFDM-based Wireless Networks over Multipath Channels," *Wireless Communication and Mobile Computing*, accepted.

A. Behnad, X. Gao and X. Wang, "Distributed Resource Allocation for Multihop Decode-and-Forward Relay systems," *IEEE Trans. Veh. Technol.*, accepted.